Facultad de Ciencias
Departamento de Biología Molecular

STUDY OF THE RIBOSOMAL STRESS PATHWAY IN PLURIPOTENCY, CANCER AND DISEASE

DOCTORAL THESIS

LUCÍA MORGADO PALACÍN

Madrid, 2015

Universidad Autónoma de Madrid
Facultad de Ciencias
Departamento de Biología Molecular

STUDY OF THE RIBOSOMAL STRESS PATHWAY IN PLURIPOTENCY, CANCER AND DISEASE

Lucía Morgado Palacín
BSc, Biochemistry

The work presented in this Thesis has been carried out at the Tumour Suppression Group in the Spanish National Cancer Research Centre (CNIO, Madrid), under the direction and supervision of Dr. Manuel Serrano Marugán

Madrid, 2015

Dr. **Manuel Serrano Marugán**, Director of the Molecular Oncology Program (CNIO) and Head of the Tumour Suppression Group (CNIO)

CERTIFIES:

That the Doctoral Thesis titled "**STUDY OF THE RIBOSOMAL STRESS PATHWAY IN PLURIPOTENCY, CANCER AND DISEASE**" developed by **Mrs. Lucía Morgado Palacín, BSc, MSc** meets all the requirements to obtain the degree of **Doctor of Philosophy (PhD) in Molecular Biology** and that, with the aforementioned objective, will be defended at the Universidad Autónoma de Madrid. This Thesis has been carried out under my direction and I authorize its presentation to the Tribunal.

I hereby issue this certification in Madrid in October 15th, 2015.

Manuel Serrano Marugán, PhD
PhD Thesis Director.

Manuel Serrano Marugán
Director of the Molecular Oncology Program
Head of the Tumour Suppression Group

Spanish National Cancer Research Centre (CNIO)
C/Melchor Fernández Almagro, 3
E-28029, Madrid (Spain)
Phone: 0034-91 732 80 00

A mis padres y a mi hermana

A mis tíos José Luis y Santos

A Miguel

ACKNOWLEDGMENTS

Gracias **Manolo**, mi director de tesis y mentor, por darme la oportunidad de realizar la tesis doctoral en tu laboratorio y en un centro como el CNIO. Gracias por todo el apoyo que me has dado durante estos años. Gracias por tener la puerta del despacho siempre abierta y por las maravillosas discusiones científicas. Gracias por tu incansable búsqueda de excitantes preguntas científicas (*a veces no se trata de encontrar una respuesta inmediata sino de formular la pregunta adecuada*). Gracias por saber de todo y conectarlo todo, por hacer ciencia innovadora. Gracias por no caer ni en el dogma ni en la rutina, por lanzarte sin miedo a nuevos proyectos. Sobretodo, gracias por transmitirme todo eso. Y gracias también por tu comprensión en el terreno personal.

Gracias al **Grupo de Supresión Tumoral** por toda la ayuda y apoyo brindados a lo largo de estos 5 años (y un poquitín más). Gracias **Cristina** por la infinita paciencia escuchando mis dudas existenciales de experimentos, del labo y de la vida, por los consejos sosegados, gracias por ser una gran amiga. Y cómo no, gracias por ser mi compi de piscina! Gracias **María A.** por tu desbordante alegría, tu brillante capacidad de abordar preguntas científicas (y no científicas), de cuestionar siempre para bien. Gracias por ser tan constructiva. Gracias por todos los momentos compartidos dentro y fuera del labo, pasando por la campana de cultivos a una carrera a toda pastilla en Neptuno. Gracias **Susana L.** por preocuparte siempre de mí, por compartir tus conocimientos conmigo, por tus historias. Gracias por hacerme saber que puedo contar contigo. Gracias **Elena** por nuestro pasillo y nuestros cajones comunes, por tu "ains, Luci" seguido de un abrazo, por toda la ternura que me brindas siempre, por preocuparte de mí. Gracias **Ade** por tu perseverancia y constancia, por ser tan diferente a mí. Te siento muy cerca (y eso que estás muy lejos!). Gracias **Lluc** por ser un torbellino de energía, por tu alegría, tu cariño y tus charlas. Gracias **Pablo** por tu candidez, tus ánimos, tu buen humor (y tus coplas con la Meri) y por tu manera de ver la vida. Gracias **Daniela** por tus consejos, tu rigurosidad científica y tu cariño, por hacerme compañía en el labo a las mil de la noche. Gracias **Ana** por estar siempre dispuesta a ayudar con la mejor de tus sonrisas, por ser tan eficiente y tan organizada. Gracias **Maribel** por enseñarme con tanta paciencia a trabajar con ratones, gracias por tu buen humor y tu diligencia. **Han**, *thanks for sharing the secrets of reprogramming with me, for being with me during my first steps, for your support*. Gracias **Antonio** y **Dani M.** por vuestro desenfado, por vuestros ánimos. **Cian**, *thanks for the chatting in tissue culture, for your calm attitude and your kindness*. **Tim**, *thanks for the talks and discussions, for taking care of me*. **Sandrina**, gracias por la serenidad que le aportabas a nuestro pasillo. Gracias **Gianluca** por tu disponibilidad y ayuda en el proyecto de RPL11, por ser tan majo y tan atento, ha sido un placer trabajar contigo! Gracias **Gema** por tu eficiencia, tu sintonía y por tu disponibilidad (es muy fácil trabajar contigo!). Gracias por cuidar de nuestros ratoncitos con tanto esmero.

Gracias al **Grupo de Telómeros y Telomerasa** por ser parte de nuestro grupo y dejarnos ser parte del suyo. Gracias **Ianire** por haber estado siempre ahí, aunque sean las dos de la mañana de un verano plagado de cucarachas. Gracias por estar aquí, porque tenerte cerca me hace olvidar que estoy lejos. Gracias porque sé que estarás allí, con nosotros, en un futuro. Gracias por poder contar siempre contigo, por compartir llantos y risas y por las charlas sin fin. Gracias **María G.** por tu bondad, por sacar siempre lo bueno de cualquier causa perdida, por tu admirable constancia en el labo. Gracias también por brindarnos tantos inolvidables y divertidos momentos (bien trabajado!). Gracias **Gina** por tu amistad, tus ánimos, tus charlas y tu candor. Gracias por ser tan profesional y hacer todo con tanto esmero. Gracias **Martina** por ser tan cariñosa y *of course*, gracias por tus tartas! Gracias **Nora**, por tu amistad, tu buena vibra y tu jovialidad. Gracias **Águeda** por ser tan pulcra trabajando, por preocuparte de nosotros. Gracias **Elisa**, mi compañera de desk, por tus charlas, tus consejos y tu alegría. Gracias **Isabel** por tus conversaciones y tu delicadeza trabajando. Gracias **Merche**, **Nani**, **Paula** y **Marinela**

por vuestro buen humor, vuestras divertidas historias y por preocuparos de mí. Gracias **Ralph**, mi otro compi de desk, por tu amistad y por el SOLA. Gracias **Fabian** por hacer del pasillo un sitio tan divertido, por tu alegría y tu ilusión. **Ben**, *thanks for your spontaneity, your joy and your support*. **Christian**, *thanks for your kindness and joy*. **Bruno**, *thanks for your calmness and your good sense of humour*. Gracias **Iole** por ser tan maja (*mucho ánimo con la tesis, tú puedes!*). **Rosa**! Gracias por ese buen rollo que transmites, por ser mega-eficiente y rigurosa en tu trabajo, por tus "*me meo, tía*" y gracias por toda tu ayuda con mis dudas murinas, eres genial!

Gracias a los miembros pasados de Supresión Tumoral y Telómeros con los que he coincidido. Gracias **Dani H.**, **Arantza**, **Susana V.**, **Manuel C.** (gracias por los contrapuntos), **Elsa** y **Gerdine**. Gracias **Luis Enrique** por brindarnos tantos extravagantes momentos tan divertidos (*Quién es Victoria Eugenia? Victoria Eugenia puso la primera piedra del CNIO*). Gracias a la nueva remesa de predocs y postdocs de ambos grupos (sois todos muy majos!), **Noelia**, **Raquel**, **Juanma**, **Aksinya**, **Miguel A.**, **Montero**, y **Kurt**.

Gracias a **Patri N.** y **Laia** (pero qué majas que sois!)**, Alba M.**, **Ana del R.** y **Silvia** (por las desesperaciones compartidas, por los ánimos y el buen rollo, sois un encanto!), **Eva**, **Laura**, **Direna** y **Bárbara** (por esas fugaces y alegres conversaciones), **Marta A.** (por tu alegría y por cuidar de mi *sis*), **Enara** (muchas gracias por tu ternura, tus ánimos y por tus consejos, por preocuparte de mí), **Ara**, **Nuria**, **Oli** y **Juanma F.** (gracias por vuestros ánimos!).

Gracias, y muy grandes, a las **Unidades del CNIO**, sin vuestra ayuda los resultados de esta tesis no hubieran sido posibles. Gracias **Sagrario** por toda tu ayuda con la generación del ratón, gracias **Carmen y Patri** por prepararnos los medios de las ES y iPS. Gracias **Orlando** por tus consejos y sugerencias con el RNAseq, gracias **Guada** y **Jorge** por encargaros de las muestras. Gracias **Gonzalo** por tu disposición con el análisis bioinfórmatico y responder con tanta amabilidad mis dudas. Gracias **Lola** por tus conocimientos, por la flexibilidad y por el aguante con esas citometrías interminables. Y además, gracias por ser tan maja y tan divertida, gracias por tu amistad. Gracias **Ultan, Miguel Ángel** y **Elena** por vuestra ayuda en el citómetro, por rescatar experimentos que dábamos por perdidos. Gracias **Diego** por tu tiempo, tus ánimos y por emocionarte con nuestras experimentos en el confocal, y especialmente gracias por toda tu ayuda en la elaboración del screening y el script del Definiens. Gracias **Manu y Ximo** por estar siempre dispuestos con una sonrisa de oreja a oreja, por vuestros consejos técnicos. Gracias **Alba** por tu ayudan con las histologías y tus explicaciones. Gracias **Patri, Virginia, María G., María U.** por hacer de la unidad de inmunohistoquímica sinónimo de eficiencia. Gracias **María L.** por ese tiempo tan preciado y tu tenacidad hasta que nos funcionaba el análisis. Gracias **Geno** por la puesta a punto de la librería de compuestos. Gracias **Manolo U.-C.** por tu ayuda con el segundo screening, los análisis bioinfórmaticos de los otros candidatos y por estar siempre dispuesto a ayudar. Gracias **Carmen B.-A.** y **Joaquín Pastor** por vuestra ayuda con el screening. Gracias **José A. Cámara** por las ecos, siento que no funcionara el proyecto. Gracias **Isabel** por hacer del animalario del CNIO algo de lo que estar muy orgullosos, por mantener el nivel de calidad tan alto, por preocuparte del bienestar de los animales por encima de cualquier cosa. Gracias al resto del equipo del animalario que se han preocupado de que todo esté bajo control en el mundo de las fieras.

Thanks to my Thesis Committee, **Oskar Fernández-Capetillo**, **Nabil Djouder** y **Jesús Paramio**, *for all your suggestions regarding the projects and support*.

Gracias **Paloma** y **Susa** por vuestra eficiencia, por hacer que el papeleo parezca hasta sencillo. En especial, gracias **Paloma** por todas las gestiones de la tesis.

Gracias a Cafetería, gracias **Enma** por acordarte siempre de nuestros cafés, por ser tan eficiente y maja. Gracias a Limpieza, gracias **Celeste** por estar siempre tan sonriente, por tus mini-charlas. Gracias a Mantenimiento, **Jesús, Paco, Emilio y Edu** por ser tan eficientes, por arreglarlo todo en un plis-plas. Un particular gracias a **Jesús** por sus ánimos a las mil en cultivos. Gracias a Seguridad, por atender las llamadas de una madre preocupada a las tantas de la noche. Gracias a Sistemas de la Información, **Alberto** con el PC y **Jorge** con el MAC, por salvarme de más de una crisis.

Y por último, gracias a **María Blasco** y a **Mariano Barbacid**, así como al resto de grupos del CNIO, porque, a pesar del poco "entusiasmo" de nuestros gobiernos por la ciencia, han conseguido hacer un centro puntero mundialmente.

He llegado a este punto en parte a todas esas personas que me ha transmitido una motivación infinita por la ciencia. Gracias a **Pepa Hazen**, **José "Stuart"**, **Paloma**, **Vero** y **Ana** por dejarme mirar a través del microscopio entre clase y clase, por hacerme sentir bienvenida en vuestro labo. Gracias a **Jesús Blázquez** y su labo (**Elena**, **Güelfo** y **Alex**), por ser los primeros en enseñarme los entresijos del laboratorio, por cuidarme. Gracias a **José Ramón Naranjo** y su labo (**Begoña**, **Judit**, **Paz**, **Marcos**, **Britt**, **Sofía**, **Tomasso** y **Clara**), en especial gracias a **Begoña** por enseñarme con paciencia y por alentarme a exponer mis ideas y a **Judit** por todas las cuantitativas que hemos compartido juntas. Gracias a **Enrique Samper** por haberse preocupado siempre de mí, por ampliar mis horizontes, por sus consejos, por ser mi mentor. Gracias al labo de Antonio Bernad por hacerme sentir muy a gusto en mis dos estancias con ellos. Gracias a **Susana Gonzalo** (para mí eres la jefa perfecta!) por tu dedicación a la ciencia, por tu ilusión desbordante, por tu análisis crítico y tus críticas constructivas. Además, gracias por haberme hecho sentir como una más de vuestra familia. Gracias al labo de Susana G. (**Nacho**, **Abena**, **Dave** y **Stephanie**) por estar siempre dispuestos a ayudarme y hacer de mi experiencia en St. Louis algo inolvidable.

No seríamos quiénes somos sin la impronta de nuestro pasado y sin "*When Conrad Waddington*"! Gracias **Alfonso**, **Pilar** y **Marta** por haber compartido esta aventura juntos. Gracias **Alfonso** por introducirme en el mundo del café, gracias por tantas risas y buenos momentos compartidos (y por los que quedan por venir!) y por estar siempre ahí, desde el principio y hasta el final, en las alegrías y en los momentos difíciles. Gracias **Pili** por ser única, por amar tanto la vida y sacar a relucir la belleza de las pequeñas cosas, por tu creatividad y tu delicadeza, por ser nuestro pilar. Gracias **Marta** por tu visión de la vida, tu alegría contagiosa, tus ganas de hacer cosas, tu tolerancia y empatía, por las noches del *Shock*. Os quiero mucho, chicos. Soy muy afortunada de teneros como amigos. Gracias al grupo de Bioquímica, **Alejo**, **Cris G.**, **Inés**, **Alex**, **Elisa**, **Bea**, **Jara**, **David**, **Jaime de Juan**, **Lara**, **Piñero**, **Irene**, por tanto buenos momentos, por hacerme sentir que no pasa el tiempo aunque no nos veamos en años. Gracias al grupo "prestado" del Máster, porque aunque no lo hice con vosotros me siento una más. Gracias **Dani**, **Edu**, **Jesús C.** y **Jaime R**.

Gracias a mi universidad, la **UAM**, por tener el elenco de profesores que tiene. Porque siempre han ido más allá del estándar establecido. Por ser un crisol de ideas. Gracias por no enseñarnos a "recitar", gracias por enseñarnos a "criticar constructivamente". Vosotros nos disteis las herramientas, ahora depende de nosotros convertir nuestros sueños en proyectos. Gracias a mi profe de

Biología del I.E.S. Laboral de Cáceres, por "saltarse" el libro y transmitirnos esa gran pasión por la ciencia.

And thanks to my Edinburgh friends and labmates for all your support and understanding (I'll be free soon!).

Gracias **Isa**, mi *sis*, por ser un ejemplo a seguir. Gracias por todo el amor y cariño que me das (te echo mucho de menos). Gracias por nuestras discusiones acerca de todo, por tus maravillosas argumentaciones, por no dejarte "llevar por la corriente". Gracias por mostrar esa entereza en tiempos "revueltos", por mantenerte firme y seguir luchando, por hacer siempre un trabajo tan bien hecho y tan perfecto. Estoy muy orgullosa de ser tu hermana. Y cómo no, gracias por tus divertidas historias. Gracias **Guille** por tu serenidad, por tus agradables conversaciones, por lo detallista y cuidadoso que eres, por el empeño que pones en que todo esté bien hecho.

Gracias a mis **padres**, y en especial a mi **mamá**, por quererme con locura y haber hecho tantos sacrificios para darme una educación y así hacerme una persona libre. Gracias por ser tan luchadora, te quiero mucho, mamá! Y gracias por tus noches en vela cuando me quedaba hasta tarde estudiando y tus cola-caos (*sólo una madre hace esto!*). Gracias a mis tíos **José Luis** y **Santos** por haberme querido tanto, por haber estado siempre tan orgullosos de mí, por llevarme en bici a los dos molinos y a ver los cabezudos. Gracias por todo vuestro amor (os echo mucho de menos). Y también gracias a mi abuela **Esperanza**, la mujer más buena y más guapa del mundo entero.

Gracias a **Marga**, **Antonio**, **Victor**, **Nines**, **Jesús**, **David**, **Ali y Rafa**, que ya llevan unos cuantos años siendo también mi familia. Muchas gracias por vuestro cariño infinito, por quererme como a una más y por preocuparos siempre por mí.

Gracias **Miguel**, por ser mi compañero de vida. Por darme tu amor incondicional sin esperar nada a cambio. Por poner el mundo entero a mis pies.

Gracias *Sigur Rós* y *GYBE!* por ser bálsamo para mi estrés durante la escritura de esta tesis.

Muchas gracias a todos! Me ha encantado compartir esta aventura con todos vosotros.

RESUMEN

La vía de estrés ribosomal se describió hace más de una década como una nueva vía activadora de p53. Dicha vía monitoriza la homeostasis de la biogénesis ribosomal. Perturbaciones en cualquiera de las etapas de la biosíntesis del ribosoma, transcripción del DNA ribosomal, procesamiento del RNA ribosomal, ensamblaje o transporte nuclear, conllevan un exceso de proteínas ribosomales no unidas al ribosoma. En este contexto, el complejo pre-ribosomal RPL11/RPL5/5S rRNA inhibe MDM2, activando así al supresor tumoral p53. La activación de p53 puede resultar en diferentes respuestas celulares que impiden que las células dañadas se conviertan en tumorales.

Una de las preguntas que hemos abordado en este trabajo es si las células madre pluripotentes de ratón, caracterizadas por altas tasas de división celular, presentan mecanismos que monitoricen la homeostasis de la biogénesis ribosomal para salvaguardar la integridad de la progenie. Aquí demostramos que dichas células tienen funcional la vía de estrés ribosomal y que esta vía activa p53 en respuesta al estrés ribosomal y elimina aquellas células dañadas mediante un proceso de apoptosis.

Las células tumorales requieren a una mayor producción de ribosomas para mantener las altas tasas de división celular que las caracterizan. En este trabajo hemos llevado a cabo un rastreo de compuestos que tengan como diana el nucléolo, la fábrica de ribosomas de la célula, con la finalidad de perturbar la producción de ribosomas y eliminar así las células cancerígenas. Hemos testado dos colecciones de compuestos químicos y hemos identificado un grupo de derivados de acridina que inhiben la transcripción del ADN ribosomal y, por tanto, generan la pérdida de la integridad del nucleolo. Esto resulta en la activación de p53 en ausencia de daño a través de la vía de estrés ribosomal. Finalmente, estos compuestos ralentizan el crecimiento celular y activan un proceso de apoptosis en distintas líneas de células tumorales.

RPL11, proteína clave en la vía de estrés ribosomal, se encuentra mutada en heterozigosis en pacientes de anemia de Diamond-Blackfan. Hemos generado un alelo nulo condicional para *Rpl11* y hemos demostrado que la pérdida de un alelo de *Rpl11* en ratones adultos recapitula las principales características de la enfermedad, incluyendo un procesamiento inadecuado del ARN ribosomal, anemia macrocítica debida a una maduración eritroide defectuosa y una mayor predisposición a cáncer. Los ratones haploinsuficientes para *Rpl11* muestran una linfomagénesis acelerada, lo que puede deberse a dos mecanismos no excluyentes: una vía de estrés ribosomal defectuosa y mayores niveles basales de la proto-oncoproteína c-MYC.

En resumen, nuestro trabajo pone de manifiesto la importancia de la vía de estrés ribosomal y, en particular de RPL11, en la fisiología, incluyendo células madre embrionarias y el organismo adulto, así como para el desarrollo del cancer y su terapia.

ABSTRACT

The ribosomal stress (RbS) pathway was described more than a decade ago as a new p53-activating pathway. This pathway monitors the homeostasis of the ribosome biogenesis. Perturbations in any of the steps comprising ribosome biosynthesis, rDNA transcription, rRNA processing and ribosome assembly and export, lead to the accumulation of ribosome-free ribosomal proteins. In this situation, RPL11/RPL5/5S rRNA pre-ribosomal complexes bind and inhibit MDM2, thus activating p53. Activation of p53 can result in different cellular outcomes that prevent damaged cells from becoming malignant.

We wanted to explore whether mouse pluripotent stem cells, characterized by a rapid growth rate, present mechanisms to monitor the homeostasis of ribosome biogenesis as a way to ensure an optimal quality of their progeny. We have demonstrated that mouse pluripotent stem cells rely on an operative ribosomal stress pathway to eliminate damaged cells upon RbS. Importantly, p53 plays a key role in this process by eliciting apoptsis in embryonic stem cells following RbS.

Cancer cells require high rates of ribosome biogenesis to sustain their rapid growth. To target this Achilles' heel of cancer cells we have designed a cellular screen that monitors the integrity of the nucleolus, the ribosome factory, to identify small molecule compounds that disrupt ribosome biogenesis. By performing chemical library screens, we have identified a group of acridine derivatives that inhibits rDNA transcription, and thus cause nucleolar disruption. This results in p53 activation through the RbS pathway, and in the absence of detectable DNA damage. Remarkably, these compounds hamper proliferation and trigger apoptosis of different cancer cell lines, providing new therapeutical opportunities against cancer.

Heterozygous mutations of *RPL11*, a key player in the RbS pathway, have been found in Diamond-Blackfan Anaemia (DBA) patients. To that end, we generated a conditional knockout mouse model for *Rpl11*. Here we demonstrate that partial loss of *Rpl11* recapitulates the main pathologies of DBA, including impaired rRNA processing, macrocytic anaemia and cancer predisposition. *Rpl11* haploinsufficient mice have reduced number of erythroid progenitors and delayed erythroid differentiation. These animals show accelerated lymphomagenesis, probably due to two non-exclusive mechanisms: defective activation of p53 through the RbS pathway and increased basal levels of c-MYC.

In summary, our work provide insights into the biological relevance of the RbS pathway and, in particular of RPL11, in the physiology, including mouse pluripotent stem cells and the adult organism, as well as in cancer development and possible treatments.

ABBREVIATIONS

ActD	Actinomycin D
ADN	Ácido deoxirribonucleico
ARN	Ácido ribonucleico
DBA	Diamond-Blackfan Anaemia
DDR	DNA Damage Response
DNA	Deoxyrribonucleic Acid
DSB	Double Strand Break
E	Embryonic day
HSCs	Hematopoietic Stem Cells
iPSCs	Induced Pluripotent Stem Cells
MDM2	Mouse Double Minute 2
MDS	Myelodysplastic Syndrome
MEF	Mouse Embryonic Fibroblast
mESCs	Mouse Embryonic Stem Cells
Pol	Polymerase
RbS	Ribosomal Stress
RS	Replicative Stress
RNA	Ribonucleic Acid
RP	Ribosomal Protein
RPL	Ribosomal Protein (Large subunit)
RPS	Ribosomal Protein (Small subunit)
rRNA	Ribosomal RNA
TCS	Treacher Collins Syndrome

INDEX

INTRODUCTION

1. THE TUMOUR SUPPRESSOR P53

In 1979 four different groups described by the first time the p53 protein as a tumour antigen (DeLeo et al., 1979; Kress et al., 1979; Lane and Crawford, 1979; Linzer and Levine, 1979). Levels of p53 were shown to be very high in transformed cells and forming a complex with distinct oncoviral proteins (Lane and Crawford, 1979; Sarnow et al., 1982; Scheffner et al., 1990). In addition, many of the isolated p53 cDNA clones were able to transform cells in combination with the Ras oncogene (Eliyahu et al., 1984; Jenkins et al., 1984; Parada et al., 1984). Based on these findings, p53 was considered at that time as an oncogene. Ten years later it was verified that those transforming p53 cDNA clones carried a mutation (Finlay et al., 1989; Hinds et al., 1989). Moreover, their transformation potential in combination with Ras was abolished when wt p53 cDNA was expressed at the same time (Finlay et al., 1989). These unexpected results led to the credence that, contrary to what was previously stated, p53 acts as a tumour suppressor. The tumour suppressor function of p53 was firmly established when (Baker et al., 1989) found p53 mutated in one allele and lost in the second allele in two human colon cancers. Supporting this, somatic p53 mutations or deletions are reported in around 50% of human sporadic cancers, while the remaining percentage presents alterations in its signalling pathways (Vogelstein et al., 2000). Mice with genetic deletion of p53 develop spontaneous tumours with 100% penetrance (Donehower et al., 1992; Jacks et al., 1994). Moreover, families with germline mutations in the *TP53* gene, Li-Fraumeni syndrome and Li-Fraumeni-like syndrome, are more susceptible to cancer (McBride et al., 2014). Correspondingly, restoration of wild type p53 function in animal models can induce tumour regression and significantly extend survival (Martins et al., 2006; Ventura et al., 2007; Xue et al., 2007). In support of this, mice carrying additional extra copies of p53, under its own promoter, show high resistance to spontaneous and chemically-induced tumours (Garcia-Cao, 2002). These genetic models have revealed the crucial role of p53 in suppressing tumourigenesis

1.1. Tumour suppressive function of p53 – transcriptional activity

p53 prevents genetically compromised cells from becoming malignant by eliciting different cellular responses that execute through its activity as a transcription factor. The p53 transcriptional program is regulated in a stress-specific manner (Beckerman and Prives, 2010), whereby distinct subsets of p53 target genes are induced in response to different p53-activating agents, including oncogene activation, chronic DNA damage, oxidative stress, nutrient deprivation, hypoxia, telomere erosion or ribosome biogenesis dysfunction. How p53 is able to discriminate between different loci in response to a particular stress is the subject of intense research and it is thought that specific patterns of p53 post-translation modifications trigger individual transcriptional programs that lead to different cellular outcomes (Beckerman and Prives, 2010; Bieging et al., 2014).

The sequence analysis of the p53 protein revealed two N-terminal transcriptional activation domains (TAD), a large DNA binding domain (DBD), a tetramerization domain (4D) and a basic C-terminal domain (CTD) (Toledo and Wahl, 2006). The DNA binding domain directs the p53 tetramer to p53-responsive elements (p53 RE), located in specific RNA pol II-transcribed gene promoters. Once p53 is bound to the p53 RE, it recruits, through its transactivation domain, both general and specific transcriptional co-regulators whose depending on their nature, co-activator or co-repressor, can activate or inhibit expression of different p53 target genes, respectively (Laptenko and Prives, 2006). Special attention has been placed in the DNA binding domain since most mutations in p53 in human cancers occurs in this region (Olivier et al., 2010). For instance, mutations in the arginine 175 (R175H) or arginine 273 (R273H), both within the DNA binding domain, are hot spot mutations in human cancers (Joerger and Fersht, 2007). This suggests that the transcription factor activity of p53 is crucial for tumour suppression.

Cell cycle arrest, senescence and apoptosis have been extensively accepted as the major mechanisms by which p53 suppresses cancer onset and development. However, these p53-mediated responses have been mainly evaluated in response to acute DNA damage, which in addition of being a non-physiological stimulus is irrelevant for p53-mediated tumour suppression (Christophorou et al., 2006; Efeyan et al., 2006; Hinkal et al., 2009). Engineered mouse models in which p53 function can be restored in a time controllable manner have revealed that cell cycle arrest, senescence and apoptosis are likely to result in tumour suppression depending on the cell type context (Bieging et al., 2014; Ventura et al., 2007). However, no single or compound knockout mouse model for p53 target genes involved in these cellular responses has recapitulated the dramatic tumour predisposition that characterizes p53-null mice. This suggests that p53 executes its tumour suppressive function by additional mechanisms. In agreement, it has been shown recently that cell cycle arrest, senescence and apoptosis may be dispensable for tumour suppression and that other important cancer-relevant p53 activities such as metabolic regulation or antioxidant function migth be required to limit tumorigenesis (Bieging et al., 2014; Li et al., 2012b; Valente et al., 2013).

1.2. Regulation of p53. p53-MDM2: the negative regulatory feedback loop

The half-life of p53 is extremely short in unstressed cells, being about 30 min, but it is extended to longer times, about 24 hours, in SV-40 transformed fibroblasts (Oren et al., 1981). This fact led researchers to hypothesize the existence of post-translational mechanisms controlling p53 stability and in the early 90's they discovered the main regulator of p53 stability, namely, the proto-oncoprotein MDM2 (murine double minutes-2) (Momand et al., 1992). *Mdm2*-null mice die around implantation (Jones et al., 1995; Montes de Oca Luna et al., 1995) because of unrestrained p53-

dependent apoptosis (de Rozieres et al., 2000). The embryonic lethality of *Mdm2*-null mice is overcome in the absence of p53 (Jones et al., 1995; Montes de Oca Luna et al., 1995) highlighting the negative regulation of MDM2 on p53 function *in vivo*, and specially during the extremely proliferative gastrulation stage (Snow, 1977). *Mmd2* haploinsufficient mice are more resistant to tumour formation in an oncogenic context due to high p53 activity (Alt et al., 2003; Mendrysa et al., 2006). On the contrary, transgenic mice overexpressing *Mdm2* develop carcinoma (Lundgren et al., 1997) and lymphomas or sarcomas (Jones et al., 1998) and the onset of tumorigenesis is not accelerated when these mice are crossed with p53-null animals. In addition, the *Mdm2* gene is amplified in many human cancers, especially frequent in osteosarcomas and soft tissue sarcomas (Wade et al., 2013). All these reports provide additional evidence for the role of MDM2 in mediating p53 inhibition.

MDM2 and p53 form an autoregulatory feedback loop. P53 stimulates the transcriptional expression of MDM2 (Barak et al., 1993; Perry et al., 1993; Wade et al., 2013), which in turn negatively regulates p53. MDM2 maintains levels of p53 low in unstressed cells by regulating three different aspects: function, stability and subcellular localization of p53. MDM2 binds to the N-terminal p53 transactivation domain, thus impairing p53 transcriptional activity (Kussie et al., 1996). In addition, MDM2 promotes ubiquitylation and proteasome-mediated degradation of p53 (Haupt et al., 1997; Honda et al., 1997; Kubbutat et al., 1997). MDM2 contains a C2H2C4 RING (*r*eally *i*nteresting *n*ew *g*ene) domain with intrinsic E3 ubiquitin ligase activity that promotes the transfer of ubiquitin molecules from an E2 conjugating enzyme to a cluster of lysine residues within the C-terminus of p53 (Lohrum et al., 2001; Rodriguez et al., 2000). Low levels of MDM2 activity induce monoubiquitylation and nuclear export of p53, controlling in this manner p53 subcellular localization, while high levels of MDM2 activity promote p53 polyubiquitylation and nuclear degradation (Li et al., 2003). The phenotype of mice bearing a homozygous MDM2 mutation (C462A) that abolishes the E3 ubiquitin ligase activity without affecting p53-binding (Itahana et al., 2007) resembles *Mdm2*-null mice. This strongly support p53 degradation rather than impairment of its transcriptional activity as the primarily source of MDM2 regulation on p53 function. Furthermore, MDM2 can also negatively regulate p53 transcription activity by catalysing the transfer of the NEDD8 ubiquitin-like molecule (Xirodimas et al., 2004). Besides MDM2, there are several ubiquitin ligases involved in p53-mediated proteosomal degradation and nuclear export, such as Pirh2, COP1 or Ubc13 (Lee and Gu, 2010), although their biological relevance remains to be addressed in genetic models. Likewise, additional proteins mediating p53 NEDDylation and SUMOylation, such as FBX011 and the family of PIAS ligases, respectively, have been described to modulate p53 protein stability (Horn and Vousden, 2007).

Stabilization of p53 is crucial for its tumour suppressor function in response to various types of stress and can be achieved through 1) direct p53 deubiquitylation by ubiquitin-specific proteases, such as HAUSP or USP10 (Li et al., 2002; Yuan et al., 2010), 2) abrogation of MDM2-mediated

ubiquitin ligase activity and, so far the most studied mechanism, 3) inhibition of MDM2-p53 interaction. A simplified graph of the p53-activating pathways is depicted below (**Figure 1**).

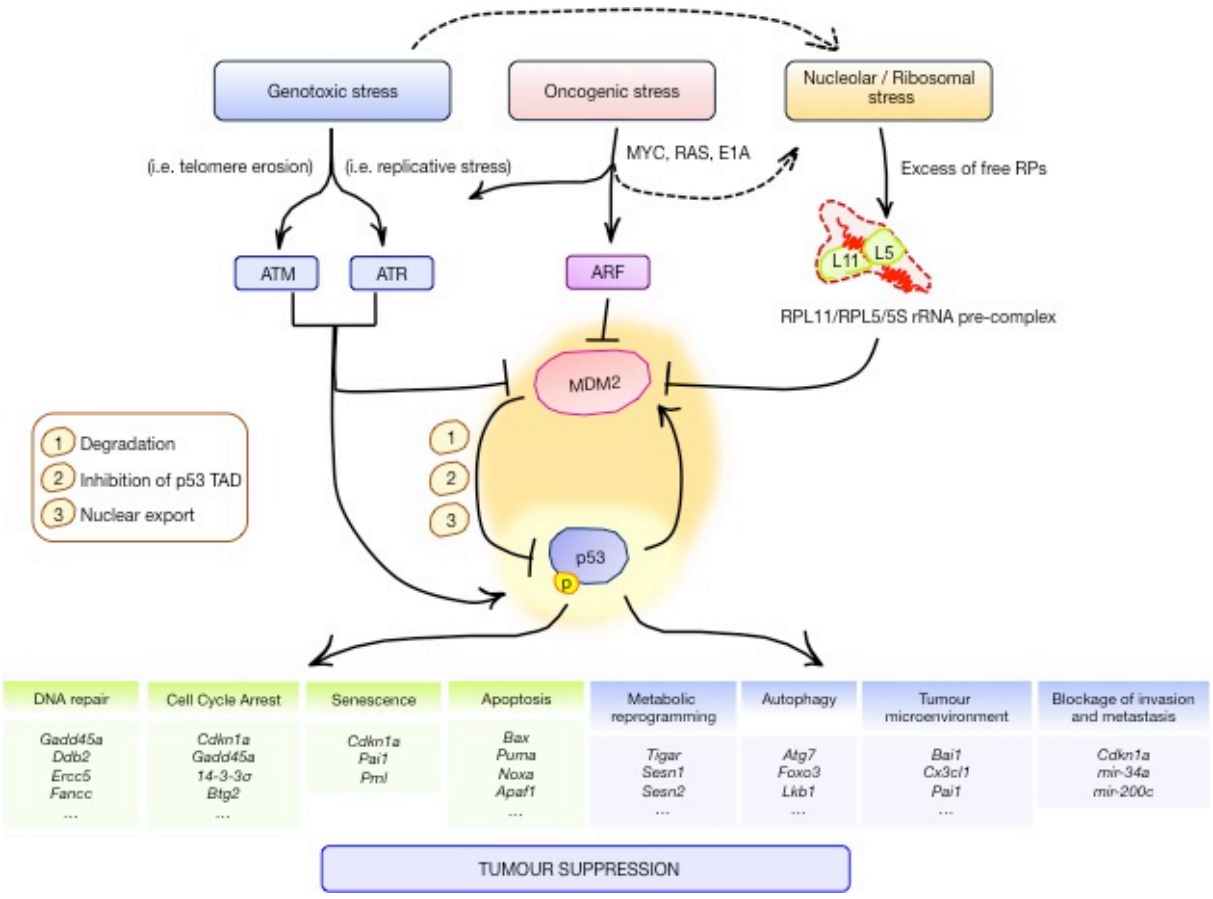

Figure 1. p53-activating pathways.
Insults and mediators triggering activation of p53 are depicted in the figure. Note that MDM2 is central to all pathways, denoting its important function in the regulation of p53. At the bottom part, p53 target genes involved in the different celular outcomes. Coloured in green are highligthed the classical p53-mediated responses while in blue are represented emerging cellular outcomes driven by p53 and relevant for tumour suppression.

1.2.1. Disruption of the MDM2-p53 interaction: MDM2 post-translational modifications and binding of basic proteins (ARF and RPs)

Impairment of MDM2-mediated ubiquitylation activity can be accomplished following genotoxic stress by MDM2 post-translational modifications (PMTs) that affect its stability and E3 ligase processivity (Cheng et al., 2009; Wade et al., 2013). Additionally, MDM2 transcripts levels can be downregulated by p53-mediated expression of a set of miRNAs (miR-*192*, *194*, and *215*) thus indirectly contributing to p53 stabilization (Pichiorri et al., 2010). Although MDM2 post-translational modifications have been shown to be involved in rapid p53 stabilization upon DNA damage, the p53 response can only be executed if its interaction with its inhibitor MDM2 is abolished. A group of basic

proteins that binds to the acidic domain of MDM2 in response to mitogenic or ribosomal stress disrupt MDM2-p53 interaction and impair MDM2-mediated p53 ubiquitylation and nuclear export. The central acidic domain of MDM2 is critical for efficient p53 ubiquitylation (Kawai et al., 2003; Meulmeester et al., 2003) so interfering with it results in cancellation of the MDM2 E3 ubiquitin ligase activity and subsequent p53 activation.

The tumour suppressor $p19^{Arf}$ ($p14^{Arf}$ in humans; ARF thereafter) is among these basic proteins and binds MDM2 (Kamijo et al., 1997; Pomerantz et al., 1998; Zhang et al., 1998) in the presence of oncogenic stress, such as aberrant expression of E2F1, c-MYC, RAS and the viral oncoprotein E1A (Bates et al., 1998; Palmero et al., 1998; Sherr, 1998; De Stanchina et al., 1998; Zindy et al., 1998). ARF null mice are prone to cancer to a similar extent as p53 knockout mice (Kamijo et al., 1997), highlighting the tumour suppressor role of ARF by inhibiting MDM2. However, ARF null animals retain p53 activation in response to DNA damage or pRb inactivation which indicates the existence of complementary p53-activating pathways (Kamijo et al., 1999; Tolbert et al., 2002).

In the presence of oncogenic c-MYC or ribosomal stress (explained in more detail in following sections), ribosomal proteins RPL11 and RPL5 bind to the MDM2 acidic domain without overlapping ARF binding (Lindström et al., 2007; Macias et al., 2010), forming a quaternary complex with p53 (Zhang et al., 2003). Mice with a mutation in MDM2 (C305F) that selectively disrupts RPL11/RPL5 binding exhibit accelerated lymphomagenesis in an Eμ-MYC background (Macias et al., 2010), highlighting the importance of the MDM2-p53 interaction also in response to ribosomal stress.

1.2.2. Disruption of the MDM2-p53 interaction: p53 post-translational modifications.

More than 36 residues can undergo post-translational modifications in p53, including phosphorylation, acetylation, ubiquitylation, methylation, sumoylation and neddylation, modulate p53 function. They are involved in controlling 1) p53 stabilization, 2) DNA binding, and 3) transcriptional activation in response to oncogene expression or DNA damage, among other stresses. Post-transcriptional modifications controlling stability and activation are usually circumscribed to the p53 transactivation domain and C-terminus domain (TAD and CTD). Ubiquitylation in the CTD largely contributes to the regulation of p53 stability, as above discussed, while stress-induced phosphorylation of serines in the TAD of p53 attenuates MDM2-p53 interaction, thus prolonging p53 half-life. p53 phosphorylation occurs very rapidly within the first 30 minutes following different stimuli, most notably DNA damage, and can be catalysed by a broad range of kinases, including ATM/ATR/DNA-PK, CHK1/CHK2, CK2 or JNK (Loughery and Meek, 2013). Experiments *in vitro* have shown that

phosphorylation of certain p53 residues in response to DNA damage disrupts MDM2-p53 association, thus stabilizing p53, and is crucial for promoting binding of co-regulators (Loughery and Meek, 2013). Finally, acetylation levels of p53 significantly increase in response to stress and correlate well with p53 activation and stabilization. Moreover, acetylation of lysine residues in the C-terminus of p53 is required for p53 transcriptional activities in a cell type-dependent context (Feng et al., 2005; Tang et al., 2008) and p53 deacetylation by SIRT1 and HDAC1 impairs its stability and transcriptional activation (Brooks and Gu, 2011). Interestingly, acetylation of p53 occurs in the same lysines targeted for MDM2-mediated ubiquitylation so it is considered to prevent p53 degradation.

Although p53 post-translational modifications have been shown to be necessary for p53 activation *in vitro*, genetic studies in mice claim that they play a subtle role in the stress-induced tumour suppressive function of p53 *in vivo*. Mutant mice for all major targeted residues of serines in the TAD and lysines in the CTD show modest phenotypes and do not prevent p53 activation upon genotoxic stress (Bieging et al., 2014; Toledo and Wahl, 2006). This suggests that p53 can still be stabilized, by means of other mechanisms, in the absence of post-translational modifications.

1.2.3. Chemical disruption of the MDM2-p53 interaction: Reactivation of p53 in tumours with wild-type p53

Half percent of human cancers bear mutations or deletions in the *p53* gene while the other half percent present alterations in p53-activating pathways. One of the mechanisms preventing activation of p53 is overexpression of MDM2 and MDM4. The *Mdm2* gene is found amplified in many human cancers, being amplification of *Mdm2* especially frequent in osteosarcomas and soft tissue sarcomas (Oliner et al., 1992; Wade et al., 2013). Numerous attempts have been made to develop small molecules that target and block the MDM2-p53 interaction to reactivate p53 levels in p53-proficient cancers. The key of the interaction between MDM2 and p53 relies in just three lipophylic residues of p53, required for p53 transactivation, that fit deeply into the hydrophobic pocket of the MDM2 N-terminal domain (Kussie et al., 1996). Fortunately, the size of the MDM2 cleft can be fully occupied by small molecules that mimic this interaction. Three groups of chemical compounds, nutlins, benzodiazepines and spirooxindole-containing molecules, have been successfully used *in vitro* to restore p53 function in human cancer cells and xenograft models with minimal side effects (Brown et al., 2009; Wade et al., 2013; Zhao et al., 2013). Importantly, several of these compounds have been advanced into phase I clinical trials for treating multiple human cancers (Ray-Coquard et al., 2012; Zhao et al., 2013), such as two nutlin derivatives, RG-7112 and RO5503781 (ROCHE), the spirooxindole analog SAR405848 (Sanofi) or the dihydroisoquinolinone derivative CGM097 (Novartis). RITA is another effective compound that blocks MDM2-p53 interaction by direct binding to p53 and induces apoptosis more efficiently than nutlins, although its mechanism of action needs

further clarification (Brown et al., 2009). Although the main efforts have been made in chemically disrupting p53-MDM2 interaction, the ubiquitin ligase activity of MDM2 has also been targeted although with less success. This is the case of the HLI98 inhibitor, which activates p53-dependent apoptosis in cancer cells but with low potency and selectivity (Wade et al., 2013).

Additional cell-based screens have identified chemical compounds that activate p53 by indirectly promoting MDM2 inhibition and reduce tumour growth in cancer cell lines and xenografts. This is the case, for instance, of tenovins that inhibit the p53 deacetylase SIRT1, tubulin inhibitors (taxol and vinca alkaloids), or compounds that inhibit rRNA synthesis (actinomycin D, mycophenolic acid or 5-fluorouracil). This last set of compounds cause nucleolar disruption and the release of ribosome-free RPL11 and RPL5 that bind and inactivate MDM2 (Sun et al., 2008, 2007; Zhang et al., 2003).

1.3. p53 and stem cells

Mouse embryonic stem cells (mESCs) possess unlimited self-renewal capacity with the potential to differentiate into all cell lineages in the body, including germ cells (Young, 2011). Both self-renewal and pluripotentcy are maintained by the coordinated action of a core of transcription factors, such as Oct4, Sox2 and Nanog (Mitsui et al., 2003; Nichols et al., 1998). Among other features, mESCs are characterized by extremely high rates of proliferation with an average generation time of 8-10 hours (Orford and Scadden, 2008; White and Dalton, 2005). Rapid cell divisions are achieved by means of their particular cell cycle structure. In contrast to somatic or adult stem cells, mESCs do not undergo quiescence or present gap phases so they dedicate the majority of the time (around 60%) to alternate between replication and mitosis. mESCs present a very short G1 period that lacks the restriction (R-) point control (White and Dalton, 2005). This is possible by elevated levels of Cdk activity that maintain RB phosphorylated and absence of Ink4a and Cip/Kip cyclin-dependent kinases inhibitors such p16, p21 and p27 (Orford and Scadden, 2008; Sage, 2012; White and Dalton, 2005). Furthermore, Cdc25A, required for progression from G1 to S phase, cannot be inactivated by CHK2 kinase in response to ionizing radiation (Hong and Stambrook, 2004). The inability of mESCs to undergo G1/S cell cycle arrest or senescence in response to genotoxic insults would make them especially susceptible to accumulate large mutational burdens, which might result in teratogenesis during embryo development. However, mESCs present a lower frequency of spontaneous mutations (10^{-6}) than differentiated cells (10^{-4}) (Cervantes et al., 2002). This might be due to the fact that mESCs can be halted at G2/M (Chuykin et al., 2008), are hypersensitive to DNA damage and readily undergo either apoptosis or differentiation to eliminate damaged cells from the pool (Giachino et al., 2013; Heyer et al., 2000; Hong and Stambrook, 2004). The exact mechanisms by which mESCs insure that

intact genomes are transferred to identical daughter cells have been of interest during many years. Special interest has been placed on the tumour suppressor p53 although its role in the maintenance of genomic stability in mESCs remains controversial as explained below.

P53 constitutes a barrier for reprogramming of differentiated cells to induced pluripotent stem cells (iPSCs) (Hong et al., 2009; Kawamura et al., 2010; Li et al., 2009; Marion et al., 2009; Utikal et al., 2009). mESCs present abundant amounts of cytoplasmic p53 that remains inactive as a transcription factor (Aladjem et al., 1998; Sabapathy et al., 1997a; Solozobova et al., 2009). Unlike differentiated cells, mESCs cannot activate p53 through ARF-mediated inhibition of MDM2 since the locus comprising ARF, *Ink4/Arf* locus, is epigenetically silenced in mESCs and iPSCs (Li et al., 2009). In addition, several studies have reported the absence of a p53-dependent G1/S checkpoint or apoptosis following ionizing radiation of mESCs (Aladjem et al., 1998; Chao et al., 2000a; Chuykin et al., 2008; Corbet et al., 1999; Hong and Stambrook, 2004; Solozobova et al., 2009). All these facts together could lead us to consider that p53 is dispensable for maintenance of genomic integrity and pluripotency features in mESCs. Lack of p53 does not affect self-renewal of mESCs, however, it causes developmental abnormalities and accelerated appearance of tumours (Donehower et al., 1992; Jacks et al., 1994), suggesting an important role for p53 during embryo development. Contrary to what stated above that p53 is not required for keeping stem cells in check following DNA damage, p53 can be functional depending on the nature of the genotoxic insult. In this manner, p53 can be translocated to the nucleus (Han et al., 2008; Solozobova et al., 2009), mainly in response to UV radiation (Corbet et al., 1999; Sabapathy et al., 1997b) and oxidative stress (Han et al., 2008). UV and oxidative stress and the radiomimetic compound doxorubicin elicit p53-dependent apoptosis or differentiation in mESCs, respectively (Chao et al., 2000b; Corbet et al., 1999; Han et al., 2008; Li et al., 2012a; Sabapathy et al., 1997a). mESCs differentiation results from p53-mediated repression of the pluripotency factor NANOG (Lin et al., 2005) and other stemness master regulators (Li et al., 2012a). Additionally, studies through early gastrulation (E6.5 to E7.5) show that low dose of radiation (<0.5 Gy) cause a ATM- and p53-dependent apoptosis (Heyer et al., 2000). A summary table of p53 responses in mESCs is shown below (**Table 1**).

Highly proliferating mESCs need to increase ribosome biogenesis rate in order to meet the elevated energetic demands. Consistent with this, ribosomal proteins are more abundantly expressed in mESCs compared to differentiated cells (Kondrashov et al., 2011), and, interestingly, a decrease in rDNA transcription is associated to differentiation in certain type of cells (Larson et al., 1993). In somatic cells, proliferative signals, such as serum stimulation or activation of the MAPK signalling pathway, result in elevated rDNA transcription to support cell growth and replication (Drygin et al., 2010). In addition, ribosome biogenesis and cell cycle are tightly coupled processes, being levels of rRNA synthesis increased during S and G2 phases, when cells demand newly synthesized proteins to

progress into mitosis (Drygin et al., 2010). Data from hepatectomized mice deficient for the 40S ribosomal protein S6 (RPS6) have revealed that normal protein synthesis but ribosome dysfunction prevents re-entry in the cell cycle (Volarevic et al., 2000), indicating that both ribosome biogenesis and cell cycle are coupled. Somatic cells count on the p53-activating ribosomal stress pathway (explained in following sections), to safeguard homeostasis of ribosome biogenesis and ensure intact genetic transmission to daughter cells. But, do mESCs also count on the p53-activating ribosomal stress pathway? Due to the controversial role of p53 in mESCs, this question is fundamental to us in order to better understand the mechanisms that mESCs use to preserve the pool of "bona fide" stem cells.

Table 1. Summary of the p53 responses in mESCs following different stresses.

DNA damage type	Activation of p53	Cellular outcome	References
Non-ionizing radiation			
UV radiation	Nuclear translocation	N/A	(Solozobova et al., 2009)
	Yes (phospho-S315)	Differentiation	(Lin et al., 2005)
	Yes	Apoptosis	(Corbet et al., 1999)
	Yes	Apoptosis	(Sabapathy et al., 1997a)
	Yes	Apoptosis	(Chao et al., 2000b)
Ionizing radiation			
γ-irradiation	Transient stabilization	Reduced clonogenic survival	(Corbet et al., 1999)
	Transient stabilization	N/A	(Solozobova et al., 2009)
	Transient stabilization	N/A	(Chao et al., 2000a)
	Stabilization + phosphoS23	Absence of G1 arrest	(Hong and Stambrook, 2004)
	No	Apoptosis	(Aladjem et al., 1998)
	No	Absence of G1 arrest	(Chuykin et al., 2008)
	Yes	Apoptosis (E6.5)	(Heyer et al., 2000)
Other stresses			
rNTP depletion	No	Apoptosis	(Aladjem et al., 1998)
Doxorubicin	No	Apoptosis	(Aladjem et al., 1998)
	Yes	Differentiation	(Li et al., 2012a)
Oxidative stress	Mitochondrial translocation	Apoptosis	(Han et al., 2008)

2. RIBOSOME BIOGENESIS

Ribosome biogenesis is one of the most demanding energetic processes of a proliferating cell. In a yeast cell, approximately 40 nascent ribosomes per second are exported from the nucleolus, the major site of ribosome biogenesis, into the cytoplasm. Per generation, a cell produces 1-2 millions of ribosomes (Warner, 1999). Ribosome biogenesis consumes up to the 80% of the energy of a

eukaryotic cell (Schmidt, 1999) and requires a complete synchronization of all three RNA polymerases. RNA polymerase I (RNA pol I) transcribes the clusters of rDNA genes, repeated in tandem, generating long primary transcripts (47S) that will be afterwards processed into mature 28S, 18S and 5.8S rRNAs. RNA polymerase III (RNA pol III) is in charge of transcribing the fourth rRNA specie (5S) that integrates the ribosome, as well as small nuclear RNAs (snRNAs) that participate in rRNA processing and transfer RNA (tRNA) that are required for protein synthesis. Simultaneously, RNA polymerase II (RNA pol II) transcribes the r-proteins or ribosomal proteins (RPs) as well as other factors that participate in the maturation of the primary rRNA, assembly and exporting of the ribosomal subunits. Ribosomes are made of equimolar amounts of the four rRNA species (28S, 18S, 5.8S and 5S rRNA) and more than 70 RPs. 18S rRNA along with 30 r-proteins makes the small ribosomal subunit (40S) while the 28S, 5.8S and 5S rRNA together with 45 r-proteins compose the large ribosomal subunit (60S).

Ribosome biogenesis comprises three different steps: 1) rDNA transcription, 2) rRNA processing and 3) ribosome subunits assembly and export. All these three steps, except nuclear transport, are carried out in the nucleolus. In mammalian cells, the synthesis of ribosomes is tightly regulated to cell cycle progression. rDNA transcription is absent during mitosis, where nucleoli are disassembled (Dousset et al., 2000), and gradually increases during G1, peaking S and G2 phases (Russell and Zomerdijk, 2005). The length of the cell cycle mainly depends on the time employed by the cell to pass through the G1 phase. During G1 phase cells need to surpass the restriction point (-R point) to proceed into DNA replication and they need to grow sufficiently in order to do so. Consequently, an accelerated or delayed G1/S phase progression results from accelerated or delayed achievement of an appropriate ribosome production during G1 (Derenzini et al., 2005). Nucleolar size increases between G1 and G2 phases (Russell and Zomerdijk, 2005) and, accordingly, proliferating cells display larger nucleoli than the corresponding resting cells (Derenzini et al., 2009). Increase in nucleolar size is mainly due to elevated rates of rDNA transcription, positively regulated by mitogens, nutrient availability and growth factors, through a complex signalling network that integrates the mammalian target of rapamycin (mTOR), phosphatidyl inositol-3 kinase (PI3K) and mitogen-activated protein kinase (MAPK) signalling pathways (James and Zomerdijk, 2004; Zhong et al., 2004).

2.1. The Nucleolus

The nucleolus is “an organelle formed by the act of building a ribosome” (Mélèse and Xue, 1995). Thus, nucleoli are the ribosome factories of the cell. Unlike cytoplasmic organelles, such as the Golgi apparatus or the mitochondria, nucleoli are not enveloped by a membrane. Thus, nucleoli are

not isolated inside the nucleus, although they are very distinct from the surrounding nuclear material, being about twice as dense and roughly 100,000 times more viscous than the nucleoplasm (Brangwynne et al., 2011). The particular density of the nucleolus is due to the multiple interactions of macromolecular complexes (more than 4,000 proteins) that msotly participate in ribosome biogenesis (Ahmad et al., 2009). The high density and great refractive index allow the nucleolus to be easily visualized by phase contrast microscopy and electron microscopy.

Nucleoli assemble around specific genetic loci, called nucleolar organizer regions (NORs), firstly described by B. McClintock (1934) in plant cells. NORs comprise tandemly repeated clusters of rDNA genes located in different chromosomes in mammals and with number variation across species (Goodpasture and Bloom, 1975). In humans, each NOR contain around 40 repeats consisting of 18S, 5.8S and 28S rRNA coding sequences, transcribed internal and external spacers (ITS and ETS), a non-transcribed intergenic spacer, an origin of replication, transcriptional terminators and a replication fork barrier that prevents collisions between replication and transcription (Fatica and Tollervey, 2002; Labib and Hodgson, 2007). Only 50% of the approximately 400 rDNA repeats in the human diploid genome are transcriptionally active. Counter-intuitively, when cells need higher rDNA transcription rates for growth they increase the efficiency of transcription from active rDNA repeats instead of activating those transcriptionally "silent" repeats (McStay and Grummt, 2008). The number, size and position of nucleoli depend on the cellular metabolic activity.

The nucleolus carries out three different steps during the synthesis of ribosomes:

1. rDNA transcription. Transcription of rDNA requires the recruitment and assembly of the preinitiation complex (PIC) during G1 phase to the rDNA core promoter. This complex is comprised by the RNA pol I and, in mammals, at least 3 other basal factors: the transcription initiation factor I A (TIF-IA), the selectivity factor complex (SL1 in humans, TIF-IB in mouse), and the upstream binding factor (UBF). UBF bends the DNA and bring into close proximity the core promoter and the upstream control element, as well as recruits RNA pol I to rDNA promoter and stabilizes TIF-IA and SL1 binding (Grummt, 2003). TIF-1A, SL1, and UBF are essential for transcription by RNA Pol I and are modulated by different signalling pathways in response to changes in environmental conditions. For example, in response to nutrients availability mTOR promotes pre-rRNA synthesis by regulating the localization and/or activity of TIF-1A, SL1, and UBF, as well as translation of RPs (Mayer and Grummt, 2006).

2. rRNA processing. rRNA is firstly transcribed as an immature precursor (47S) species that needs to be modified (pseudourylation and methylation) for further processed into 18S, 28S and 5.8S by endo- and exonucleolytic cleavages. Maturation of rRNA and assembly of pre-ribosomal units

occur in the nucleolus before export. More than 700 non-ribosomal factors, conserved from yeast to humans, participate in this complex process (Couté et al., 2006). These factors include small nucleolar ribonucleoproteins (snoRNPs) and numerous non-ribosomal proteins that process or modify the pre-RNAs (i.e. endo- and exonucleases, pseudouridine synthases or methyltransferases), mediate RNP folding/remodelling (RNA helicases, RNA chaperones) or facilitate protein association/dissociation (GTPases, AAA-ATPases) (Zemp and Kutay, 2007).

3. Ribosome assembly and nuclear transport. RPs, similar to the rest of RNA pol II-transcribed genes, are translated in the cytoplasm. For assembly, newly synthesized RPs must be firstly imported into the nucleus. Nuclear import of RPs is controlled, among others, by importin β, transportin, RanBP5 and RanBP7 (also known as importin 7, IPO7) (Jäkel and Gürlich, 1998). The mTOR kinase activity has been recently described to be essential in nuclear import of RPs (Kazyken et al., 2014). Once inside the nucleus, RPs accumulate in the nucleolus, bind to rRNA precursors and participates in their processing while they assembly together (Kressler et al., 2010). 60S and 40S pre-ribosomal subunits need to be exported to the cytoplasm for final maturation before achieving translational competence. Both subunits interact with the nuclear export receptor exportin 1 (XPO1) and are exported as independent entities through the nuclear pore complex in a Ran-GTP-dependent manner (Zemp and Kutay, 2007). Nuclear transport is tightly controlled by c-MYC and p53. c-MYC, a master regulator of ribosome biogenesis, upregulates the transcription of *IPO7* and *XPO1* while p53 transcriptionally represses both (Golomb et al., 2012). Finally in the cytoplasm, in order to achieve translational competence, non-ribosomal protein factors are released from the 60S ribosome subunit, while 20S rRNA in the 40S ribosome subunit is further processed by dimethylation and cleavage into the final mature 18S rRNA (Zemp and Kutay, 2007).

2.1.1. The tripartite structure and function of the nucleolus

In high eukaryotes, the nucleolus has a tripartite structure that comprises three distinguishable regions by electron microscopy: the fibrillar centre (FC), the dense fibrillar component (DFC) and the granular component (GC) (Hernandez-Verdun et al., 2010). Each topological region in the nucleolus is in charge of a different function during ribosome biogenesis. rDNA transcription occurs at the interface between the FC and the DFC, early rRNA processing in the DFC and finally, late rRNA processing and ribosomal subunits assembly ensue in the GC (**Figure 2**).

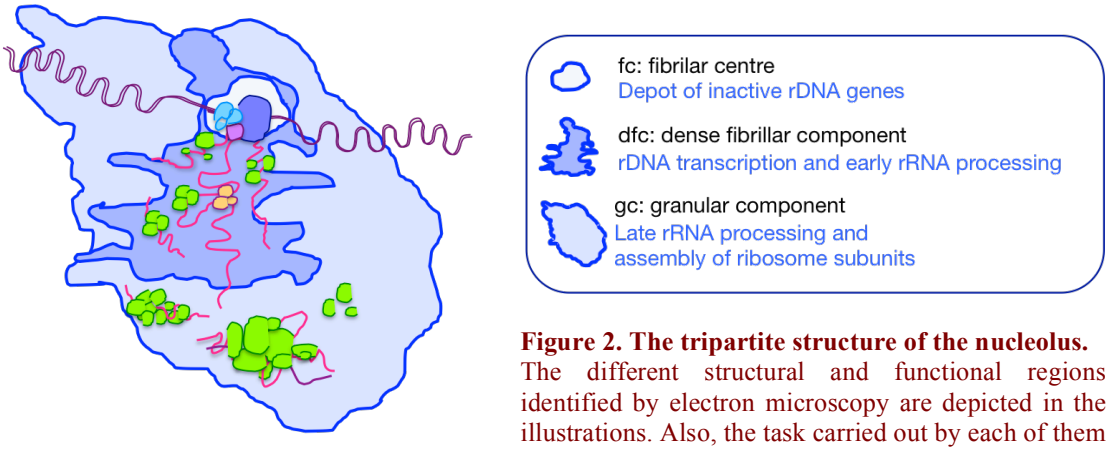

Figure 2. The tripartite structure of the nucleolus. The different structural and functional regions identified by electron microscopy are depicted in the illustrations. Also, the task carried out by each of them is shown.

2.1.2. Nucleolar stress

The nucleolus is well known to be a hub in the stress response. Approximately 70% of the ~4000 nucleolus-associated proteins are involved in functions other than ribosome biogenesis, including cell cycle control, apoptosis, DNA repair or the assembling and storage of the components of the telomerase complex (Boulon et al., 2010). Thus, the nucleolus is an important integrator between ribosome synthesis, cell cycle progression and stress signalling. Because of the high energetic demands for ribosome biogenesis, almost any perturbation that slows down cell growth or protein synthesis will lead to an immediate shutdown of rDNA transcription. Perturbations affecting rDNA transcription and early rRNA processing produce structural alterations in the dynamics of nucleolar proteins and rRNA, typically segregation (condensation followed by separation) of the nucleolar compartments and formation of "nucleolar caps" around the nucleolus remnant (Shav-tal et al., 2005). These structural changes were visualized many decades ago, in 1964, by phase-contrast microscopy. Cell treatment with actinomycin D, an inhibitor of rDNA and gene transcription, dramatically reduced the nucleolar size and changed the nucleolar morphology from irregular to spherical, what it was denominated as nucleolar "caps" (Reynolds et al., 1964). Nowadays, it is known that "nucleolar caps" are condensed remnants of FC or DFC components, such as UBF or fibrillarin, and that proteins located in the granular compartment diffuse throughout the nucleoplasm, such as nucleophosmin, being excluded from the residual nucleolar structures (Kurki et al., 2004; Shav-tal et al., 2005) (**Figure 3**). This total vanishing of nucleoli is referred to as "nucleolar disruption" and it is different from nucleolar fragmentation, which occurs following inhibition of either RNA pol II (by daunorubicin or CK2 inhibitors) or protein kinases leading to unravelling to the FC into necklace structures (Boulon et al., 2010).

It is well established that nucleolar disruptions occur in response to DNA damage (i.e. UV irradiation or inhibition of topoisomerase II by drugs such as etoposide) or Pol I-mediated

transcription inhibition (i.e. ActD) (Al-Baker et al., 2005; Shav-tal et al., 2005). In a very elegant manner, Rubbi and Milner showed that UV-induced DNA damage triggers p53 activation by disrupting the nucleolus (Rubbi and Milner, 2003). The precise mechanisms by which DNA damage can alter nucleolar morphology still remain elusive. Many chemotherapeutic drugs that activate p53 cause nucleolar disruption by blocking rDNA transcription or early steps of rRNA processing (Burger et al., 2010; Hein et al., 2013). Similarly, depletion or overexpression of mutant nucleolar proteins, such as TIF-IA ablation (Yuan et al., 2005) or the dominant negative mutant Bop1 (Pestov et al., 2001), leads to destabilization of nucleolar morphology and activation of p53-mediated cell cycle arrest and apoptosis. In turn, p53 represses RNA pol I transcription by preventing binding of SL1 to UBF (Zhai and Comai, 2000), as well as elicits a p53-mediated cell cycle arrest that hampers rDNA transcription, reinforcing the halt on ribosome synthesis. Interestingly, blockage of nuclear import of ribosomal proteins or nuclear export of ribosomal subunits by genetic ablation of *IPO7* and *XPO-1*, respectively, also cause nucleolar disruption and activates p53 (Golomb et al., 2012).

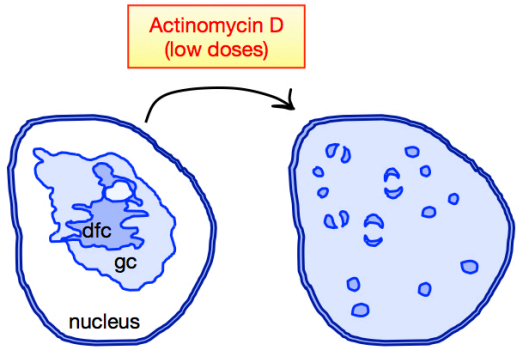

Figure 3. Nucleolar Disruption.
Following ribosomal stress, proteins located in the dense fibrillar centre, such as fibrillarin, condense in nucleolar caps around the remaining nucleolar component, while proteins in the granular compartment, such as nucleophosmin (NPM), diffuse throughout the nucleoplasm. **dfc**, dense fibrillar center; **gc**, granular component.

2.1.3. Nucleoli and cancer

Notably, changes in number, size and morphology of nucleoli have been long recognized as a reliable feature of cancer cells. Cancer cells are characterized by presenting large nucleoli, described by pathologists more than 100 years ago as "prominent nucleoli" (Derenzini et al., 2009). Proliferating and cancer cells have higher demands on protein synthesis due to growth factors signalling and oncogenes that increase proliferation and upregulate rRNA synthesis, thus increasing the size and number of nucleoli. Therefore, the size and number of nucleoli is a reflection of how active ribosome production is in a cell. Cancer cells of a given type of tumour have larger nucleoli than the corresponding benign lesion and, therefore, a malignant lesion can be distinguished from a benign lesion in the same tissue on the basis of different nucleolar size. As an example, aggressive breast cancer cell lines increase their nucleolar size around 30% resulting in elevated ribosome biogenesis (Belin et al., 2009). In contrast, terminally differentiated cells, such as lymphocytes, present small nucleoli. UBF levels are, in many cases, indicative of high ribosome biogenesis in cancer cells

(Derenzini et al., 1998). For instance, hepatocellular carcinoma samples often overexpress UBF which is sufficient to activate rDNA transcription and accelerate tumour growth (Huang et al., 2002).

Silver-staining has been used to detect nucleolar size based on the argyrophilic nature of nucleolar proteins. This particular staining is known as AgNOR staining (Trerè, 2000). Nucleolar size evaluated by AgNOR staining is considered as an independent prognosis factor for many human cancers, the larger size of the nucleolus the worse the prognosis of the disease (Derenzini et al., 2009) (**Figure 4**).

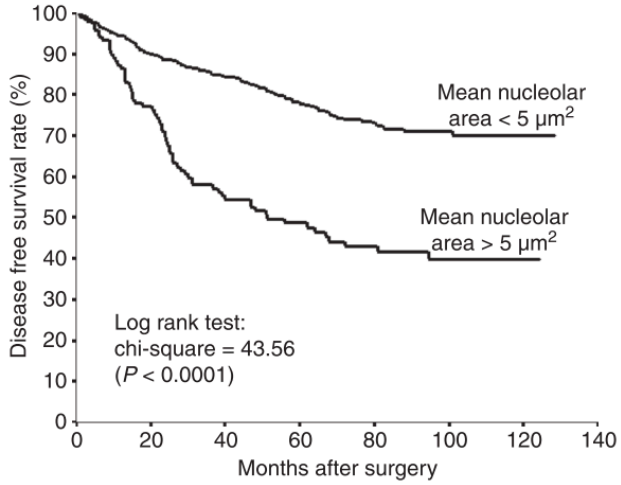

Figure 4. Nucleolar size as a prognosis factor.
Disease-free survival curves (Kaplan-Meier estimates) for 504 breast cancer paperns with respect to the nucleolar area per cell nucleus, measured by image analysis on specifically silver-stained tissue sections, granular component. Figure taken from Derenzini et al., 2009.

Cancer cells can regulate the nucleolus activity by means of overexpression of proto-oncogenes and repression of tumour suppressors. In this manner, oncogenic c-MYC stimulates ribosome biogenesis by activating RNA pol I transcription (Arabi et al., 2005; Grandori et al., 2005). Particularly, two major tumour suppressors, retinoblastoma protein (pRb) and p53 can control nucleolar function by inhibiting rDNA transcription. pRb binds to UBF and p53 to SL1 and, in both cases, the formation of the UBF-SL1 complex, required for RNA pol I recruitment at rDNA gene promoters, is hampered and consequently, ribosome biogenesis is downregulated (Hannan et al., 2000; Voit et al., 1997; Zhai and Comai, 2000). Accordingly, tumours bearing deletion in Rb or inactivated pRb or mutated p53 present larger nucleolus than tumours with normal Rb and p53 status (Derenzini et al., 2009). Moreover, activation of the tumour suppressor PTEN has been shown to block recruitment of SL1 complexes to the promoter of rDNA genes, thus reducing Pol I transcription (Zhang et al., 2011a). In agreement, repression of PTEN is often observed in cancer and enhances cell growth, proliferation and survival. The tumour suppressor ARF, in addition to inhibit MDM2 activity and activate p53, can directly control rDNA transcription by altering phosphorylation of UBF and thus preventing its ability to recruit the PIC, and by preventing Pol I transcription termination factor (TTF-1) nucleolar import (Ayrault et al., 2006; Lessard et al., 2010).

2.1.4. Drugs targeting nucleoli

Chemotherapeutic drugs have been developed to halt proliferation of cancer cells. Cancer cells require increased ribosome biogenesis to fulfil the energetic needs of highly proliferating cells. Many of the current drugs used in the clinics mostly target ribosome biogenesis at different levels (Burger et al., 2010). For example, ActD (Dactinomycin) is a natural antibiotic approved for Wilms tumour that intercalates into GC-rich DNA regions, commonly found in rDNA genes, and prevents elongation of rDNA transcription by Pol I (Fetherston et al., 1984). As a consequence of inhibited transcription, ActD causes nucleolar disruption and activates p53 (Choong et al., 2009). Similar to ActD, the ellipticine derivative 9-hydroxyellipticine (9-HE) intercalates into GC-rich regions of the rDNA and prevents the interaction between SL-1 and the rDNA promoter (Andrews et al., 2013). Cisplatin inhibits Pol I transcription by cross-linking DNA at HMG-protein affinity sites thus preventing UBF from association with the rDNA promoter (Treiber et al., 1994). Topoisomerase I inhibitors (camptothecin, irinotecan and topotecan) also disrupt Pol I transcription (Garg et al., 1987). In addition, 5'-fluorouracil (5'-FU), an inhibitor of nucleotide synthesis, disrupts rRNA processing (Ghoshal and Jacob, 1997).

Alternatively, inhibitors of certain kinases controlling cellular growth and proliferation signalling pathways have been shown to inhibit ribosome biogenesis. In this manner, Cdk2 inhibitors (roscovitien and olomoucine), the casein kinase 2 (CK2) inhibitor 5,6-dichoro-1-beta-ribofuranosyl benzimidazole (DRB) or the Cdk9 inhibitor flavopiridol disrupt nucleolar integrity and hinder rRNA processing (David-Pfeuty et al., 2001; Louvet et al., 2006). As previously mentioned, mTOR kinase is one the key players in modulating rDNA transcription in response to nutrients and growth factors availability. mTOR signalling pathway phosphorylates TIF-IA and UBF promoting their binding to SL-1 (Hannan et al., 2003; Mayer et al., 2004). Accordingly, the mTORC1 inhibitor, rapamycin, suppress rDNA transcription by impairing signalling downstream of mTORC1 (Hannan et al., 2003; Mayer et al., 2004). Additionally, inhibitors of the protein kinase AKT (AKTi-1/2 and MK-2206), upstream mTORC1, also suppress rDNA and have effectively shown anti-tumorigenic properties in c-MYC driven lymphomas, characterized for higher rDNA transcription rates (Chan et al., 2011; Devlin et al., 2013).

An important approach to target nucleolar function is impairing the formation of the rDNA pre-initiation complex. In this regard, several drugs targeting components of the Pol I machinery have been described. The most noteworthy examples are the small molecule compounds CX-3543 and CX-5461, developed by Cylene Pharmaceuticals, and BMH-21. CX-3543 (quarfloxin) binds to G-quadruplex regions, higher order structures formed within G-rich regions of rDNA, and prevents nucleolin (NCL) interactions thus inhibiting elongation of Pol I transcription (Drygin et al., 2009).

NCL stabilizes G-quadruplex structures in the rDNA gene and facilitates rapid Pol I transcription by preventing renaturation of template DNA in the GC-rich rDNA. CX-3543 has shown anti-tumorigenic properties in a broad panel of cancer cell lines, as well as in xenograft models of breast and pancreatic cancers (Drygin et al., 2009), and has progressed into phase I and phase II clinical trials (but they were withdrawn due to bioavailability problems). CX-5461 directly binds to SL-1 complexes impairing its binding to rDNA promoters and further recruitment of RNA Pol I co-factors thus blocking Pol I transcription initiation (Drygin et al., 2011). CX-5461 is a highly selective inhibitor of Pol I activity (300-400 fold more selective than for Pol II or Pol III activity) and its anti-proliferative efficacy has been exhibited over a broad panel of cancer cell lines, in melanoma and pancreatic xenograft models and in engineered models of c-MYC driven B-cell lymphomas (Bywater et al., 2012; Drygin et al., 2011). Importantly, the apoptotic effect of CX-5461 is specific for c-MYC overexpressing lymphoma cells without damaging normal B-lymphocyte cells and does not cause genotoxic stress (Bywater et al., 2012). Currently, CX-5461 is being tested in patients with advanced haematological malignancies (phase I; clinical trial ID ACTRN12613001061729). Lastly, BMH-21, an acridine derivative, causes nucleolar disruption and activates p53 in the absence of DNA damage (Peltonen et al., 2010, 2014). BMH-21 intercalates into GC-rich regions of rDNA, similar to ActD, and promotes degradation of the catalytic subunit of the RNA pol I, RPA194 (Peltonen et al., 2014). The efficacy of these drugs *in vivo* reinforce that cancer cells depend on enhanced ribosome biogenesis characterized by increased rDNA transcription rates and Pol I machinery abundance.

2.2. The ribosomal stress pathway (RP-MDM2-p53)

The surveillance RP-MDM2-p53 pathway, also known as the ribosomal/nucleolar stress pathway, emerged more than ten years ago as a new p53-signalling pathway that monitor coupling between cell growth and cell cycle. The stimulus that activates this pathway is the so-called nucleolar or ribosomal stress. Ribosomal stress (RbS) results from perturbations at any level of the ribosome biogenesis. Ribosome is formed by equimolar amounts of the four rRNA species and the ribosomal proteins. These perturbations generate an imbalance in ribosome biosynthesis leading to the release of free ribosomal proteins from the nucleolar into the nucleoplasm. In turn, free ribosomal proteins and pre-ribosomal complex, in particular the RPL11/RPL5/5S rRNA pre-complex, bind and inhibit MDM2 ubiquitin ligase activity (**Figure 4**). Of note, coordinated downregulation of rRNA and RPs synthesis, by serum deprivation or rapamycin treatment, does not lead to free RPL11 so p53 is not activated (Donati et al., 2011). Several RPs has been shown to bind and inhibit MDM2 activity: RPL23 (Dai et al., 2004), RPS7 (Chen et al., 2007), RPS3 (Yadavilli et al., 2009), RPS14 (Zhou et al., 2013), RPS27 and RPS27-like (Xiong et al., 2011), RPL37, RPS15 and RPS20 (Daftuar et al., 2013), although an increasingly numbers of reports claim that inhibition of MDM2 relies solely on the

interaction with the RPL11/RPL5/5S rRNA pre-complex (Bursać et al., 2012a; Dai and Lu, 2004a; Donati et al., 2013; Horn and Vousden, 2008; Lohrum et al., 2003; Zhang et al., 2003). This is proposed based on 1) interaction studies in yeast in which orthologs RPL11 and RPL5 are detected in a pre-ribosomal complex together with 5S rRNA before being incorporated into the nascent 90S processome (Zhang et al., 2007), 2) dependence on 5S rRNA for RPL11/RPL5 binding to MDM2 and cooperation between RPL11 and RPL5 to fully activate p53 (Donati et al., 2013; Fumagalli et al., 2012; Horn and Vousden, 2008), and 3) RPL11 and RPL5 mutually protects each other from proteosomal degradation (Bursać et al., 2012a). In addition, only depletion of RPL11 or RPL5, but not other RPs shown to bind MDM2 (i.e. RPS7 or RPL23), rescues the p53-mediated cell cycle arrest provoked by ribosome biogenesis imbalance (Fumagalli et al., 2012).

Notably, none RP has been described to bind MDMX, an MDM2-related ubiquitin ligase that also modulates p53 transcriptional activity. MDM2 and MDMX share a similar structure; however, RPL11 selectively binds to the C4 zinc finger domain of MDM2 (Zheng et al., 2015), but not to MDMX (Gilkes et al., 2006). Specific binding to MDM2 is due to the presence of hydrophobic residues (PPLP motif) in its C4 zinc finger domain, not present in MDMX, that are required for RPL11 interaction (Zheng et al., 2015). Importantly, human cancer-derived mutations, such as C305F (found in osteosarcomas) targeting the cysteine residues (C4) in the MDM2 central zinc finger, abrogate RPL11 and RPL5, but not ARF, binding (Lindström et al., 2007; Macias et al., 2010; Zheng et al., 2015). The MDM2 C305F mutant retains p53 ubiquitylation and transcriptional repression activities but attenuates p53 degradation due to impaired nuclear export (Lindström et al., 2007). This rises the possibility that RPL11 and RPL5 may help MDM2 to undergo nuclear export, in addition to prevent MDM2 from ubiquitinating p53 and repressing its transactivation (Zhang et al., 2003). Thus, MDM2 with mutations disrupting RPL11 and RPL5 binding could evade ribosomal stress-induced growth arrest, which could explain the origin of these zinc finger mutations in human cancer.

In vivo studies of RPs deletion strongly support the notion that impairment in ribosome biogenesis activates p53. Genetic inactivation of p53 in *Rps6* and *Rpl22* heterozygous mice and in *Rpl24* (Belly Spot and Tail, *Bst*) mutant mice rescues all the pathological phenotypes observed in these animals, suggesting that they are caused by p53 activation (Bursac et al., 2014).

Insults affecting rDNA transcription or early rRNA processing activate p53 through the RbS pathway in the absence of nucleolar disruption. This is the case, for instance, of low doses (1-5 nM) of actinomycin D (ActD), that selectively stalls RNA pol I-mediated rDNA transcription (Perry and Kelley, 1970), resulting in the release of free RPs from the nucleolus into the nucleoplasm and the subsequent inhibition of MDM2 (Choong et al., 2009; Dai and Lu, 2004b; Dai et al., 2004; Jin et al., 2004; Lohrum et al., 2003; Zhang et al., 2003). Similar to ActD, additional drugs affecting rDNA

transcription, such as CX-5461, CX-3543, or the immunosuppressant mycophenolic acid (MPA), cause nucleolar disorganization and activate the RPL11/RPL5-MDM2-p53 pathway (Bywater et al., 2012; Sun et al., 2008). Genetic models also support this notion. Deletion of the RNA pol I transcription initiation factor TIF-IA (Yuan et al., 2005) or silencing the *Polr1a* gene coding for the Pol I catalytic subunit (RPA 194) (Donati et al., 2011) leads to nucleolar disruption and elicits a p53-mediated cell cycle arrest and apoptosis through the RbS pathway. Notably, ARF does not play a substantial role in this scenario (Yuan et al., 2005), indicating that RPL11 is the main p53 activator when ribosome biogenesis is disturbed.

On the other hand, insults affecting later steps during ribosome biogenesis or equimolar amounts of RPs can drive the RbS pathway in the presence or absence of nucleolar disruption, depending on the particular stimulus. Drugs affecting later steps in rRNA processing, such as 5'-fluorouracil (5'-FU), activate the RbS pathway in the absence of nucleolar disruption (Sun et al., 2007). Depletion of *IPO7* and *XPO1*, involved in nuclear transport of RPs and subunits, also activates the RbS pathway by causing nucleolar stress (Golomb et al., 2012). Regarding the assembly of the distinct ribosomal subunits, impaired assembly of the 60S large ribosomal subunit by knockdown of certain large-subunit ribosomal protein, such as RPL23 or RPL37 (Fumagalli et al., 2012; Llanos and Serrano, 2010), results in ribosome free-RPL11 that binds to MDM2 in the absence of nucleolar disruption while depletion of RPL29 or RPL30, which equally activates the ribosomal stress pathway, provokes nucleolar disorganization (Sun et al., 2010). Interestingly, depletion of small-subunit ribosomal proteins (i.e. RPS6, RPS7 or RPS14) activates the RbS pathway, in the absence of nucleolar disruption, through a novel mechanism. Knockdown of RPS proteins selectively enhances the translation of a group of mRNAs containing a 5' terminal oligopyrimidine tract (5' TOP) in the leader sequence, including the RPL11 mRNA, which results in higher amounts of available RPL11 to inhibit MDM2 (Dutt et al., 2013; Fumagalli et al., 2009).

In addition to inactivation of MDM2 by binding of RPL11/RPL5/5S rRNA complex, there are other mechanisms that collaborate in the p53 activation upon ribosome dysfunction. MDMX forms oligomers with MDM2 and prevents MDM2 self-ubiquitylation (Tanimura et al., 1999). RPS15 and RPS20 interact with MDMX and downregulate its protein levels, while RPL37 downregulates *Mdmx* mRNA levels (Daftuar et al., 2013), thus contributing to full p53 activation. RPL11 promotes MDMX degradation upon ribosomal stress in an MDM2-dependent manner, and concomitantly, MDMX overexpression abrogates p53 activation and prevents growth arrest (Gilkes et al., 2006). An additional regulator of the ribosomal stress pathway is the Myb-binding protein 1a (MYBBP1A). MYBBP1A localizes in the nucleolus and, following impairment of ribosome biogenesis, is translocated, in an RPL11- and RPL5-dependent manner, to the nucleoplasm where it increases the interaction between p53 and p300/CBP to enhance p53 acetylation (Kuroda et al., 2011). The promyelocytic leukemia

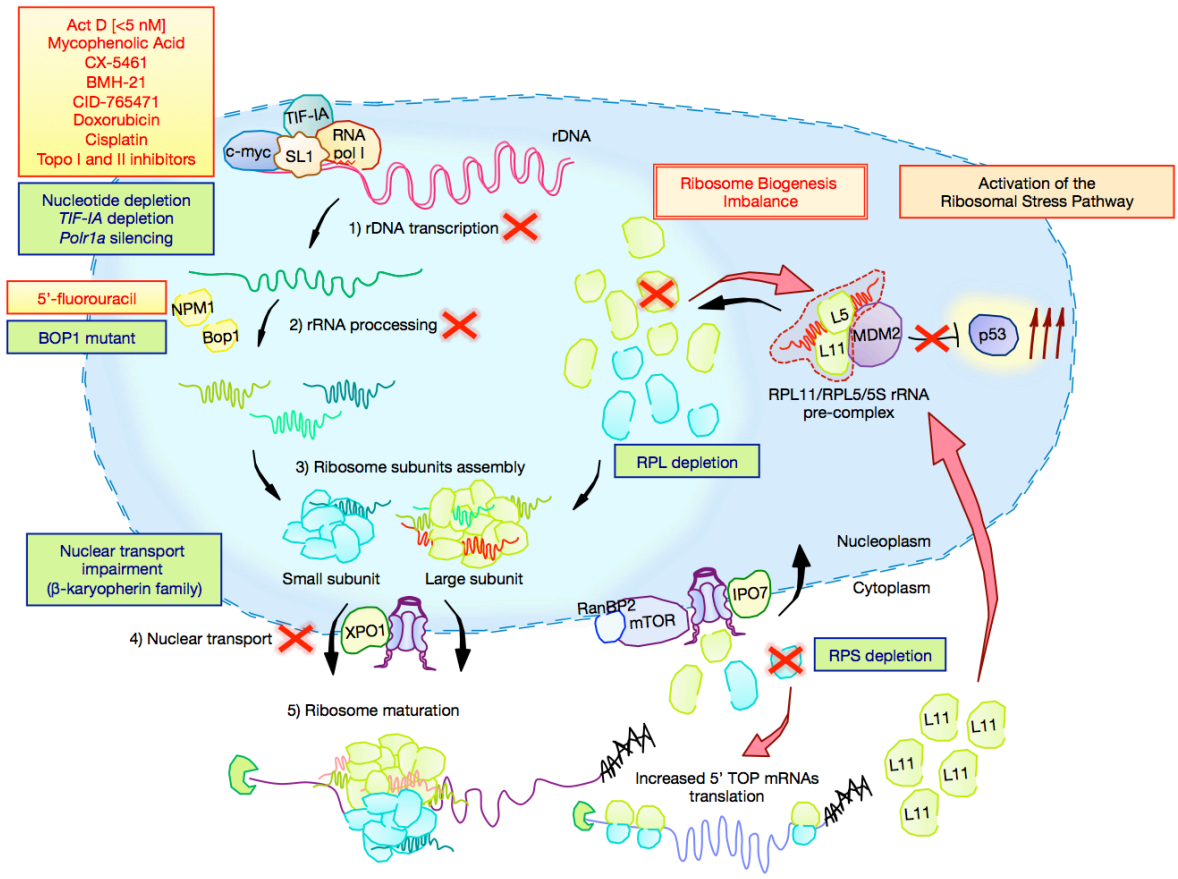

Figure 4. Perturbations in ribosome biogenesis activate the Ribosomal Stress Pathway.
Chemical compounds (yellow boxes) or genetic depletion (green boxes) affecting the different steps of ribosome biosynthesis (rDNA transcription, rRNA processing, ribosome assembly, nucleolar transport and availability of RPs) can lead to ribosome-free RPL11 or increased translation of 5'TOP mRNAs, including *Rpl11*. Then, ribosome-free RPL11 can bind and inhibit MDM2, thus activating p53.

(PML) tumour suppressor is also implicated in regulation of p53 acetylation upon ribosomal stress by low doses of ActD. PML co-localizes with p53, acetylated p53 and MDM2 in disrupted nucleoli in an RPL11- and RPL5-dependent manner (Bursać et al., 2012b). These observations indicate that the ribosomal stress pathway also modulate p53 transactivation by promoting its acetylation. Also, p53 activity can be boosted by augmented p53 mRNA translation. Ribosomal protein L26 (RPL26) binds to the duplex 5'/3'-UTR of p53 mRNA following ionizing radiation and enhances translation of the p53 mRNA without affecting global translation, thus increasing the number of cells undergoing p53-dependent G1 cell cycle arrest and apoptosis (Chen and Kastan, 2010; Takagi et al., 2005).

The most convincingly work, besides cell-based studies, demonstrating the biological relevance of the ribosomal stress pathway *in vivo* is the mouse model engineered by Macias and co-workers (Macias et al., 2010). They generated mutant C305F MDM2 mice, in which RPL11 and RPL5 binding to MDM2 is abolished and thus, that fail to activate p53 in response to ribosomal stress (ActD, 5'-FU and MPA), but not to DNA damage (Doxorubicin, UV and whole body ionizing radiation). Remarkably, mutant MDM2 mice develop an accelerated lymphomagenesis in an Eμ-MYC oncogenic

context. cMYC stimulate translation of ribosomal proteins (van Riggelen et al., 2010) and under oncogenic conditions it may produce an excess of ribosomal proteins that activate the ribosomal stress pathway. This study highlights the important contribution of the ribosomal stress pathway, in parallel with the ARF/MDM2/p53 pathway, in p53-mediated tumour suppression. Notably, mutant MDM2 mice do not present accelerated onset of tumorogenesis in other oncogenic contexts, such as inactivation of pRb or RAS overexpression (Pan et al., 2011), which indicates a context-dependency of the biological activity of the ribosomal stress pathway.

2.2.1. The Ribosomal Protein L11 (RPL11)

The ribosomal protein L11 (RPL11) is encoded by chromosome 1 (1p36.1-p35; *Homo sapiens*) in human and chromosome 4 in mouse (4; 4 D3; *Mus musculus*). In healthy tissues, RPL11 mRNA expression varies, being strikingly high in ovary and relatively low in the nervous system (GTEx Portal; RPL11 Entrez Gene ID: 6315). RPL11 is part of the large subunit of the ribosome. RPL11 together with RPL5 and 5S rRNA are part of the 60S protrusion of the large ribosome subunit that binds 28S rRNA (Zheng et al., 2015).

Beyond its function as part of the ribosome, the ribosome-free RPL11/RPL5/5S rRNA pre-complex activates p53 through the so-called ribosomal/nucleolar stress pathway (Bursać et al., 2012b; Donati et al., 2013; Horn and Vousden, 2008; Zhang and Lu, 2009). In addition, RPL11 enhances p53 activation by promoting MDM2 self-ubiquitylation (Dai et al., 2006). Moreover, upon ribosome biogenesis dysfunction, RPL11 is rapidly but transiently recruited at the promoter sites of p53 target genes, in an MDM2-dependent manner, and helps recruiting the p53 co-activators p300/CBP that subsequently induce p53 K382 acetylation (Mahata et al., 2012).

RPL11 has a hand-like conformation structure conserved from prokaryotes to eukaryotes. It selectively binds to MDM2, but not MDMX, through the C4 zing finger domain of MDM2 in a similar manner to that of 28S rRNA (Zheng et al., 2015). Hydrophilic critical residues for binding to MDM2 have been identified in the centre of the palm of RPL11 (Dai et al., 2006; Zhang et al., 2011b, 2003; Zheng et al., 2015). Mutations in several of these residues, for instance Lysine 52, Arginine 75 and Aspartate 136, abolish binding of RPL11 to MDM2 (Zhang et al., 2011b), therefore inactivating the ribosomal stress pathway. So far, 46 mutations in RPL11 have been described in several cancers, including melanoma and prostate cancer (COSMIC, International Cancer Genome Consortium (ICGC)), although it seems that key residues for MDM2 binding are not affected. *Rpl11* mRNA expression is particularly high in blood malignancies and Ewing sarcoma (Cancer Cell Line Enciclopedia). Unlike *Rpl5*, *Rpl10* and *Rps15*, which have been found recurrently mutated in T cell-

acute lymphoblastic leukaemia (T-ALL) and chronic lymphocytic leukaemia (CLL) patients (De Keersmaecker et al., 2013; Landau et al., 2015), mutations in *Rpl11* have not been described in blood malignancies yet. On the other hand, *Rpl11* mutations resulting in *Rpl11* heterozygosity have been found in Diamond-Blackfan Anemia (DBA) patients (Boria et al., 2010; Cmejla et al., 2009; Gazda et al., 2008; Quarello et al., 2010). Strikingly, mutations in *Rpl11* are preferentially associated to thumb malformations, in particular triphalangeal or dysplastic thumbs and additional bilateral small thumbs (Cmejla et al., 2009; Gazda et al., 2008; Quarello et al., 2010).

Depletion of *Rpl11* has been performed *in vitro* in somatic and tumor cells, but so far, deletion of *Rpl11* only has been conducted in a few studies in *Zebrafish* (Amsterdam et al., 2004a; Chakraborty et al., 2009; Danilova et al., 2011; Zhang et al., 2013b). Ablation of *Rpl11* by morpholinos in *Zebrafish* causes brain development, hematopoietic and metabolic defects (Chakraborty et al., 2009; Danilova et al., 2011; Zhang et al., 2013b). Importantly, the hematopoietic related phenotype recapitulates DBA symptoms. Contrary to what was observed in cells, *Rpl11* haploinsufficiency-associated pathologies (brain development and hematopoietic defects) are totally or partially alleviated in a p53 null background (Chakraborty et al., 2009; Danilova et al., 2011). This supports the existence of a p53 checkpoint *in vivo* that monitors homeostasis of the ribosome biogenesis. All these studies have mainly focused on developmental and hematopoietic defects upon deletion of *Rpl11* but cancer predisposition, an important feature of DBA patients, has not been assessed yet.

2.2.2. Regulation of RPL11

NEDDylation

Neddylation is a "tagging" protein process that controls localization and stability of many proteins. The ubiquitin-like protein NEDD8 is conjugated to its target proteins by specific E1 and E2 enzymes (Enchev et al., 2015). In normal conditions, NEDDylation of RPL11 by MDM2 protects it from degradation and retain its nucleolar localization (Sundqvist et al., 2009). However, impairment of ribosome biogenesis by treatment with ActD causes rapid de-NEDDylation of RPL11 and, subsequently, its re-localization from the nucleolus to the nucleoplasm where it binds to MDM2, thus increasing p53 stability (Sundqvist et al., 2009).

PICT1

PICT1 (protein interacting with the C terminus 1 of the tumour suppressor PTEN; also known as GLTSCR2) is a negative regulator of the RPL11-dependent p53 activation (Sasaki et al., 2011). PICT1 retains RPL11 in the nucleolus preventing, in this manner, binding to MDM2 in the nucleoplasm and activation of the ribosomal stress pathway. In line with this, patients with oligodendrogliomas with *PICT1* haploinsufficiency have a better prognosis than their counterparts

(Cairncross et al., 1998; Mariani et al., 2006; Smith et al., 1999). Likewise, colon and oesophageal cancer patients bearing tumours that retain p53 wild-type and lower expression of PICT1 have a better prognosis (Sasaki et al., 2011). Similarly, PICT1 heterozygous mice are more resistant to develop chemically-induced papillomas when compared to wild-type mice (Sasaki et al., 2011).

c-MYC, ribosome biogenesis and RPL11: a negative feedback loop

MYC is a proto-oncogene discovered three decades ago (Dang, 2012). c-MYC is one of the members of the Myc family of transcription factors, that also includes MYCN (n-MYC) and MYCL (l-MYC). Overexpression of c-MYC is found in 20% of many different human cancers; being chromosomal translocation, as observed in human Burkitt's lymphoma, one of the major causes of c-MYC deregulation (Dang, 2012). c-MYC modulates around 15% of genome transcription, controlling cell growth and proliferation, among other vital cellular processes (Patel et al., 2004). c-MYC activates or represses transcription mainly by chromatin remodelling. In one hand, c-MYC dimerizes with MAX and binds to E-boxes DNA sequences in gene promoters when chromatin is partially open (Guccione et al., 2006). MYC/MAX complexes recruit co-regulatory factors, such as GCN5, TIP60 and TRRAP, which promote acetylation of nucleosome histones, resulting in further opening of the chromatin and greater levels of gene transcription (Cole and Nikiforov, 2006). On the other hand, MYC/MAX heterodimers can also repress transcription of MIZ1 target genes, including cyclin-dependent kinase inhibitors p21 (*CDKN1A*) and p15 (*CDKN2B*), by binding to the transcriptional factor MIZ-1 and recruitment of DNA methyltransferase DNMT3a, ultimately resulting in epigenetic silencing (Brenner et al., 2005). Transactivation of genes involved in cell growth and proliferation, as well as transcriptional repression of tumour suppressors, count for the oncogenic role of cMYC in the onset and development of tumorogenesis.

Additionally, c-MYC is considered a master regulator of ribosome biogenesis (van Riggelen et al., 2010). In this regard, c-MYC facilitates rDNA transcription by chromatin remodelling of rDNA loci and recruitment of RNA pol I co-factors to rDNA promoters (Arabi et al., 2005; Grandori et al., 2005; Shiue et al., 2009), promotes transcription of ribosomal proteins and other factors involved in ribosome biogenesis by RNA pol II (Golomb et al., 2012; van Riggelen et al., 2010; Schlosser et al., 2003), and activates RNA pol III-mediated transcription of 5S rRNA and tRNA (Gomez-Roman et al., 2003). Supporting the role in controlling ribosome biogenesis, Eμ-MYC mice with *Rpl24* half gene dose presented a slower onset of tumorogenesis, possibly because of the inability of c-MYC to upregulate nascent ribosome biogenesis due to limiting amounts of RPL24 (Barna et al., 2008). Alternatively, *Rpl24* deletion could result in activation of the ribosomal stress pathway; so increased levels of p53 and/or downregulation of c-MYC by ribosome-free RPL11 might explain the decelerated tumorogenesis in these mice. *Rpl11* is a "bona-fide" c-MYC transcriptional target and, in turn, RPL11 represses c-MYC transcriptionally activity by multiple mechanisms. RPL11 directly binds to c-MYC

at c-MYC target gene promoters inhibiting the recruitment of the c-MYC co-activator TRRAP to these regions by competing with TRRAP for c-MYC binding (Dai et al., 2007a). In this manner, RPL11 can reduce histone acetylation of the target gene promoters (open conformation) and suppress c-MYC transcriptional activity. RPL11 knockdown increases c-MYC mRNA and protein levels and overexpression of RPL11 re-locate ectopic c-MYC into the nucleolus (Dai et al., 2007b). Association of RPL11 to c-MYC in the nucleolus might prevent c-MYC functions. Also, ribosome-free RPL11 promotes c-MYC mRNA degradation by binding to c-MYC 3'UTR and recruitment of mir-24/miRISC complex, and this mechanism is further enhanced upon ribosomal stress (Challagundla et al., 2011). Importantly, activation of p53, which can be elicited by increased ribosome-free RPL11 levels, can repress c-MYC transcription (Ho et al., 2005; Sachdeva et al., 2009). An illustration summarizing the c-MYC-RPL11 feedback loop is shown (**Figure 5**).

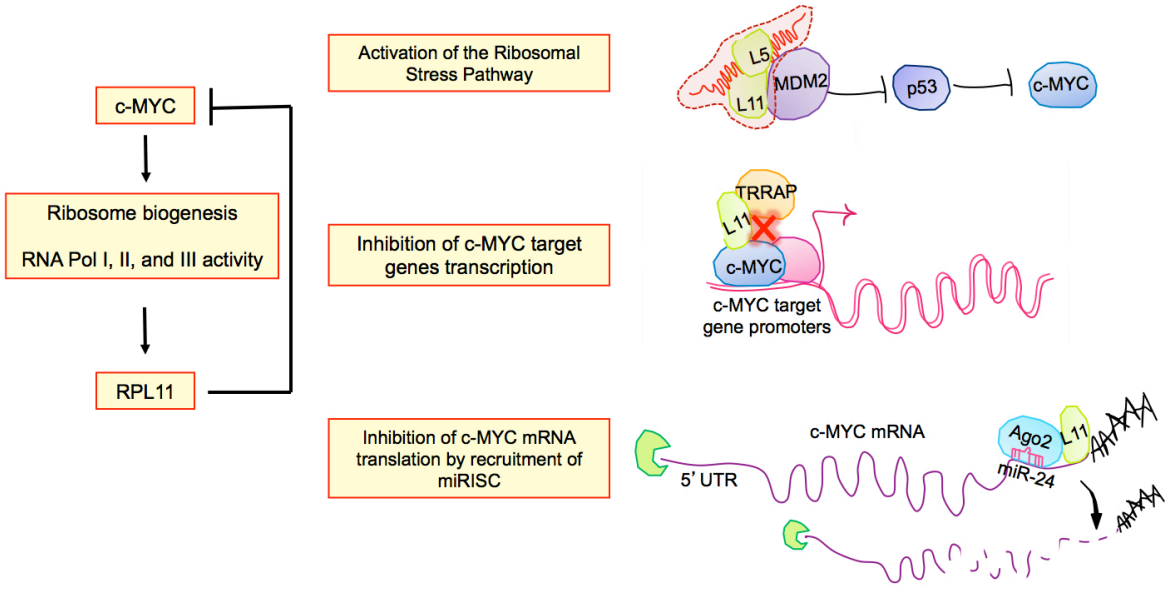

Figure 5. c-MYC-RPL11 feedback regulation.
c-MYC promotes ribosome biogenesis by controlling all the RNA polymerases involved in this cellular process. In turn, RPL11 negatively modulates c-MYC activity by different mechanisms, including p53 activation, impaired recruitment of c-MYC co-activators and c-MYC mRNA miRISC-mediated degradation.

3. RIBOSOMOPATHIES

Ribosomopathies refers to a group of inherited diseases caused by haploinsuficiency of genes involved in ribosome biogenesis, such as RPs or factors involved in rRNA processing (Narla and Ebert, 2010). Most of the diseases comprising this group are characterized by similar pathologies, including bone marrow failure, anaemia and higher predisposition to cancer (**Table 2**). Diamond-Blackfan anaemia (DBA) and the 5q- myelodysplasic syndrome (5q- MDS) are caused by mutations in RP genes, while other congenital syndromes, such as Schwachman-Diamond syndrome (SDS), X-

linked dyskeratosis congenital (DKC), cartilage hair hypoplasia (CHH) and Treacher Collins syndrome (TCS), present mutations in non-RPs factors.

Ribosomopathies: characterization and molecular defects

Disease	Genetic defect	Gene function	Congenital or acquired?	Clinical characteristics	Cancer risk
Diamond Blackfan Anemia (DBA)	RPS19, RPS24, RPL35a, RPS17, RPL5, RPL11, RPS7, RPS10, RPS26	Ribosomal proteins required for ribosome biogenesis	Congenital	Macrocytic anemia; growth retardation; craniofacial malformations; thumb, limb and heart defects	Myelodysplastic syndrome (MDS), AML and solid tumors
5q- syndrome	RPS14, one of ~40 genes in CDR	Ribosomal protein required for ribosome biogenesis	Acquired	Macrocytic anemia; micromegakaryocytosis and thrombocytosis	Acute myeloblastic leukemia (AML)
Shwachman–Diamond syndrome (SDS)	SBDS	Maturation of 60S ribosomal subunit and 60S–40S subunit joining	Congenital	Bone marrow dysfunction; pancreatic insufficiency; skeletal abnormalities; short stature	AML and MDS
X-linked dyskeratosis congenital (DKC)	DKC1	Nucleolar protein associated with snoRNPs. Modifies rRNA. Component of telomerase complex	Congenital	Skin and nail abnormalities; bone marrow failure	High risk of cancer
Cartilage hair hypoplasia (CHH)	RMRP	RNA component of RNase MRP complex. Cleaves precursor rRNA. Role in mitochondrial DNA replication	Congenital	Short-limbed dwarfism, hypoplastic hair, defective erythropoiesis and immunity	7-Fold higher incidence of cancer
Treacher Collins syndrome (TCS)	TCOF1 POLR1D POLR1C	Nucleolar protein with role in pre-ribosomal processing and ribosome biogenesis. RNA polymerase I and III components	Congenital	Craniofacial abnormalities	None known

Table 2. Ribosomopathies: characterization and molecular features.
Molecular features as well as the pathologies and cancer risk of the different diseases comprising the group of ribosomopathies are shown in this table. Adapted from Teng et al., 2013.

It is now widely accept that p53 activation is one of the molecular mechanisms underlying the pathologies of ribosomopathies (Teng et al., 2013a). In this manner, p53 has been found activated in animal models and patient samples of DBA, 5q- MDS and SDS (Dutt et al., 2013; Elghetany and Alter, 2002; Pellagati et al., 2015), as well as in *RPS19* and *RPS14*-depleted human cells (Dutt et al., 2013) and in *Rps19*, *Rps14* and *Tcof1* haploinsufficient mouse models for DBA, 5q- MDS and TCS, respectively (Barlow et al., 2010; Jaako et al., 2011; McGowan et al., 2008). Interestingly, macrocytic anaemia in *Rps6* haploinsufficient mice, similar to that of DBA and 5q- MDS patients, is rescued in a p53-null background (McGowan et al., 2011). In this model it was also shown that p53 activation depends on the ribosomal stress pathway (Dutt et al., 2013; Fumagalli et al., 2009).

Patients with ribosomopathies present higher risk to develop cancer and are particularly inclined towards blood malignancies (acute myeloid leukaemia and myelodysplastic syndrome) (**Table 2**). It is counter-intuitive the fact that deficient protein synthesis by ribosome dysfunction incline cells to oncogenic events, as observed in patients with ribosomopathies. Ablation of *Rps6* in *Drosophila* and deletion of several RPs in *Zebrafish* lead to tumour predisposition (Amsterdam et al.,

2004b; Stewart and Denell, 1993; Watson et al., 1992), providing *in vivo* evidences for an oncogenic role of aberrant ribosome biogenesis.

3.1. Diamond-Blackfan Anaemia (DBA)

Diamond-Blackfan anaemia (DBA; OMIM105650) is a rare inherited disease characterized by normocytic or macrocytic anaemia and defects in erythroid progenitors (Ruggero and Shimamura, 2015). DBA affects to 5-10 persons per million and is usually diagnosed in the first year of life according to the Diamond-Blackfan Anaemia Registry (DBAR) of North America. Patients are severely anaemic although they can have a healthy life under blood transfusion therapy, corticosteroid treatment or bone marrow transplant. In addition to anaemia, 47% of DBA patients present congenital anomalies, including malformations in head, hand, heart, kidney, urinary tract and genital organs. Malformations are more frequently associated to specific mutated genes, such as the case for cleft palate and thumb abnormalities associated to RPL5 and RPL11 mutations, respectively (Boria et al., 2010; Cmejla et al., 2009; Gazda et al., 2008). Currently, thirteen genes encoding for both large (*RPL5*, *RPL11*, *RPL35a*, *RPL19*, *RPL26 and RPL31*) and small ribosomal proteins (*RPS19*, *RPS24*, *RPS26*, *RPS17*, *RPS7*, *RPS10* and *RPS29*) and *GATA1* gene have been identified by deep sequencing mutated in around 50% of DBA patients, while the genetic cause remains unknown for the rest of patients (Boria et al., 2010; Chae et al., 2014; Doherty et al., 2010; Farrar et al., 2014; Gazda et al., 2012; Kuramitsu et al., 2012; Landowski et al., 2013; Mirabello et al., 2014; Sankaran et al., 2012). More than 25% of DBA patients bear mutations in *RPS19*, followed by a 7% and 5-10% in *RPL5* and *RPL11*, respectively (Vlachos et al., 2013). Minor symptoms include elevated levels of erythrocyte adenosine deaminase activity (eADA) and fetal haemoglobin (HbF).

DBA is also a cancer predisposition syndrome. 22% of DBA patients develop some type of cancer by age 46 years, including leukaemia and solid tumours (Vlachos et al., 2012). The age at which cancer appears in DBA patients is sooner than that observed for the type of cancers in the healthy population. So far, cancer predisposition has been underestimated in DBA community, mainly because of the lack of proper follow-ups and research.

3.1.1. Modelling DBA

To date, it is widely accepted that DBA is a disease resulting from ribosome dysfunction. Animal models, cells from DBA patients and DBA derived-iPSCs have helped in unravelling the molecular mechanisms underlying this disease. Mice with mutant *Rps19* or reduced *Rps19* gene dose develop symptoms like patients with DBA. In both animal models, as well as in *Rps19*, *Rpl11*, *Rpl5*,

Rpl19, *Rps7*, *Rps10*, *Rps26*, *Rps24*, *Rps29*, *Rpl26*, *Rpl35a* and *Rpl31* mutant DBA patient-derived cells and in RP-depleted cells, impaired rRNA processing is observed (Choesmel et al., 2008; Devlin et al., 2010; Doherty et al., 2010; Farrar et al., 2014; Flygare et al., 2007; Garçon et al., 2013; Gazda et al., 2008, 2012; Jaako et al., 2011; Mirabello et al., 2014; Robledo et al., 2008a).

Regarding the erythroid defects, macrocytic anaemia and reduction in the number of erythroid progenitors (BFU-Es), but not other lineages, is reported in *Rps19* mutant or deficient models (Danilova et al., 2008; Devlin et al., 2010; Ebert et al., 2005; Flygare et al., 2005; Garçon et al., 2013; Jaako et al., 2011; Miyake et al., 2008; Moniz et al., 2012), as well as in *Rps29* null *Zebrafish* (Taylor et al., 2012). Some studies show that anaemia in *Rps19* haploinsufficient mice is due to impaired erythroid differentiation (Danilova et al., 2008; Ebert et al., 2005; Flygare et al., 2005; Jaako et al., 2011), while others do not report abnormalities during maturation (Miyake et al., 2008; Moniz et al., 2012). Most of these reports state that erythroid defects in *Rps19* haploinsufficient progenitors are caused by p53 activation. In this regard, normal erythroid behaviour is restored in *Rps19* deficient mice either by rescuing the anaemia in a *p53*-null background or by treating with pifithrin α, an p53 inhibitor (Danilova et al., 2008; Dutt et al., 2011; Jaako et al., 2011; McGowan et al., 2008; Miyake et al., 2008; Moniz et al., 2012; Sieff et al., 2010). However, there is some controversy concerning the *Rps19* deficient DBA *Zebrafish* model. While Danilova and colleagues claim that the erythroid phenotype is caused by p53 activation and, concomitantly, defects are amelliorated by p53 suppression (Danilova et al., 2008), Torihara and co-workers can not rescue the erythroid defects when they deplete p53 (Torihara et al., 2011). In the case of *Rps29* deficient *Zebrafish*, erythroid defects are rescued in a p53 null background (Taylor et al., 2012).

Strikingly, *Rps19* heterozygous mice are normal and they do not develop hematopoietic or erythroid defects (Matsson et al., 2006). Similarly, *Rps7* disruption in mice do not lead to anaemia, although it causes several malformations and neuroanatomical defects that are rescued in a p53-null background (Watkins-Chow et al., 2013). This suggests that *Rps19* or *Rps7* mutations in DBA patients act as dominant negative or compensatory effects exist in mice, but not in humans, for retaining a normal RP activity.

Special relevance must be given to *Rpl11* and *Rpl5* deficient models. Since these two proteins are key in the p53-activating ribosomal stress pathway it is expected that erythroid failure is not caused by p53 accumulation. However, contrary to *in vitro* studies with cell lines, DBA *Rpl11* mutation caused a dramatic decrease in erythroid progenitor and a delayed differentiation because of augmented p53-mediated apoptosis and cell cycle arrest (Moniz et al., 2012). Concomitantly, erythroid defects observed in *Rpl11* mutant *Zebrafish* were partially alleviated following p53 depletion (Danilova et al., 2011). Brain development defects reported upon *Rpl11* knockdwon in *Zebrafish* were

also rescued upon p53 abrogation (Chakraborty et al., 2009). In the case of RPL5, *Rpl5* mutant DBA patient-derived iPSCs present erythroid defects which can be corrected by gene targeting (Garçon et al., 2013). Nonetheless, p53 levels remain normal in *Rpl5* mutant ES cells and suppression of p53 do not rescue the observed G2/M cell cycle arrest (Singh et al., 2014).

Although numerous studies have been carried out in cells from DBA patients and several animal models recapitulating the erythroid failure have been generated, DBA pathogenesis is not clearly understood. Yet some disagreement can be encountered in certain DBA models, activation of p53 seems to largely be a common molecular feature observed in DBA RP-deficient cells. Indeed, p53 levels are increased in other RP-deficient mice that present anaemia, such as is the case of *Rpl24* or *Rps6* (Anderson et al., 2007; Barkić et al., 2009; Dutt et al., 2011; McGowan et al., 2008). This indicates that p53 safeguards erythroid cells in a ribosome dysfunctional context.

3.1.2. Current DBA treatments and hints from DBA models

Existing treatments for DBA patients present side effects, some of them can negatively impact on their health status (Vlachos and Muir, 2010). Corticosteroids medication, such as dexamethasone, enhances production of red blood cells by increasing self-renewal of burst-forming unit erythroid progenitors (Zhang et al., 2013a). It has been shown recently that glucocorticoids improve red blood cells production by dampening the p53 response in affected erythroid cells (Sjögren et al., 2015). However, corticosteroids can cause short-term and long-term side effects, ranging from swelling to pathological fractures and physical and neurocognitive development in children. Moreover, not all DBA patients respond to corticosteroids and those who do not remain on corticosteroid treatment or are steroid non-responsive (20%) are subjected to blood transfusions. Iron overload is frequently observed in DBA patients dependent on chronic blood transfusions as consequence of improper recycling in new blood cells, which are not generated due to impaired erythropoiesis. Importantly, excess of iron can damage organs if not removed by iron chelators after few blood transfusions. Other than transplantation-related mortality, transfusion-associated iron overload is the leading cause of death for DBA patients. Stem cell transplant is the alternative to overcome DBA. However, this medical procedure involves serious risks, including the finding of an HLA-matched related donor, the administration of chemotherapy and radiation for killing the unhealthy patient's bone marrow or the possibility of dying because of complications of the treatment.

Harmless compounds are being tested in phase I/II clinical trials for amelioration of anemia, such as the nutrional supplement L-leucine (ClinicalTrials.gov identifiers: NCT02386267 and NCT01362595). L-leucine is a branched-chain aminoacid that enhances protein synthesis in skeletal

muscle and adipose tissues. DBA results from ribosome dysfunction, being compromised the translation of transcripts involved in erythroid maturation (Devlin et al., 2010; Horos et al., 2012; Ludwig et al., 2014). Dietary L-leucine administration alleviates anaemia in DBA *Rps19*-deficient animals and in other anaemic RP-deficient mice by activating mTOR and thus, boosts translation of proteins in a p53-independent manner (Jaako et al., 2012; Narla et al., 2014; Payne et al., 2012; Yip et al., 2013). Presumably, L-leucine supplementation would also restore normal levels of this aminoacid, which could be potentially affected in DBA mouse models since they present reduced translation of the branched-chain aminotransferase 1 (BCAT1), required for proper branched-chain aminoacid synthesis (Pereboom et al., 2014). Notably, L-leucine administration caused remission of DBA in the first patient tested in a pilot study (Pospisilova et al., 2007).

Lastly, the thalidomide-related immunosuppressant lenalidomide has displayed large effectiveness in 5q- MDS patients. Because of both DBA and 5q- MDS share many common pathological features, lenalidomide is being currently tested in a pilot study with blood transfusion-dependent DBA patients (ClinicalTrials.gov Identifier: NCT01034592). Lenalidomide administration to *Rps6* deficient mice, which present an erythroid phenotype similar to both DBA and 5q- MDS, improves their anaemia (Keel et al., 2012). Remarkably, lenalidomide promotes p53 degradation by inhibiting MDM2 self-ubiquitylation in 5q- MDS erythroid precursors (Wei et al., 2012).

OBJETIVOS

El objetivo principal de esta tesis ha sido la caracterización de la vía de estrés ribosomal en tres contextos diferentes:

1. **Integridad de la biogénesis ribosomal en pluripotencia.**

   1a. Estudio de la funcionalidad de la vía de estrés ribosomal en células embrionarias pluripotentes de ratón.

2. **Activación no genotóxica de la vía de estrés ribosomal mediante compuestos químicos en células tumorales**

   2a. Identificación de nuevos agentes disruptivos del nucleolo para activar la vía de estrés ribosomal en ausencia de daño detectable en células tumorales.

   2b. Caracterización del mecanismo de acción de los candidatos.

3. **Relevancia de la integridad de la vía de estrés ribosomal en la fisiología y en el desarrollo de cáncer.**

   3a. Generación y caracterización de un modelo de ratón con deficiencia condicional para *Rpl11*.

   3b. Análisis de los defectos en eritropoyesis tras la pérdida de un alelo de *Rpl11*.

   3c. Estudio de la implicación de un alelo de *Rpl11* en linfomagénesis.

OBJECTIVES

The main goal of this Thesis was the characterization of the ribosomal stress pathway in three different settings:

1.- Ribosome integrity in pluripotency.

1a. To study the functionality of the ribosomal stress pathway in mouse pluripotent stem cells.

2.-Non-genotoxic activation of the ribosomal stress pathway in cancer cells with small molecule compounds.

2a. Identification of novel nucleolar disruptors that trigger the ribosomal stress pathway in the absence of DNA damage in cancer cells.

2b. Characterization of the mechanism of action of the identified compounds.

3. Biological relevance of the ribosomal stress pathway in cancer and disease.

3a. Generation and characterization of a conditional knockout mouse model for *Rpl11*.

3b. Analysis of the erythropoiesis defects upon partial loss of *Rpl11*.

3c. Study of the implication of partial loss of RPL11 in lymphomagenesis.

MATERIALS AND METHODS AND RESULTS

MANUSCRIPT I

Ribosomal stress induces L11- and p53-dependent apoptosis in mouse pluripotent stem cells

Lucia Morgado-Palacin, Susana Llanos and Manuel Serrano

Cell Cycle 11:**3**, 1-8; February 1, 2012

Objetivo: ESTUDIO DE LA VIA DE ESTRES RIBOSOMAL EN CELULAS PLURIPOTENTES DE RATON

Las células madre embrionarias de ratón (mESCs, de sus siglas en inglés) se caracterizan por su alta capacidad de auto-renovación sin perder la capacidad de dar lugar a todos los linajes celulares. La tasa de crecimiento celular es muy alta en dichas células, al igual que la tasa de biogénesis ribosomal. Ambos procesos deben estar íntimamente acoplados para no interferir en las funciones celulares de las mESCs. Nosotros hipotetizamos que la vía de estrés ribosomal debe estar operativa en las mESCs para garantizar la calidad de los ribosomas y la síntesis de proteínas y así preservar la integridad genómica y correcta función de dichas células.

El supresor tumoral p53 puede activarse en mESCs en respuesta a ciertos tipos de daño en el ADN o en respuesta a estrés oxidativo. Uno de los activadores de p53 es la proteína ARF, que se une e inhibe MDM2 ante señales aberrantes de crecimiento. Sin embargo, ARF no puede operar en mESCs debido a que su promotor está silenciado epigenéticamente. Por tanto, la vía de estrés ribosomal cobra una mayor importancia en el contexto de supresión tumoral en células mESCs. En este trabajo hemos demostrado que la vía de estrés ribosomal es funcional en células madre embrionarias y en células madre pluripotentes inducidas y responde a perturbaciones en el proceso de biogénesis del ribosoma. Además, mostramos que la activación de p53 a través de la unión de RPL11 a MDM2 provoca la apoptosis de las células embrionarias pluripotentes. Nuestros resultados aportan claridad al controvertido papel de p53 en células embrionarias pluripotentes.

Cell Cycle 11:3, 1-8; February 1, 2012; © 2012 Landes Bioscience

Ribosomal stress induces L11- and p53-dependent apoptosis in mouse pluripotent stem cells

Lucia Morgado-Palacin, Susana Llanos and Manuel Serrano*

Spanish National Cancer Research Center (CNIO); Madrid, Spain

Key words: ribosomal stress, embryonic stem cells, induced pluripotent stem cells, p53, apoptosis

Ribosome biogenesis is the most demanding energetic process in proliferating cells, and it is emerging as a critical sensor of cellular homeostasis. Upon disturbance of ribosome biogenesis, specific free ribosomal proteins, most notably, L11, bind and inhibit Mdm2, resulting in activation of the tumor suppressor p53. This pathway has been characterized in somatic and cancer cells, but its function in embryonic pluripotent cells has remained unexplored. Here, we show that treatment with low doses of actinomycin D or depletion of ribosomal protein L37, two well-established inducers of ribosomal stress, activate p53 in an L11-dependent manner in mouse embryonic stem cells (ESCs) and in induced pluripotent stem cells (iPSCs). Activation of p53 results in transcriptional induction of p53 targets, including *p21*, *Mdm2*, *Pidd*, *Puma*, *Noxa* and *Bax*. Finally, ribosomal stress elicits L11- and p53-dependent apoptosis in ESCs/iPSCs. These results extend the functionality of the ribosomal stress pathway to pluripotent cells, and therefore it could be a relevant cellular checkpoint during early embryogenesis.

The p53 protein is a key tumor suppressor that is activated in response to a variety of cellular insults, triggering cellular responses that ultimately prevent the proliferation of damaged cells.[1,2] In normal cells, p53 activity is limited by the proto-oncoprotein Mdm2, an ubiquitin-ligase that targets p53 for degradation in the absence of cellular stress.[3,4] Inhibition of Mdm2 is a universal requirement for p53 activation that occurs in response to genotoxic and oncogenic stresses.[1,2] In addition, disruption of ribosomal biogenesis has recently emerged as a new p53-activating stress.[5,6] This new pathway, known as the ribosomal stress pathway, is initiated when ribosome assembly is unbalanced, which results in free ribosomal proteins that shuttle from nucleoli to the nucleoplasm.[5] Importantly, some specific free ribosomal proteins have the capacity to bind and inhibit Mdm2. In particular, L11 has been extensively reported as a main inhibitor of Mdm2.[7-10] In addition to L11, other ribosomal proteins, such as L5, L23 and S7, also have the ability to bind and inhibit Mdm2.[11-14]

During the last years, a number of human syndromes have been identified associated to deficiencies in ribosomal proteins, which are characterized by a wide range of pathologies, from bone marrow failure to craniofacial defects.[15] In addition, several animal models with ribosomal deficiencies have been reported showing a variety of phenotypes, from mild growth retardation to embryonic lethality.[16] Interestingly, most of these phenotypes can be rescued at least partially by genetic inactivation of p53, thus demonstrating in vivo the existence of a p53-dependent checkpoint that monitors the integrity of ribosome biogenesis.[16]

The ribosomal stress pathway can be experimentally induced in cultured cells by depletion of many ribosomal proteins or nucleolar components as well as by chemicals that disturb ribosome biogenesis, most notably including low doses of actinomycin D.[5] In addition, the ribosomal stress pathway is connected to the genotoxic and oncogenic p53-activating pathways. In particular, there are evidences indicating that many types of DNA damaging agents activate the ribosomal stress pathway, which contributes to the full activation of p53 in concert with the canonical DNA damage pathway.[14,17] Also, it has been recently reported in mice that oncogenic c-Myc engages the ribosomal stress pathway and contributes to activation of p53-mediated tumor suppression.[10] Therefore, the ribosomal stress pathway participates in the activation of p53 by genotoxic and by oncogenic stresses.

Mouse embryonic stem cells (ESCs) present special adaptations in their cell cycle that afford them extremely rapid proliferation rates (8–10 h per division cycle).[18,19] It is conceivable that this intense proliferative activity could render them particularly susceptible to alterations in ribosome biogenesis, which, in turn, is the most energy-consuming process in the cell (spending more than 60% of the cell resources).[6] Protein p53 is particularly abundant in ESCs compared with differentiated cells;[20] however, its functional relevance in response to stress remains to be clarified. For example, UV and oxidative damage produce p53-dependent apoptosis in ESCs,[21-23] whereas ionizing radiation or radiomimetic agents activate p53, but apoptosis occurs independently of p53.[21,24-26] Based on this, we have considered of

*Correspondence to: Manuel Serrano; Email: mserrano@cnio.es
Submitted: 12/08/11; Accepted: 12/10/11
http://dx.doi.org/10.4161/cc.11.3.19002

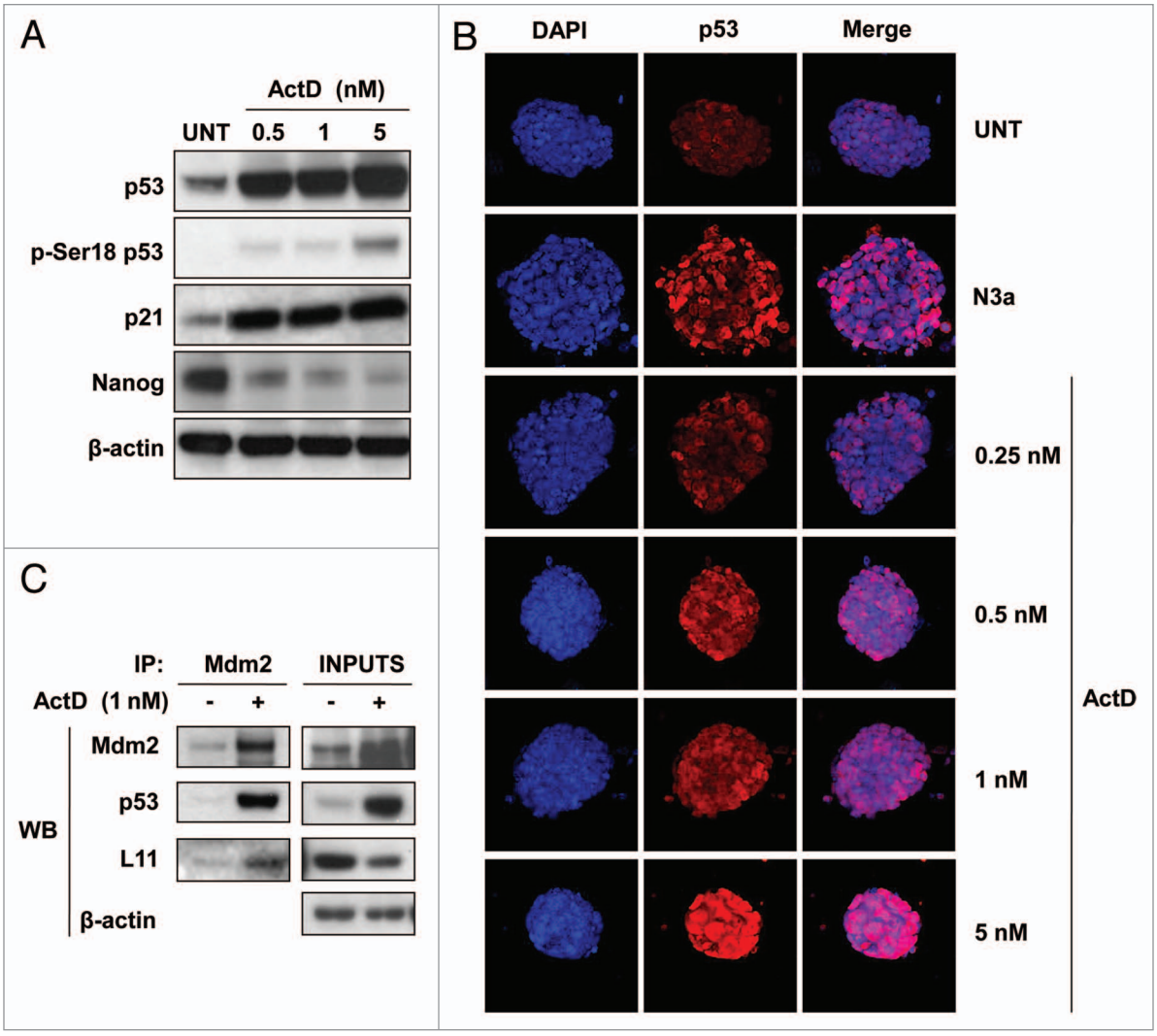

Figure 1. Actinomycin D induces binding of L11 to Mdm2. (A) ESCs were treated for 24 h with increasing concentrations of ActD. The levels of the indicated proteins were detected by immunoblotting. (B) ESCs were treated for 24 h with nutlin-3a (N3a, 5 μM), as a control for p53 activation, or with increasing concentrations of ActD, and fixed for immunofluorescence against p53. (C) ESCs were treated with 1 nM of ActD and, 6 h later, identical amounts of cellular lysates were inmunoprecipitated with anti-Mdm2 antibody. Protein levels were determined by immunobloting.

relevance to determine whether the ribosomal stress pathway is operative in mouse embryonic stem cells and whether it induces p53-dependent apoptosis.

Results

Activation of the ribosomal stress pathway by low doses of actinomycin D. It has been well-established that low doses of actinomycin D (ActD), lower than 5 nM, selectively impair the transcription of rRNAs by RNA polymerase I, thus resulting in activation of the ribosomal stress pathway.[5,7,8] We began by testing whether low doses of ActD activate p53 in mouse embryonic stem cells (ESCs). Indeed, p53 was strongly activated 24 h after treatment with 0.5 nM of ActD (**Fig. 1A**). Activation of p53 was accompanied by upregulation of its transcriptional target p21 and repression of Nanog, which is known to be repressed by p53.[27] Of note, the degree of activation of p53 was not proportional to its phosphorylation at serine 18, which is a residue normally associated with p53 activation through the DNA damage response pathway.[3] These results were confirmed by immunofluorescence on ESC colonies, where we also used nutlin-3a (N3a) as a positive control to induce the stabilization of p53 (**Fig. 1B**). It is important to mention that cells treated with low doses of ActD (0.5 nM and 1 nM) maintained normal levels of Oct4 and a normal ESC morphology, thus indicating that low doses of ActD are not producing a general loss of stemness despite the decreased levels of Nanog (**Fig. S1**). To directly implicate the ribosomal stress pathway in the stabilization of p53, we performed co-immunoprecipitation assays of endogenous Mdm2 in the absence or presence of ActD. As anticipated, in the presence of ActD the total levels of p53 were increased together with the levels of Mdm2, which is a well-established transcriptional target of p53, while the levels of L11 were not induced by ActD (**Fig. 1C**). Interestingly, the amount of L11 bound to Mdm2 was clearly increased upon

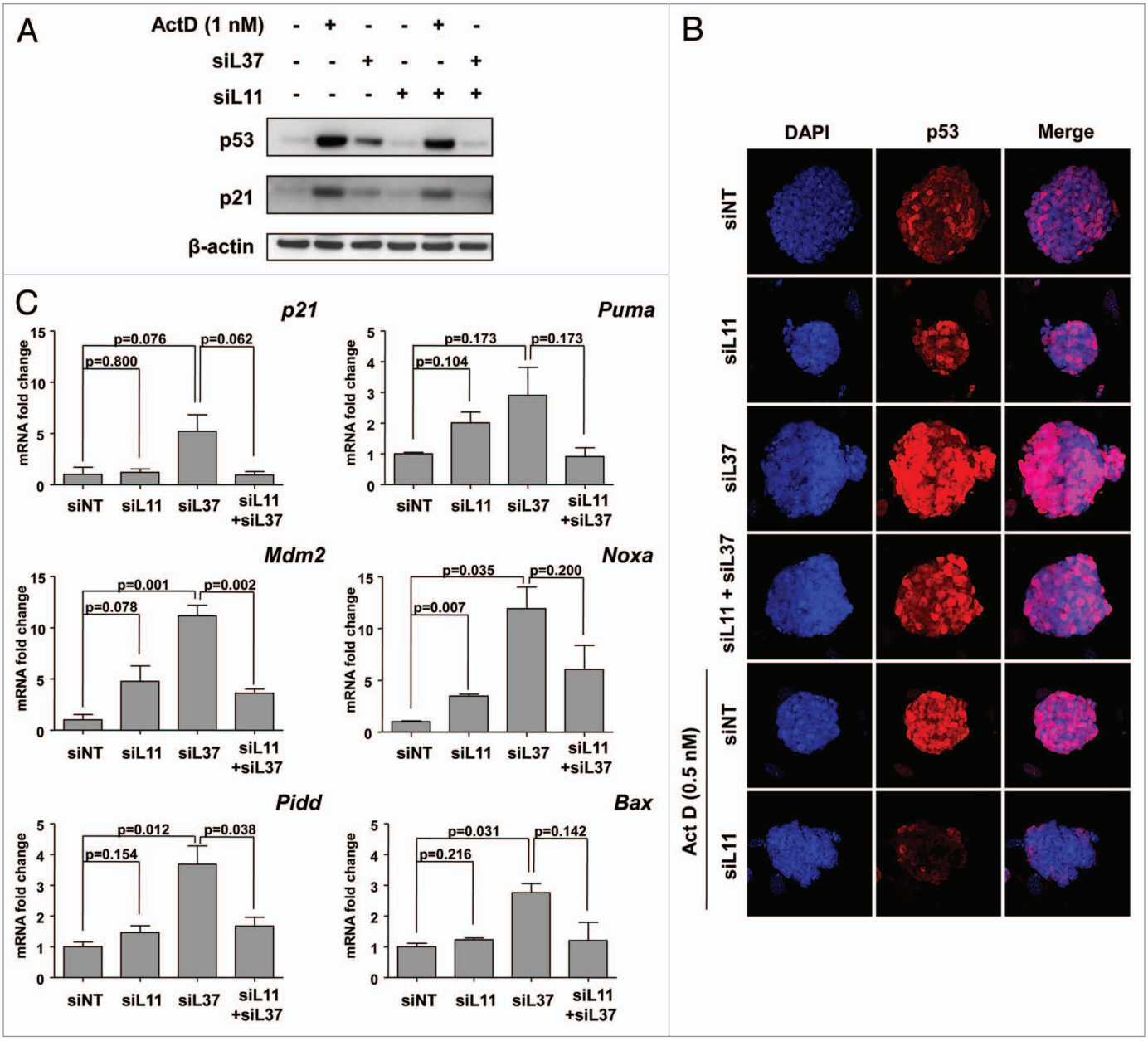

Figure 2. The ribosomal stress pathway is operative in ESCs. (A) ESCs were interfered with the indicated siRNAs for 48 h. ActD was added 32 h post-transfection and maintained o/n (16 h). Levels of the indicated proteins were determined by immunoblotting. The immunoblotting is representative of three independent experiments. (B) ESCs were transfected with the indicated siRNAs for 48 h (siNT, non-targeting siRNA) and ActD was added 32 h post-transfection and maintained o/n (16 h). Cells were fixed and immunostained for p53 and DAPI. (C) ESCs were transfected with the indicated siRNAs for 48 h and mRNA levels of the indicated genes were quantified by qRT-PCR. Values were corrected by *Gapdh* and fold change was calculated relative to siNT. Data are mean ± SD of three independent experiments. Unpaired two-tailed Student's t-test was performed and p-values of the resulting tests are indicated.

treatment with ActD (**Fig. 1C**). Similar results were obtained when cells were treated with ActD in the presence of the proteasome inhibitor MG132 (data not shown). These observations strongly suggest that low doses of ActD induce the activation of p53 in ESCs through the ribosomal stress pathway.

Activation of the ribosomal stress pathway by depletion of L37. We wanted to use a more direct inducer of ribosomal stress, and for this, we depleted the levels of the ribosomal protein L37, which engages the ribosomal stress pathway in differentiated cells.[17] Treatment of ESCs with a siRNA against L37 (siL37, for 48 h) increased p53 and p21 levels, although less efficiently than ActD (**Fig. 2A**). Importantly, concomitant inhibition of L11 cancelled the effects of siL37 on p53 and p21 and partially reverted the effects of ActD (**Fig. 2A**). These observations were corroborated by immunofluresence, where the induction of p53 by ActD or siL37 was reduced in the presence of simultaneous treatment with siL11 (**Fig. 2B**). The activation of the p53 transcriptional program by siL37-induced ribosomal

stress was documented by examining several p53 transcriptional targets, including *p21*, *Mdm2*, the Mdm2 inhibitor *Pidd*[28] and the pro-apoptotic genes *Puma, Noxa* and *Bax* (**Figs. 2C and S2**). In all these cases, induction of ribosomal stress by siL37 resulted in upregulation of the mRNA levels of these genes, and this was cancelled by the simultaneous presence of siL11 (**Fig. 2C**).

We also wanted to extend these data to induced pluripotent stem cells (iPSCs). Treatment of wild-type iPSCs with ActD or siL37 efficiently increased p53 and p21 protein levels (**Fig. 3A and B**) and the mRNA levels of *p21*, *Mdm2*, *Pidd*, *Puma, Noxa* and *Bax* (**Fig. 3C**). We also examined the antioxidant p53 targets *Sestrin1* and *Sestrin2*, although we only saw significant induction in the case of *Sestrin2* (**Fig. S3**). Importantly, all the effects of siL37 were cancelled by the concomittant presence of siL11 (**Figs. 3B and C and S3**). Moreover, we took advantage of *p53*-null iPSCs to demonstrate that the effects of ActD and siL37 were dependent on p53. As expected, *p53*-null iPSCs did not show upregulation of p21 protein levels in response to ActD or siL37 and did not show changes in the above mentioned p53 transcriptional targets (**Figs. 3A–C and S3**). Together, these results indicate that impairment of ribosome biogenesis by depletion of L37 activates the p53 transcriptional program in an L11-dependent manner.

Induction of p53-dependent apoptosis by the ribosomal stress pathway. Finally, we wanted to determine the impact of the ribosomal stress pathway on the viability of ESCs/iPSCs. We first observed that treatment of ESCs with siL37 resulted in a significant induction of apoptosis that was almost completely rescued by the simultaneous knockdown of L11 (**Fig. 4A**). Interestingly, similar results were obtained in wt iPSCs treated with ActD or with siL37, but no apoptosis was observed in *p53*-null iPSCs (**Fig. 4B**). In an attempt to determine the role of the pro-apoptotic p53-transcriptional targets, we examined *Puma*-null and *Bax*-null iPSCs. Interestingly, we did not observe ribosomal stress-induced apoptosis in *Puma*-null or in *Bax*-null iPSCs (**Fig. S4**), suggesting that these p53 transcriptional targets are relevant mediators of p53-induced apoptosis. Together, these results demonstrate that the ribosomal stress pathway induces p53-dependent apoptosis in pluripotent stem cells.

Discussion

The ribosomal stress pathway has emerged as a new p53-activating pathway, whose relevance is now firmly established.[5,6,15,16] Ribosome biogenesis is the most demanding energetic process of the cell,[6] and therefore, it is well placed to sense whether a cell is optimally fitted for intense proliferation, acting as a quality checkpoint. Embryonic pluripotent stem cells are unique because of their extremely fast proliferation rates (8–10 h), reaching cell cycles of less than 5 h in the epiblast.[18,19] However, the operation of the ribosomal stress pathway in pluripotent stem cells has remained unexplored. Moreover, the role of p53 in embryonic stem cells (ESCs) remains to be clarified, and it may depend on the particular stress or pathway that activates p53. For example, treatment of ESCs with UV or oxidative damage triggers p53-dependent apoptosis,[22,23] but ionizing radiation or radiomimetic agents activate p53 in ESCs without producing p53-dependent apoptosis.[24-26] In this context, we considered important to determine the response of pluripotent stem cells to ribosomal stress and the involvement of p53. It should be mentioned that a recent report has shown that ablation of the nucleolar protein Pict1 results in free nucleoplasmic L11 and in p53-dependent apoptosis of ESCs.[29]

Here, we demonstrate that the ribosomal stress pathway can be activated in ESCs and in induced pluripotent stem cells (iPSCs) by two standard procedures, namely, low concentrations of actinomycin D (1 nM ActD)[5] or depletion of ribosomal protein L37.[17] Activation of the pathway in ESCs results in association of the critical effector protein L11 with Mdm2, which is the hallmark of the ribosomal stress pathway responsible for the activation of p53.[5] We show that the ribosomal stress pathway in ESCs/iPSCs results in upregulation of the p53-transcriptional program, including *p21*, *Mdm2*, *Pidd*, *Puma*, *Noxa*, *Bax* and *Sestrin2*, and this transcriptional program requires L11 and p53. Finally, we demonstrate that the ribosomal stress pathway efficiently triggers apoptosis in pluripotent stem cells and this occurs in a manner dependent on L11 and p53. We also examined *Puma*-null or *Bax*-null iPSCs, and, interestingly, we did not observe ribosomal stress-induced apoptosis, suggesting that these p53 transcriptional targets are relevant mediators of p53-induced apoptosis. Collectively, these data add the ribosomal stress pathway as a relevant pathway to ensure the optimal fitness of pluripotent stem cells and identify L11 and p53 as its critical mediators. It is conceivable that the ribosomal stress pathway could constitute an important checkpoint during early embryogenesis, when pluripotent stem cells undergo an intense proliferative activity.

The fact that ESCs/iPSCs are sensitive to the ribosomal stress pathway could help to explain apparently paradoxical results about the role of p53 in ESCs. Namely, ESCs undergo p53-dependent apoptosis in response to UVC[21-23] but not in response to ionizing radiation (IR).[21,24-26] Suggestively, a key difference between these stimuli is that UVC induces ribosomal stress in cancer cells,[17,30-32] while IR does not.[32] Based on this, we speculate that the activation of the ribosomal stress pathway by UV could explain its ability to induce p53-dependent apoptosis in ESCs.

Materials and Methods

Cells and reagents. Wild-type C57BL/6 mouse ESCs (clone BL3.10) were isolated at the CNIO from blastocyst-stage embryos using established methods. ESCs were cultured on a feeder monolayer in DMEM with Glutamax, high glucose and sodium pyruvate supplemented with 10^3 U/mL LIF (ESGRO, Millipore ESG1107), 15% of fetal bovine serum (FBS), non-essential amino acids, β-mercaptoethanol and penicillin/streptomycin (all from Invitrogen). Media was replaced daily, and ESCs were passed every 2 d by trypsinization. WT, *p53*-null, *Bax*-null and *Puma*-null iPSCs were obtained from the corresponding C57BL/6 mouse embryonic fibroblasts (MEFs), respectively, by retroviral transduction with the three reprogramming factors pMXs-Sox2 (Addgene, 13367), pMXs-Oct4 (Addgene, 13366), and pMXs-Klf4 (Addgene, 13370), as previously described.[33]

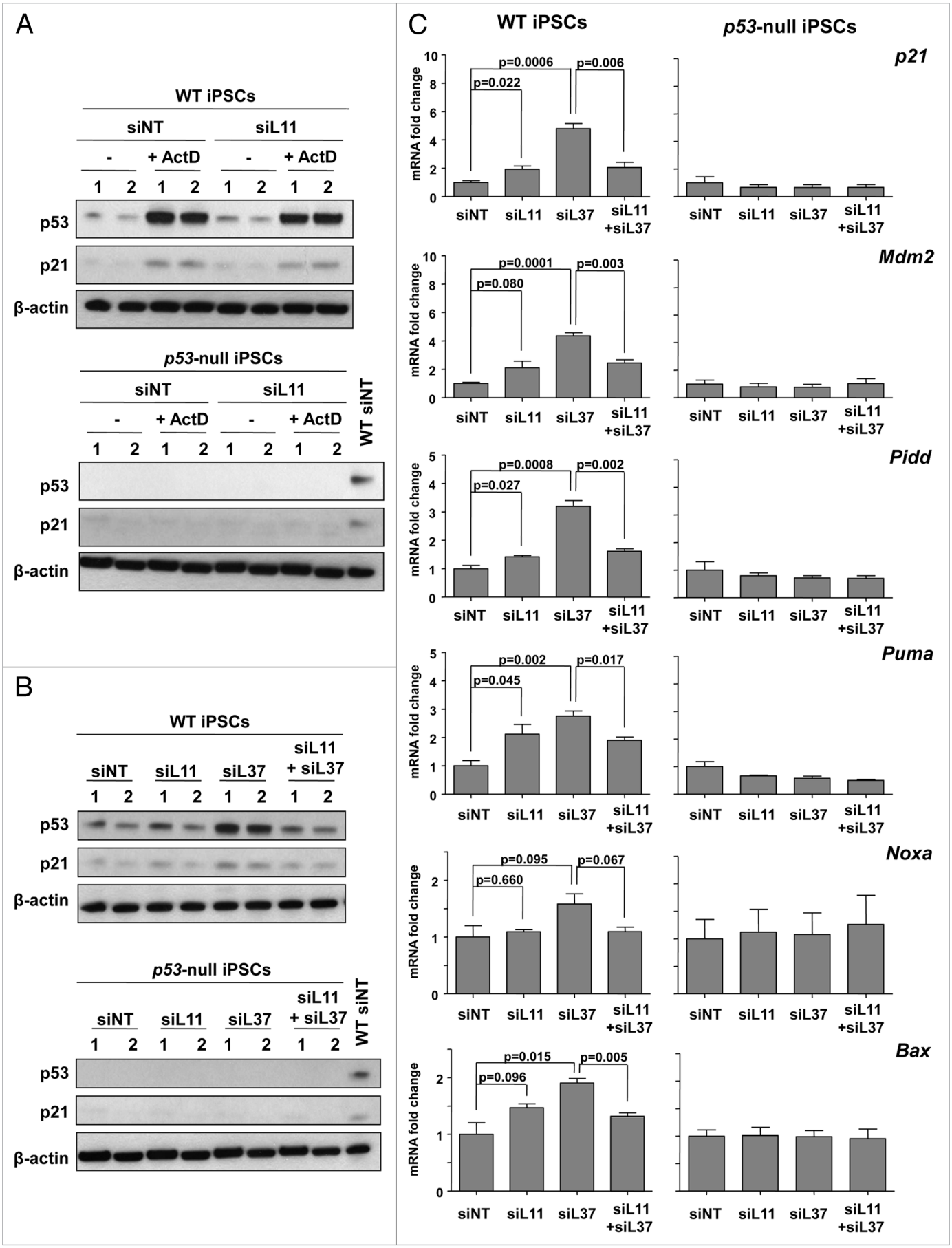
A
WT iPSCs
siNT
siL11
- + ActD - + ActD
1 2 1 2 1 2 1 2
p53
p21
β-actin
p53-null iPSCs
WT siNT
B
WT iPSCs
siNT siL11 siL37 siL11 + siL37
p53-null iPSCs
C
WT iPSCs
p53-null iPSCs
p21
Mdm2
Pidd
Puma
Noxa
Bax
mRNA fold change
p=0.0006
p=0.006
p=0.022
p=0.0001
p=0.003
p=0.080
p=0.0008
p=0.002
p=0.027
p=0.002
p=0.017
p=0.045
p=0.095
p=0.067
p=0.660
p=0.015
p=0.005
p=0.096
siNT siL11 siL37 siL11 +siL37

Figure 3. The ribosomal stress pathway is operative in iPSCs. (A) WT iPSCs clones (n = 2, upper part) and *p53*-null iPSCs clones (n = 2, bottom part) were transfected with non-targeting (NT) or L11 siRNAs and, 32 h later, cells were treated with ActD (1 nM) for an additional 16 h. Levels of the indicated proteins were detected by immunoblotting. (B) WT iPSCs clones (n = 2, upper part) and *p53*-null iPSCs clones (n = 2, bottom part) were transfected with the indicated siRNAs for 48 h. Levels of the indicated proteins were detected by immunoblotting. (C) WT or *p53*-null iPSCs were transfected with the indicated siRNAs and mRNA levels of the indicated genes were quantified by qRT-PCR. Values were corrected by *Gapdh* and fold change was calculated relative to siNT. Data are mean ± SD of three independent clones per genotype. Unpaired two-tailed Student's t-test was performed and p-values of the resulting tests are indicated.

iPSCs were cultured on feeders in the same manner as ESCs, except that 15% Knockout Serum Replacement (Invitrogen) was used instead of FBS in the culture media. Feeders were obtained from MEFs inactivated with 10 μg/mL of Mitomycin C (Sigma). ESCs/iPSCs were adapted to non-feeder conditions onto gelatin-coated plates (0.1% porcine gelatin, Sigma), previous treatment with actinomycin D (ActD) or interference with siRNA. ActD was purchased from Sigma and added at the indicated concentrations to the culture media. After 24 h, cells were harvested for protein extraction or immunofluorescence analysis.

RNA interference. ESCs/iPSCs (2.5 x 10^5 cells per 6-well plate) were transfected in suspension with 100 nM of siRNA using DharmaFECT1 (Dharmacon) and harvested 48 h later for RNA, protein extraction or immunofluorescence analysis. siRNA duplexes were purchased from Dharmacon (L37: GCG CAA GAG GAA GUA UAA C; L11 ON-TARGET plus J-064528-11-0010; and non-targeting ON-TARGET plus D-001810-01-20). ActD was added 32 h post-transfection and maintained in the culture media o/n (16 h).

Quantitative real-time PCR (qRT-PCR). Total RNA was isolated from ESCs/iPSCs using TRIzol reagent (Invitrogen) following the manufacter's instructions. Five μg of total RNA was retrotranscribed into cDNA using Ready-To-Go You-Prime First Strands beads (GE Healthcare). Real-time PCR was performed using FAST SYBR Green master mix (Applied Biosystems) in a 7500 Fast Real-Time PCR system (Applied Biosystems). All reactions were performed in triplicates and normalized to *Gapdh*, as an endogenous control. Levels of mouse mRNAs were analyzed using the following specific primers: L37-Fw, CAT CCT TTG GTA AGC GTC GCA; L37-Rv, TGG CAC TCC AGT TAT ACT TCC T; L11-Fw, ATG GCG CAA GAT CAA GGG G; L11-Rv, GAC TGT GCA GTG AAC AGC AAT; p21-Fw, GTG GGT CTG ACT CCA GCC C; p21-Rv, CCT TCT CGT GAG ACG CTT AC; Mdm2-Fw, GGT CCC TGT CCT TTG ATC CGA G; Mdm2-Rv, GCA GTG TGA TGG AAG GGG AGG A; Pidd-Fw, GGG AAC CAG TTG AAC TTG GAC; Pidd-Rv, CCG CAA AAA CTC CAC TTG CAG; Puma-Fw, AGC AGC ACT TAG AGT CGC C; Puma-Rv, CCT GGG TAA GGG GAG GAG T; Noxa-Fw, GCA GAG CTA CCA CCT GAG TTC; Noxa-Rv, CTT TTG CGA CTT CCC AGG CA; Bax-Fw, GAC AGG GGC CTT TTT GCT A; Bax-Rv, TGT CCA CGT CAG CAA TCA TC; Sesn1-Fw, GTC TGG ATA ACA TCA CAT TAG; Sesn1-Rv, CCA GGT AGG AAC ACT GAT GC; Sesn2-Fw, CTC ACA GCT GGT CTG TGT G; Sesn2-Rv, CCT CCG TGT GGC AAT ACC; Gapdh-Fw, TTC ACC ACC ATG GAG AAG GC; Gapdh-Rv, CCC TTT TGG CTC CAC CCT.

Immunoblotting. Cells were harvested after ActD treatment or siRNA transfection in RIPA buffer. Identical amounts of whole lysates were resolved in 4–12% SDS/PAGE gels (NuPAGE Invitrogen) and transferred to nitrocellulose membranes. Blots were incubated with the primary antibodies anti-p53 (1C12, Cell Signaling), anti-phosphoSer18 p53 (Cell Signaling, 9284), anti-p21 (C-19, SCBT), anti-Nanog (Millipore, AB5731), anti-β-actin (AC-15, Sigma), and subsequently incubated with the corresponding secondary anti-IgG HRP antibodies (DAKO). Blots were developed with ECL (Amersham).

Immunofluorescence. ESCs/iPSCs (1 x 10^5 cells per 24-well plate) were seeded on a feeder monolayer onto glass coverslips and treated with ActD or transfected in suspension for siRNA interference. Cells were fixed at 24 or 48 h with 4% paraformaldehyde for 15 min and permeabilized with 0.1% Triton X-100 30 min. Then, cells were blocked in 5% BSA during 1 h at R.T. and incubated o/n at 4°C with the primary antibodies anti-p53 (1C12, Cell Signaling), anti-Nanog (NOVUS, NB100-588), or anti-Oct3/4 (BD Biosciences, 611203). Alexa-555 or Alexa-488 conjugated goat anti-mouse or anti-rabbit antibodies (Molecular Probes) were used for detection of the reported proteins by confocal microscopy. Nuclei were counterstained with DAPI bath and coverslips mounted with ProLong (Molecular Probes). Sections of 1 μm were acquired with a Leica TCS-SP5 multiphoton confocal microscope.

Immunoprecipitation. ESCs grown on gelatin were treated with ActD (1 nM) for 6 h and subsequently collected for immunoprecipitation. Endogenous Mdm2 was immunoprecipitated with 5 μg of antibody to Mdm2 (SMP14, Santa Cruz) and TrueBlot anti-mouse IgG beads (eBioscience) starting from 1 mg of whole lysate. The immuprecipitated proteins were detected with a monoclonal antibody to Mdm2 (2A10, Abcam), a monoclonal antibody to p53 (1C12, Cell Signaling), a polyclonal antibody to L11 (SCBT catalog #25931) and a monoclonal antibody to β-actin (AC-15, Sigma). TrueBlot anti-mouse IgG (eBiosciences) and anti-goat IgG HRP (DAKO) were used as secondary antibodies for detection of proteins with ECL (Amersham). Forty μg of whole lysates were loaded as inputs.

Annexin V staining. ESCs/iPSCs were collected for Annexin V staining 48 h after siRNA transfection. Cells were trypsinized, washed once in cold PBS at 1,500 rpm for 5 min and then resuspended in 300 μL of Annexin V binding buffer 1x (BD Pharmigen). Three μL of FITC-Annexin V (BD Pharmigen) were added, and cells were incubated in dark for 15 min. Then, cells were stained with 2 μL of DAPI and, at least, 10,000 events were analyzed by flow cytometry on a LSR-Fortessa (BD Biosciences) with FACSDiva software. Early-stage apoptotic cells were quantified as FITC-Annexin V positive (+) DAPI negative (-) with the FlowJo 7.6.1. program.

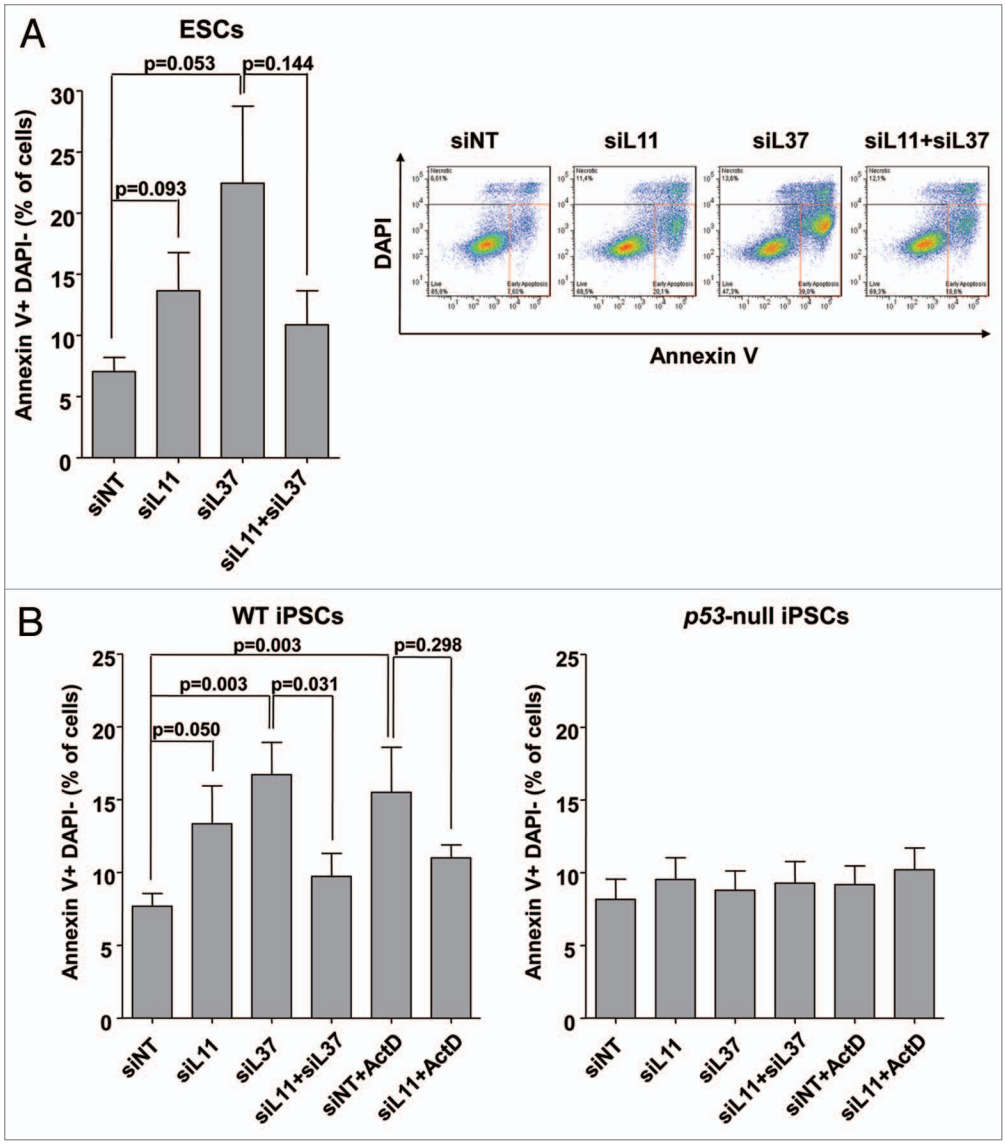

Figure 4. The ribosomal stress pathway induces p53-dependent apoptosis in ESCs and iPSCs. (A) ESCs were transfected with the indicated siRNAs for 48 h and early-stage apoptotic cells were quantified by FACS analysis as Annexin V positive (+) DAPI negative (-). Data are mean ± SD of four independent experiments. Early-stage apoptotic cell population is labeled inside the red box (right part; representative FACS profiles). (B) WT and *p53*-null iPSCs were transfected with the indicated siRNAs for 48 h or treated with ActD o/n 32 h post-transfection. Early-stage apoptotic cells were measured as in (A). Data are mean ± SD of five independent clones per genotype. Unpaired two-tailed Student's t-test was performed and p-values of the resulting tests are indicated.

Disclosure of Potential Conflicts of Interest

No potential conflicts of interest were disclosed.

Acknowledgements

We thank Maria Abad (CNIO) for helping us with the generation of iPSCs and the Flow Cytometry and Confocal Microscopy Units of the CNIO for technical help. L.M.P. is supported by a predoctoral fellowship from the Spanish Ministry of Education. Work in the laboratory of M.S. is funded by the CNIO and by grants from the Spanish Ministry of Science (SAF and CONSOLIDER), the European Research Council (ERC Advanced Grant), and the "Marcelino Botin" Foundation.

Note

Supplemental materials can be found at:
www.landesbioscience.com/journals/cc/article/19002

References

1. Junttila MR, Evan GI. p53—a Jack of all trades but master of none. Nat Rev Cancer 2009; 9:821-9; PMID:19776747; http://dx.doi.org/10.1038/nrc2728.
2. Meek DW. Tumour suppression by p53: a role for the DNA damage response? Nat Rev Cancer 2009; 9:714-23; PMID:19730431.
3. Kruse JP, Gu W. Modes of p53 regulation. Cell 2009; 137:609-22; PMID:19450511; http://dx.doi.org/10.1016/j.cell.2009.04.050.
4. Marine JC, Lozano G. Mdm2-mediated ubiquitylation: p53 and beyond. Cell Death Differ 2010; 17:93-102; PMID:19498444; http://dx.doi.org/10.1038/cdd.2009.68.
5. Zhang Y, Lu H. Signaling to p53: ribosomal proteins find their way. Cancer Cell 2009; 16:369-77; PMID:19878869; http://dx.doi.org/10.1016/j.ccr.2009.09.024.
6. Deisenroth C, Zhang Y. Ribosome biogenesis surveillance: probing the ribosomal protein-Mdm2-p53 pathway. Oncogene 2010; 29:4253-60; PMID:20498634; http://dx.doi.org/10.1038/onc.2010.189.
7. Lohrum MA, Ludwig RL, Kubbutat MH, Hanlon M, Vousden KH. Regulation of HDM2 activity by the ribosomal protein L11. Cancer Cell 2003; 3:577-87; PMID:12842086; http://dx.doi.org/10.1016/S1535-6108(03)00134-X.
8. Zhang Y, Wolf GW, Bhat K, Jin A, Allio T, Burkhart WA, et al. Ribosomal protein L11 negatively regulates oncoprotein MDM2 and mediates a p53-dependent ribosomal-stress checkpoint pathway. Mol Cell Biol 2003; 23:8902-12; PMID:14612427; http://dx.doi.org/10.1128/MCB.23.23.8902-8912.2003.
9. Fumagalli S, Di Cara A, Neb-Gulati A, Natt F, Schwemberger S, Hall J, et al. Absence of nucleolar disruption after impairment of 40S ribosome biogenesis reveals an rpL11-translation-dependent mechanism of p53 induction. Nat Cell Biol 2009; 11:501-8; PMID:19287375; http://dx.doi.org/10.1038/ncb1858.
10. Macias E, Jin A, Deisenroth C, Bhat K, Mao H, Lindström MS, et al. An ARF-independent c-MYC-activated tumor suppression pathway mediated by ribosomal protein-Mdm2 Interaction. Cancer Cell 2010; 18:231-43; PMID:20832751; http://dx.doi.org/10.1016/j.ccr.2010.08.007.
11. Dai MS, Lu H. Inhibition of MDM2-mediated p53 ubiquitination and degradation by ribosomal protein L5. J Biol Chem 2004; 279:44475-82; PMID:15308643; http://dx.doi.org/10.1074/jbc.M403722200.
12. Jin A, Itahana K, O'Keefe K, Zhang Y. Inhibition of HDM2 and activation of p53 by ribosomal protein L23. Mol Cell Biol 2004; 24:7669-80; PMID:15314174; http://dx.doi.org/10.1128/MCB.24.17.7669-7680.2004.
13. Chen D, Zhang Z, Li M, Wang W, Li Y, Rayburn ER, et al. Ribosomal protein S7 as a novel modulator of p53-MDM2 interaction: binding to MDM2, stabilization of p53 protein and activation of p53 function. Oncogene 2007; 26:5029-37; PMID:17310983; http://dx.doi.org/10.1038/sj.onc.1210327.
14. Zhu Y, Poyurovsky MV, Li Y, Biderman L, Stahl J, Jacq X, et al. Ribosomal protein S7 is both a regulator and a substrate of MDM2. Mol Cell 2009; 35:316-26; PMID:19683495; http://dx.doi.org/10.1016/j.molcel.2009.07.014.
15. Narla A, Ebert BL. Ribosomopathies: human disorders of ribosome dysfunction. Blood 2010; 115:3196-205; PMID:20194897; http://dx.doi.org/10.1182/blood-2009-10-178129.
16. Caldarola S, De Stefano MC, Amaldi F, Loreni F. Synthesis and function of ribosomal proteins—fading models and new perspectives. FEBS J 2009; 276:3199-210; PMID:19438715; http://dx.doi.org/10.1111/j.1742-4658.2009.07036.x.
17. Llanos S, Serrano M. Depletion of ribosomal protein L37 occurs in response to DNA damage and activates p53 through the L11/MDM2 pathway. Cell Cycle 2010; 9:4005-12; PMID:20935493; http://dx.doi.org/10.4161/cc.9.19.13299.
18. White J, Dalton S. Cell cycle control of embryonic stem cells. Stem Cell Rev 2005; 1:131-8; PMID:17142847; http://dx.doi.org/10.1385/SCR:1:2:131.
19. Ballabeni A, Park IH, Zhao R, Wang W, Lerou PH, Daley GQ, et al. Cell cycle adaptations of embryonic stem cells. Proc Natl Acad Sci USA 2011; 108:19252-7; PMID:22084091; http://dx.doi.org/10.1073/pnas.1116794108.
20. Sabapathy K, Klemm M, Jaenisch R, Wagner EF. Regulation of ES cell differentiation by functional and conformational modulation of p53. EMBO J 1997; 16:6217-29; PMID:9321401; http://dx.doi.org/10.1093/emboj/16.20.6217.
21. Corbet SW, Clarke AR, Gledhill S, Wyllie AH. P53-dependent and -independent links between DNA-damage, apoptosis and mutation frequency in ES cells. Oncogene 1999; 18:1537-44; PMID:10102623; http://dx.doi.org/10.1038/sj.onc.1202436.
22. Chao C, Saito S, Kang J, Anderson CW, Appella E, Xu Y. p53 transcriptional activity is essential for p53-dependent apoptosis following DNA damage. EMBO J 2000; 19:4967-75; PMID:10990460; http://dx.doi.org/10.1093/emboj/19.18.4967.
23. Han MK, Song EK, Guo Y, Ou X, Mantel C, Broxmeyer HE. SIRT1 regulates apoptosis and Nanog expression in mouse embryonic stem cells by controlling p53 subcellular localization. Cell Stem Cell 2008; 2:241-51; PMID:18371449; http://dx.doi.org/10.1016/j.stem.2008.01.002.
24. Aladjem MI, Spike BT, Rodewald LW, Hope TJ, Klemm M, Jaenisch R, et al. ES cells do not activate p53-dependent stress responses and undergo p53-independent apoptosis in response to DNA damage. Curr Biol 1998; 8:145-55; PMID:9443911; http://dx.doi.org/10.1016/S0960-9822(98)70061-2.
25. Qin H, Yu T, Qing T, Liu Y, Zhao Y, Cai J, et al. Regulation of apoptosis and differentiation by p53 in human embryonic stem cells. J Biol Chem 2007; 282:5842-52; PMID:17179143; http://dx.doi.org/10.1074/jbc.M610464200.
26. Solozobova V, Rolletschek A, Blattner C. Nuclear accumulation and activation of p53 in embryonic stem cells after DNA damage. BMC Cell Biol 2009; 10:46; PMID:19534768; http://dx.doi.org/10.1186/1471-2121-10-46.
27. Lin T, Chao C, Saito S, Mazur SJ, Murphy ME, Appella E, et al. p53 induces differentiation of mouse embryonic stem cells by suppressing Nanog expression. Nat Cell Biol 2005; 7:165-71; PMID:15619621; http://dx.doi.org/10.1038/ncb1211.
28. Oliver TG, Meylan E, Chang GP, Xue W, Burke JR, Humpton TJ, et al. Caspase-2-mediated cleavage of Mdm2 creates a p53-induced positive feedback loop. Mol Cell 2011; 43:57-71; PMID:21726810; http://dx.doi.org/10.1016/j.molcel.2011.06.012.
29. Sasaki M, Kawahara K, Nishio M, Mimori K, Kogo R, Hamada K, et al. Regulation of the MDM2-p53 pathway and tumor growth by PICT1 via nucleolar RPL11. Nat Med 2011; 17:944-51; PMID:21804542; http://dx.doi.org/10.1038/nm.2392.
30. Rubbi CP, Milner J. Disruption of the nucleolus mediates stabilization of p53 in response to DNA damage and other stresses. EMBO J 2003; 22:6068-77; PMID:14609953; http://dx.doi.org/10.1093/emboj/cdg579.
31. Kurki S, Peltonen K, Latonen L, Kiviharju TM, Ojala PM, Meek D, et al. Nucleolar protein NPM interacts with HDM2 and protects tumor suppressor protein p53 from HDM2-mediated degradation. Cancer Cell 2004; 5:465-75; PMID:15144954; http://dx.doi.org/10.1016/S1535-6108(04)00110-2.
32. Al-Baker EA, Boyle J, Harry R, Kill IR. A p53-independent pathway regulates nucleolar segregation and antigen translocation in response to DNA damage induced by UV irradiation. Exp Cell Res 2004; 292:179-86; PMID:14720517; http://dx.doi.org/10.1016/j.yexcr.2003.09.006.
33. Li H, Collado M, Villasante A, Strati K, Ortega S, Cañamero M, et al. The Ink4/Arf locus is a barrier for iPS cell reprogramming. Nature 2009; 460:1136-9; PMID:19668188; http://dx.doi.org/10.1038/nature08290.

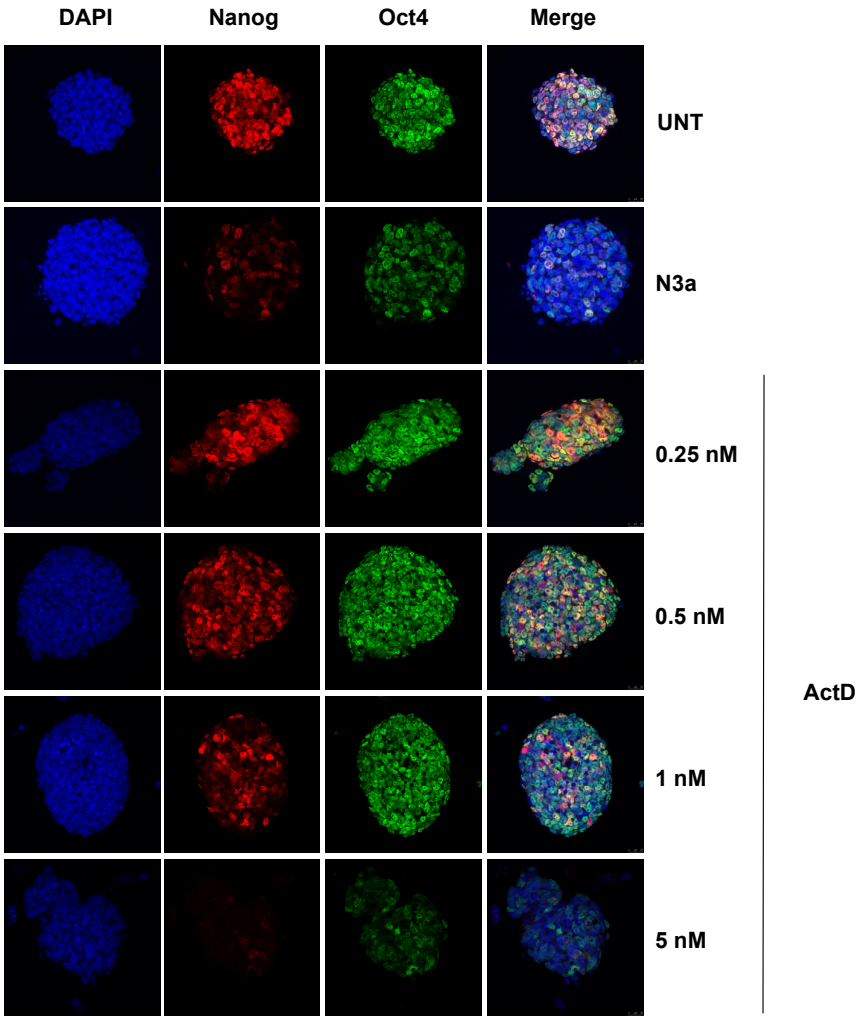

Supplementary Figure S1

ESCs treated as in **Figure 1** of the main paper for 24 h with Nutlin-3a (N3a, 5 μM), as control for p53 activation, or increasing concentrations of ActD, then, cells were fixed and stained for Nanog (red) and Oct4 (green) to evaluate stemness integrity.

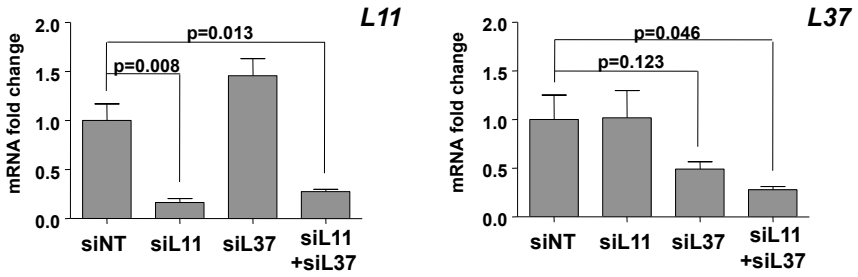

Supplementary Figure S2

ESCs were transfected with the indicated siRNAs and efficiency of the knockdown for L11 and L37 genes was measured by qRT-PCR. Values were corrected by *Gapdh* and fold change was calculated relative to siNT. Data are mean ±SD of three independent experiments (those corresponding to **Figure 2A-C**). Unpaired two-tailed Student's *t*-test was performed and p-values of the resulting tests are indicated.

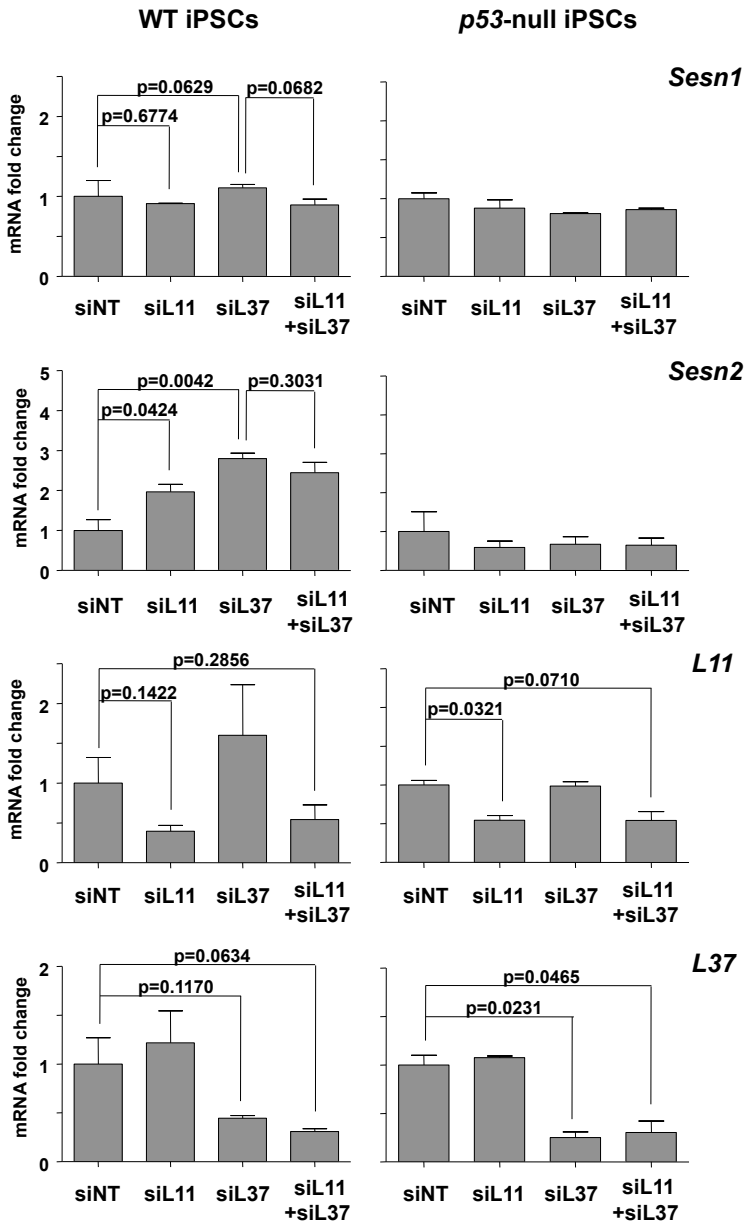

Supplementary Figure S3

WT or *p53*-null iPSCs were transfected with the indicated siRNAs for 48 h and mRNA levels of the indicated genes were quantified by qRT-PCR. Values were corrected by *Gapdh* and fold change was calculated relative to siNT. Data are mean ±SD of three independent clones per genotype. Unpaired two-tailed Student's *t*-test was performed and p-values of the resulting tests are indicated.

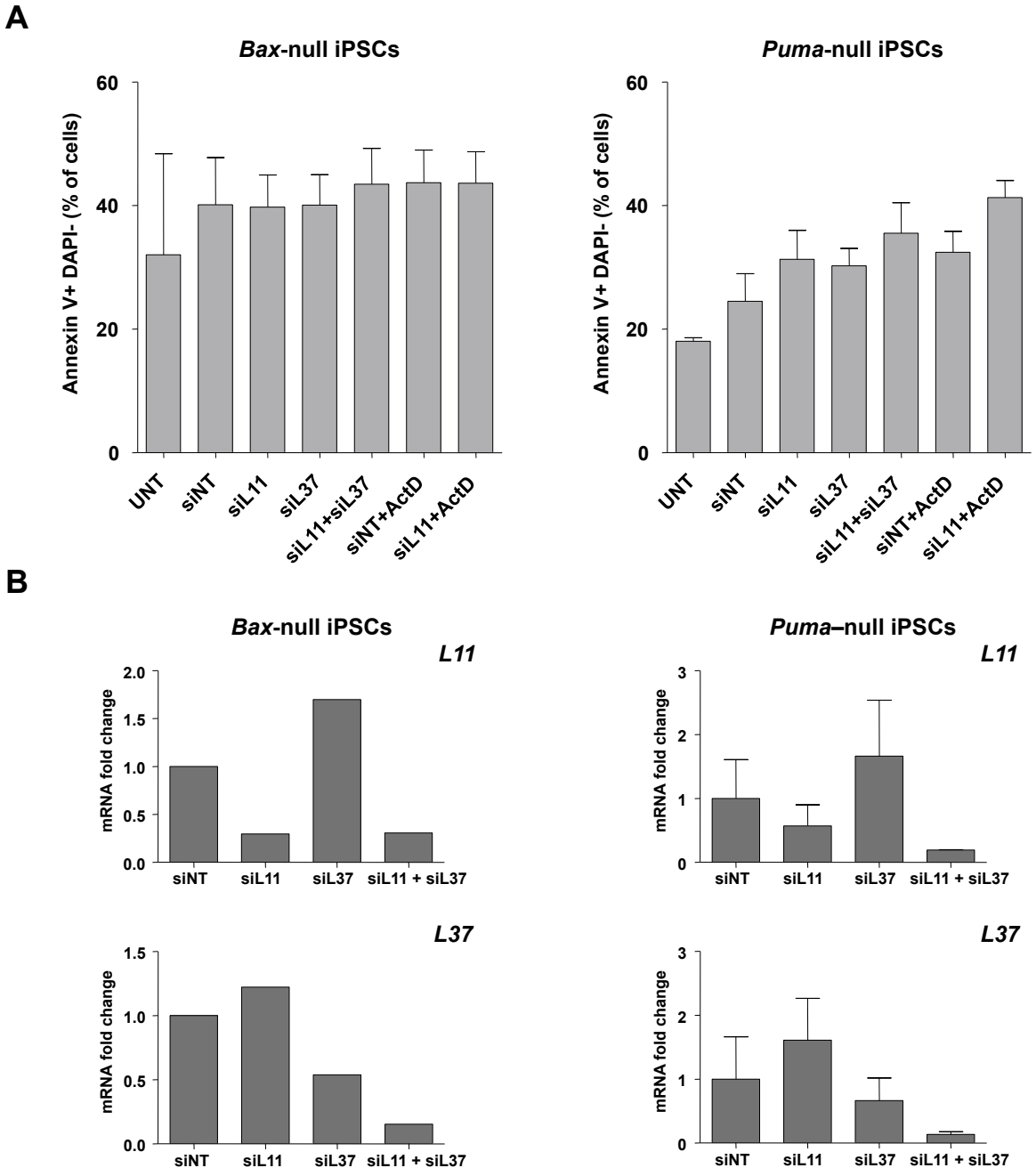

Supplementary Figure S4

(A) *Bax*-null and *Puma*-null iPSCs were interfered with the indicated siRNAs for 48 h, and ActD (1 nM) was added 32 h post-transfection and maintained in the culture media o/n (16 h). Early-stage apoptotic cells were measured by FACS as Annexin V positive (+) DAPI negative (-). Data are mean ±SD of two independent clones per genotype.

(B) *Bax*-null and *Puma*-null iPSCs were interfered with the indicated siRNAs for 48 h, and levels of L11 and L37 mRNA were quantified by qRT-PCR to check the knockdown efficiency.

MANUSCRIPT II

Non-genotoxic activation of p53 through the RPL11-dependent ribosomal stress pathway

Lucia Morgado-Palacin, Susana Llanos, Manuel Urbano-Cuadrado, Carmen Blanco-Aparicio, Diego Megias, Joaquín Pastor and Manuel Serrano

Carcinogenesis 35:**12**, 2822-2830; October 24, 2014

Objetivo: IDENTIFICACIÓN DE NUEVOS AGENTES DISRUPTIVOS DEL NUCLEOLO PARA ELIMINAR CELLULAR TUMORALES A TRAVÉS DE LA VÍA DE ESTRÉS RIBOSOMAL

Las células tumorales dependen de elevados niveles de biogénesis ribosomal para satisfacer las altas demandas energéticas que implica su mayor tasa de síntesis proteica. La biogénesis ribosomal tiene lugar en el nucleolo. Perturbaciones de la integridad nucleolar activan p53 a través de la vía de estrés ribosomal (RPL11/RPL5-MDM2-p53), resultando en la parada o apoptosis de las células tumorales. Muchos de los agentes quimioterapéuticos empleados para el tratamiento del cáncer han sido seleccionados por su capacidad de causar daño genotóxico, aunque posteriormente se ha demostrado que muchos de ellos causan además estrés ribosomal. El daño genotóxico sistémico que suponen los tratamientos quimioterapeúticos es responsable de la alta incidencia de cáncer de novo en los pacientes tratados. Sería ideal disponer de drogas quimioterapeúticas que activen p53 y que no produzcan daños en el ADN.

El objetivo de este trabajo ha sido la identificación de nuevos agentes disruptivos de nucleolo que activaran p53 en ausencia de de daño detectable en el ADN. Para ello, hemos diseñado un cribado de sustancias químicas en células de osteosarcoma que expresan la construcción GFP-RPL37. La proteína ribosomal L37 (RPL37, de sus siglas en inglés) se acumula en el nucleolo y nos sirve para monitorizar su estructura. Los candidatos de dicho cribado han sido seleccionados en base a su potencia para generar pérdida de la integridad nucleolar. Entre ellos, hemos caracterizado el mecanismo de acción de un grupo de derivados de acridinas, los cuales inhiben la transcripción mediada por la ARN polimerasa I, encargada de la síntesis de ARN ribosomales. La inhibición de la transcripción de ARN ribosomales causa la pérdida de la integridad del nucleolo y esto conlleva la activación de p53 a través de la unión de RPL11 a MDM2. Es reseñable el hecho de que la activación de p53 ocurre en ausencia de daño detectable en el DNA y sin embargo es capaz de causar la muerte celular de las diferentes líneas tumorales evaluadas.

Carcinogenesis vol.35 no.12 pp.2822–2830, 2014
doi:10.1093/carcin/bgu220
Advance Access publication October 24, 2014

Non-genotoxic activation of p53 through the RPL11-dependent ribosomal stress pathway

Lucia Morgado-Palacin, Susana Llanos, Manuel Urbano-Cuadrado[1], Carmen Blanco-Aparicio[1], Diego Megias[2], Joaquín Pastor[1] and Manuel Serrano*

Tumour Suppression Group, [1]Experimental Therapeutics Program and [2]Confocal Microscopy Unit, Spanish National Cancer Research Centre (CNIO), Madrid, E28029, Spain

*To whom correspondence should be addressed. Tel: +34 91 7328000; Fax: +34 91 2246980;
Email: mserrano@cnio.es

Nucleolar disruption has recently emerged as a relevant means to activate p53 through inhibition of HDM2 by ribosome-free RPL11. Most drugs that induce nucleolar disruption also possess important genotoxic activity, which can have lasting mutagenic effects. Therefore, it is of interest to identify compounds that selectively produce nucleolar disruption in the absence of DNA damage. Here, we have performed a high-throughput screening to search for nucleolar disruptors. We have identified an acridine derivative (PubChem CID-765471) previously known for its capacity to activate p53 independently of DNA damage, although the molecular mechanism underlying p53 activation had remained uncharacterized. We report that CID-765471 produces nucleolar disruption by inhibiting ribosomal DNA transcription in a process that includes the selective degradation of the RPA194 subunit of RNA polymerase I. Following nucleolar disruption, CID-765471 activates p53 through the RPL11/HDM2 pathway in the absence of detectable DNA damage. In a secondary screening of compounds approved for medical use, we identify two additional acridine derivatives, aminacrine and ethacridine, that operate in a similar manner as CID-765471. These findings provide the basis for non-genotoxic chemotherapeutic approaches that selectively target the nucleolus.

Introduction

Highly proliferative cells have an enormous demand of ribosome biogenesis (1). The relevance of monitoring ribosome biogenesis is highlighted by the fact that there is a dedicated molecular pathway connecting ribosomal perturbations with p53 (2). In particular, unbalanced ribosome assembly results in free preribosomal complex RPL11/RPL5/5SrRNA, which binds and inhibits HDM2, thereby resulting in stabilization and activation of p53 (3–6). Increasing experimental and mutational data supports the relevance of this pathway for cancer protection. In mice, a genetically engineered mutant HDM2 that cannot bind RPL11 and RPL5 results in failure to sense ribosomal unbalances and favors cMyc-driven lymphoma (7). In humans, RPL5 is somatically mutated in a small percentage of glioblastomas (3% [8]) and T-cell leukemias (2% [9]); and RPL11 is mutated in endometrial cancers (2%) (http://icgc.org). When analysed, these cancer-associated mutations have been found in heterozygosis (9), consistent with the fact that RPL11 and RPL5 are essential for cell viability (10) and suggesting that a partial decrease in their levels is sufficient to favor cancer. Indeed, patients with germline heterozygous mutations in ribosomal genes have an increased incidence of cancer (11). Impaired activity of the ribosomal stress pathway can be advantageous to cancer cells because it partially alleviates surveillance of ribosome integrity by p53. According to this rationale, the ribosomal stress pathway has emerged as an attractive target for p53 activation and cancer therapy (12).

Most genotoxic chemotherapeutic agents not only produce DNA damage, but also produce ribosomal stress, which is often visualized by the disruption of nucleoli (12–15). Accordingly, genotoxic drugs activate p53 through two simultaneous pathways, namely, the DNA damage response (DDR) pathway and the ribosomal stress pathway (16–18). Despite its undeniable benefits, genotoxic chemotherapy has serious drawbacks, most prominently the mutational load imposed on surviving cells and the ensuing risk of *de novo* tumorigenesis. In this regard, it is of high interest to identify chemotherapeutic agents that activate p53 without producing DNA damage. Here, we perform a drug screening to search for compounds that activate p53 through the ribosomal stress pathway and in the absence of detectable DNA damage.

Abbreviations: ActD, actinomycin D; CNIO, Spanish National Cancer Research Centre; DAPI, 4′,6-diamidino-2-phenylindole; DDR, DNA damage response; DMSO, dimethyl sulfoxide; NPM, nucleophosmin; PBS, phosphate-buffered saline.

Materials and methods

Cell culture and drugs

Cell lines U2OS (human osteosarcoma), its derivative expressing GFP-RPL37 (U2OS/GFP-RPL37 [16]), and HCT116 (human colon carcinoma) p53WT and p53KO (19) were maintained in DMEM, supplemented with 10% fetal bovine serum and antibiotic-antimicotic (all from Gibco), and incubated in 20% O_2 and 5% CO_2 at 37°C. Human cell lines were purchased from ATCC and were authenticated after completion of this work. Cell line authentication was performed by analysing a total of 10 microsatellites at the authentication service (Genomic Unit) of the Institute of Biomedical Research 'Alberto Sols' in Madrid. CID-765471 (2,4,7,9-tetramethylbenzo[b][1,8] naphthyridin-5-amine), actinomycin D (ActD), doxorubicin (Doxo), nutlin-3 (N3), MG132 (proteosome inhibitor) and hydroxyurea (HU) were purchased from Sigma. Aminacrine and ethacridine lactate were purchased from Selleckchem. The ataxia telangiectasia and Rad3-related protein inhibitor (ETP-46464 [20]) was obtained from the Spanish National Cancer Research Centre (CNIO). For those assays using cyclohexamide (CHX), cells were treated with 20 µM CHX (Sigma) during the indicated time.

High-throughput screening

We tested two libraries of chemical compounds. The first library (CNIO-640 library) comprises 640 compounds representative of the full collection (50 000 compounds) of the Experimental Therapeutics Programme at the Spanish National Cancer Research Centre (CNIO). The second library was acquired from the Johns Hopkins University (Johns Hopkins Clinical Compound Library or JHCCL, version 1.3) and comprises 1524 compounds approved for medical use. U2OS cells expressing GFP-RPL37 (U2OS/GFP-RPL37) were seeded in cell-carrier black 384-well microplates (Perkin Elmer) at a density of 5000 cells per well 24 h before adding the compounds. Compounds were weighed out and diluted with dimethyl sulfoxide (DMSO) to a final concentration of 10 mM. From here, a 'mother plate' was prepared at 80× the final concentration in the culture, resulting the final concentration of DMSO in the tissue culture media in 1.25%. Viability of cells was previously tested in a dose curve with increasing concentrations of DMSO. The appropriate volume of the compound solution (1.5 µl) was added automatically (Beckman FX 96 tip) to media to make it up to the final concentration (5 µM) for each drug. This concentration was assayed in triplicate. After 4.5 h of incubation with the compounds, cells were fixed in 4% paraformaldehyde in phosphate-buffered saline (PBS) for 15 min at room temperature and washed three times with PBS. The last wash of PBS was left in the wells to prevent drying of cells, and microplates were sealed with aluminium adhesive foil to avoid fading away of GFP fluorescence. Those compounds that killed cells at 5 µM for 4.5 h were retested at a lower concentration (2.5 µM). For the validation assays, two different U2OS/GFP-RPL37 clones were seeded in µClear black 96-well microplates (Greiner Bio-One) at a density of 25 000–30 000 cells per well in triplicates, and they were assessed at 5 µM and 2.5 µM in the case of the CNIO-640 library or at 5 µM in the case of the JHCCL screening for 4.5 h. 384-well and 96-well microplates were run in the Opera High Content Screening (HCS) system (Perkin Elmer) by taking images of 27 or 42 random fields per well, respectively, with a ×20 magnification lens. Images were then analysed with Definiens Developer XD software by using a morphology-based script that classifies nucleoli (defined by GFP signal) in two classes depending on

their roundness (>0.15 as irregular, 'normal', and ≤0.15 as round, 'disrupted', spots). At least, 5000 nucleoli per well were analysed. After classification, the average of normal and disrupted nucleoli per well was calculated to assign a 'nucleolar disruption score' (ratio between the number of disrupted and normal nucleoli). The Z'-factor to statistically measure the assay quality of the screening was calculated as defined $(1 - 3 \times (\sigma_p + \sigma_n)/|\mu_p - \mu_n|$ where σ_p and σ_n are the standard deviations of the positive and negative controls, and μ_p and μ_n are the means of the positive and negative controls), taking the nucleolar disruption score of ActD-treated cells as the positive control and DMSO-treated cells as the negative control. Z'-factor was 0.65 for the screen.

RNA extraction and quantitative real-time PCR

Total RNA was isolated from cells using TRI-reagent (Sigma) following the manufacturer's instructions. 2.5 µg of total RNA was reverse transcribed into cDNA using iScript Advanced First Strand cDNA synthesis kit (BioRad). Real-time PCR was performed using FAST SYBR Green master mix (Applied Biosystems) in a 7500 Fast Real-Time PCR (Applied Biosystems). All reactions were performed in triplicates and normalized to β-*Actin* mRNA levels as an endogenous control. Sequences of the human primers used for quantitative real-time PCR in this work are listed: *P21*-Fw: 5′-GAT TAG CAG CGG AAC AAG GAG T-3′, *P21*-Rv: 5′-TAC AGT CTA GGT GGA GAA ACG GG-3′; *HDM2*-Fw: 5′-TAC AGG GAC GCC ATC GAA TC-3′, *HDM2*-Rv: 5′-TGA AGT GCA TTT CCA ATA GTC AGC-3′; *GADD45A*-Fw: 5′-GGC TGG AGA GCA GAA GAC CGA A-3′, *GADD45A*-Rv: 5′-CTG ACG CGC AGG ATG TTG ATG-3′; *BAX*-Fw: 5′-CTC AGG ATG CGT CCA CCA AGA A-3′, *BAX* -Rv: 5′-CTC CCG GAG GAA GTC CAA TGT C-3′; *ITS1 rRNA*-Fw: 5′-AGT CGG GTT GCT TGG GAA TG-3′, *ITS1 rRNA*-Rv: 5′-GAC ACG CCC TTC TTT CTC TC-3′; *5S rRNA*-Fw: 5′-GTC TAC GGC CAT ACC ACC CTG-3′, *5S rRNA*-Rv: 5′-AAA GCC TAC AGC ACC CGG TAT-3′; *UBF*-Fw: 5′-GGC CAG ATG CCA CTA CGA-3′, *UBF*-Rv: 5′-CTC CAG GGC CTT ATG AAT CCA-3′; *Nucleolin*-Fw: 5′-ACC CAG GGG ATC ACC TAA TG-3′, *Nucleolin*-Rv: 5′-CCT TTG GAG GAC CCA GTT TC-3′; *NPM1*-Fw: 5′-GTA CAG CCA ACG GTA A-3′, *NPM1*-Rv: 5′-AGA CCG CTT TCC AGA T-3′; β-*Actin* Fw: 5′-GGC ACC ACA CCT TCT ACA ATG-3′, β-*Actin*-Rv: 5′-GTG GTG GTG AAG CTG TAG CC-3′.

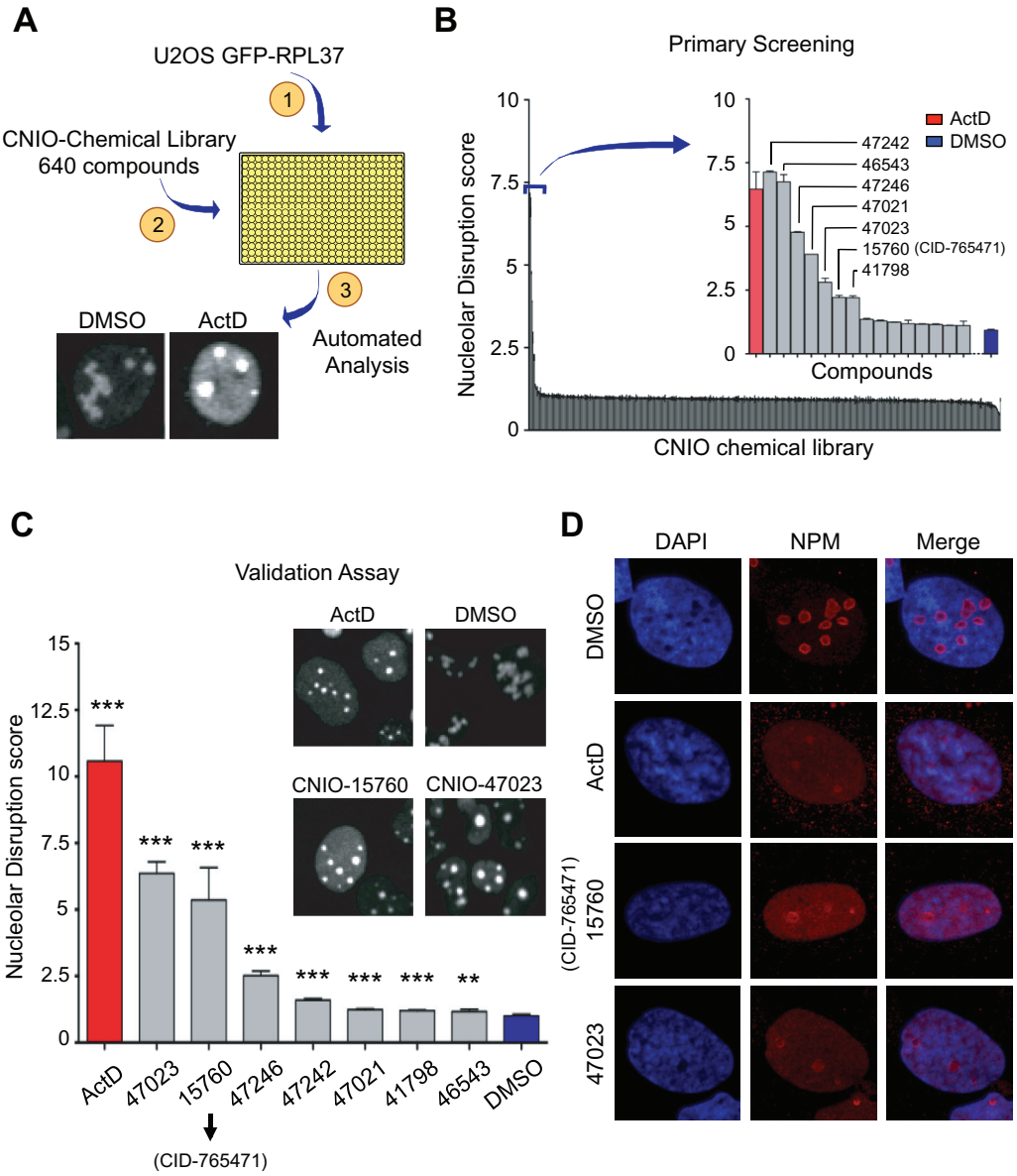

Fig. 1. A cell-based high-content screen for nucleolar disruptors. (**A**) Outline of the screening. (**B**) Result of the primary screening with 640 compounds (all at 5 µM for 4.5 h) in 384-well microplates. A zoom in of the 15 best-scored compounds is shown at the right top corner. Values correspond to the average ± SD of technical triplicates (n=3). CNIO compound 15760 corresponds to CID-765471. (**C**) Validation of the primary hits in a secondary screen in 96-well microplates. Compounds were tested in triplicates (all at 5 µM for 4.5 h) in two different clones of U2OS/GFP-RPL37 cells. Values correspond to the average ± SD of the two biological replicates (n=2) normalized to DMSO treatment. Statistical significance was calculated by the Student's t-test: $^{**}P \leq 0.01$; $^{***}P \leq 0.005$. Representative images of the GFP fluorescence. (**D**) Immunofluorescence of NPM, which marks the granular component of nucleoli, 72 h after treatment of U2OS cells with ActD (5 nM) or the indicated CNIO compounds (5 µM).

Northern Blot analysis of pre-RNA intermediates

U2OS cells were treated for 6 h with the indicated compounds and then collected and processed for isolation of total RNA by using TRI-reagent (Sigma) and following the manufacturer's instructions. 3 µg of total RNA, resuspended in formamide, were loaded into a 1.2% MOPS/formaldehyde agarose gel and run in the same buffer at 30V o/n. RNAs were transferred to a Hybond N+ nylon membrane (Amersham) and fixed by UV cross-linking. Membranes were prehybridized and incubated with the 5′ITS1 (5′-CCT CGC CCT CCG GGC TCC GTT AAT GAT C-3′) and ITS2 (an equal amount of 5′- CTG CGA GGG AAC CCC CAG CCG CGC A-3′ and 5′-GCG CGA CGG CGG ACG ACA CCG CGG CGT C-3′) probes as described (21).

RNA interference

U2OS cells were plated the day before of transfection. siRNA duplexes (Dharmacon) against a non-targeting sequence (ON-TARGET plus D-001810-01-20) or human RPL11 (sequence: 5′- AAG GUG CGG GAG UAU GAG UUA UU-3′) were added at 100 nM by using DharmaFECT1 (Dharmacon), and transfection media was replaced 24 h later by fresh media containing the corresponding drugs. Cells were incubated with the corresponding drugs for additional 24 h and then collected for immunoblotting. For the lentiviral assay, we used MISSION non-target shRNA control SHC016 and MISSION shRNA against RPL11 clone ID: NM_000975.2-287s1c1 (sequence: 5′- CCG GGC GGG AGT ATG AGT TAA GAA A-3′).

Immunoblotting

Cells were harvested after treatment with the indicated compounds or siRNA transfection in RIPA buffer. Identical amounts of whole lysates were resolved in 4–12% SDS/PAGE gels (NuPAGE Invitrogen) and transferred to nitrocellulose membranes. Blots were incubated with the primary antibodies anti-p53 (DO-1, SCBT), anti-p21 (C-19, SCBT), anti-HDM2 (clone SMP14, SCBT), anti-RPL11 (Proteintech), anti-RPA194 (H-300, SCBT), anti-RPA135 (H-15, SCBT), anti-NPM (7H10B9, NOVUS Biologicals), anti-β-actin (AC-15, Sigma), and subsequently incubated with the corresponding secondary anti-IgG HRP antibodies. For uncropped images of the blots and links to the commercial antibodies, see Supplementary Figure 7, available at *Carcinogenesis* online.

Immunofluorescence

Cells were plated onto glass coverslips or Greiner Bio-One µClear black 96-well plate (7.5×10^4 cells per well) and treated with the indicated drugs for 6 or 72 h. Then, cells were fixed with 4% paraformaldehyde for 15 min, permeabilized with 0.1% Triton X-100 for 30 min and blocked in 5% bovine serum albumin during 1 h at room temperature. Incubation with primary antibodies against fibrillarin (C13C3, Cell Signaling), nucleophosmin (NPM) (7H10B9, NOVUS Biologicals), p53 (DO-1, SCBT),or γH2A.X Ser139 (JBW301, Millipore) were carried out o/n at 4°C. Alexa-555 or Alexa-488 conjugated anti-mouse or anti-rabbit antibodies (Molecular Probes) were used for detection of the reported proteins by confocal microscopy. Nuclei were counterstained with 4′,6-diamidino-2-phenylindole (DAPI) bath. In the case of coverslips, samples were mounted with ProLong and sections of 1 µm were acquired with a ×40 magnification lens in a Leica TCS-SP5 (WLL) multiphoton confocal microscope. A total of 27 fields per well were acquired with a ×40 magnification lens for those samples run in the Opera HCS system (Perkin Elmer). In the case of p53 and γH2A.X, images were segmented using the DAPI staining to generate masks matching cell nuclei from which fluorescence intensity signals were calculated by using Acapella High Content Imaging and Analysis software (Perkin Elmer). In the case of nucleophosmin, images were segmented using the DAPI staining and the coefficient of variation of nucleophosmin intensity per nucleus was calculated using Definiens Developer XD software.

Immunoprecipitation

U2OS cells were treated with CID-765471 (5 and 10 µM) for 24 h and with MG132 (25 µM) during 3 h before collecting them. RPL11 was immunprecipitated with 5 µg of antibody to RPL11 (Proteintech) and TrueBlot anti-rabbit IgG beads (eBioscience) starting from 1 mg of whole lysate. The immunoprecipitated proteins were detected with a monoclonal antibody to HDM2 (clone SMP14, SCBT) and a polyclonal antibody to RPL11 (Proteintech). TrueBlot anti-rabbit IgG (eBiosciences) and anti-mouse IgG HRP (DAKO) were used as secondary antibody for detection of proteins with ECL (Amersham). Twenty micrograms of whole lysates were loaded as input.

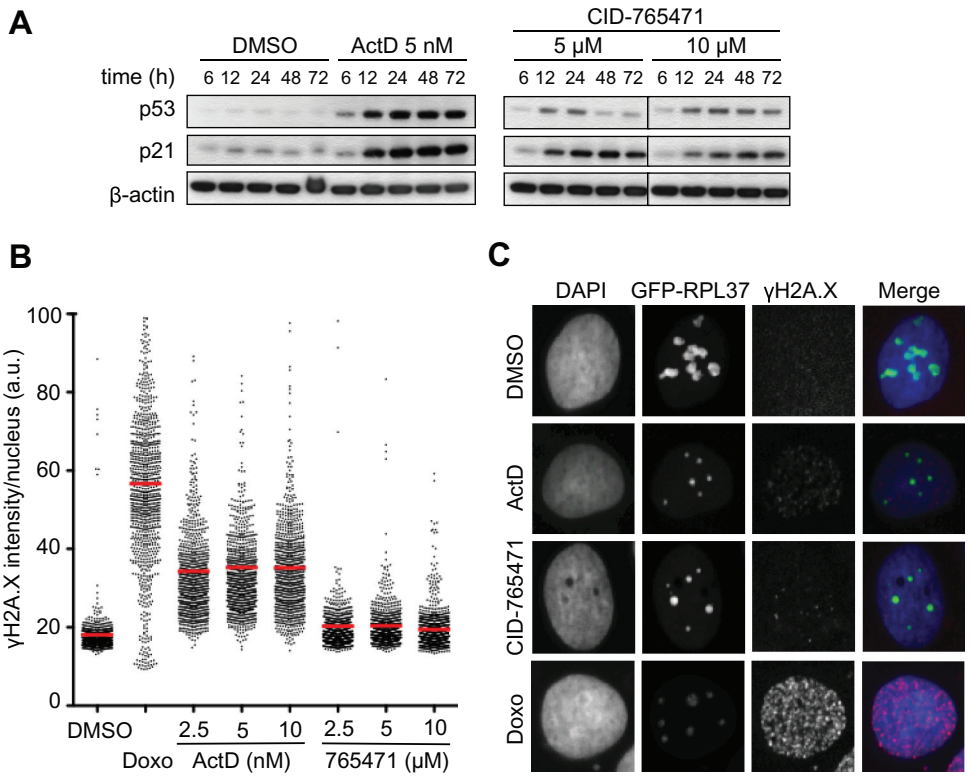

Fig. 2. CID-765471 activates p53 in the absence of DNA damage. (**A**) U2OS cells were treated as indicated and protein levels of p53 and p21 were measured by immunoblotting. β-actin was used as a loading control. (**B**) Quantification of γH2A.X immunofluorescence in U2OS/GFP-RPL37 cells treated with the indicated compounds for 6 h (doxorubicin is abbreviated as Doxo). Immunofluorescence was quantified by high-throughput microscopy (each dot corresponds to a single nucleus). At least, 900 nuclei were quantified per condition. (**C**) Representative images of γH2A.X immunofluorescence in U2OS/GFP-RPL37 cells treated with the indicated compounds (ActD at 5 nM, CID-765471 at 5 µM and Doxorubicin, as Doxo, at 1 µM).

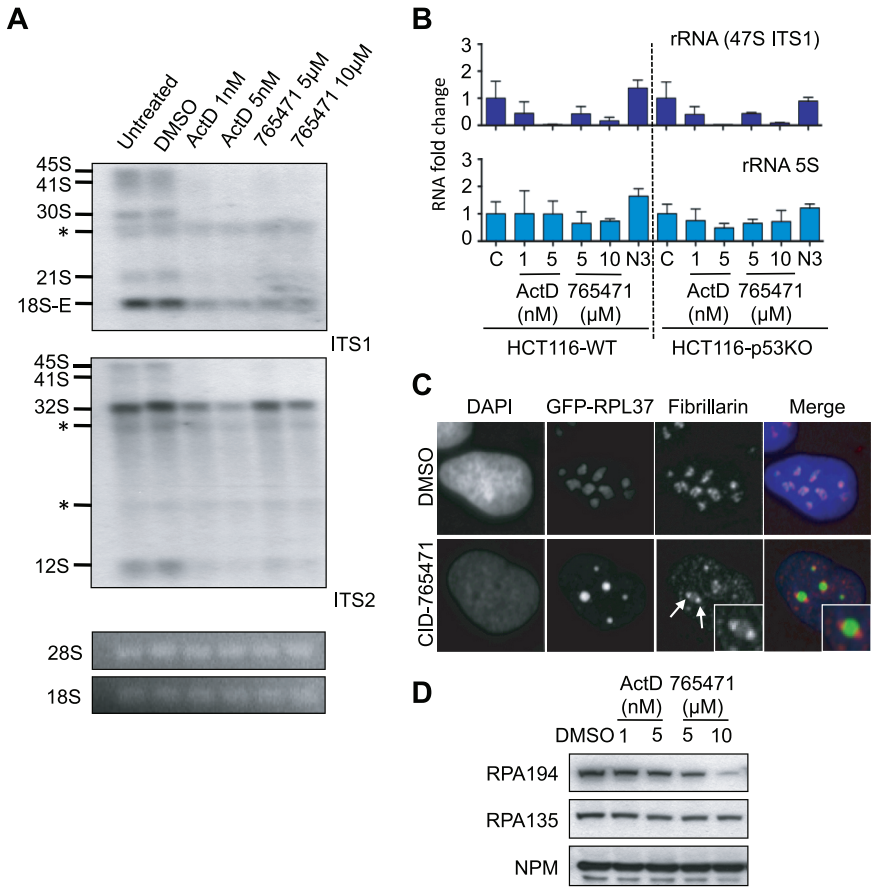

Fig. 3. CID-765471 inhibits ribosomal DNA transcription. (**A**) Northern blot analysis of pre-rRNA intermediates in U2OS cells treated with the indicated compounds for 6 h. Probes against ITS1 or ITS2 regions were used to identify all the intermediates, as indicated to the left (asterisks correspond to non-specific signals). Mature 28S and 18S rRNA levels were detected by staining with ethidium bromide. This Northern blot is representative of two independent assays. (**B**) RNA levels of 47S ITS1 (RNA pol I-transcribed) and 5S rRNA (RNA pol III-transcribed) were measured by quantitative real time PCR in HCT116-WT and HCT116-p53KO cells treated as indicated for 24 h. Nutlin-3 (N3) was used at 20 μM, as a positive control for p53 activation. Values correspond to the average ± SD of two independent assays (n=2). (**C**). Immunofluorescence of fibrillarin in U2OS/GFP-RPL37 cells after treatment (6 h) with CID-765471 (5 μM). In normal cells (DMSO treated), fibrillarin marks the dense fibrillar center of nucleoli and coincides with GFP-RPL37. Upon nucleolar disruption, fibrillarin segregates and forms the so-called fibrillarin caps around the remaining central body of nucleoli (containing GFP-RPL37). (**D**) RPA194 and RPA135 protein levels were measured by immunoblotting following the indicated treatments for 24 h. The immunoblot is representative of three independent assays.

Flow cytometry assays

For flow cytometry assays, 3×10^5 or 5×10^5 of U2OS or HCT116 (p53WT or p53KO) cells, respectively, were seeded in multi six-well plates and compounds were added the following day or 24 h after RNA interference. For cell cycle profiles, cells were collected 24 h after addition of compounds and fixed in 70% EtOH o/n, washed twice in PBS and stained in propidium iodide solution (25 μg/ml, Sigma, in PBS) with RNase A (0.2 mg/ml, Qiagen) for 3–4 h. About 20 000 events were at least acquired with FACS Calibur (BD Bioscience; FACSDiva software) and data were analysed with FlowJo 9.6.2 software. For apoptosis experiments, cells were collected 96 h after addition of compounds, washed once in cold PBS (1500 r.p.m. for 5 min) and incubated in TMRE (30 nM in PBS) for 10 min at 37°C in waterbath (protecting samples from light). Then, cells were spun down and incubated in dark for 20 min at room temperature in 300 μl of Annexin V binding buffer with 3 μl of APC-Annexin (BD Pharmigen). DAPI was used as viability marker. At least 10 000 events were collected in LSR-Fortessa (BD Biosciences; FACSDiva software) and apoptotic cells were quantified as DAPI negative (-) TMRE negative (-) APC-Annexin V positive (+) with FlowJo 9.6.2 software.

Results

High-content screening for drugs that induce nucleolar disruption

Ribosomal proteins accumulate in nucleoli when they are newly synthesized (22) and associate to precursor rRNAs (23). We took advantage of U2OS cells stably expressing the ribosomal protein L37 (RPL37) fused to GFP (16) to monitor nucleolar integrity in a high-content screen based on automated confocal microscopy. In the absence of nucleolar stress, GFP-RPL37 marks foci of irregular shape and rough borders (Figure 1A), which correspond to nucleoli as demonstrated by their colocalization with fibrillarin and NPM (Supplementary Figure 1A and B, available at *Carcinogenesis* online). Shortly upon treatment with ActD, a well-characterized nucleolar disruptor (13,15), the GFP-RPL37 signal became compacted and rounded (Figure 1A) and nucleolar proteins changed their localizations: fibrillarin segregated into caps around the GFP-RPL37 foci and NPM mislocalized over the nucleoplasm (Supplementary Figure 1A and B, available at *Carcinogenesis* online). All these changes constitute hallmarks of nucleolar disruption (24). Several parameters were tested to quantify nucleolar disruption, including fluorescence intensity, and we found that the morphological change was the most robust feature altered upon loss of nucleolar integrity. Changes in nucleolar morphology were quantified with a 'roundness' algorithm that classified nucleoli into two classes: irregular or rounded (Supplementary Figure 1C, available at *Carcinogenesis* online). This served as the basis to calculate the ratio between disrupted (rounded) and normal (irregular) nucleoli in a given cell population and we refer to this ratio as 'nucleolar disruption score'.

In agreement with previous reports (15), we observed that nucleolar disruption by ActD occurs very rapidly, reaching a maximum in 1 h and being stably maintained for at least 6 h (Supplementary Figure 1D, available at *Carcinogenesis* online). Based on this, we set the readout

of our screening at 4.5 h after addition of the compounds to the cells. We tested an in-house made library of 640 compounds chosen to cover a large chemical space (CNIO-640 chemical library). This primary screening on U2OS/GFP-RPL37 cells yielded seven hits with high nucleolar disruption scores (Figure 1B) and two of them were confirmed in a subsequent validation assay (Figure 1C). Compound CNIO-15760 (which we will refer to by its PubChem identifier CID-765471) and CNIO-47023 also induced nucleolar disruption in parental U2OS cells (not carrying GFP-RPL37), as demonstrated by the dissolution of NPM foci (Figure 1D), and nucleolar disruption was detectable at least 22 h after treatment (not shown). These two compounds presented a similar dose-response profile at μM range, being CID-765471 more efficient than CNIO-47023 (Supplementary Figure 1E, available at *Carcinogenesis* online). Based on the better capacity of CID-765471 to induce nucleolar disruption, we focus hereafter on this compound.

CID-765471 activates p53 in the absence of DNA damage

Nucleolar disruption by ActD or other chemotherapeutic agents results in the activation of the tumour suppressor p53 (13,15). As expected, CID-765471 also increased p53 and p21 levels (Figure 2A and Supplementary Figure 2A and B, available at *Carcinogenesis* online). Interestingly, CID-765471, an acridine derivative whose chemical structure is 2,4,7,9-tetramethylbenzo[b][1,8] naphthyridin-5-amine, had been previously identified in two screenings for p53-activating compounds under the names of BMH-22 (25) and SID-17433115 (26). Also, acridine and a number of derivatives closely related to CID-765471 have been found to be efficient activators of p53 (27). As suggested by their planar heteroaromatic ring structure, acridine derivatives are DNA intercalating agents and indeed CID-765471 has been directly demonstrated to intercalate into DNA (25). Many DNA intercalators carry reactive groups and are genotoxic, thereby efficiently triggering a DDR and activating p53. Intriguingly, however,

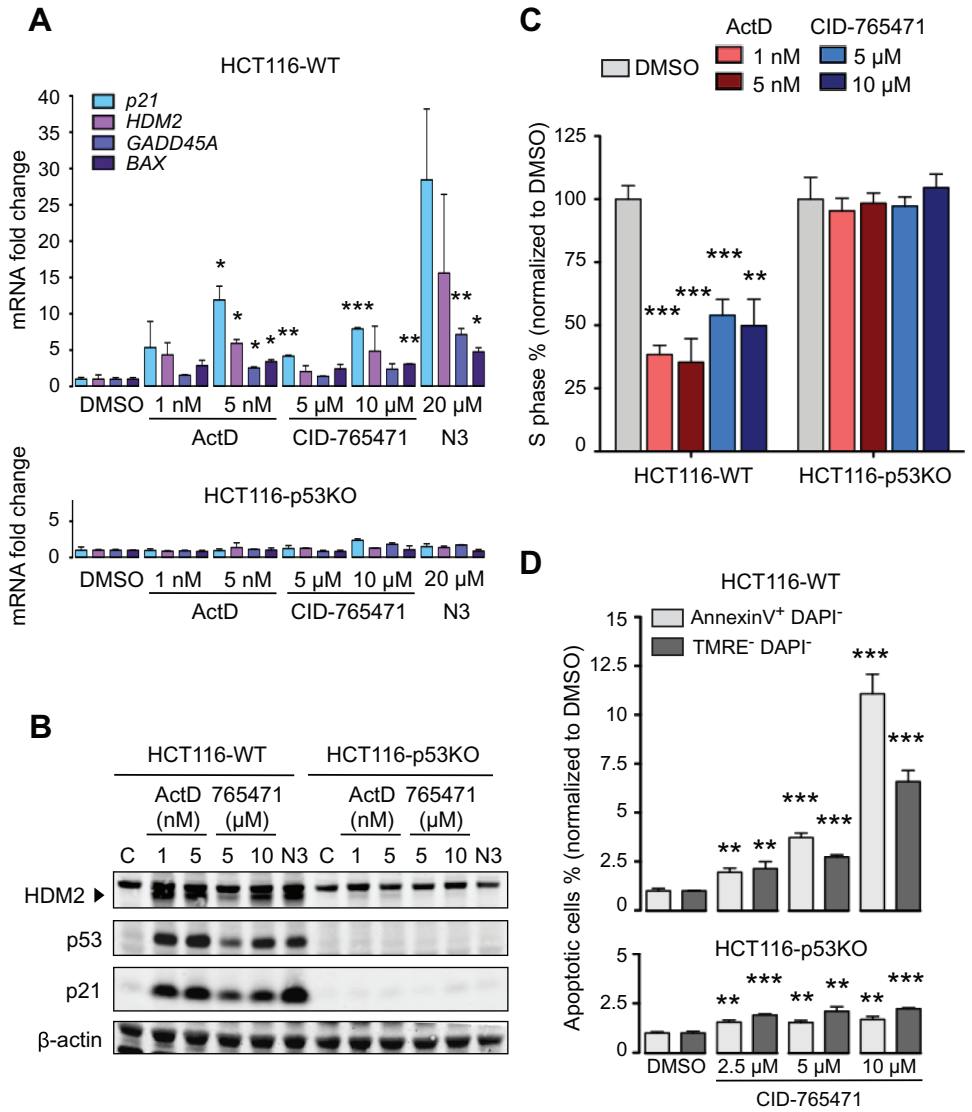

Fig. 4. CID-765471 activates a p53-dependent transcriptional program. (**A**) Transcriptional activation of p53 target genes measured by quantitative real-time PCR after the indicated treatments, for 24 h. N3 corresponds to Nutlin-3. All mRNA levels were normalized by the endogenous β-actin mRNA levels. Fold induction is relative to negative controls (DMSO treatment). Values correspond to the average ± SD of two independent assays (n=2). (**B**) Protein levels of the indicated p53 targets detected by immunoblotting. The upper band in the HDM2 immunoblot is non-specific; the specific band is indicated with an arrowhead. This immunoblot is representative of a total of two independent assays. (**C**) Percentage of cells in S phase after the indicated treatments, for 24 h. S phase was measured by flow cytometry of propidium iodide-stained cells. Data correspond to one assay representative of four independent assays. Each assay was performed in triplicates. (**D**) Percentage of apoptotic cells after the indicated treatments, for 96 h. Apoptotic cells were measured by flow cytometry using two stainings, AnnexinV or TMRE, in viable cells (DAPI-negative). Data correspond to one assay representative of a total of two independent assays. Each assay was performed in triplicates. All values correspond to the average ± SD. Statistical significance was calculated by the Student's t-test: *$P \leq 0.05$; **$P \leq 0.01$; ***$P \leq 0.005$.

some acridine derivatives and, in particular, CID-765471 have been reported to activate p53 in the absence of genotoxic damage and independently of the DDR pathway (25–27). We wanted to confirm if this was the case in our experimental system. In agreement with the above-mentioned reports, we did not observe γH2A.X foci, indicative of DNA damage, in cells treated with CID-765471 (Figure 2B and C). In contrast to this, non-intercalating genotoxic agents that efficiently activate the DDR and p53, such as ataxia telangiectasia and Rad3-related protein inhibitors or hydroxyurea, were unable to produce nucleolar disruption (Supplementary Figure 2C, available at *Carcinogenesis* online). These observations support the notion than nucleolar stress can be triggered in the absence of genotoxic damage.

CID-765471 inhibits rDNA transcription

Previous studies have indicated that DNA intercalators cause nucleolar disruption by inhibiting rDNA transcription by RNA polymerase I (15). Based on our nucleolar disruption screen, we hypothesized that CID-765471 could cause nucleolar disruption in association with inhibition of rDNA transcription. Northern blot analysis of rRNA from U2OS cells treated with ActD or CID-765471 revealed that both drugs dramatically reduced the levels of the longest rRNA intermediate (45S) and its smaller derivatives (Figure 3A). These results were confirmed by quantitative real-time PCR amplification of the internally transcribed spacer 1 (ITS1) present in 45S and in many of its derivatives (Figure 3B). Of note, no effect was observed on the levels of 5S rRNA (transcribed by RNA polymerase III), neither on the mRNA levels of three important regulators of ribosome biogenesis (transcribed by RNA polymerase II), namely, *UBF*, *nucleolin* and *NPM1* (Supplementary Figure 3, available at *Carcinogenesis* online). Additionally, the inhibition of RNA polymerase I-mediated rDNA transcription by ActD and CID-765471 does not appear to be secondary to p53 because activation of p53 with nutlin-3 (N3) did not affect ITS1-containing transcripts (Figure 3B). Moreover, immunofluorescence of fibrillarin, which localizes in the dense fibrillar center in normal conditions, revealed that treatment with CID-765471 provokes its segregation to nucleolar caps (Figure 3C), which is a hallmark of rDNA transcriptional inhibition (24).

While this work was in preparation, another non-genotoxic acridine derivative, BMH-21, was reported to produce nucleolar disruption and to inhibit RNA polymerase I in a process that includes the degradation of RPA194, an essential and specific subunit of the RNA polymerase I (28). Of note, nucleolar disruption by ActD is not accompanied by the degradation of RPA194 (28). In agreement with the above, RPA194 protein levels were remarkably diminished following treatment with CID-765471, but not with ActD (Figure 3D). As a control, the levels of RPA135, which strongly interacts with RPA194 (29), remained stable (Figure 3D). Collectively, these findings support the notion that the primary effect of CID-765471 is to inhibit RNA polymerase I-mediated rDNA transcription.

CID-765471 induces p53-dependent transcription

To investigate whether CID-765471 initiates a p53-dependent transcriptional program, we tested the effects of this compound on well-established p53 transcriptional targets. Treatment with CID-765471 and ActD strongly increased *p21* mRNA levels in WT, but not in p53KO, HCT116 cells (Figure 4A). A similar trend was observed for p53-transcriptional targets *HDM2*, *GADD45A* and *BAX* (Figure 4A). No changes were observed in the levels of *p53* mRNA (data not shown). In agreement with the above, protein levels of p21 and HDM2 were also significantly increased after treatment with ActD or CID-765471 in a p53-dependent manner (Figure 4B).

To explore the cellular consequences of CID-765471-mediated p53 activation, we analysed the cell cycle profiles of cells treated with this compound. We observed that ActD and CID-765471 significantly decreased the percentage of HCT116-WT cells in S-phase, but had not effect on HCT116-p53KO cells (Figure 4C and Supplementary Figure 4A, available at *Carcinogenesis* online). The analysis of the proliferation rates of both U2OS and HCT116 cell lines confirmed that CID-765471 impairs cell proliferation and it is more effective in p53-proficient cells (Supplementary Figure 4B, available at

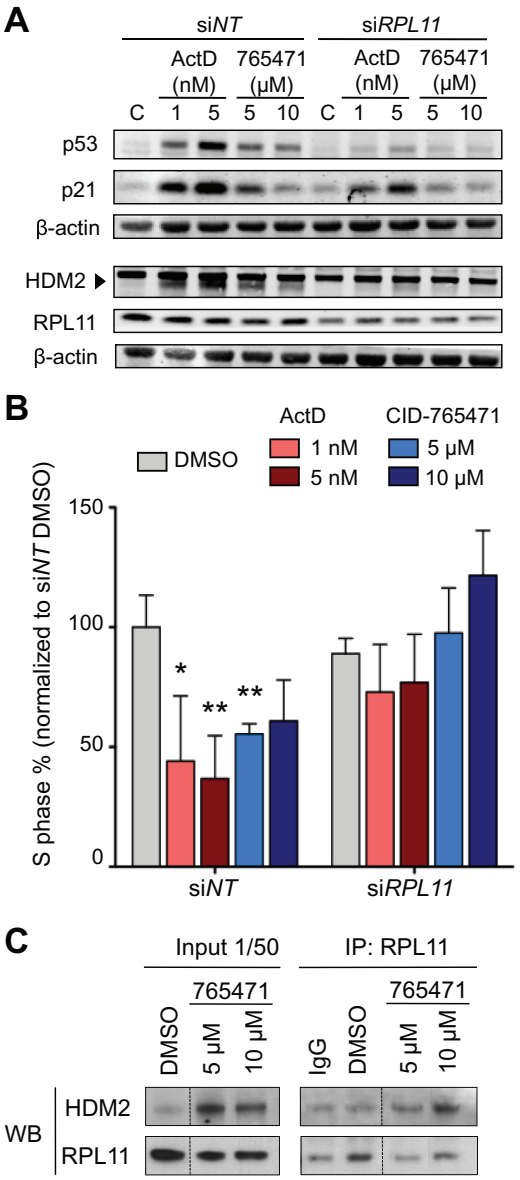

Fig. 5. CID-765471 requires RPL11 to activate p53. (**A**) RPL11 protein levels were partially depleted by siRNA in U2OS cells and, 24 h later, compounds were added as indicated for another period of 24 h. U2OS cells transfected with non-targeting siRNA (abbreviated as siNT) are used as negative control. Protein levels of p53 target genes were detected by immunoblotting. This immunoblot is representative of a total of two independent assays. (**B**). Percentage of cells in S phase treated as in panel A. S phase was measured by flow cytometry of propidium iodide-stained cells. Data correspond to the average ± SD normalized to siNT DMSO treatment of three independent assays. Statistical significance was calculated by the Student *t* test: $*P \leq 0.05$; $**P \leq 0.01$. (**C**) Immunoprecipitation of RPL11 in U2OS cells after treatment with CID-765471 (5 μM and 10 μM) and subsequent immunoblotting against HDM2 and RPL11. To increase the levels of HDM2 and RPL11, cells were treated with the proteasome inhibitor MG132 (25 μM) for 3 h prior to cell extract preparation. This assay is representative of a total of two independent assays.

Carcinogenesis online). Apoptosis was measured by cell cytometry of alive cells (DAPI-negative) that have lost plasma membrane phospholipid asymmetry (AnnexinV-positive) or that have lost mitochondiral function (TMRE-negative). After prolonged exposure of cells to CID-765471 (4 days), apoptosis was more pronounced in HCT116-WT compared to HCT116-p53KO cells (Figure 4D). Cell death was confirmed by live imaging using TO-PRO-3 iodide as a dead cell indicator (Supplementary Figure 4B, available at *Carcinogenesis* online). It

should be pointed out that nucleolar disruption is incompatible with cell proliferation regardless of the status of p53, but proliferation arrest and cell death are remarkably faster in the presence of functional p53 (see for example [30]). Together, we conclude that inhibition of ribosome biogenesis by CID-765471 activates a full p53 response.

CID-765471 activates p53 through binding of RPL11 to HDM2

Nucleolar stress causes the accumulation of the preribosomal complex RPL11/RPL5/5SrRNA that binds to HDM2, causing its inhibition and resulting in the stabilization of p53 (3–5). Based on this, we wondered whether the activation of p53 by CID-765471 is mediated by RPL11. For this, we interfered U2OS cells with a siRNA against the ribosomal protein L11 (si*RPL11*) that was able to reduce RPL11 protein levels by about 50%. Interestingly, *RPL11* knockdown abolished the accumulation of p53 after treatment with ActD or CID-765471, and it also decreased the accumulation of p21 and HDM2 (Figure 5A). Similar results were obtained with a lentiviral construct expressing an shRNA targeting a different sequence of the *RPL11* mRNA (Supplementary Figure 5A, available at *Carcinogenesis* online). Inhibition of *RPL11* also protected cells from cell-cycle arrest upon treatment with ActD or CID-765471 (Figure 5B and Supplementary Figure 5B, available at *Carcinogenesis* online). Finally, imunoprecipitation of RPL11 revealed increased binding to HDM2 after treatment with 10 µM CID-765471, consistent with the concept that CID-765471 triggers the RPL11-HDM2-p53 pathway (Figure 5C). Taken together we conclude that CID-765471 activates p53 through the RPL11/HDM2 pathway.

Identification of non-genotoxic p53-activating acridines approved for medical use

Based on the above and previous data on the ability of some acridine derivatives to activate p53 in a non-genotoxic manner (25–28), we considered of interest to identify acridine derivatives that have been approved for medical use and with capacity to activate p53 without causing DNA damage. For this, we screened the Johns Hopkins Clinical Compound Library that comprises 1524 compounds

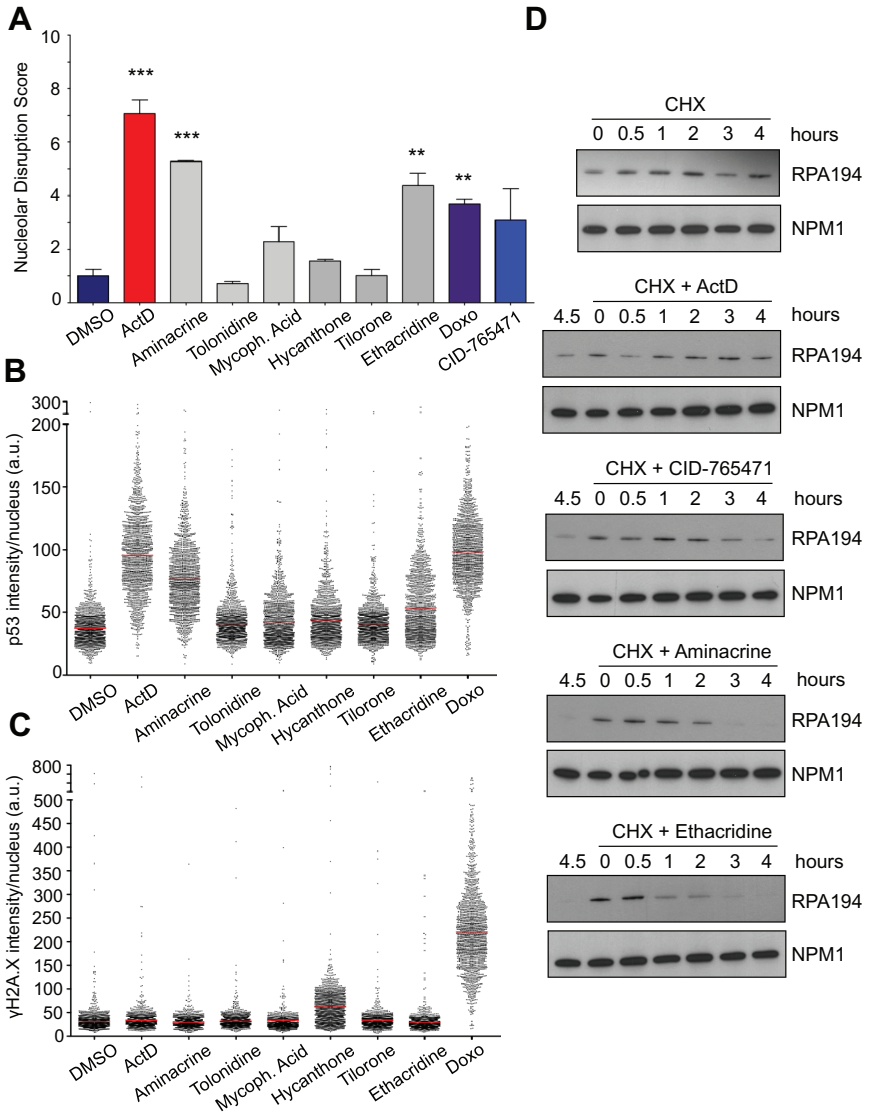

Fig. 6. Non-genotoxic acridine derivatives cause nucleolar disruption, activate p53 and degrade RPA194. (**A**) Validation of the primary hits from the Johns Hopkins Clinical Compound Library, version 1.3, in 96-well microplates. Compounds were tested in triplicates (all at 5 µM for 4.5 h) in two different clones of U2OS/GFP-RPL37 cells. Values correspond to the average ± SD of the two biological replicates (n=2) normalized to DMSO treatment. Statistical significance was calculated by the Student's t-test: $^{**}P \leq 0.01$; $^{***}P \leq 0.005$. (**B**) Levels of p53 after 4.5 h of treatment with the candidates from the JHCCL were detected by immunofluorescence and quantified by a script using Acapella High Content Image Analysis software. Mean values correspond to two different clones of U2OS/GFP-RPL37. Doxorubicin (1 µM) is abbreviated as Doxo. (**C**). Levels of γH2A.X were detected and quantified in the same manner as in B. (**D**). Cycloheximide kinetics of RPA194 protein stability after treatment with the indicated drugs at 5 nM (ActD) or 5 µM (CID-765471, aminacrine and ethacridine), during the indicated periods of time (0.5, 1, 2, 3 or 4 h).

approved for medical use. The screening was performed using U2OS/GFP-RPL37 cells in the same manner as before (see above Figure 1). We identified a total of six compounds in the primary screening, two of which were confirmed in a validation assay and, remarkably, these two compounds correspond to acridine derivatives aminacrine and ethacridine (Figure 6A). This finding reinforces once more the concept that acridine derivatives are potent nucleolar disruptors. We performed dose-response assays measuring nucleolar disruption (by nucleophosmin immunofluorescence dispersion) and cell viability in U2OS, HCT116-WT and HCT116-p53KO cells. For each acridine derivative, the obtained EC50 values were similar across the three cell lines; and, when compared, the three compounds had EC50s within a similar range although with a reproducible nucleolar disruption potency ranking of aminacrine>CID-765471>ethacridine (Supplementary Figure 6A, available at *Carcinogenesis* online). Cell viability assays confirmed the same potency ranking (Supplementary Figure 6B, available at *Carcinogenesis* online). Of note, cell viability inhibition was more pronounced in HCT116-WT than in U2OS cells, and HCT116-p53KO cells were less sensitive than HCT116-WT (Supplementary Figure 6B, available at *Carcinogenesis* online). As expected, aminacrine and, to a lesser extent, ethacridine were both efficient activators of p53 (Figure 6B) in the absence of detectable DNA damage (Figure 6C). Moreover, in agreement with previous observations with BMH-21 (28) and CID-765471 (see Figure 3D), both aminacrine and ethacridine efficiently induced the degradation of RPA194 (Figure 6D). Therefore, aminacrine and ethacridine are two medically-approved compounds that upregulate p53 in a non-genotoxic manner. These data also suggest that destruction of RPA194 is a hallmark of ribosomal RNA inhibition by non-genotoxic acridines.

Discussion

The identification of compounds that produce nucleolar disruption with minimal or no DNA damage is of interest because of their possible antitumoral activity without undesirable mutagenic effects. Acridine is a DNA intercalating agent that has given rise to a large family of derivatives. Some acridine derivatives carry reactive groups with potent genotoxic activity (31). Interestingly, there is an emerging group of acridine derivatives, including acridine itself and CID-765471, that activate p53 in the absence of genotoxic activity (25–28) (see also Figure 2). However, the mechanism by which these compounds activate p53 had remained unexplored. Here, we show that CID-765471 inhibits ribosomal DNA transcription and this results in activation of p53 through the HDM2 inhibitor RPL11. Moreover, we have found two acridine derivatives approved for medical use, namely aminacrine and ethacridine, that also produce nucleolar disruption and non-genotoxic activation of p53.

Our current findings on CID-765471 are in-line with the recent identification of CX-5461 (32). This novel acridine-unrelated compound inhibits rDNA transcription, produces nucleolar disruption, does not produce genotoxic damage and activates p53 through the RPL11 ribosomal stress pathway (32). Therefore, CID-765471 and possibly other acridines share with CX-5461 a similar mechanism of activation of p53.

Recently, it has been reported that another acridine derivative, BMH-21, inhibits ribosomal DNA transcription through a mechanism that includes the degradation of the RNA polymerase subunit RPA194 (28). Notably, this feature is not common to other inhibitors of ribosomal transcription, such as ActD (28). We have found that CID-765471, aminacrine and ethacridine induce the degradation of RPA194. Therefore, RPA194 destruction could be a distinctive feature of nucleolar disruption by non-genotoxic acridines.

In summary, we identify the ribosomal stress pathway as the mechanism by which compound CID-765471 activates p53 in a non-genotoxic manner. We also identify two acridine derivatives approved for medical use, aminacrine and ethacridine, with similar effects as CID-765471. The clarification of the mechanism of action of CID-765471 on p53 sets the bases for further studies on the possible chemotherapeutic value of non-genotoxic acridine derivatives.

Supplementary material

Supplementary Figures 1–7 can be found at http://carcin.oxfordjournals.org/

Funding

A predoctoral fellowship (FPU) from the Spanish Ministry of Education (to L.M.-P); Funding to laboratory work of M.S: the Spanish National Cancer Research Center; the European Research Council (Advanced ERC Grant 2008, reference 233270); the Framework Program 7 of the European Union (RISK-IR, reference 323267); the Spanish Ministry of Economy (SAF2008-02959); the Regional Government of Madrid (S2010/BMD-2303); the Botín Foundation; the Ramón Areces Foundation and the AXA Foundation.

Acknowledgments

We are thankful to Oscar Fernandez-Capetillo for reagents and to the confocal microscopy and flow cytometry units of the CNIO.

Conflict of Interest Statement: None declared.

References

1. Thomson,E. *et al*. (2013) Eukaryotic ribosome biogenesis at a glance. *J Cell Sci.*, **126**, 4815–4821.
2. Deisenroth,C. *et al*. (2010) Ribosome biogenesis surveillance: probing the ribosomal protein-Mdm2-p53 pathway. *Oncogene*, **29**, 4253–4260.
3. Horn,H.F. *et al*. (2008) Cooperation between the ribosomal proteins L5 and L11 in the p53 pathway. *Oncogene*, **27**, 5774–5784.
4. Bursać,S. *et al*. (2012) Mutual protection of ribosomal proteins L5 and L11 from degradation is essential for p53 activation upon ribosomal biogenesis stress. *Proc. Natl Acad. Sci. USA*, **109**, 20467–20472.
5. Fumagalli,S. *et al*. (2012) Suprainduction of p53 by disruption of 40S and 60S ribosome biogenesis leads to the activation of a novel G2/M checkpoint. *Genes Dev*., **26**, 1028–1040.
6. Donati,G. *et al*. (2013) 5S ribosomal RNA is an essential component of a nascent ribosomal precursor complex that regulates the Hdm2-p53 checkpoint. *Cell Rep*., **4**, 87–98.
7. Macias,E. *et al*. (2010) An ARF-independent c-MYC-activated tumor suppression pathway mediated by ribosomal protein-Mdm2 Interaction. *Cancer Cell*, **18**, 231–243.
8. Lawrence,M.S. *et al*. (2014) Discovery and saturation analysis of cancer genes across 21 tumour types. *Nature*, **505**, 495–501.
9. De Keersmaecker,K. *et al*. (2013) Exome sequencing identifies mutation in CNOT3 and ribosomal genes RPL5 and RPL10 in T-cell acute lymphoblastic leukemia. *Nat. Genet*., **45**, 186–190.
10. Dresios,J. *et al*. (2006) Eukaryotic ribosomal proteins lacking a eubacterial counterpart: important players in ribosomal function. *Mol. Microbiol*., **59**, 1651–1663.
11. Teng,T. *et al*. (2013) Growth control and ribosomopathies. *Curr. Opin. Genet. Dev*., **23**, 63–71.
12. Hein,N. *et al*. (2013) The nucleolus: an emerging target for cancer therapy. *Trends Mol. Med*., **19**, 643–654.
13. Rubbi,C.P. *et al*. (2003) Disruption of the nucleolus mediates stabilization of p53 in response to DNA damage and other stresses. *EMBO J*., **22**, 6068–6077.
14. Boisvert,F.M. *et al*. (2007) The multifunctional nucleolus. *Nat. Rev. Mol. Cell Biol*., **8**, 574–585.
15. Burger,K. *et al*. (2010) Chemotherapeutic drugs inhibit ribosome biogenesis at various levels. *J. Biol. Chem*., **285**, 12416–12425.
16. Llanos,S. *et al*. (2010) Depletion of ribosomal protein L37 occurs in response to DNA damage and activates p53 through the L11/MDM2 pathway. *Cell Cycle*, **9**, 4005–4012.
17. Zhu,Y. *et al*. (2009) Ribosomal protein S7 is both a regulator and a substrate of MDM2. *Mol. Cell*, **35**, 316–326.
18. Cui,D. *et al*. (2014) The ribosomal protein S26 regulates p53 activity in response to DNA damage. *Oncogene*, **33**, 2225–2235.
19. Bunz,F. *et al*. (1998) Requirement for p53 and p21 to sustain G2 arrest after DNA damage. *Science*, **282**, 1497–1501.
20. Toledo,L.I. *et al*. (2011) A cell-based screen identifies ATR inhibitors with synthetic lethal properties for cancer-associated mutations. *Nat. Struct. Mol. Biol*., **18**, 721–727.

21. O'Donohue,M.F. *et al*. (2010) Functional dichotomy of ribosomal proteins during the synthesis of mammalian 40S ribosomal subunits. *J. Cell Biol*., **190**, 853–866.
22. Lam,Y.W. *et al*. (2007) Analysis of nucleolar protein dynamics reveals the nuclear degradation of ribosomal proteins. *Curr. Biol*., **17**, 749–760.
23. Kressler,D. *et al*. (2010) Driving ribosome assembly. *Biochim. Biophys. Acta*, **1803**, 673–683.
24. Shav-Tal,Y. *et al*. (2005) Dynamic sorting of nuclear components into distinct nucleolar caps during transcriptional inhibition. *Mol. Biol. Cell*, **16**, 2395–2413.
25. Peltonen,K. *et al*. (2010) Identification of novel p53 pathway activating small-molecule compounds reveals unexpected similarities with known therapeutic agents. *PLoS One*, **5**, e12996.
26. Dudgeon,D.D. *et al*. (2010) Implementation of a 220,000-compound HCS campaign to identify disruptors of the interaction between p53 and hDM2 and characterization of the confirmed hits. *J. Biomol. Screen*., **15**, 766–782.
27. Wang,W. *et al*. (2005) Acridine derivatives activate p53 and induce tumor cell death through Bax. *Cancer Biol. Ther*., **4**, 893–898.
28. Peltonen,K. *et al*. (2014) A targeting modality for destruction of RNA polymerase I that possesses anticancer activity. *Cancer Cell*, **25**, 77–90.
29. Lane,L.A. *et al*. (2011) Mass spectrometry reveals stable modules in holo and apo RNA polymerases I and III. *Structure*, **19**, 90–100.
30. Drygin,D. *et al*. (2011) Targeting RNA polymerase I with an oral small molecule CX-5461 inhibits ribosomal RNA synthesis and solid tumor growth. *Cancer Res*., **71**, 1418–1430.
31. Galdino-Pitta,M.R. *et al*. (2013) Niche for acridine derivatives in anticancer therapy. *Mini Rev. Med. Chem*., **13**, 1256–1271.
32. Bywater,M.J. *et al*. (2012) Inhibition of RNA polymerase I as a therapeutic strategy to promote cancer-specific activation of p53. *Cancer Cell*, **22**, 51–65.

Received June 5, 2014; revised October 6, 2014; accepted October 19, 2014

Non-genotoxic activation of p53 through the RPL11-dependent ribosomal stress pathway

Lucia Morgado-Palacin[1], Susana Llanos[1], Manuel Urbano[2], Carmen Blanco-Aparicio[2], Diego Megias[3], Joaquin Pastor[2], and Manuel Serrano[1]

INDEX OF SUPPLEMENTARY MATERIALS

LEGENDS TO SUPPLEMENTARY FIGURES

Supplementary Figure 1

A. Immunofluorescence of fibrillarin in U2OS/GFP-RPL37 cells. In control cells (DMSO), fibrillarin marks the dense fibrillar component of nucleoli. After treatment with ActD (5 nM), for 4.5 h, fibrillarin segregates to nucleolar caps and GFP-RPL37 concentrates in the central body of the nucleolus. In the merged image, green corresponds to GFP-RPL37 and red corresponds to fibrillarin (see also magnification).

B. Immunofluorescence of nucleophosmin (NPM) in U2OS/GFP-RPL37 cells. In control cells (DMSO), NPM marks the granular component of nucleoli. After treatment with ActD (5 nM), for 4.5 h, NPM diffuses throughout the nucleoplasm and GFP-RPL37 concentrates in the central body of the nucleolus. In the merged image, green corresponds to GFP-RPL37 and red corresponds to NPM.

C. Schematic explanation of the nucleolar disruption score. The Definiens Developer XD software identifies nucleoli and calculates their roundness.

D. Individual nucleoli were classified as normal or disrupted, according to panel C, and their relative abundance is plotted over time upon treatment with ActD (5 nM).

E. Dose-response curve for CNIO-15760 (CID-765471) and CNIO-47023 compounds in U2OS/GFP-RPL37 cells treated with the indicated concentrations, for 4.5 h.

Supplementary Figure 2

A. Immunofluorescence of p53 in U2OS/GFP-RPL37 cells treated for 72 h with the indicated compounds (ActD at 5 nM and CID-765471 at 5 μM).

B. U2OS/GFP-RPL37 cells were treated for 6 h with the indicated compounds and concentrations. Levels of p53 were detected by immunofluorescence and quantified by a script using Acapella High Content Image Analysis software. Doxorubicin (1 μM) is abbreviated as Doxo.

C. Nucleolar disruption score calculated for U2OS/GFP-RPL37 cells treated with the indicated compounds and concentrations. This experiment was performed in duplicates in two different U2OS/GFP-RPL37 clones.

Supplementary Figure 3

Fold change of the mRNA levels of the indicated nucleolar processing factors measured by qRT-PCR, 24 h after treatment with the indicated compounds. All mRNA levels were normalized by the endogenous β-actin mRNA levels. Fold induction is relative to controls (DMSO treatment). Values correspond to the average ± SD of two independent assays (n=2). Statistical significance was calculated by the Student t-test: ** $P \leq 0.01$; * $P \leq 0.05$.

Supplementary Figure 4

A. Sub-G1, G0/G1, S, G2/M phases and polyploidy are shown for HCT116 (WT and p53KO) treated with the indicated compounds and concentrations for 24 h.

B. Proliferation assay was carried out by staining with crystal violet at the indicated times. Cells were plated in triplicates.

C. Live imaging was performed for 54.5 hours in U2OS/GFP-RPL37 cells treated with DMSO or CID-765471 (5 μM). Green marks nucleoli (GFP-RPL37) and red is the viability dye (To-Pro-3 iodide) (dead cells incorporate the dye). Representative frames are shown.

Supplementary Figure 5

A. U2OS/GFP-RPL37 cells were lentivirally transduced with an shRNA against RPL11 (different from the siRNA used in main Figure 5). Cells were puromycin-selected for 4 days and cells were treated as indicated for 4 h. Protein levels were measured by immunoblotting.

B. Sub-G1, G0/G1, S, G2/M phases and polyploidy are shown for U2OS interfered with si*NT* or si*RPL11* treated with the indicated compounds and concentrations for 24 h.

Supplementary Figure 6

A. EC50 values for nucleolar disruption of the indicated compounds in the three cell lines used in this study. Nucleolar disruption was measured in triplicates by immunofluorescence against nucleophosmin using a dedicated software (see Materials and Methods).

B. Cell viability assays of the indicated compounds in the three cell lines used in this study. Cell viability was measured using the MTS method. The assay was performed once in quatriplicates. Values correspond to the average and standard deviation (n=4 technical replicates).

Supplementary Figure 7

Uncropped blots of bands shown in the main figures and supplementary figure 5. Membranes were sliced to incubate upper and bottom parts with different antibodies. Links to antibodies datasheets, where articles in which antibodies have been successfully used, are as follows: anti-p53 DO-1 SCBT (http://datasheets.scbt.com/sc-126.pdf), anti-p21 C-19 SCBT (http://datasheets.scbt.com/sc-397.pdf), anti-HDM2 SMP14 SCBT (http://datasheets.scbt.com/sc-965.pdf), anti-RPL11 Proteintech (http://www.ptglab.com/Products/RPL11-Antibody-16277-1-AP.htm), anti-RPA194 H-300 SCBT (http://datasheets.scbt.com/sc-28714.pdf), anti-RPA135 H-15 SCBT (http://datasheets.scbt.com/sc-17914.pdf), anti-NPM1 7H10B9 NOVUS Biologicals (http://www.novusbio.com/Nucleophosmin-Antibody-7H10B9_NBP1-47354.html), and anti-β-actin AC-15 SIGMA (http://www.sigmaaldrich.com/content/dam/sigma-aldrich/docs/Sigma/Datasheet/6/a5441dat.pdf).

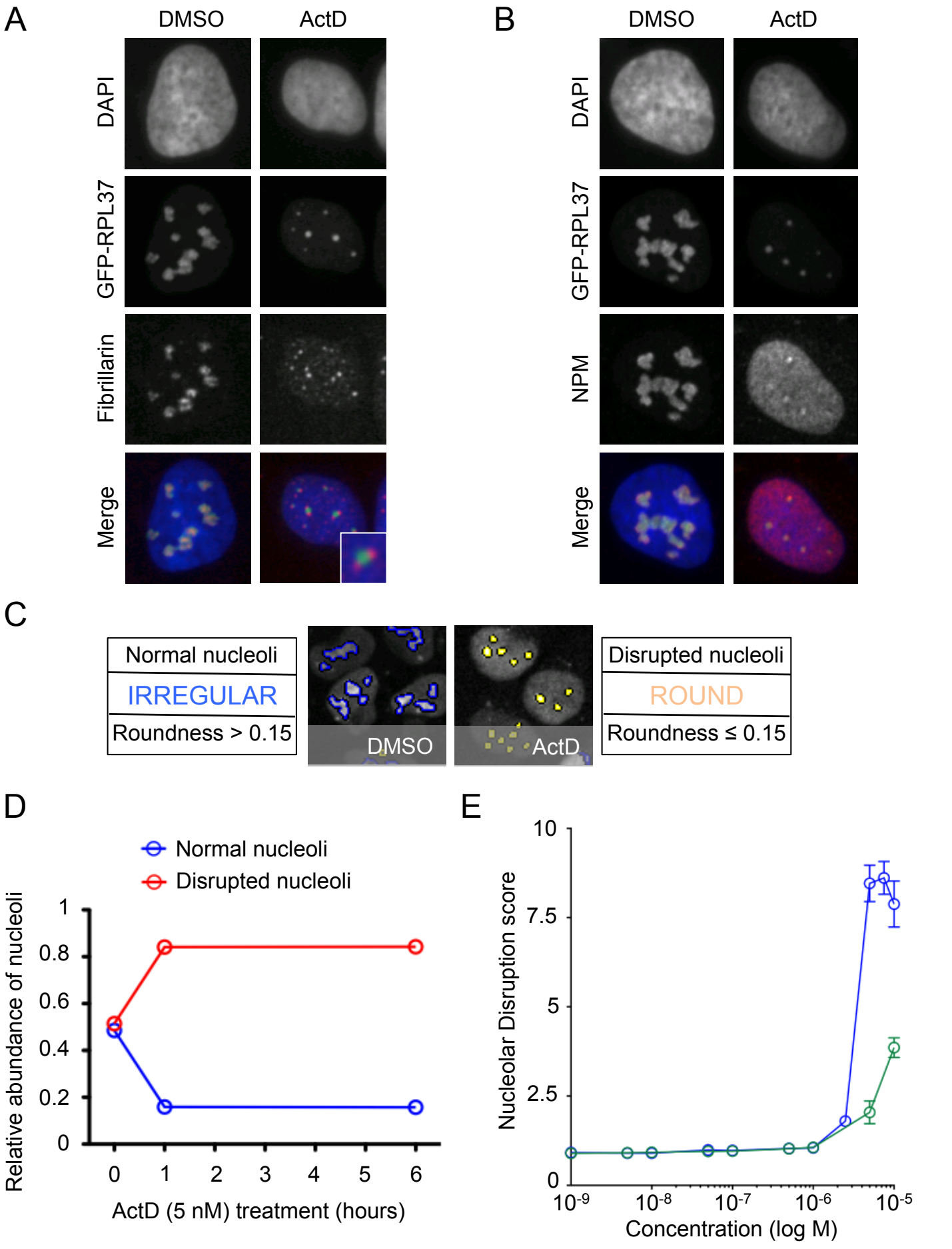
A
DMSO
ActD
DAPI
GFP-RPL37
Fibrillarin
Merge
B
DMSO
ActD
DAPI
GFP-RPL37
NPM
Merge
C
Normal nucleoli
IRREGULAR
Roundness > 0.15
DMSO
ActD
Disrupted nucleoli
ROUND
Roundness ≤ 0.15
D
Normal nucleoli
Disrupted nucleoli
Relative abundance of nucleoli
0
0.2
0.4
0.6
0.8
1
0
1
2
3
4
5
6
ActD (5 nM) treatment (hours)
E
Nucleolar Disruption score
0
2.5
5
7.5
10
10-9
10-8
10-7
10-6
10-5
Concentration (log M)

Morgado-Palacin et al., Supplementary Fig. 2

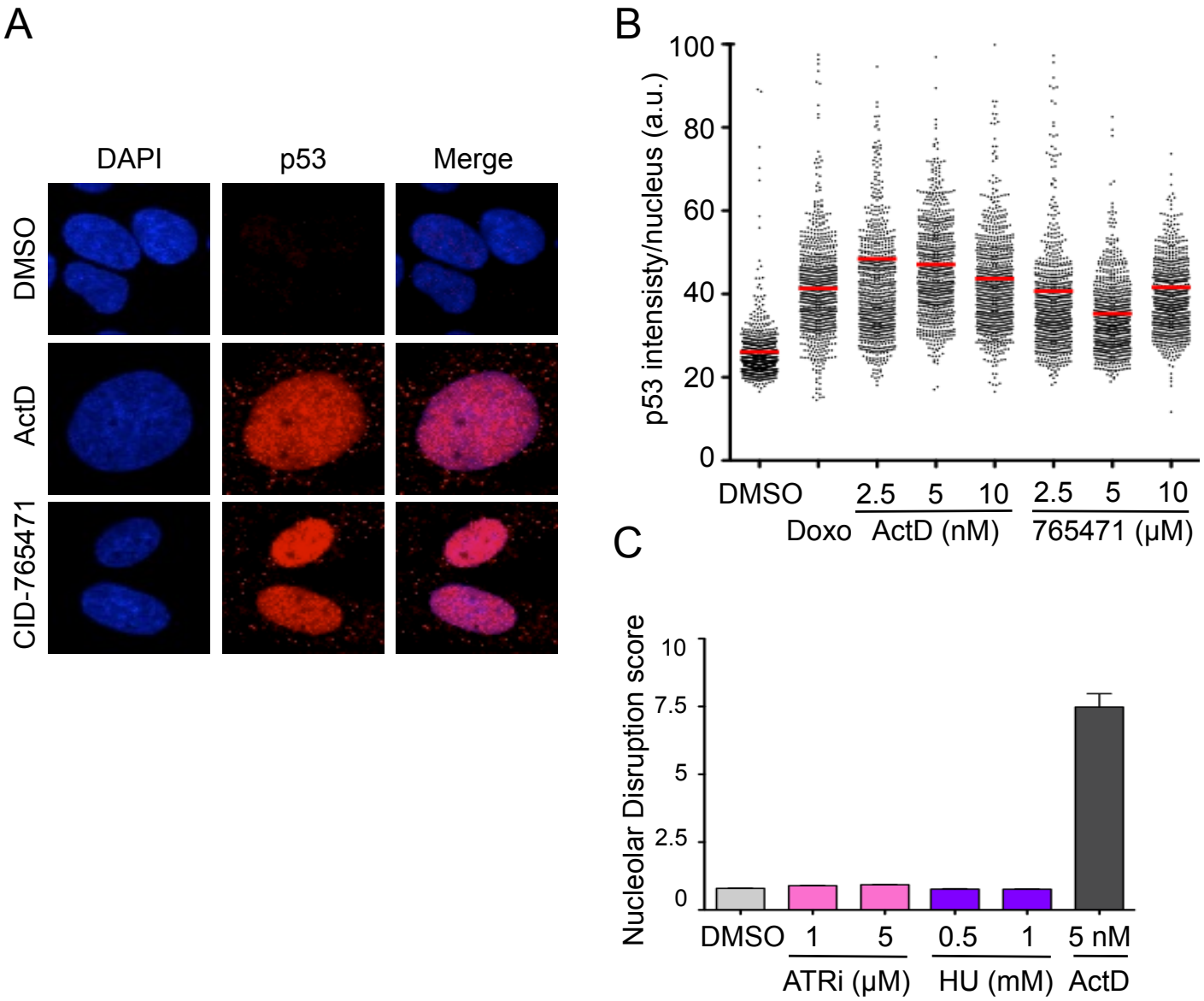

Morgado-Palacin et al., Supplementary Fig. 3

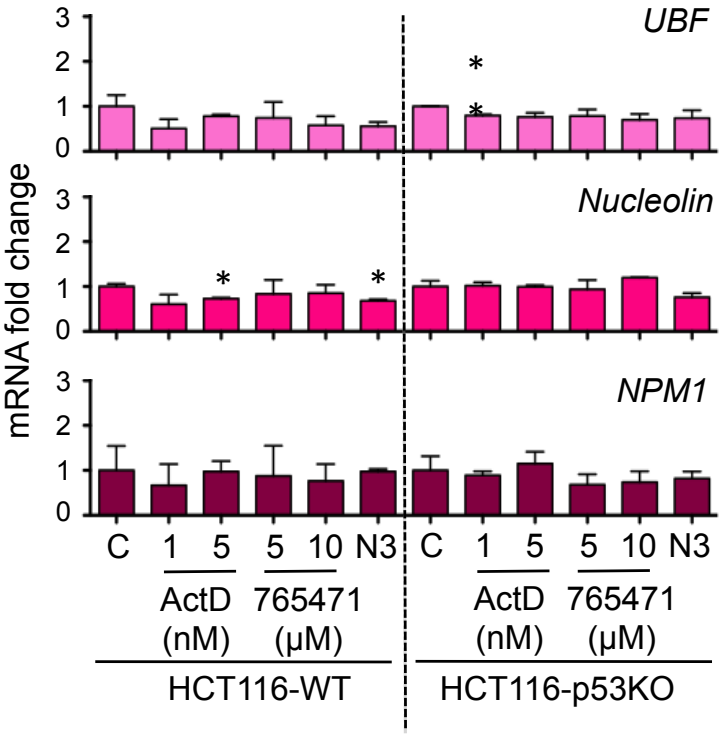

Morgado-Palacin et al., Supplementary Fig. 4

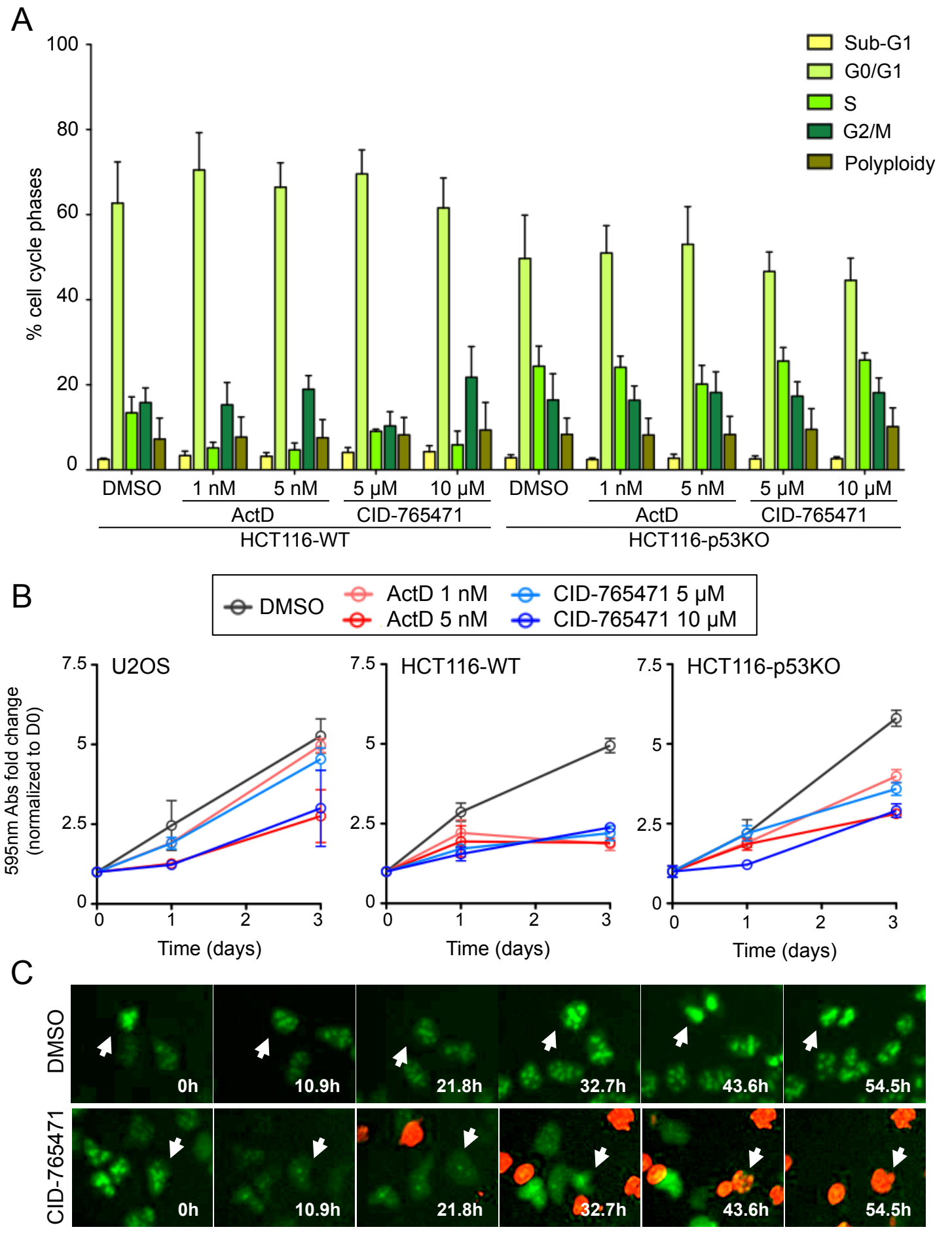

Morgado-Palacin et al., Supplementary Fig. 5

A

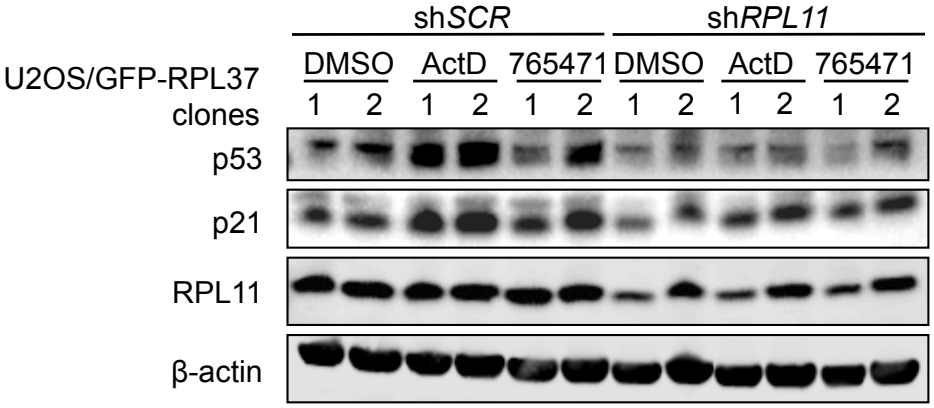

B

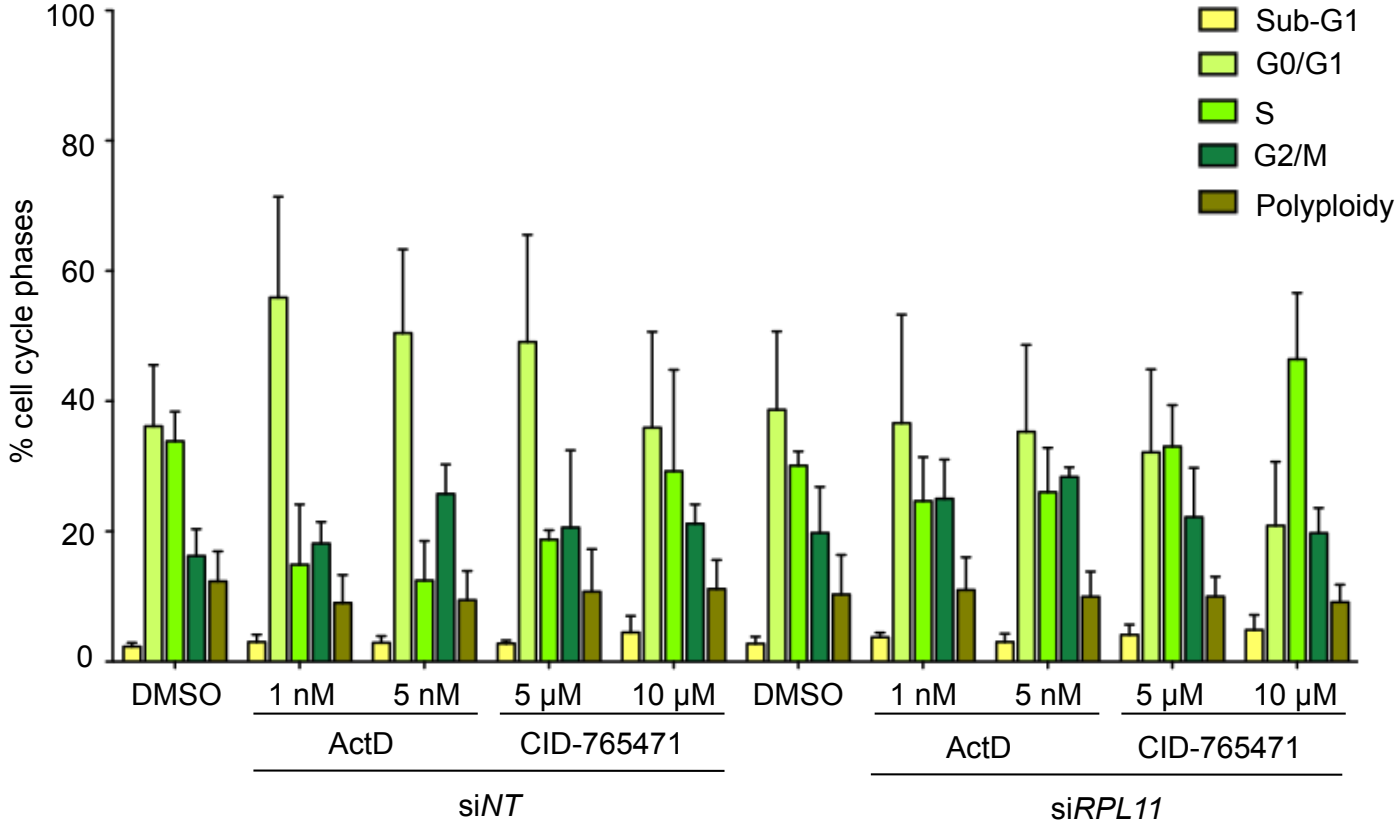

Morgado-Palacin et al., Supplementary Fig. 6

A

EC50 values	U2OS	HCT116-WT	HCT116-p53KO
CID-765471	2.4 μM	2.3 μM	2.3 μM
Ethacridine	3.6 μM	4.8 μM	5.6 μM
Aminacrine	1.0 μM	0.5 μM	1.0 μM

B

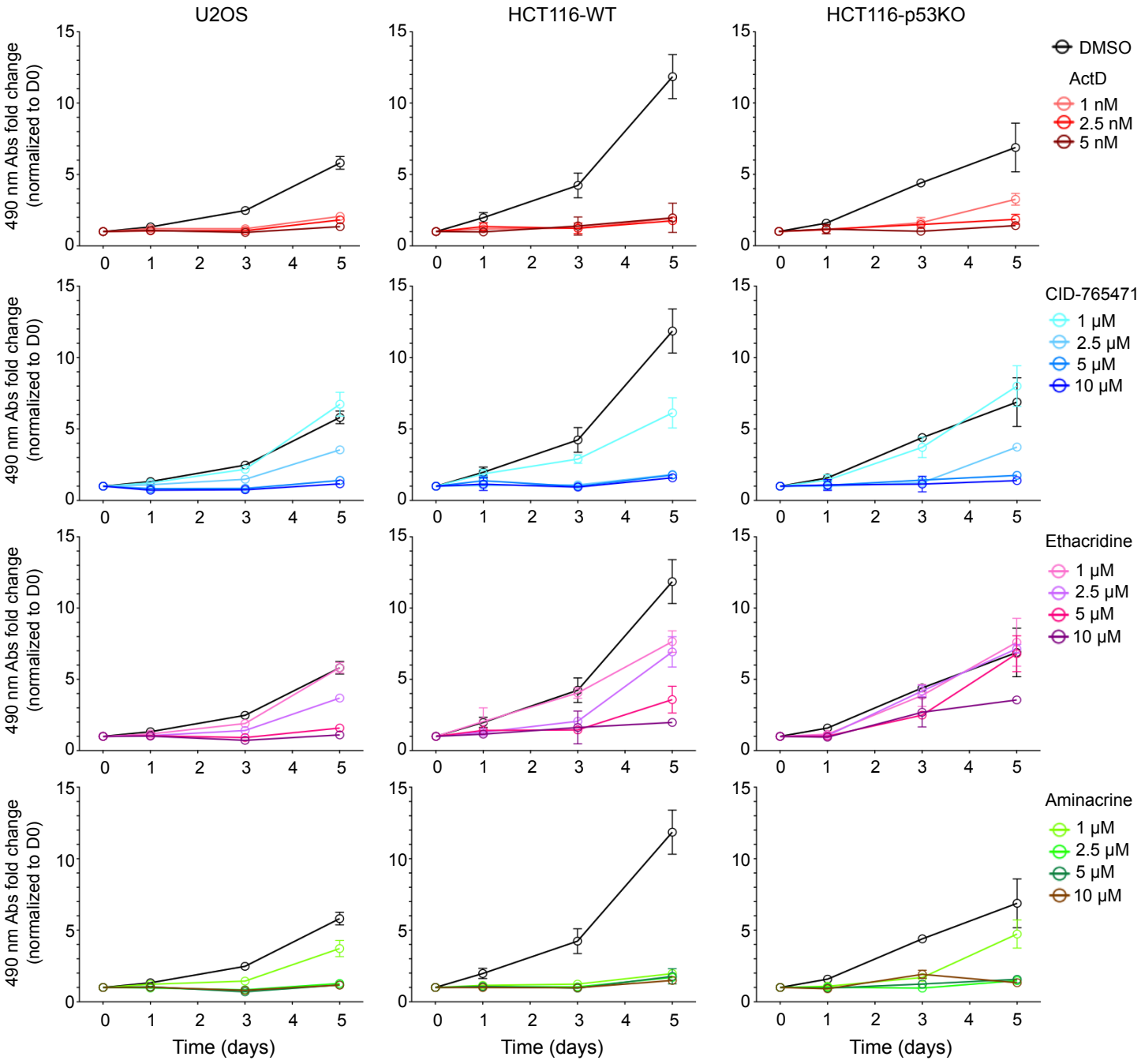

Figure 2A

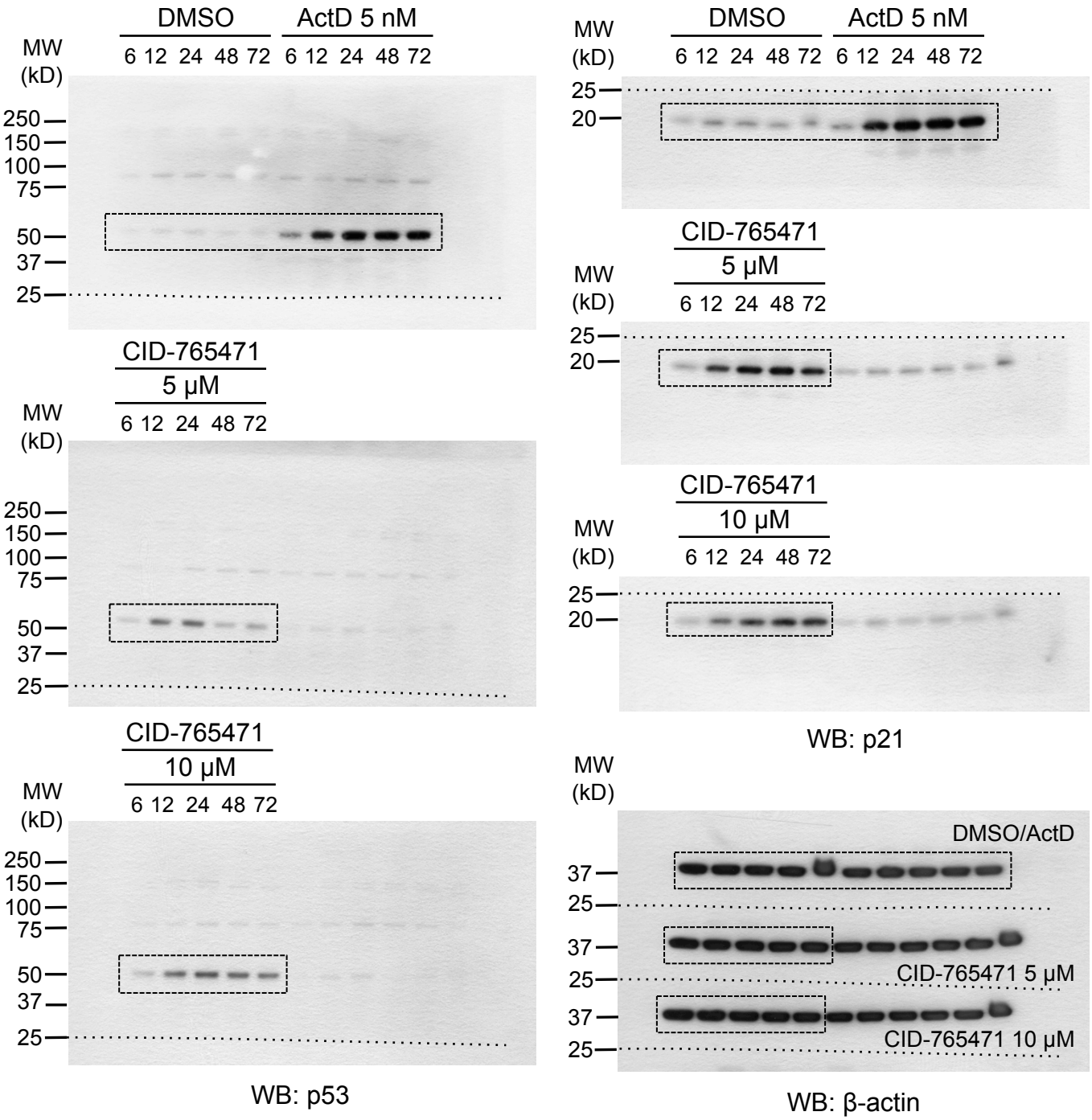
DMSO
ActD 5 nM
MW (kD)
6 12 24 48 72 6 12 24 48 72
250
150
100
75
50
37
25
CID-765471
5 μM
6 12 24 48 72
CID-765471
10 μM
WB: p53
20
WB: p21
DMSO/ActD
CID-765471 5 μM
CID-765471 10 μM
WB: β-actin

Figure 3A

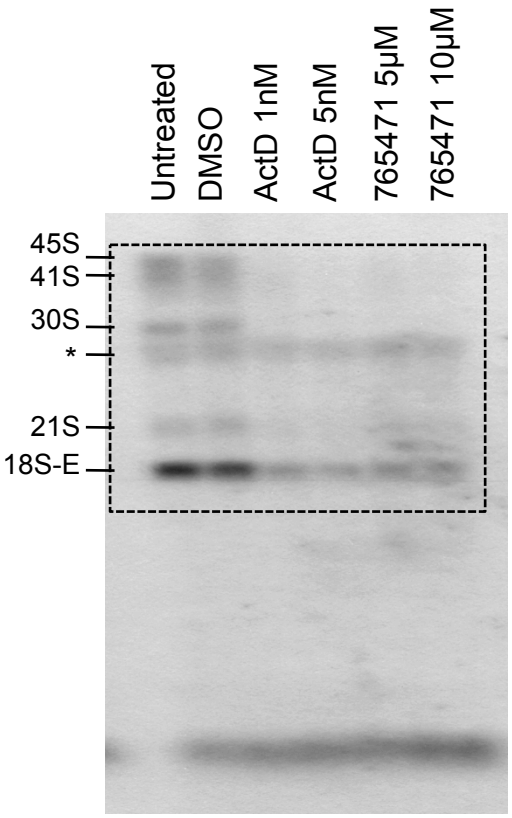

probe: ITS1

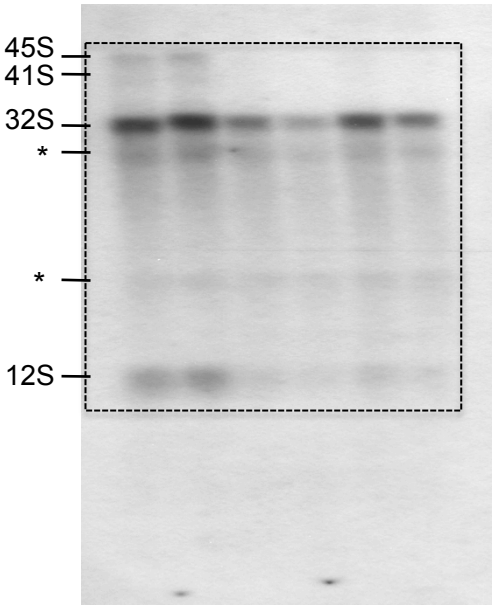

probe: ITS2

Figure 3D

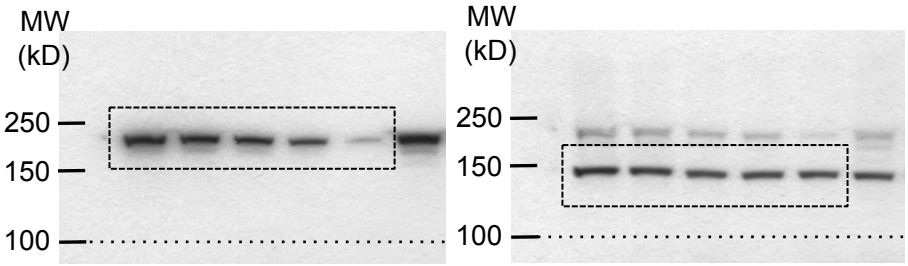

WB: RPA194 WB: RPA135

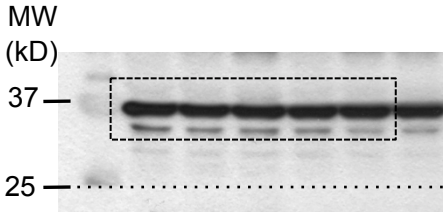

WB: NPM1

Figure 4B

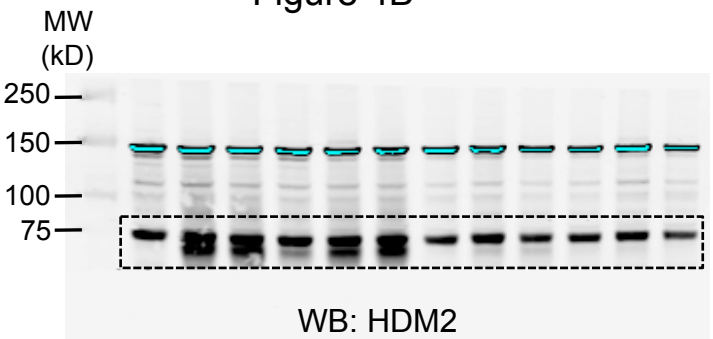

WB: HDM2

WB: p53

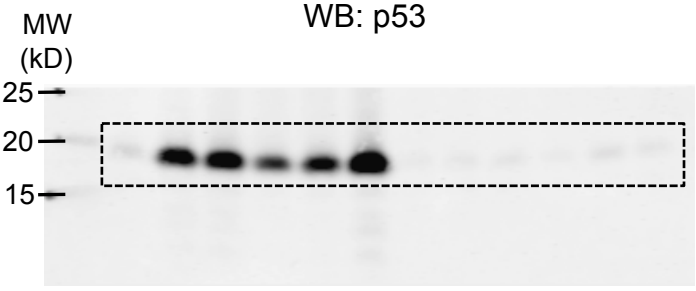

WB: p21

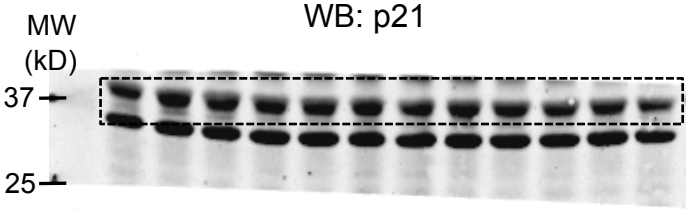

WB: β-actin

Morgado-Palacin et al., Supplementary Fig. 7. continued

Figure 5A

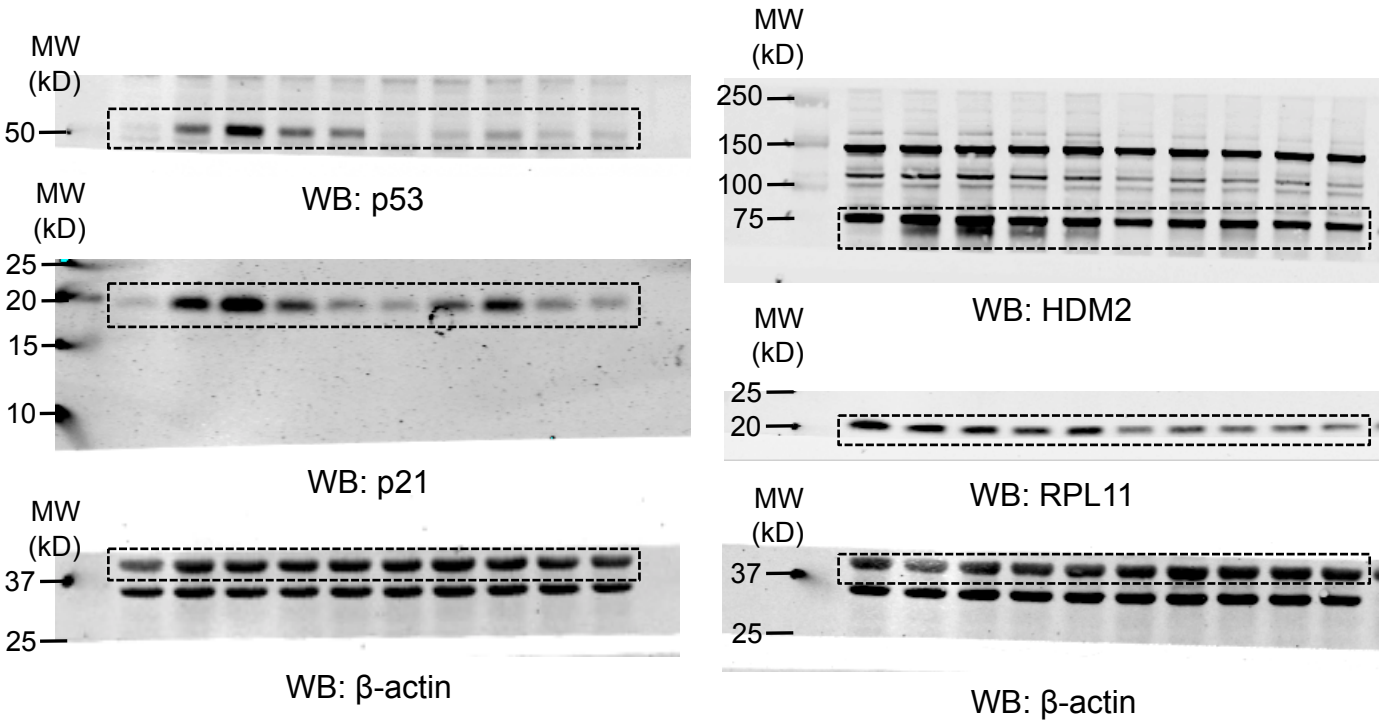

Figure 5C

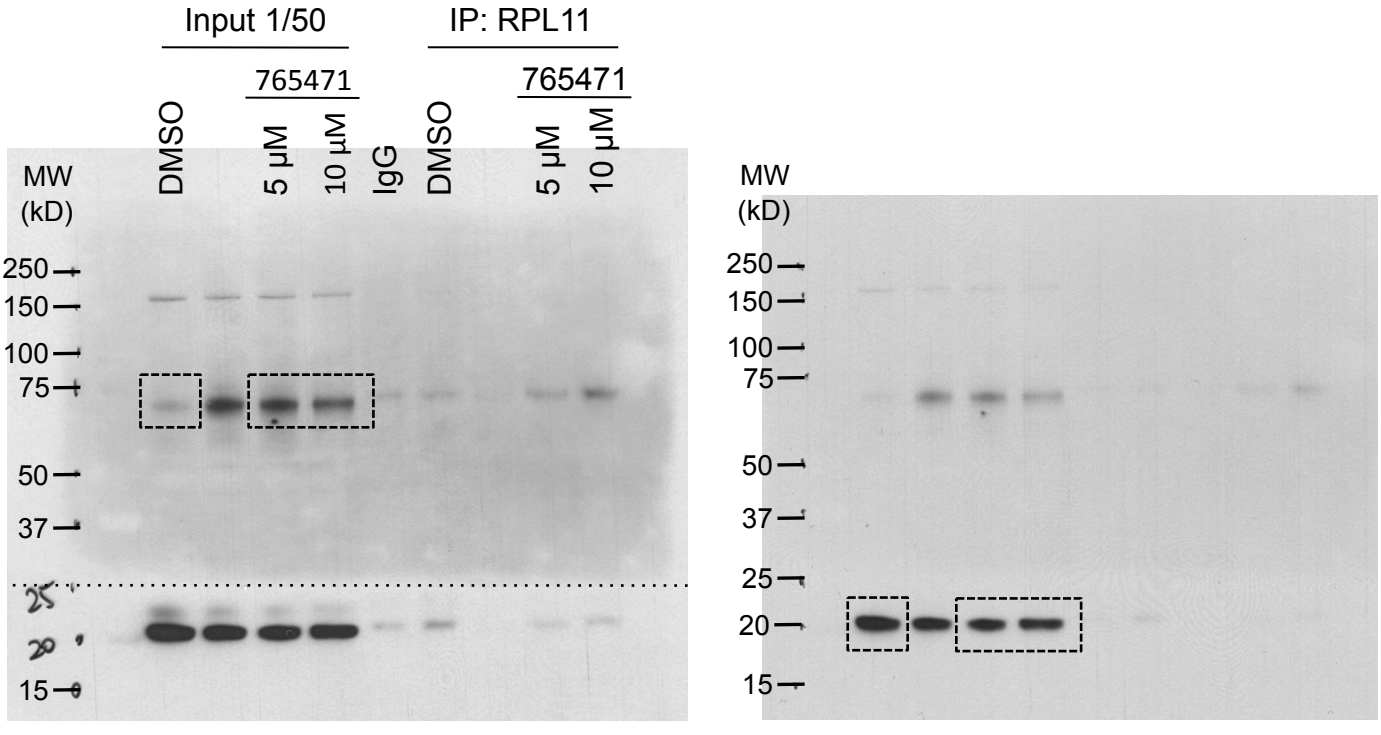

Figure 5C (continued)

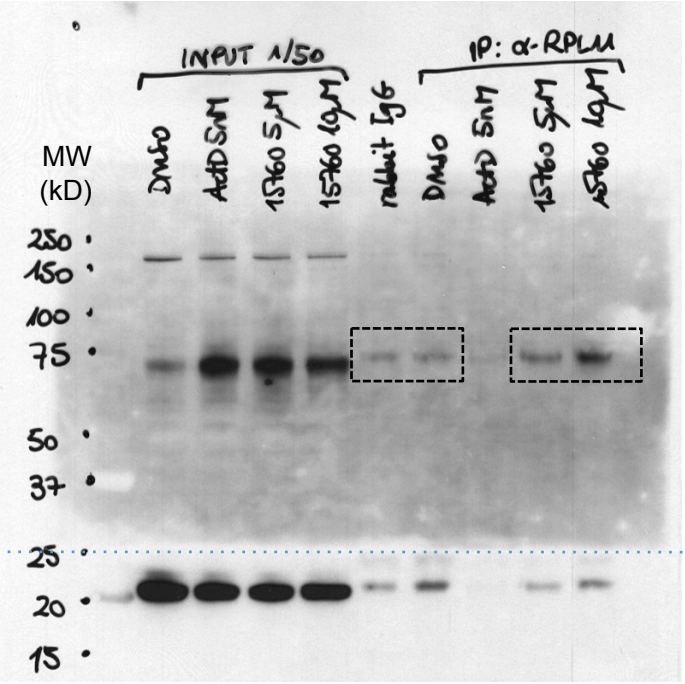

WB: HMD2, RPL11 (high contrast)

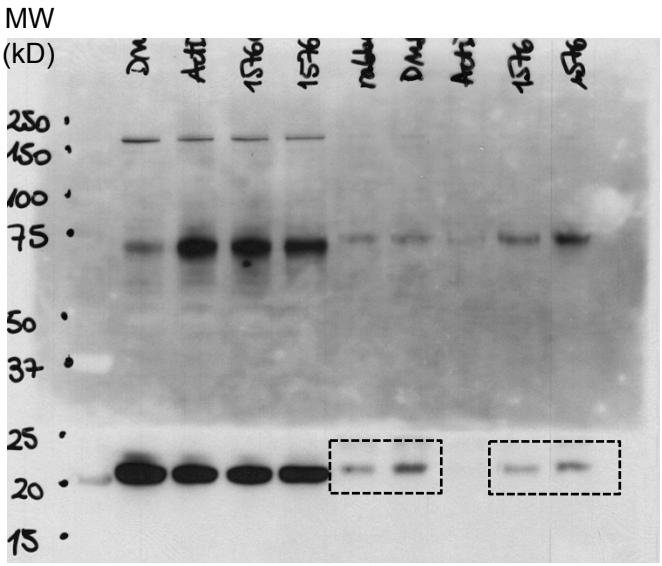

WB: HMD2, RPL11 (low contrast)

Figure 6D

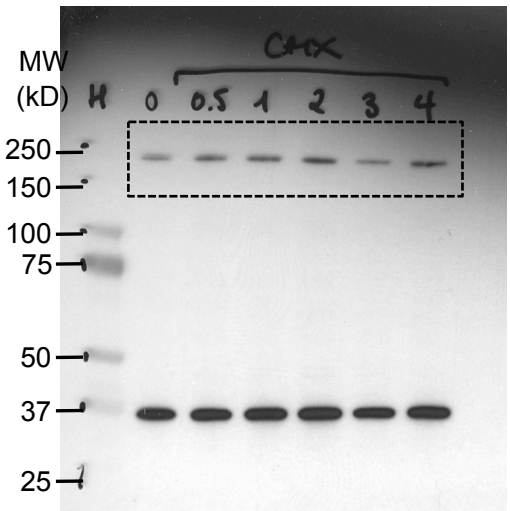

WB: RPA194, NPM1 (high contrast)

Morgado-Palacin et al., Supplementary Fig. 7. continued

Figure 6D (continued)

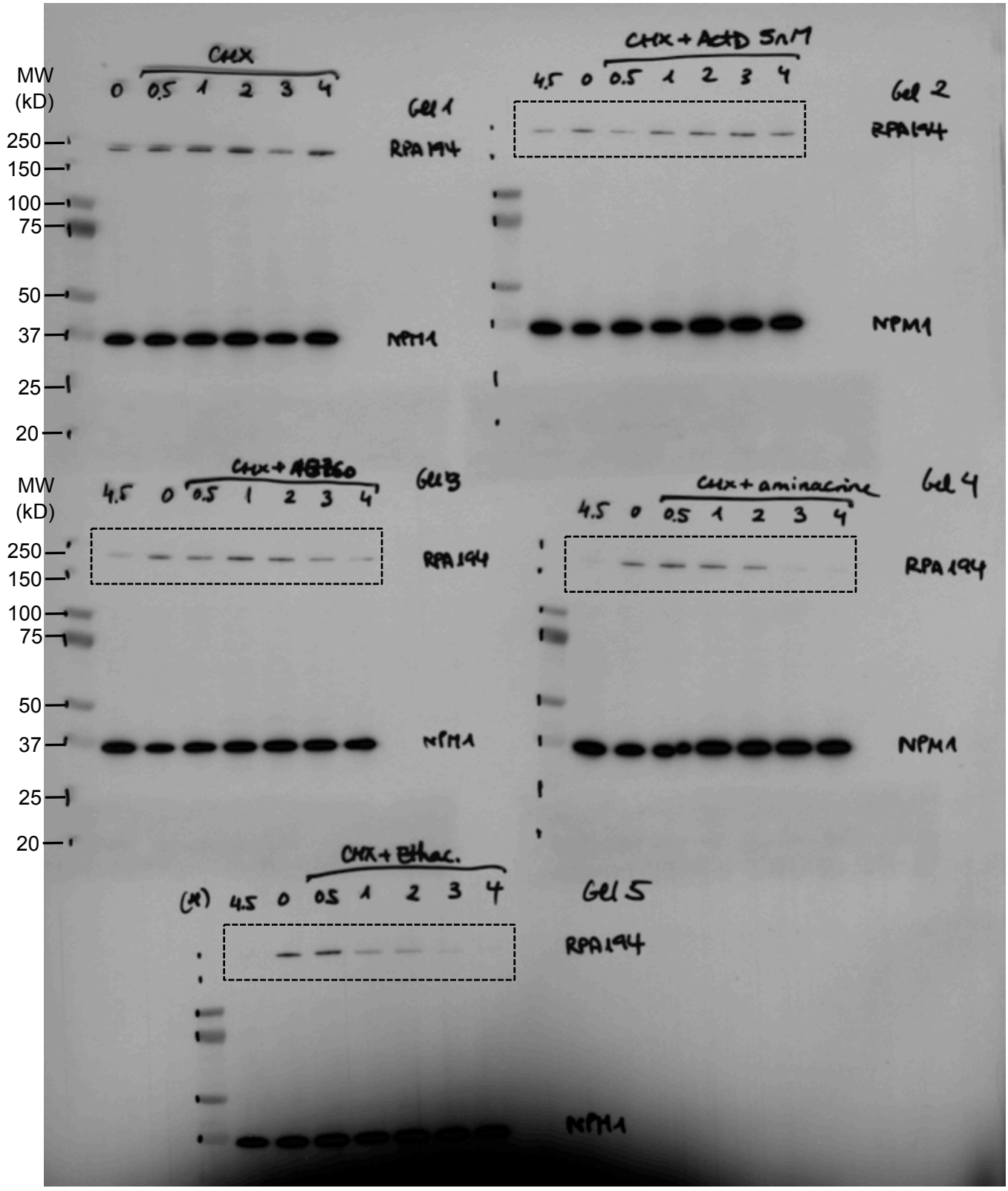

WB: RPA194, NPM1 (high exp)

Figure 6D (continued)

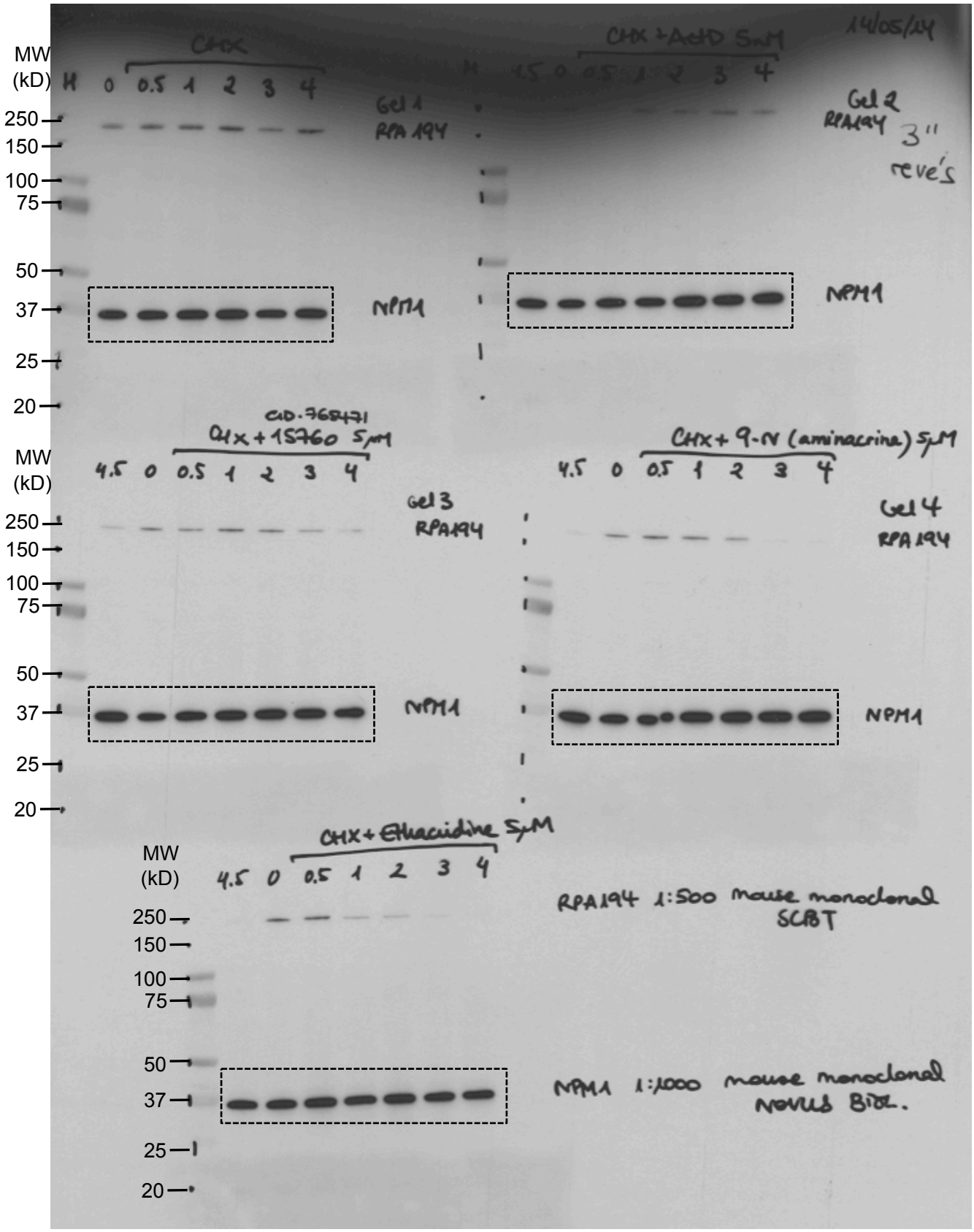

WB: RPA194 (low exp), NPM1

Morgado-Palacin et al., Supplementary Fig. 7. continued

Supp. Figure 5A

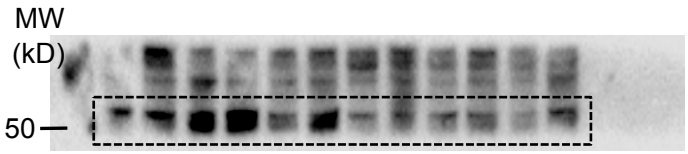

WB: p53

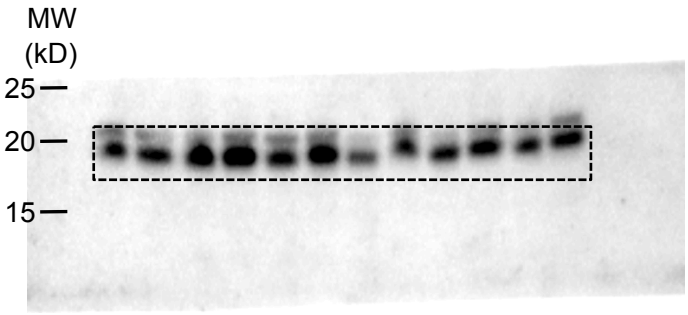

WB: p21

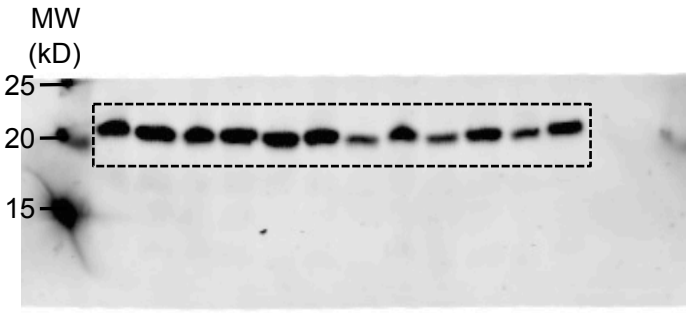

WB: RPL11

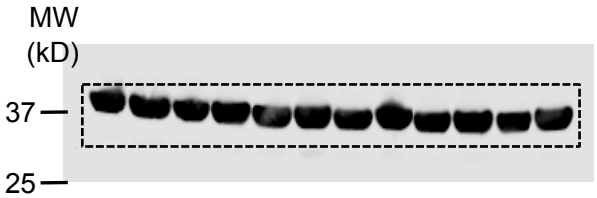

WB: β-actin

SUPPLEMENTARY MATERIALS AND METHODS

Dose-response curves

For the determination of the nucleolar disruption score in a dose-response curve, at least 12-points of increasing concentrations of the indicated compounds were added for 4.5 hours to two clones of U2OS/GFP-RPL37 cells previously plated in triplicates. GraphPad Prism 5 software was used to plot data to log(concentrations).

Proliferation and viability assays

U2OS and isogenic HCT116 cells (WT and p53KO) were seeded in triplicates at a density of 3,000 and 5,000 cells/well respectively in 96-well flat bottom tissue culture plates. Then, cells were fixed at the indicated days with 1% glutaraldeyde in PBS for 15 min. at R.T., washed twice with PBS, and stained with 0.1% cristal violet in PBS for 30 min. After removing excess of crystal violet and drying the plates, 10% acetic acid was added and the colorimetric signal was measured at an optical density of 590 nm. Values were normalized by day 0 (baseline).

For cell viability, U2OS and isogenic HCT116 cells (WT and p53KO) were seeded in quadruplicates at a density of 2,500 and 2,000 cells/well respectively in 96-well flat bottom tissue culture plates. Then, MTS was added to the cells and, after incubation for 1 hour at 37 ºC 5% CO2, absorbance at 490 nm was measured. Values were normalized by day 0 (baseline).

Time-lapse videomicroscopy

U2OS/GFP-RPL37 cells were seeded 2 days before of time-lapse analysis at a density of 7,500 cells/well in chamber slides (Lab-Tek II) and maintained in tissue culture in a humidified incubator at 37 ºC and 5% CO2. DeltaVision Live-cell microscope was set up to maintain the same temperature and CO2 conditions than in tissue culture. To-Pro-3 iodide (Life Technologies) was added to the media culture at the beginning of the experiment at a final concentration of 1 μM. Images from 10 different positions in each well were acquired every 6 min. by using the fluorescence FITC and Cy5 channels. Z position was defined as the best focus for each fluorescence channel. After 1 hour of live imaging, DMSO or CID-765471 were added at 2X, containing To-Pro-3 iodide, by a syringe-system connected to the chambers. Final concentration of CID-765471 was 5

μM. Live imaging continued for additional 53.5 hours adjusting focus every day. Analysis was performed with FIJI software.

MANUSCRIPT III

Partial loss of Rpl11 in adult mice recapitulates Diamond-Blackfan anemia and promotes lymphomagenesis

Lucia Morgado-Palacin, Gianluca Varetti, Susana Llanos, Gonzalo Gómez-López, Dolores Martinez and Manuel Serrano

Cell Reports 13:**4**, 712-722; October 27, 2015

Objetivo: ESTUDIO DE LA DEFICIENCIA DE *Rpl11* EN ERITROPOYESIS Y CANCER. UN MODELO DE ANEMIA DE DIAMOND-BLACKFAN (DBA)

La proteína ribosomal L11 (RPL11, de sus siglas en inglés) es una de las proteínas ribosomales más extensamente estudiadas. Además de ser parte de la subunidad mayor del ribosoma, RPL11 activa p53 en respuesta a estrés ribosomal o nucleolar. El interés en RPL11 ha aumentado notablemente en los últimos años al describirse mutaciones en heterozigosis que comprometen la función de dicha proteína en pacientes de anemia de Diamond-Blackfan (DBA, de sus siglas en inglés). Los pacientes de DBA presentan anemia severa y una mayor predisposición al cáncer, entre otros síntomas.

Hasta ahora, sólo se ha descrito *in vivo* en el modelo animal *zebrafish* que la deficiencia de RPL11 recapitula parte de la patogénesis de DBA. Sin embargo, no existen modelos de ratón deficientes en RPL11 y aún quedan muchas preguntas abiertas en relación a los mecanismos moleculares que gobiernan esta enfermedad, especialmente aquellos relacionados con la predisposición al cáncer. En este trabajo, hemos generado y caracterizado un modelo inducible de ratón deficiente para RPL11. Hemos descrito que la pérdida constitutiva de un alelo de *Rpl11* es incompatible con el desarrollo embrionario, al igual que la deleción de ambos alelos en el ratón adulto. Cuando se produce en el ratón adulto, la eliminación de ambos alelos de *Rpl11* provoca atrofia intestinal y aplasia en la médula ósea. La pérdida de un alelo de *Rpl11* en ratones adultos recapitula gran parte de la sintomatología observada en los pacientes de DBA. Los ratones adultos RPL11 heterozigotos presentan anemia macrocítica debida a una disminución en progenitores eritroides y a una diferenciación eritropoyética defectuosa. Los eritroblastos de estos ratones tienen niveles elevados de los ARN mensajeros de *p21* y *Bax*, un inhibidor del ciclo celular y un gen implicado en apoptosis, respectivamente. Además, hemos observado una reducción en los niveles de ARN mensajero de genes

implicados en desarrollo y función de los eritrocitos, como *Uros* o *Gypa*. También, hemos detectado que el procesamiento del ARN ribosomal es anormal en los fibroblastos y tejidos de estos animales. Es destacable que los ratones adultos desarrollan linfomas de timo con mayor celeridad ante un protocolo de radiación ionizante. Nuestros resultados indican que esta mayor predisposición al cáncer en los ratones RPL11 heterozigotos puede atribuirse, al menos en parte, a dos mecanismos no excluyentes, 1) una deficiente activación de p53 en respuesta a estrés ribosomal, tal y como hemos observado en fibroblastos de estos ratones, y 2) unos mayores niveles de la oncoproteína c-MYC en fibroblastos y tejidos hematopoyéticos de los ratones RPL11 heterozigotos. Dichos hallazgos proporcionan una evidencia molecular para explicar la elevada propensión a lcáncer pacientes de DBA con mutaciones en RPL11.

Article

Cell Reports

Partial Loss of *Rpl11* in Adult Mice Recapitulates Diamond-Blackfan Anemia and Promotes Lymphomagenesis

Graphical Abstract

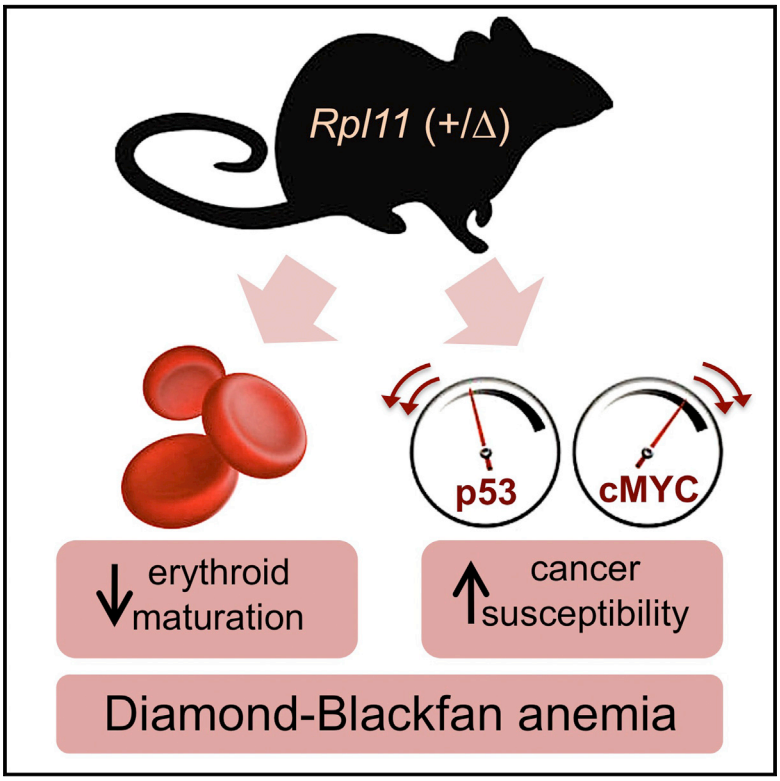

Authors

Lucia Morgado-Palacin, Gianluca Varetti, Susana Llanos, Gonzalo Gómez-López, Dolores Martinez, Manuel Serrano

Correspondence

mserrano@cnio.es

In Brief

Protein RPL11 is critical for ribosome activity and also has extra-ribosomal functions. Morgado-Palacin et al. demonstrate that elimination of one allele of *Rpl11* in adult mice impairs erythrocyte maturation, reduces p53 responses, and increases cMYC levels. Together these defects result in anemia and cancer susceptibility, thereby recapitulating human Diamond-Blackfan anemia.

Highlights

- *Rpl11*-haploinsufficient mice develop anemia, recapitulating the human disorder DBA
- *Rpl11*-deficient erythroid precursors mature inefficiently
- *Rpl11*-deficient cells present impaired p53 responses and high cMYC levels
- *Rpl11*-deficient mice are prone to radiation-induced lymphomagenesis

Accession Numbers

GSE72537

Morgado-Palacin et al., 2015, Cell Reports *13*, 1–11
October 27, 2015 ©2015 The Authors
http://dx.doi.org/10.1016/j.celrep.2015.09.038

Please cite this article in press as: Morgado-Palacin et al., Partial Loss of *Rpl11* in Adult Mice Recapitulates Diamond-Blackfan Anemia and Promotes Lymphomagenesis, Cell Reports (2015), http://dx.doi.org/10.1016/j.celrep.2015.09.038

Cell Reports
Article

Partial Loss of *Rpl11* in Adult Mice Recapitulates Diamond-Blackfan Anemia and Promotes Lymphomagenesis

Lucia Morgado-Palacin,[1] Gianluca Varetti,[1] Susana Llanos,[1] Gonzalo Gómez-López,[2] Dolores Martinez,[3] and Manuel Serrano[1,*]
[1]Tumor Suppression Group, Molecular Oncology Programme, Spanish National Cancer Research Centre (CNIO), Madrid E28029, Spain
[2]Bioinformatics Unit, Structural Biology and Biocomputing Programme, Spanish National Cancer Research Centre (CNIO), Madrid E28029, Spain
[3]Flow Cytometry Unit, Biotechnology Programme, Spanish National Cancer Research Centre (CNIO), Madrid E28029, Spain
*Correspondence: mserrano@cnio.es
http://dx.doi.org/10.1016/j.celrep.2015.09.038

SUMMARY

Diamond-Blackfan anemia (DBA) is characterized by anemia and cancer susceptibility and is caused by mutations in ribosomal genes, including *RPL11*. Here, we report that *Rpl11*-heterozygous mouse embryos are not viable and that *Rpl11* homozygous deletion in adult mice results in death within a few weeks, accompanied by bone marrow aplasia and intestinal atrophy. Importantly, *Rpl11* heterozygous deletion in adult mice results in anemia associated with decreased erythroid progenitors and defective erythroid maturation. These defects are also present in mice transplanted with inducible heterozygous *Rpl11* bone marrow and, therefore, are intrinsic to the hematopoietic system. Additionally, heterozygous *Rpl11* mice present increased susceptibility to radiation-induced lymphomagenesis. In this regard, total or partial deletion of *Rpl11* compromises p53 activation upon ribosomal stress or DNA damage in fibroblasts. Moreover, fibroblasts and hematopoietic tissues from heterozygous *Rpl11* mice present higher basal cMYC levels. We conclude that *Rpl11*-deficient mice recapitulate DBA disorder, including cancer predisposition.

INTRODUCTION

The ribosomal protein L11 (RPL11) is one the most relevant and extensively studied ribosomal proteins. Interest in this protein has notably increased during the last years because of its connections with Diamond-Blackfan anemia (DBA) and with oncogenic pathways. In particular, a subset of Diamond-Blackfan anemia (DBA) patients carry loss-of-function haploid mutations in the *RPL11* gene (Boria et al., 2010; Cmejla et al., 2009; Gazda et al., 2008; Quarello et al., 2010). Mutations in several other ribosomal proteins also produce DBA, being *RPS19* the most frequently mutated gene in DBA (Boria et al., 2010). DBA is a congenital disease mainly characterized by a moderate to severe anemia and by increased susceptibility to cancer (Narla and Ebert, 2010; Teng et al., 2013). A major feature of the red blood cell aplasia in DBA patients is a reduction in erythroid progenitors and impaired erythroid maturation (Miyake et al., 2008; Moniz et al., 2012). In addition, mutations in *RPL11* are associated with characteristic thumb malformations (Gazda et al., 2008).

Beyond its function as part of the ribosome, ribosome-free RPL11 activates p53 through the so-called ribosomal/nucleolar stress pathway. Specifically, conditions that perturb ribosome biogenesis, such as certain DNA damaging agents or cMYC overexpression, result in ribosome-free RPL11, which binds to and inhibits MDM2, thereby stabilizing p53 (Bhat et al., 2004; Bursać et al., 2012; Donati et al., 2013; Lohrum et al., 2003; Macias et al., 2010; Zhang et al., 2003b). This pathway has received additional support by the recent resolution of the 3D structure of the RPL11/MDM2 complex (Zheng et al., 2015). Another emerging role of ribosome-free RPL11 is to decrease the levels and activity of cMYC. This has been reported to occur through binding of RPL11 to the *cMYC* mRNA and recruitment of the RISC complex (Challagundla et al., 2011) and also by direct binding of RPL11 to cMYC protein and competition with transcriptional coactivators (Dai et al., 2007, 2010). Therefore, ribosome-free RPL11 may be part of a tumor suppressive response through its combined ability to activate p53 and inhibit cMYC.

Work in zebrafish has demonstrated that inhibition of RPL11 recapitulates DBA anemia (Danilova et al., 2011; Zhang et al., 2013). However, there are no mouse models of RPL11 deficiency. Here, we have generated mice with an inducible *Rpl11*-null allele, and we show that heterozygous loss of *Rpl11* in adult mice recapitulates DBA, including a higher predisposition to cancer. We present evidence suggesting that impaired p53 activity and abnormally high levels of cMYC could underlie the cancer susceptibility associated with *Rpl11* deficiency.

RESULTS

Rpl11 Heterozygosity Cannot Sustain Embryonic Development

To evaluate the impact of *Rpl11* deficiency in vivo, we generated a conditional knockout mouse model in which deletion of the

Please cite this article in press as: Morgado-Palacin et al., Partial Loss of *Rpl11* in Adult Mice Recapitulates Diamond-Blackfan Anemia and Promotes Lymphomagenesis, Cell Reports (2015), http://dx.doi.org/10.1016/j.celrep.2015.09.038

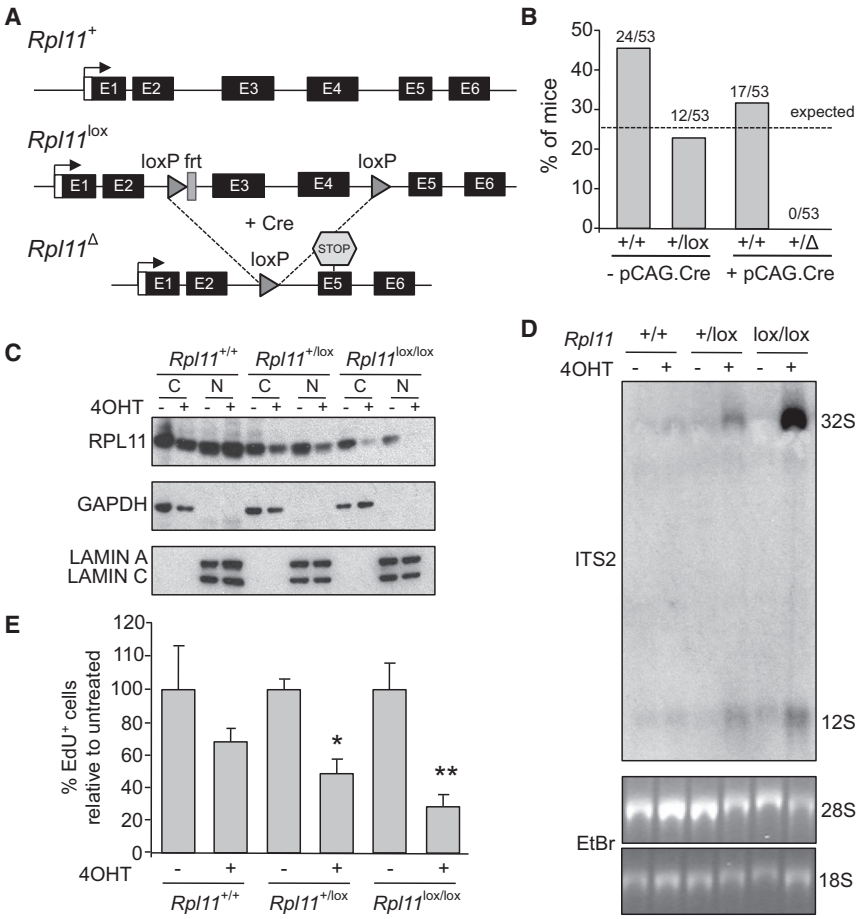

Figure 1. Diploid *Rpl11* Is Required for Embryo Development and Complete Loss of *Rpl11* Severely Compromises Cell Proliferation

(A) Scheme of the wt (+), lox, and delta (Δ) *Rpl11* alleles. Upon Cre recombinase activation, exons 3 and 4 of the $Rpl11^{lox}$ allele are excised resulting in the $Rpl11^{\Delta}$ allele where exon 2 is spliced out-of-frame with exon 5.

(B) Observed and expected Mendelian ratios for viable genotypes. The Cre recombinase used is under a strong synthetic promoter (CAG), being expressed constitutively and ubiquitously in the organism from early developmental stages.

(C) Immunoblot analysis of RPL11 protein levels in cytosolic (C) and nuclear (N) fractions from immortalized MEFs of the indicated genotypes, bearing the Tg.hUbC-*CreERT2* transgene, in the absence or presence of 4OHT for 72 hr. GAPDH and LAMIN A/C were used as cytosolic and nuclear markers, respectively. Similar results were obtained with two additional clones per genotype.

(D) Northern blot analysis of 32S and 12S rRNA precursors in immortalized MEFs as in (C). A probe specific for the ITS2 region was used to detect rRNA intermediates. The mature 28S and 18S forms were visualized by ethidium bromide staining. Similar results were obtained with two additional clones per genotype.

(E) Quantification of EdU-labeled cells in $Rpl11^{+/+}$, $Rpl11^{+/lox}$, and $Rpl11^{lox/lox}$ primary MEFs, bearing the Tg.hUbC-*CreERT2* transgene, grown in the absence or presence of 4OHT for 72 hr. For each genotype, the percentage of EdU^+ cells was normalized to the untreated cells (set as 100%).

Data correspond to the average ± SD of two to three independent MEF clones per genotype. Statistical t test analysis was performed to calculate significance (*$p < 0.05$, **$p < 0.01$). See also Figure S1.

Rpl11 gene can be controlled by the Cre recombinase (Figure 1A; Figures S1A–S1F). We first crossed $Rpl11^{+/lox}$ mice with a ubiquitous Cre recombinase (Tg.pCAG-*Cre*) constitutively expressed from early developmental stages (Sakai and Miyazaki, 1997). However, we could not detect any $Rpl11^{+/\Delta}$ pup in the offspring of these animals (Figure 1B). Therefore, a single gene dose of *Rpl11* is not sufficient to support embryonic development.

Rpl11 Deficiency Impairs rRNA Processing and Cellular Proliferation

To bypass the lethality of $Rpl11^{+/\Delta}$ embryos, we combined the Cre-excisable *Rpl11* allele ($Rpl11^{lox}$) with a ubiquitous tamoxifen-inducible Cre transgene (Tg.UbC-*CreERT2* (Ruzankina et al., 2007)). We isolated mouse embryonic fibroblasts (MEFs) at E13.5 from embryos of the three relevant *Rpl11* genotypes (+/+, +/lox, lox/lox) carrying transgenic *Cre* in hemizygosity, and treated them with 4-hydroxy-tamoxifen (4OHT). First, we evaluated whether Cre activation in $Rpl11^{+/lox}$ and $Rpl11^{lox/lox}$ cells resulted in a measurable reduction in RPL11 protein levels. After 3 days of treatment with 4OHT, RPL11 was essentially undetectable in the nuclear fraction of 4OHT-$Rpl11^{lox/lox}$ cells, and its levels were dramatically reduced in the cytoplasmic fraction (Figure 1C). In the case of 4OHT-$Rpl11^{+/lox}$ cells, there was a partial, but clear, reduction in RPL11 levels both in the nuclear and in the cytoplasmic fractions (Figure 1C). RPL11 participates in the maturation of rRNA precursors and, particularly, in the processing of the 32S and 12S precursors into mature 28S and 5.8S rRNAs, respectively (Gazda et al., 2008; Robledo et al., 2008; Sloan et al., 2013). To assess the functional impact of *Rpl11* deficiency, we measured the levels of 32S and 12S rRNA precursors by northern blotting. Of note, we observed a remarkable accumulation of the 32S and 12S precursors in 4OHT-$Rpl11^{lox/lox}$ cells (Figure 1D). Accumulation of these precursors was also evident in 4OHT-$Rpl11^{+/lox}$ cells albeit at lower levels than in 4OHT-$Rpl11^{lox/lox}$ cells (Figure 1D). These observations were paralleled by a severe reduction of proliferation in 4OHT-$Rpl11^{lox/lox}$ cells and a partial reduction in 4OHT-$Rpl11^{+/lox}$ cells (Figure 1E). Therefore, deletion of *Rpl11* in cells impairs rRNA processing and cell proliferation, being the effects severe upon total *Rpl11* deletion and moderate upon heterozygous deletion.

Deletion of *Rpl11* in Adult Mice

To test the impact of RPL11 elimination in adult organisms, mice of the three relevant genotypes ($Rpl11^{+/+}$, $Rpl11^{+/lox}$, and $Rpl11^{lox/lox}$, all carrying the Tg.UbC-*CreERT2* transgene in hemizygosity) were fed a tamoxifen (TAM) diet starting 1.5–2 months

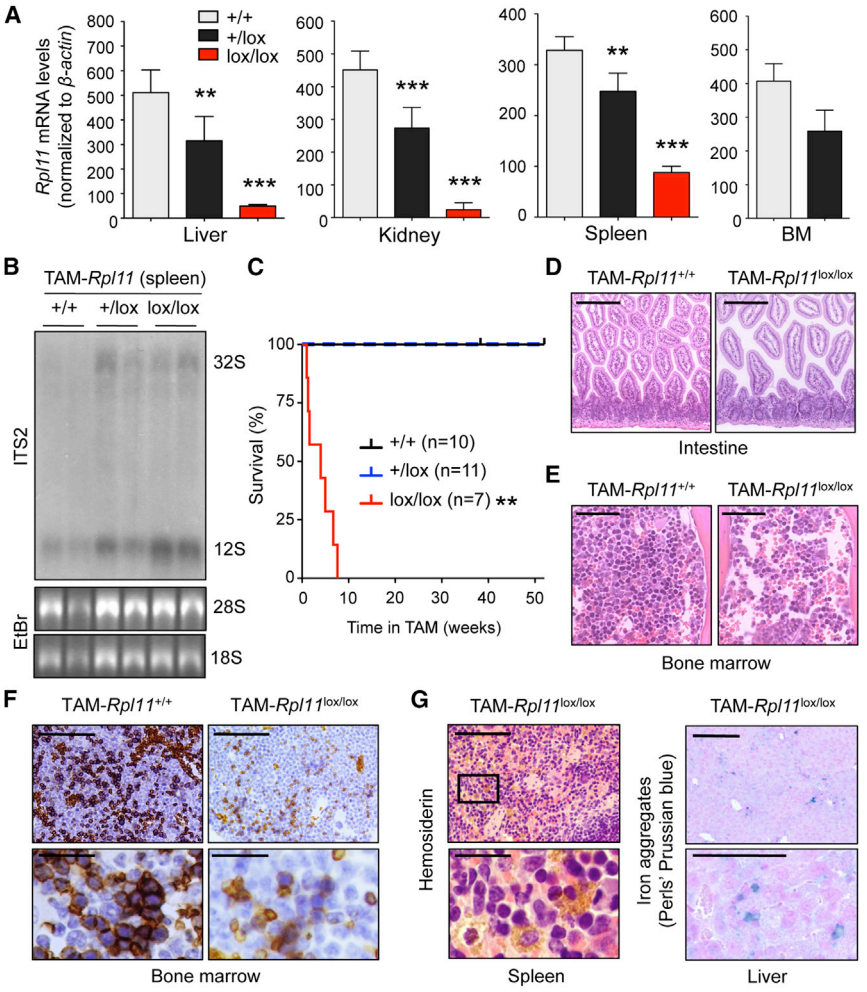

Figure 2. Adult Homozygous Deletion of *Rpl11* Is Lethal and Is Associated with Intestinal Atrophy and Bone Marrow Aplasia

(A) *Rpl11* mRNA levels measured by qRT-PCR in different tissues of TAM-mice of the indicated genotypes. Data correspond to +/+ or +/lox treated with TAM for 8 weeks (n = 4–5) or lox/lox treated with TAM for 1 week (n = 2). β-actin mRNA levels were used as an endogenous control.

(B) Northern blot analysis of 32S and 12S rRNA precursors in spleens of two animals of each genotype fed with TAM for 1 week. A probe specific for the ITS2 region was used to detect rRNA intermediates. The mature 28S and 18S forms were visualized by ethidium bromide staining.

(C) Kaplan-Meyer survival curve for TAM-treated *Rpl11*$^{+/+}$, *Rpl11*$^{+/lox}$, and *Rpl11*$^{lox/lox}$ animals. Log-rank (Mantel-Cox) test was performed to calculate significance of *Rpl11*$^{lox/lox}$ relative to the two other groups of mice (**p ≤ 0.01).

(D) Representative histological sections of intestine stained with H&E from TAM-*Rpl11*$^{+/+}$ and TAM-*Rpl11*$^{lox/lox}$ animals after 1 week of treatment. A total of three animals per genotype were analyzed. Scale bars, 200 μm.

(E) Representative histological sections of bone marrow stained with H&E. A total of two animals per genotype were analyzed. Scale bars, 100 μm.

(F) Representative histological sections of bone marrow stained with TER119. A total of two animals per genotype were analyzed. Scale bars, 100 and 25 μm in the top and bottom images, respectively.

(G) Representative histological sections of spleen (left) and liver (right) from TAM-*Rpl11*$^{lox/lox}$ animals showing accumulation of hemosiderin (spleen) and iron aggregates (Perls' Prussian blue staining in liver).

Scale bars, 100 and 25 μm in the images and zoom, respectively, in the spleen sections, and 25 μm in the liver sections. In (A), values correspond to the average ± SD. Statistical t test analysis was performed to calculate significance (*p ≤ 0.05; **p ≤ 0.01; ***p ≤ 0.005). For (C), see legend. See also Figure S2.

of age. Deletion of the *Rpl11*^{lox} allele was detected in the genomic DNA of the tail (Figure S2). More importantly, *Rpl11* mRNA levels were markedly reduced in TAM-*Rpl11*$^{lox/lox}$ mice (remaining levels in the range of 5%–30% depending on the tissue) and partially reduced in TAM-*Rpl11*$^{+/lox}$ mice (remaining levels in the range of 60%–75%) (Figure 2A). Of relevance, *Rpl11* reduction had a detectable impact on the maturation of rRNA as reflected by a clear accumulation of 32S and 12S rRNA precursors in the spleen of *Rpl11*$^{+/lox}$ and *Rpl11*$^{lox/lox}$ mice after 1 week of TAM treatment (Figure 2B). Therefore, mice carrying the inducible *Rpl11*^{lox} allele constitute a suitable model for the analysis of the in vivo effects of RPL11 deficiency in a mammalian organism.

Adult Homozygous Deletion of *Rpl11* Is Lethal

Treatment of mice with TAM starting at 1.5 months of age resulted to be lethal in the case of *Rpl11*$^{lox/lox}$ mice with no animals surviving beyond 8 weeks of TAM treatment (Figure 2C). Upon extensive histological analyses, the most obvious defects in these mice consisted in intestinal atrophy (which probably caused malnutrition) and bone marrow aplasia (Figures 2D and 2E). This suggests that highly proliferative tissues are the first to manifest defects upon severe reduction of RPL11. At the time of death, TAM-*Rpl11*$^{lox/lox}$ mice presented signs of developing anemia, including a pronounced decrease in bone marrow (BM) erythroblasts, as measured by nucleated TER119^{+} cells (Figure 2F), and a noticeable accumulation of hemosiderin in the spleen and iron in the liver, both consistent with defective erythropoiesis (Figure 2G). Therefore, complete loss of *Rpl11* is lethal in adult mice, probably due to intestinal atrophy, and it is accompanied by erythropoietic defects.

Adult Heterozygous Deletion of *Rpl11* Results in Chronic Anemia

Continuous TAM treatment of *Rpl11*$^{+/lox}$ mice did not compromise viability, at least during the first year of life (Figure 2C). DBA patients typically present macrocytic anemia (Ruggero and Shimamura, 2014), consisting in reduced red blood cell (RBC) counts with increased cellular size (mean corpuscular volume or MCV). Considering the involvement of human *RPL11*

Please cite this article in press as: Morgado-Palacin et al., Partial Loss of *Rpl11* in Adult Mice Recapitulates Diamond-Blackfan Anemia and Promotes Lymphomagenesis, Cell Reports (2015), http://dx.doi.org/10.1016/j.celrep.2015.09.038

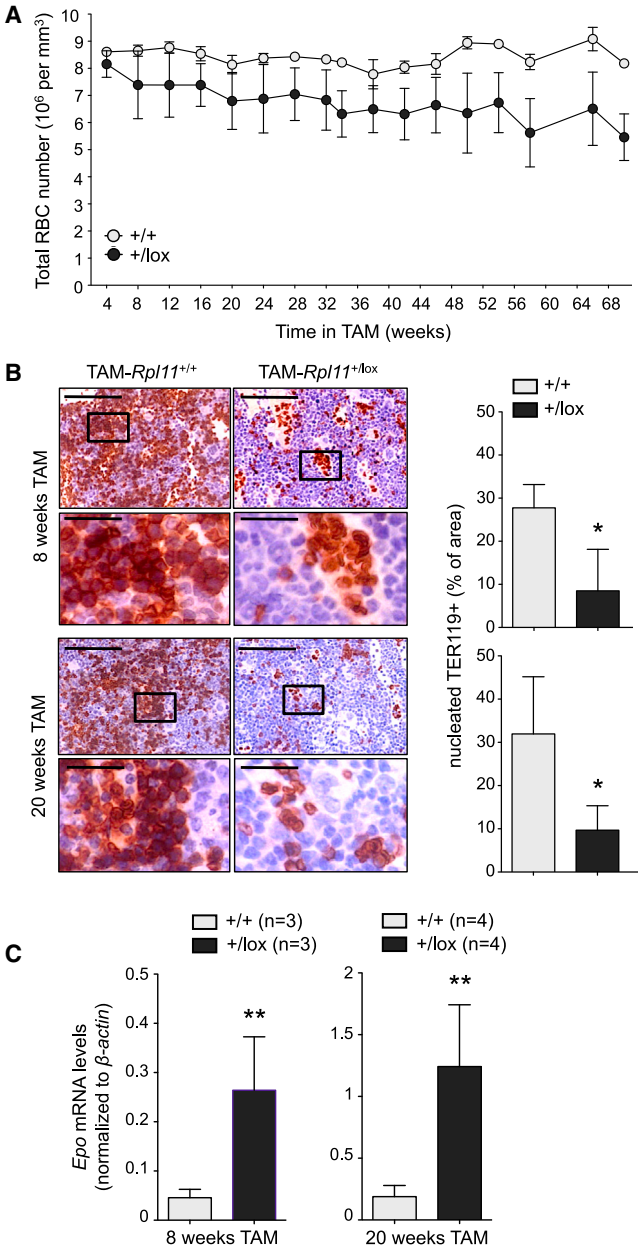

Figure 3. *Rpl11* Deficiency in Adult Mice Leads to Anemia and Reduction of Erythroid Progenitors

(A) Red blood cell (RBC) values for *Rpl11*$^{+/+}$ and *Rpl11*$^{+/lox}$ mice in TAM diet. Mice were fed TAM diet at 6 weeks of age. Data correspond to the average ± SD of six (*Rpl11*$^{+/+}$) or seven (*Rpl11*$^{+/lox}$) animals. Statistical t test analysis was performed per time point to calculate significance. Differences between genotypes were significant (*p ≤ 0.05 or **p ≤ 0.01) starting from 12 weeks of TAM treatment and beyond.

(B) Representative images of TER119-stained histological sections of bone marrows from mice that were TAM-treated during 8 (upper panel) or 20 (bottom panel) weeks. Zoom in pictures shows nucleated TER119^{+} cells. Scale bars, 100 and 25 μm in the images and zoom in pictures, respectively. Quantification of the positive area for nucleated cells expressing TER119 is shown. Data correspond to 8 weeks (n = 3 independent mice per genotype) or 20 weeks (n = 4) of TAM treatment.

(C) Erythropoietin (*Epo*) mRNA levels measured by qRT-PCR in kidneys from TAM-treated animals. Data correspond to the same mice as in (B). β-actin mRNA levels are used as an endogenous control.

Values correspond to the average ± SD. Statistical t test analysis was performed to calculate significance (*p ≤ 0.05; **p ≤ 0.01). For (A), see legend. See also Figure S3.

heterozygous mutations in DBA, we examined TAM-*Rpl11*$^{+/lox}$ mice for signs of anemia. Interestingly, TAM-*Rpl11*$^{+/lox}$ mice had lower RBC levels and macrocytosis compared to TAM-*Rpl11*$^{+/+}$ animals, being these effects more pronounced as animals aged (Figure 3A; Figure S3A). Histological examination of the BM indicated a significant decrease in the number of erythroblasts, as measured by nucleated TER119^{+} cells (Figure 3B). In support of this, the total mRNA levels of genes involved in erythrocyte function (*Epor*, *Hbb-h1*, *Trfc*, *Alas2*, and *Ireb2*) were all decreased in TAM-*Rpl11*$^{+/lox}$ BM (Figure S3B). Furthermore, we observed higher levels of erythropoietin (*Epo*) mRNA levels in the kidney, which is indicative of a compensatory response to stimulate eythropoiesis (Figure 3C). Despite the pronounced decrease in erythroblasts, the BM of TAM-*Rpl11*$^{+/lox}$ mice was histologically normocellular (Figure S3C) and had normal ratios of hematopoietic stem cells (HSCs, Lin^{-}Sca^{+}cKit^{+}) and progenitor cells (Figure S3D). Also, the sub-populations of thymic T cells and splenic B cells were all normal in TAM-*Rpl11*$^{+/lox}$ mice (data not shown). We conclude that partial loss of *Rpl11* produces a non-lethal anemia as a result of reduced erythropoiesis.

Direct Involvement of *Rpl11* in Erythropoiesis

To test if the BM precursors of TAM-*Rpl11*$^{+/lox}$ mice had a cell-autonomous defect in erythropoiesis, we first tested the capacity of BM cells to form in vitro burst-forming units-erythroid progenitors (BFU-E). We observed a tendency toward decreased BFU-E in the TAM-*Rpl11*$^{+/lox}$ BM (Figure S4A). To demonstrate that RPL11 plays a cell-autonomous role in in vivo erythropoiesis, we transplanted BM from *Rpl11*$^{+/+}$ and *Rpl11*$^{+/lox}$ donor mice, both carrying the *CreERT2* transgene, into irradiated SCID mice. Transplanted mice acquired a normal profile of mature T cells in the thymus, which was in contrast to non-transplanted SCID mice, thereby demonstrating successful BM reconstitution (data not shown). BM-transplanted (BMT) SCID mice were treated with continuous TAM diet, and we confirmed the presence of the excised *Rpl11*^{lox} allele (*Rpl11*^{Δ}) in the BM (Figure S4B). We refer to these transplanted mice and their controls as TAM-BMT-*Rpl11*$^{+/lox}$ and TAM-BMT-*Rpl11*$^{+/+}$ mice, respectively. Interestingly, RBC and hemoglobin levels decreased over time in TAM-BMT-*Rpl11*$^{+/lox}$ animals compared to TAM-*Rpl11*$^{+/+}$ BMT controls (Figure 4A). Remarkably, histological analysis of the BM indicated a severe decrease in erythroblasts (Figure 4B). Accordingly, TAM-BMT-*Rpl11*$^{+/lox}$ animals showed visible signs of weakness and paleness (Figure S4C). These observations indicate that RPL11 plays an important and cell-autonomous role in erythropoiesis.

Rpl11 Is Involved in Erythroid Maturation

Having demonstrated that *Rpl11* heterozygosity reduces the total number of erythroblasts, we wondered whether it also

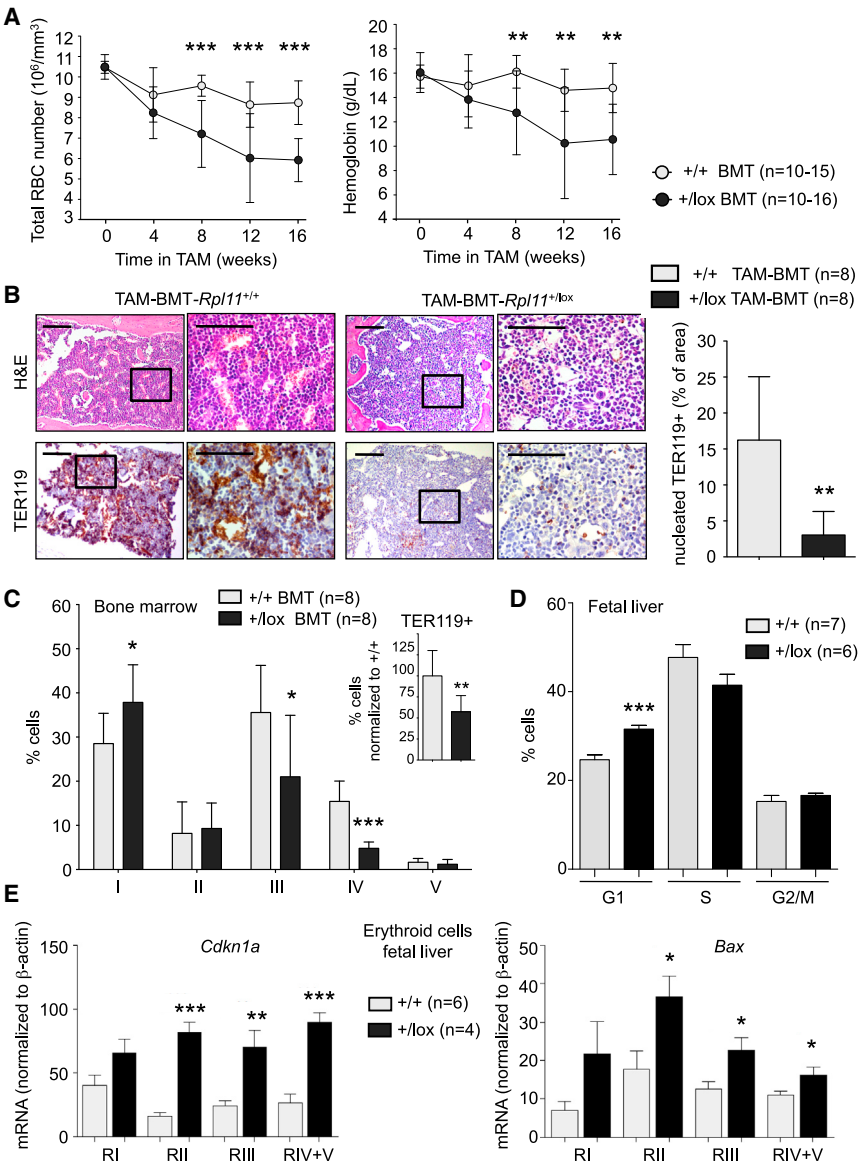

Figure 4. Intrinsic Hematopoietic Role of RPL11 in Anemia

(A) RBC and hemoglobin values from TAM-BMT-*Rpl11*$^{+/+}$ and TAM-BMT-*Rpl11*$^{+/lox}$ animals are shown along weeks in TAM diet. Data correspond to ten to 15 (*Rpl11*$^{+/+}$) or ten to 16 (*Rpl11*$^{+/lox}$) TAM-BMT animals, coming from four different donors for each genotype.

(B) Representative images of histological sections of bone marrows from TAM-BMT-*Rpl11*$^{+/+}$ and TAM-BMT-*Rpl11*$^{+/lox}$ animals stained with H&E (upper) or with an antibody against TER119 (bottom). Scale bars, 400 and 200 μm in the left and right images, respectively, for each genotype. Quantification of the positive area for nucleated cells expressing TER119 is shown. Data correspond to eight BM-transplanted animals per genotype (coming from two BM donors, for each genotype).

(C) Quantification by flow cytometry of the percentage of erythroid cells from BMs of TAM-BMT-*Rpl11*$^{+/+}$ and TAM-BMT-*Rpl11*$^{+/lox}$ animals in the different stages of erythroid maturation. Regions are defined based on the expression pattern of CD71 and TER119 markers. Data correspond to eight BM-transplanted animals per genotype (coming from two BM donors, for each genotype).

(D) Cell cycle analysis by flow cytometry after EdU incorporation and Hoechst staining of total fetal livers from *Rpl11*$^{+/+}$ and *Rpl11*$^{+/lox}$ embryos (E14.5) after daily injection of 4OHT in pregnant females from E11.5 to E13.5.

(E) mRNA levels of *Cdkn1a* and *Bax* genes in the different populations of erythroid progenitors from *Rpl11*$^{+/+}$ and *Rpl11*$^{+/lox}$ fetal livers, as in (D). mRNA levels are normalized to β-actin levels.

Values correspond to the average ±SD. Statistical t test analysis was performed to calculate significance (*p ≤ 0.05; **p ≤ 0.01; ***p ≤ 0.005). See also Figure S4.

impinges on erythroid maturation. Erythroid maturation can be divided in five stages (RI to RV) based on the patterns of TER119 signal (low or high) and CD71 signal (low, medium, or high) measured by fluorescence-activated flow cytometry (FACS) (Zhang et al., 2003a). We monitored erythroid maturation in the BM of transplanted animals (TAM-BMT-*Rpl11*$^{+/+}$ and TAM-BMT-*Rpl11*$^{+/lox}$). Interestingly, we detected a significant relative increase in the percentage of RI cells (primitive progenitors and proerythroblasts) together with a decrease in the more matured stages (RIII, RIV, and RV) (Figure 4C). Similar findings were made in the BM of whole-body TAM-*Rpl11*$^{+/lox}$ adult mice (Figure S4D), and in *Rpl11*$^{+/lox}$ fetal livers of TAM-pregnant mothers (Figure S4E). The fact that fetal livers (which are very active in erythropoiesis) manifest defective erythropoiesis prompted us to isolate erythroid progenitors and measure proliferation by FACS (using 5-ethynyl-2'-deoxyuridine [EdU] incorporation and Hoechst staining). Interestingly, as it was the case of fibroblasts (see Figure 1E), fetal liver cells also showed evidence of lower proliferation (significant increase in cells at G1, and tendency to decrease cells in S) (Figure 4D). Stage RIII erythroid precursors are the most abundant in fetal livers at E14.5 (see, for example, Figure S4E), and we also observed a significant G1 increase in RIII erythroid progenitors from fetal livers (Figure S4F). We wondered whether we could detect changes in candidate genes that could account for the impaired erythropoiesis. In particular, we focused on the cell-cycle inhibitor *Cdkn1a* and on the pro-apoptotic factor *Bax*, which have been previously found upregulated in human erythroid cells and in zebrafish embryos with *RPL11* deficiencies (Danilova et al., 2011; Moniz et al., 2012). Interestingly, several populations of erythroid progenitors from *Rpl11*$^{+/lox}$ fetal livers presented a significant upregulation of *Cdkn1a* and *Bax* (Figure 4E). We conclude that the partial loss of *Rpl11* impairs erythroid maturation, recapitulating the same cellular defects as in human DBA.

Please cite this article in press as: Morgado-Palacin et al., Partial Loss of *Rpl11* in Adult Mice Recapitulates Diamond-Blackfan Anemia and Promotes Lymphomagenesis, Cell Reports (2015), http://dx.doi.org/10.1016/j.celrep.2015.09.038

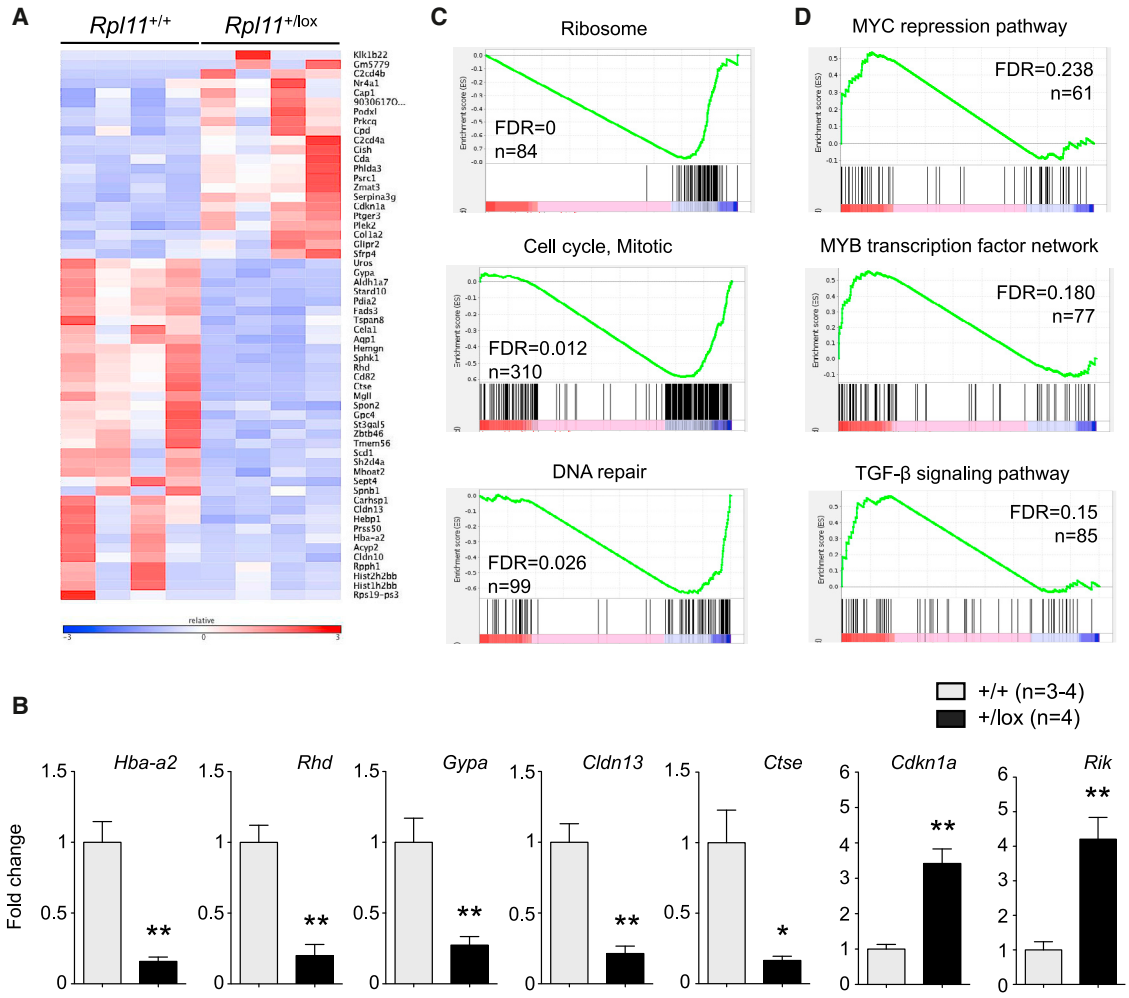

Figure 5. Impact of *Rpl11* Deficiency on the Transcriptional Profile of Bone Marrow Hematopoietic Progenitors

(A) Heatmap displaying differentially expressed genes (DEGs with FDR <0.15) as estimated by RNA-seq from *Rpl11*$^{+/+}$ and *Rpl11*$^{+/lox}$ hematopoietic progenitor cells (Lin$^-$Sca1$^-$cKIT$^+$) of TAM-treated animals (n = 4 animals per genotype; 20 weeks of TAM treatment). Gene symbols are shown and relative expression (log_2FC) is scaled in color code (indicated), from dark blue (−3) to dark red (3).

(B) Validation by qRT-PCR of some DEGs found in (A). Fold change over *Rpl11*$^{+/+}$ is shown for each gene. Data correspond to the average ± SD of three to four animals per genotype. Statistical t test analysis was performed to calculate significance (*p ≤ 0.05; **p ≤ 0.01).

(C) Enrichment plots for gene sets related to eukaryotic translation, DNA replication/cell cycle, and DNA repair pathways.

(D) Enrichment plots for gene sets related to MYC, MYB, and TGF-β.

In all the enrichment plots, *Rpl11*$^{+/lox}$ samples are located to the left. FDR and the number of genes per gene set (n) are indicated in each enrichment plot. See also Figure S5 and Tables S1 and S2.

Altered Transcriptional Profile Associated with *Rpl11* Deficiency

To further understand the molecular consequences of *Rpl11* deficiency, we performed an RNA-seq-based transcriptional profiling of the BM hematopoietic progenitors (HPCs; Lin$^-$Sca1$^-$cKIT$^+$) in TAM-*Rpl11*$^{+/lox}$ mice and in their corresponding TAM-*Rpl11*$^{+/+}$ controls (n = 4 per genotype). Previous to this, we confirmed that HPCs from TAM-*Rpl11*$^{+/lox}$ mice had lower levels of *Rpl11* mRNA than TAM-*Rpl11*$^{+/+}$ control HPCs (Figure S5A). Analysis of the RNA sequencing (RNA-seq) data revealed a number of differentially expressed genes (false discovery rate [FDR] <0.15) (Figure 5A; Table S1). In agreement with the impaired erythropoiesis observed in TAM-*Rpl11*$^{+/lox}$ mice, genes related to erythrocyte development and function, such as *Uros*, *Gypa*, *Aqp1*, *Sphk1*, *Rhd*, *Cd82*, *Hebp1*, and *Hba-a2*, were among the genes significantly downregulated in TAM-*Rpl11*$^{+/lox}$ HPCs (Figure 5A). By qRT-PCR, we confirmed that some of these genes were downregulated in *Rpl11*-deficient HPCs (Figure 5B) but were unaffected in other tissues, such as liver (Figure S5B). Other genes with diverse functions, such as cathepsin E (*Ctse*), which promotes proteolysis, or claudin 13 (*Cldn13*), which has a structural function, were also downregulated in *Rpl11*$^{+/lox}$ HPCs (Figures 5A and 5B). A description of other downregulated genes is shown in Table S1. Regarding the genes upregulated in TAM-*Rpl11*$^{+/lox}$ HPCs, we validated the cyclin-dependent kinase inhibitor p21 (*Cdkn1a*) and a gene

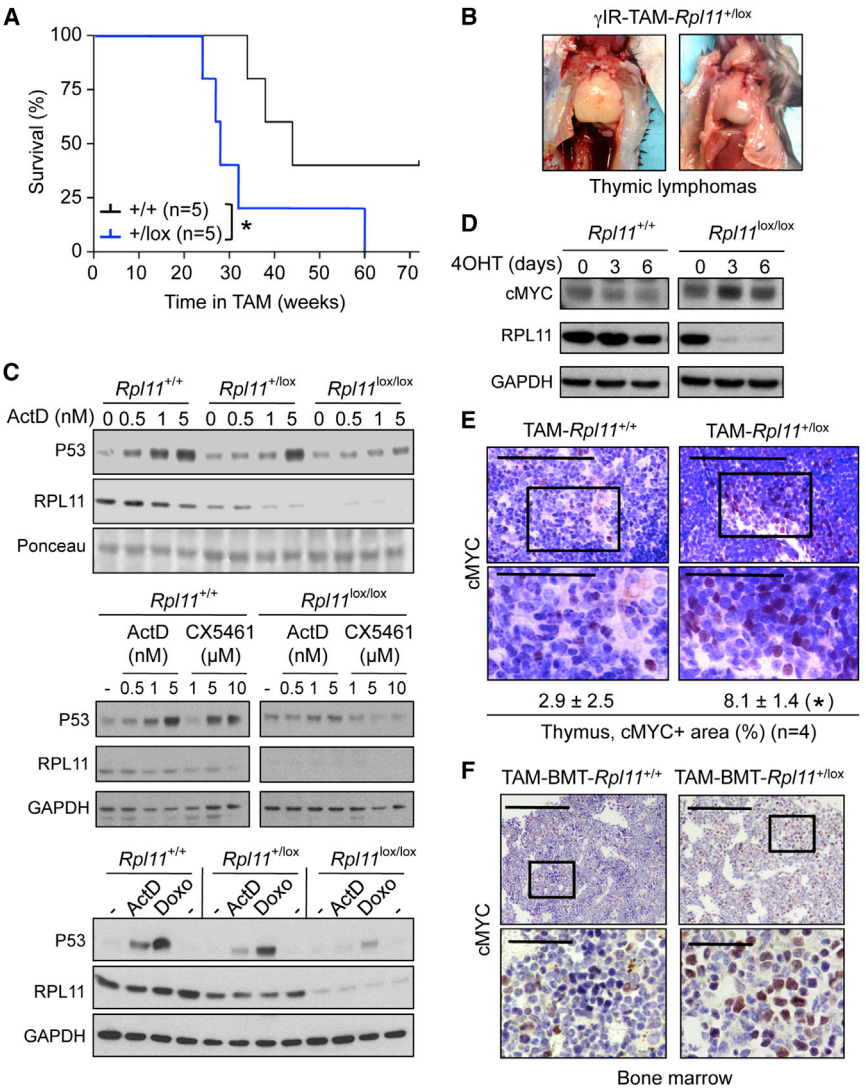

Figure 6. *Rpl11* Deficiency Increases Susceptibility to Lymphomagenesis in γ-Irradiated Mice

(A) Kaplan-Meyer survival curve for γ-irradiated *Rpl11*$^{+/+}$ and *Rpl11*$^{+/lox}$ mice fed TAM diet. Log-rank (Mantel-Cox) test was performed to calculate significance (*$p \leq 0.05$).

(B) Pictures of γ-irradiated TAM-*Rpl11*$^{+/lox}$ mice displaying thymic tumors.

(C) Immortalized *Rpl11*$^{+/+}$, *Rpl11*$^{+/lox}$, and *Rpl11*$^{lox/lox}$ MEFs, all bearing the Tg.hUbC-*CreERT2* transgene, were treated with 4OHT for 3 days and then incubated with the following drugs: ActD, for 6 hr, at the indicated concentrations or 5 nM when not specified; CX5461, for 16 hr, at the indicated concentrations; or doxorubicin, for 6 hr, at 0.5 μM. Levels of the indicated proteins were measured by immunoblotting.

(D) Primary *Rpl11*$^{+/+}$ and *Rpl11*$^{lox/lox}$ MEFs, all carrying the Tg.hUbC-CreERT2 transgene, were treated with 4OHT for the indicated times and harvested for protein extraction. Levels of the indicated proteins were measured by immunoblotting. The assay is representative of a total of two assays with different MEF preparations.

(E) Representative histological sections stained for cMYC from thymuses of *Rpl11*$^{+/+}$ and *Rpl11*$^{+/lox}$ mice (after 20 weeks of TAM diet). Scale bars, 100 (top images) and 50 (zoom in images) μm. Quantification of cMYC-positive area is shown below. Data correspond to the average ± SD of four independent animals per genotype. Statistical t test analysis was performed to calculate significance (*$p \leq 0.05$).

(F) Representative histological sections of bone marrow stained for cMYC from TAM-BMT-*Rpl11*$^{+/+}$ and TAM-BMT-*Rpl11*$^{+/lox}$ mice.

Scale bars, 200 (top images) and 50 (zoom in images) μm. Pictures are representative of a total of n = 4 per genotype. See also Figure S6.

(*9030617O03Rik*) of unknown function (Figures 5A and 5B). Gene set enrichment analysis (FDR <0.25) showed that several transcriptional gene sets related to eukaryotic translation (including the gene set "Ribosome") were downregulated in TAM-*Rpl11*$^{+/lox}$ HPCs (Figure 5C; Table S2). A high number of gene sets involved in DNA replication/cell cycle and DNA repair were also downregulated (Figure 5C; Table S2). We found particularly interesting that potentially oncogenic pathways were upregulated, such as MYC and MYB transcription networks and transforming growth factor β (TGF-β) signaling pathway (Figure 5D; Table S2). Remarkably, a very recent report has showed upregulation of the TGF-β signaling pathway in induced pluripotent stem cells derived from DBA patients with mutations in *RPS19* or *RPL15* (Ge et al., 2015).

Partial Loss of *Rpl11* Favors Lymphomagenesis

Patients with ribosomopathies, including those with DBA, are prone to develop cancer, often of hematological origin, although the mechanisms involved are poorly understood (Narla and Ebert, 2010; Teng et al., 2013). To address this issue, we tested whether partial loss of *Rpl11* predisposed mice to lymphomagenesis. We irradiated mice with a single dose of 5 Gy, and, after 1 week, we fed them with tamoxifen (abbreviated as γIR-TAM mice). As expected from our above-described findings, γIR-TAM-*Rpl11*$^{+/lox}$ mice developed anemia, as measured by the red blood numbers and hemoglobin blood content (Figure S6A). Remarkably, γIR-TAM-*Rpl11*$^{+/lox}$ mice died significantly earlier than control TAM-*Rpl11*$^{+/+}$ mice (Figure 6A). Upon necropsy, γIR-TAM-*Rpl11*$^{+/lox}$ mice presented lymphomas, particularly in the thymus, which in some cases occupied most of the thoracic cavity (Figure 6B). These observations demonstrate that partial loss of *Rpl11* predisposes to lymphomagenesis.

Rpl11 Deficiency Affects p53 Response and cMYC Levels

Based on previous literature, two conceivable and non-exclusive mechanisms could explain the observed susceptibility to cancer upon partial loss of *Rpl11*. In particular, ribosome-free RPL11

Please cite this article in press as: Morgado-Palacin et al., Partial Loss of *Rpl11* in Adult Mice Recapitulates Diamond-Blackfan Anemia and Promotes Lymphomagenesis, Cell Reports (2015), http://dx.doi.org/10.1016/j.celrep.2015.09.038

acts as a sensor of ribosome unbalance by activating p53 (Bhat et al., 2004; Bursać et al., 2012; Donati et al., 2013; Horn and Vousden, 2008; Lohrum et al., 2003; Zhang et al., 2003b) and by inhibiting cMYC (Challagundla et al., 2011; Dai et al., 2007, 2010). To evaluate the p53 response to ribosomal stress, we treated MEFs of the three relevant genotypes (all bearing the Tg.UbC-*CreERT2* transgene) with 4OHT for 3 days followed by low doses of actinomycin D (ActD), which is a well-established method to induce ribosomal stress (Burger et al., 2010). In addition to this, we used an RNA polymerase I inhibitor, CX5461, which activates p53 in an RPL11-dependent manner and has shown promising pre-clinical anti-tumoral activity (Bywater et al., 2012; Drygin et al., 2011). Finally, we also tested the radiomimetic agent doxorubicin (Doxo), which in addition to DNA damage also induces ribosomal stress (Burger et al., 2010; Llanos and Serrano, 2010; Zhu et al., 2009). Importantly, the stabilization of p53 in response to all these agents (ActD, CX5461, Doxo) was severely impaired in 4OHT-*Rpl11*$^{lox/lox}$ cells, and it was partially compromised in 4OHT-*Rpl11*$^{+/lox}$ cells (Figure 6C).

Regarding cMYC, previous investigators have reported that downregulation of RPL11 in cultured cancer cells results in increased levels of cMYC protein (Challagundla et al., 2011; Dai et al., 2007, 2010). In this regard, we have observed above that *Rpl11* heterozygous HPCs present an upregulation of MYC gene sets (see above Figure 5D). Based on this, we wondered whether reduced gene dosage of *Rpl11* could have an impact on the levels of cMYC. First, we examined cMYC levels in primary 4OHT-*Rpl11*$^{+/+}$ and 4OHT-*Rpl11*$^{lox/lox}$ MEFs. In support of the above-mentioned evidences, cMYC protein levels were increased in *Rpl11*$^{lox/lox}$ MEFs upon 4OHT treatment, whereas cMYC levels remained unchanged in *Rpl11*$^{+/+}$ MEFs (Figure 6D). Also, immunohistochemical staining of cMYC showed a clear and reproducible increase in cMYC levels in the thymus of TAM-*Rpl11*$^{+/lox}$ mice compared to TAM-*Rpl11*$^{+/+}$ controls (Figure 6E). Of note, we confirmed that TAM treatment was effective in reducing (by 40%) the levels of *Rpl11* mRNA in the thymus (Figure S6B). Similar observations regarding cMYC protein levels were made in the spleen of TAM-*Rpl11*$^{+/lox}$ mice (Figure S6C) and in the BM of TAM-BMT-*Rpl11*$^{+/lox}$ transplanted animals (Figure 6F). Therefore, *Rpl11* deficiency, even in the form of *Rpl11* heterozygosity, compromises p53 function and increases cMYC protein basal levels. These two pro-tumorigenic effects could contribute, alone or combined, to the cancer susceptibility of *Rpl11*-deficient mice.

DISCUSSION

In this work, we have set to generate a mouse model of Diamond-Blackfan anemia (DBA) based on the deficiency of the ribosomal protein RPL11. A first remarkable observation is the fact that embryonic heterozygous deletion of *Rpl11* is lethal, implying that diploid levels of RPL11 are required for embryonic development. This is an unusually extreme phenotype for mice with deficiencies in ribosomal proteins (Caldarola et al., 2009), and we are only aware of one other ribosomal gene, *RpS6*, that is embryonically lethal in heterozygosity (Panić et al., 2006). Also, inducible complete deletion of *Rpl11* in adult mice was lethal within 8 weeks post-deletion, probably due to intestinal atrophy, and it was accompanied by bone marrow aplasia and erythropoietic defects. This severe phenotype is not surprising given the essential role of RPL11 in the formation and function of ribosomes. Human DBA patients carry heterozygous loss-of-function mutations in ribosomal genes (Boria et al., 2010; Cmejla et al., 2009; Gazda et al., 2008; Quarello et al., 2010). For this reason, and considering the embryonic lethality of constitutively heterozygous mice, we have focused our work on the effects of inducible heterozygous deletion of *Rpl11* in adult mice.

A number of mouse models of DBA and ribosomopathies have been reported (McGowan and Mason, 2011; Narla and Ebert, 2010), but only a subset of them recapitulate the erythropoietic defect characteristic of human DBA patients, namely, mice with partial deficiencies of *Rps19* (Devlin et al., 2010; Jaako et al., 2011), *Rps6* (Keel et al., 2012; McGowan et al., 2011), or *Rps14* (Barlow et al., 2010). Similar to these mouse models, we show that inducible heterozygous deletion of *Rpl11* produces a non-lethal anemia characterized by a severe reduction of erythroblasts in the bone marrow. In addition, the erythroblasts of heterozygous *Rpl11* mice present a maturation defect, which is accompanied by upregulation of the cell-cycle inhibitor *Cdkn1a* and the pro-apoptotic factor *Bax*. In relation to this, erythroid progenitors from peripheral blood of *RPL11*-mutated human DBA patients present a similar erythroid differentiation defect with upregulation of *CDKN1A* (Moniz et al., 2012). In addition, we have observed that a number of genes involved in erythrocyte differentiation are downregulated in heterozygous *Rpl11* hematopoietic progenitors. Together, these observations could explain, at least in part, the reduced number of erythroblasts and their defective maturation in *Rpl11*-deficient mice.

Besides the severe defect in erythropoiesis, heterozygous *Rpl11* mice did not have other noticeable defects in the hematopoietic lineage, presenting normal levels of hematopoietic stem cells and early progenitors, B cell subpopulations, and T cell subpopulations. Despite the apparently normal production of non-erythroid lineages, the analysis of the gene expression profile of *Rpl11* heterozygous hematopoietic progenitors showed an upregulation of the cell-cycle inhibitor gene *Cdkn1a* and downregulation of a number of mitotic and cell-cycle gene sets. Compared to other hematopoietic progenitors, erythroblasts are highly proliferative, and this could render them more susceptible to a partial reduction in proliferation. Furthermore, normal mice transplanted with inducible heterozygous *Rpl11* bone marrow also developed anemia and reduced number of erythroblasts upon induction of *Rpl11* deletion. Together, these observations suggest that erythropoiesis critically relies on diploid levels of RPL11. A similar situation is encountered in DBA patients, where haploid levels of a given ribosomal gene selectively affect erythropoiesis (Narla and Ebert, 2010).

In addition to anemia, DBA patients are also characterized by an increased susceptibility to cancer (Ruggero and Shimamura, 2014); however, tumor susceptibility in mouse models of DBA has remained largely unexplored until now. We have observed that heterozygous *Rpl11* mice are highly susceptible to develop radiation-induced lymphomas. This phenotype is apparently paradoxical given the fact that an impaired ribosome production should limit cell growth and proliferation; however, it could reflect the emerging extra-ribosomal functions of RPL11 in tumor

suppression. In particular, ribosome-free RPL11 acts as a sensor of ribosome unbalance by activating p53 (Bhat et al., 2004; Lohrum et al., 2003; Zhang et al., 2003b) and by inhibiting cMYC (Challagundla et al., 2011; Dai et al., 2007, 2010). In mouse embryo fibroblasts, we have observed that complete or partial deletion of *Rpl11* impairs the activation of p53 by ribosomal stress and by DNA damage. Also, fibroblasts, bone marrow, spleen, and thymus of heterozygous *Rpl11* mice present increased basal levels of cMYC protein. Therefore, both mechanisms, namely, impaired p53 response and increased cMYC levels, can conceivably account for the observed tumor-prone phenotype of heterozygous *Rpl11* mice. As a marginal note, the upregulation of cMYC could also contribute to the impaired erythroid differentiation phenotype (Acosta et al., 2008; Coppola and Cole, 1986; Geiler et al., 2014).

In summary, we have generated and characterized a mouse model of DBA based on heterozygous deficiency of *Rpl11*. These mice recapitulate the two main features of DBA, namely, anemia and cancer susceptibility. In the case of anemia, we have identified a defect in erythroid differentiation associated with the upregulation of *Cdkn1a* and *Bax* in erythroid progenitors. Regarding tumor susceptibility, we present supporting data for two non-exclusive mechanisms based on the known capacity of ribosome-free RPL11 to activate p53 and inhibit cMYC. This mouse model may help to further understand DBA and to test possible therapeutic approaches.

EXPERIMENTAL PROCEDURES

Generation of a Conditional *Rpl11* Knockout Mouse Model

A DNA construct with exons 3 and 4 of the *Rpl11* gene flanked by loxP sites and bearing a neomycin cassette (flanked by FRT sites) in intron 2 was generated by GeneBridges and electroporated in G4 embryonic stem (ES) cells (C57BL/6Ncr × 129S6/SvEvTac) at the CNIO Transgenic Mice Unit. Recombinant ES clones were selected by neomycin resistance and screened for insertion of the construct in the 5′ and 3′ homology arms of the chromosome 4 by Southern blot and long-range PCR, respectively. The presence of both loxP sites was confirmed by PCR. One positive clone was aggregated with albino ES cells (B6(Cg)-*Tyr*$^{c-2J}$/J) and injected into pseudo-pregnant albino females. A 100% male chimera was then mated with CD-1 females in order to check for the germline transmission and establish the mouse colony. Mice bearing the neomycin (Neo) resistance gene (*Rpl11*$^{+/loxfrt}$) were viable and fertile and crossed with B6 mice expressing a flipase recombinase (pCAG-*Flpe*) (Rodríguez et al., 2000), which recognizes the FRT sites and excises the Neo cassette. *Rpl11*$^{+/lox}$ mice were mated with either constitutive (Tg.pCAG-*Cre*) (Sakai and Miyazaki, 1997) or with inducible (Tg.hUbC-*CreERT2*) (Ruzankina et al., 2007) Cre expressing mice (all in B6 background). The mice used for this work are in a mixed background (81.25% B6: 6.25% 129Sv: 12.5% CD1). All animals were maintained at the Spanish National Cancer Research Centre (CNIO) under specific pathogen-free conditions, in agreement with the recommendations of the Federation of European Laboratory Animal Science Association (FELASA). Mice were fed a standard chow diet ad libitum. When indicated, standard chow diet was replaced by tamoxifen diet (Teklad, Harlan Laboratories) to induce activation of the *CreERT2* transgene. All animal procedures were evaluated and approved by the Ethical Committee of the Carlos III Health Institute, Madrid, Spain (#54-2013-v2).

Cell Culture and Treatments

MEFs were isolated from embryos at day E13.5 and cultured in DMEM (Gibco) supplemented with 10% fetal bovine serum (Gibco) and 100 U/ml penicillin-streptomycin (Gibco) in a humidified atmosphere at 37°C, 5% CO_2. For immortalization, cells were infected with a retroviral vector expressing T121, a truncated form of the SV40 large T antigen (Sáenz Robles et al., 1994) and underwent antibiotic selection. Where indicated, cells were treated with 1 μM 4-hydroxytamoxifen (4OHT; Sigma H7904), actinomycin D (Sigma), CX5461 (Selleckchem), or doxorubicin (Sigma).

Nuclear/Cytosolic Fractionation

Immortalized MEFs were harvested and nuclear and cytosolic fractions were obtained by using the NE-PER Nuclear and Cytoplasmic Extraction Kit by Thermo Scientific, following the manufacturer's instructions.

Red Blood Cells and Hemoglobin Monitoring

Blood was obtained from submaxillary bleeding, and red blood cell counts, mean corpuscular volume, (MCV) and hemoglobin levels were measured in an Abacus Junior Vet Hematology Analyzer.

Bone Marrow Transplantation

Bone marrows (BMs) from animals 6–8 weeks old were isolated by flushing femurs and tibias (RPMI medium supplemented with 15% fetal bovine serum [FBS] and Pen/Strep) with a 25-G syringe, followed by disaggregation with a 21-G syringe and subsequent filtration through a 70-μm nylon mesh. Erythrocytes were lysed in ammonium chloride (STEMCELL Technologies) for 5 min at room temperature, neutralized with fresh medium, and counted. A total of 2.5–5 millions of cells in Leibovitz medium were injected by tail vein in immunodeficient SCID recipient mice (CB17/Icr-*Prkdc*^{scid}/Crl) of 10–12 weeks old. SCID mice were irradiated with a single dose of 3.5 Gy the day before to BM transplantation.

Isolation of Fetal Liver Cells

Pregnant females were intraperitoneally (i.p.) injected with 4OHT (Sigma, H6278), 2 mg/day dissolved in corn oil, for 3 days before fetal livers collection at E14.5. Fetal livers were disaggregated with a 25-G syringe in RPMI medium (supplemented with 15% FBS and Pen/Strep) and passed through a 40-μm nylon mesh. Erythrocytes were lysed in ammonium chloride (Stemcell Technologies) for 5 min at room temperature, and cells were counted and processed for flow cytometry. For cell-cycle analysis, fetal liver cells were incubated ex vivo with EdU (10 μM) for 30 min and then stained with the anti-TER119 and anti-CD-71 antibodies for flow cytometry. EdU was labeled through covalent binding to Alexa Fluor 647 azide using Click-iT chemistry (Invitrogen) following manufacturer's instructions. DNA was stained with Hoechst. Quantification of the different cell-cycle phases was performed in the total liver cells or in the various erythroid progenitor populations according to TER119 and CD-71 stainings.

Flow Cytometry

Cells were isolated by flushing (BM) or disaggregating tissues (spleen and thymus) followed by filtering through a nylon mesh and removal of erythrocytes by ammonium chloride lysis. 2.5–5 million cells were then blocked in a solution containing Fc block (CD16/CD32, BD Biosciences #553141) in a 1:400 dilution and incubated with the following conjugated antibodies for 30 min to 1 hr in ice (spleen and thymus) or at room temperature (BM cells): mouse hematopoietic lineage eF450 cocktail (eBioscience #88-7772-72), Sca-1-PerCP/Cy5.5 (eBioscience #45-5981-80), cKIT-APC/H7 (BD Biosciences #560250), CD34-eF660 (eBioscience #50-0341-82), IL7R-AF488 (eBioscience #53-1271-82), FcγRIII/II (CD16/32)-PE/Cy7 (eBioscience #25-0161-81), CD71-PE (eBioscience #12-0711-83) and TER119-FITC (eBioscience #11-5921-82). Fluorescence Minus One (FMO) was used to gate cell populations and commercial anti-mouse or anti-rat Igκ beads (BD Biosciences #552843 or # 552844) to compensate for fluorochrome spectral overlap during flow cytometry. Cells were analyzed in an LSR-Fortessa or FACS CANTO (BD Biosciences; FACS Diva software). Data were analyzed with FlowJo 9.6.2 software.

RNA-Seq-Based Transcriptional Profiling

RNA was prepared by using Direct-zol (Zymo Research) from BM hematopoietic progenitor cells (Lin- Sca1$^-$ cKIT$^+$) of TAM-treated animals. Mouse lineage depletion cocktail (Miltenyi #130-090-858) was used to eliminate mature hematopoietic cells. RNA Integrity Number (RIN) was in the range 7.5–9.3 (Agilent 2100 Bionalyzer). 2–8 ng of total RNA was used to synthesize the cDNA (SMARTer Ultra Low Input RNA Kit, version 3, Clontech #634848). After amplification with SeqAmp DNA Polymerase (Clontech), ~10 ng of cDNA was used

Please cite this article in press as: Morgado-Palacin et al., Partial Loss of *Rpl11* in Adult Mice Recapitulates Diamond-Blackfan Anemia and Promotes Lymphomagenesis, Cell Reports (2015), http://dx.doi.org/10.1016/j.celrep.2015.09.038

to prepare the adaptor-ligated library following the "TruSeq DNA sample preparation guide" (part #15005180). The resulting cDNA libraries were sequenced for 50 bases in a single-read format (Illumina HiSeq2000). Reads were aligned to the mouse genome (GRCm38/mm10) with TopHat-2.0.10 (Trapnell et al., 2012) using Bowtie 1.0.0 (Langmead et al., 2009) and Samtools 0.1.19 (Li et al., 2009), allowing two mismatches and five multihits. Transcripts assembly, estimation of their abundances and differential expression were calculated with Cufflinks 2.2.1 (Trapnell et al., 2012), using the mouse genome annotation data set GRCm38/mm10 from the UCSC Genome Browser. Gene Set Enrichment Analysis (GSEA) was performed using annotations from the KEGG, Reactome and NCI databases. Genes were ranked using the t statistic. After Kolmogorov-Smirnoff correction for multiple testing, only those pathways bearing a FDR <0.25 were considered significant. Enrichment plots were also obtained with GSEA and ranked according to their enrichment score (ES).

Histopathology

Mice organs were fixed in formalin and embedded in formalin/paraffin blocks. Sections and H&E and immunohistochemistry stainings were performed by the CNIO Histopathology Unit. Antibodies recognizing TER119 (BD Biosciences, #550565) and c-MYC (Abcam, clone Y69, #ab32072) were used. Positive cells for the above mentioned antibodies were quantified by using AxioVision (Zeiss) software.

ACCESSION NUMBERS

The accession number for the RNA-seq data sets is GEO: GSE72537.

SUPPLEMENTAL INFORMATION

Supplemental Information includes Supplemental Experimental Procedures, six figures, and two tables and can be found with this article online at http://dx.doi.org/10.1016/j.celrep.2015.09.038.

AUTHOR CONTRIBUTIONS

L.M.-P. performed the majority of the experimental work and contributed to experimental design, data analysis, discussion, and writing the manuscript; G.V. and S.L. helped with the experimentation, data analysis, discussion, and writing; G.G.-L. performed the bioinformatics analysis; D.M. performed and interpreted the flow cytometry analyses; M.S. designed and supervised the study, secured funding, analyzed the data, and wrote the manuscript. All authors discussed the results and commented on the manuscript.

ACKNOWLEDGMENTS

We thank M. Foronda, M. Abad, C. Pantoja, P.J. Fernandez-Marcos, A. de Martino, G. Iglesias, O. Dominguez, and S. Ortega for valuable contributions. We are also thankful to the Flow Cytometry, Genomics, Transgenics, and Histopathology Units of the CNIO. L.M.-P. was recipient of a predoctoral fellowship from the Spanish Ministry of Education. Work in the laboratory of M.S. is funded by the CNIO and by grants from the Spanish Ministry of Economy (SAF), the European Research Council (ERC Advanced Grant), the Regional Government of Madrid, the Botin Foundation and Banco Santander (Santander Universities Global Division), the Ramon Areces Foundation, and the AXA Foundation.

Received: April 11, 2015
Revised: August 10, 2015
Accepted: September 14, 2015
Published: October 15, 2015

REFERENCES

Acosta, J.C., Ferrándiz, N., Bretones, G., Torrano, V., Blanco, R., Richard, C., O'Connell, B., Sedivy, J., Delgado, M.D., and León, J. (2008). Myc inhibits p27-induced erythroid differentiation of leukemia cells by repressing erythroid master genes without reversing p27-mediated cell cycle arrest. Mol. Cell. Biol. *28*, 7286–7295.

Barlow, J.L., Drynan, L.F., Hewett, D.R., Holmes, L.R., Lorenzo-Abalde, S., Lane, A.L., Jolin, H.E., Pannell, R., Middleton, A.J., Wong, S.H., et al. (2010). A p53-dependent mechanism underlies macrocytic anemia in a mouse model of human 5q- syndrome. Nat. Med. *16*, 59–66.

Bhat, K.P., Itahana, K., Jin, A., and Zhang, Y. (2004). Essential role of ribosomal protein L11 in mediating growth inhibition-induced p53 activation. EMBO J. *23*, 2402–2412.

Boria, I., Garelli, E., Gazda, H.T., Aspesi, A., Quarello, P., Pavesi, E., Ferrante, D., Meerpohl, J.J., Kartal, M., Da Costa, L., et al. (2010). The ribosomal basis of Diamond-Blackfan Anemia: mutation and database update. Hum. Mutat. *31*, 1269–1279.

Burger, K., Mühl, B., Harasim, T., Rohrmoser, M., Malamoussi, A., Orban, M., Kellner, M., Gruber-Eber, A., Kremmer, E., Hölzel, M., and Eick, D. (2010). Chemotherapeutic drugs inhibit ribosome biogenesis at various levels. J. Biol. Chem. *285*, 12416–12425.

Bursać, S., Brdovčak, M.C., Pfannkuchen, M., Orsolić, I., Golomb, L., Zhu, Y., Katz, C., Daftuar, L., Grabušić, K., Vukelić, I., et al. (2012). Mutual protection of ribosomal proteins L5 and L11 from degradation is essential for p53 activation upon ribosomal biogenesis stress. Proc. Natl. Acad. Sci. USA *109*, 20467–20472.

Bywater, M.J., Poortinga, G., Sanij, E., Hein, N., Peck, A., Cullinane, C., Wall, M., Cluse, L., Drygin, D., Anderes, K., et al. (2012). Inhibition of RNA polymerase I as a therapeutic strategy to promote cancer-specific activation of p53. Cancer Cell *22*, 51–65.

Caldarola, S., De Stefano, M.C., Amaldi, F., and Loreni, F. (2009). Synthesis and function of ribosomal proteins–fading models and new perspectives. FEBS J. *276*, 3199–3210.

Challagundla, K.B., Sun, X.-X., Zhang, X., DeVine, T., Zhang, Q., Sears, R.C., and Dai, M.-S. (2011). Ribosomal protein L11 recruits miR-24/miRISC to repress c-Myc expression in response to ribosomal stress. Mol. Cell. Biol. *31*, 4007–4021.

Cmejla, R., Cmejlova, J., Handrkova, H., Petrak, J., Petrtylova, K., Mihal, V., Stary, J., Cerna, Z., Jabali, Y., and Pospisilova, D. (2009). Identification of mutations in the ribosomal protein L5 (RPL5) and ribosomal protein L11 (RPL11) genes in Czech patients with Diamond-Blackfan anemia. Hum. Mutat. *30*, 321–327.

Coppola, J.A., and Cole, M.D. (1986). Constitutive c-myc oncogene expression blocks mouse erythroleukaemia cell differentiation but not commitment. Nature *320*, 760–763.

Dai, M.-S., Arnold, H., Sun, X.-X., Sears, R., and Lu, H. (2007). Inhibition of c-Myc activity by ribosomal protein L11. EMBO J. *26*, 3332–3345.

Dai, M.-S., Sun, X.-X., and Lu, H. (2010). Ribosomal protein L11 associates with c-Myc at 5 S rRNA and tRNA genes and regulates their expression. J. Biol. Chem. *285*, 12587–12594.

Danilova, N., Sakamoto, K.M., and Lin, S. (2011). Ribosomal protein L11 mutation in zebrafish leads to haematopoietic and metabolic defects. Br. J. Haematol. *152*, 217–228.

Devlin, E.E., Dacosta, L., Mohandas, N., Elliott, G., and Bodine, D.M. (2010). A transgenic mouse model demonstrates a dominant negative effect of a point mutation in the RPS19 gene associated with Diamond-Blackfan anemia. Blood *116*, 2826–2835.

Donati, G., Peddigari, S., Mercer, C.A., and Thomas, G. (2013). 5S ribosomal RNA is an essential component of a nascent ribosomal precursor complex that regulates the Hdm2-p53 checkpoint. Cell Rep. *4*, 87–98.

Drygin, D., Lin, A., Bliesath, J., Ho, C.B., O'Brien, S.E., Proffitt, C., Omori, M., Haddach, M., Schwaebe, M.K., Siddiqui-Jain, A., et al. (2011). Targeting RNA polymerase I with an oral small molecule CX-5461 inhibits ribosomal RNA synthesis and solid tumor growth. Cancer Res. *71*, 1418–1430.

Gazda, H.T., Sheen, M.R., Vlachos, A., Choesmel, V., O'Donohue, M.F., Schneider, H., Darras, N., Hasman, C., Sieff, C.A., Newburger, P.E., et al. (2008). Ribosomal protein L5 and L11 mutations are associated with cleft

palate and abnormal thumbs in Diamond-Blackfan anemia patients. Am. J. Hum. Genet. *83*, 769–780.

Ge, J., Apicella, M., Mills, J.A., Garçon, L., French, D.L., Weiss, M.J., Bessler, M., and Mason, P.J. (2015). Dysregulation of the transforming growth factor β pathway in induced pluripotent stem cells generated from patients with diamond blackfan anemia. PLoS One, Published online August 10, 2015. http://dx.doi.org/10.1371/journal.pone.0134878.

Geiler, C., Andrade, I., and Greenwald, D. (2014). Exogenous c-Myc blocks differentiation and improves expansion of human erythroblasts. Int. J. Stem Cells *7*, 153–157.

Horn, H.F., and Vousden, K.H. (2008). Cooperation between the ribosomal proteins L5 and L11 in the p53 pathway. Oncogene *27*, 5774–5784.

Jaako, P., Flygare, J., Olsson, K., Quere, R., Ehinger, M., Henson, A., Ellis, S., Schambach, A., Baum, C., Richter, J., et al. (2011). Mice with ribosomal protein S19 deficiency develop bone marrow failure and symptoms like patients with Diamond-Blackfan anemia. Blood *118*, 6087–6096.

Keel, S.B., Phelps, S., Sabo, K.M., O'Leary, M.N., Kirn-Safran, C.B., and Abkowitz, J.L. (2012). Establishing Rps6 hemizygous mice as a model for studying how ribosomal protein haploinsufficiency impairs erythropoiesis. Exp. Hematol. *40*, 290–294.

Langmead, B., Trapnell, C., Pop, M., and Salzberg, S.L. (2009). Ultrafast and memory-efficient alignment of short DNA sequences to the human genome. Genome Biol. *10*, R25.

Li, H., Handsaker, B., Wysoker, A., Fennell, T., Ruan, J., Homer, N., Marth, G., Abecasis, G., and Durbin, R.; 1000 Genome Project Data Processing Subgroup (2009). The Sequence Alignment/Map format and SAMtools. Bioinformatics *25*, 2078–2079.

Llanos, S., and Serrano, M. (2010). Depletion of ribosomal protein L37 occurs in response to DNA damage and activates p53 through the L11/MDM2 pathway. Cell Cycle *9*, 4005–4012.

Lohrum, M.A., Ludwig, R.L., Kubbutat, M.H., Hanlon, M., and Vousden, K.H. (2003). Regulation of HDM2 activity by the ribosomal protein L11. Cancer Cell *3*, 577–587.

Macias, E., Jin, A., Deisenroth, C., Bhat, K., Mao, H., Lindström, M.S., and Zhang, Y. (2010). An ARF-independent c-MYC-activated tumor suppression pathway mediated by ribosomal protein-Mdm2 Interaction. Cancer Cell *18*, 231–243.

McGowan, K.A., and Mason, P.J. (2011). Animal models of Diamond Blackfan anemia. Semin. Hematol. *48*, 106–116.

McGowan, K.A., Pang, W.W., Bhardwaj, R., Perez, M.G., Pluvinage, J.V., Glader, B.E., Malek, R., Mendrysa, S.M., Weissman, I.L., Park, C.Y., and Barsh, G.S. (2011). Reduced ribosomal protein gene dosage and p53 activation in low-risk myelodysplastic syndrome. Blood *118*, 3622–3633.

Miyake, K., Utsugisawa, T., Flygare, J., Kiefer, T., Hamaguchi, I., Richter, J., and Karlsson, S. (2008). Ribosomal protein S19 deficiency leads to reduced proliferation and increased apoptosis but does not affect terminal erythroid differentiation in a cell line model of Diamond-Blackfan anemia. Stem Cells *26*, 323–329.

Moniz, H., Gastou, M., Leblanc, T., Hurtaud, C., Crétien, A., Lécluse, Y., Raslova, H., Larghero, J., Croisille, L., Faubladier, M., et al.; DBA Group of Société d'Hématologie et d'Immunologie Pédiatrique-SHIP (2012). Primary hematopoietic cells from DBA patients with mutations in RPL11 and RPS19 genes exhibit distinct erythroid phenotype in vitro. Cell Death Dis. *3*, e356.

Narla, A., and Ebert, B.L. (2010). Ribosomopathies: human disorders of ribosome dysfunction. Blood *115*, 3196–3205.

Panić, L., Tamarut, S., Sticker-Jantscheff, M., Barkić, M., Solter, D., Uzelac, M., Grabusić, K., and Volarević, S. (2006). Ribosomal protein S6 gene haploinsufficiency is associated with activation of a p53-dependent checkpoint during gastrulation. Mol. Cell. Biol. *26*, 8880–8891.

Quarello, P., Garelli, E., Carando, A., Brusco, A., Calabrese, R., Dufour, C., Longoni, D., Misuraca, A., Vinti, L., Aspesi, A., et al. (2010). Diamond-Blackfan anemia: genotype-phenotype correlations in Italian patients with RPL5 and RPL11 mutations. Haematologica *95*, 206–213.

Robledo, S., Idol, R.A., Crimmins, D.L., Ladenson, J.H., Mason, P.J., and Bessler, M. (2008). The role of human ribosomal proteins in the maturation of rRNA and ribosome production. RNA *14*, 1918–1929.

Rodríguez, C.I., Buchholz, F., Galloway, J., Sequerra, R., Kasper, J., Ayala, R., Stewart, A.F., and Dymecki, S.M. (2000). High-efficiency deleter mice show that FLPe is an alternative to Cre-loxP. Nat. Genet. *25*, 139–140.

Ruggero, D., and Shimamura, A. (2014). Marrow failure: a window into ribosome biology. Blood *124*, 2784–2792.

Ruzankina, Y., Pinzon-Guzman, C., Asare, A., Ong, T., Pontano, L., Cotsarelis, G., Zediak, V.P., Velez, M., Bhandoola, A., and Brown, E.J. (2007). Deletion of the developmentally essential gene ATR in adult mice leads to age-related phenotypes and stem cell loss. Cell Stem Cell *1*, 113–126.

Sáenz Robles, M.T., Symonds, H., Chen, J., and Van Dyke, T. (1994). Induction versus progression of brain tumor development: differential functions for the pRB- and p53-targeting domains of simian virus 40 T antigen. Mol. Cell. Biol. *14*, 2686–2698.

Sakai, K., and Miyazaki, Ji. (1997). A transgenic mouse line that retains Cre recombinase activity in mature oocytes irrespective of the cre transgene transmission. Biochem. Biophys. Res. Commun. *237*, 318–324.

Sloan, K.E., Bohnsack, M.T., and Watkins, N.J. (2013). The 5S RNP couples p53 homeostasis to ribosome biogenesis and nucleolar stress. Cell Rep. *5*, 237–247.

Teng, T., Thomas, G., and Mercer, C.A. (2013). Growth control and ribosomopathies. Curr. Opin. Genet. Dev. *23*, 63–71.

Trapnell, C., Roberts, A., Goff, L., Pertea, G., Kim, D., Kelley, D.R., Pimentel, H., Salzberg, S.L., Rinn, J.L., and Pachter, L. (2012). Differential gene and transcript expression analysis of RNA-seq experiments with TopHat and Cufflinks. Nat. Protoc. *7*, 562–578.

Zhang, J., Socolovsky, M., Gross, A.W., and Lodish, H.F. (2003a). Role of Ras signaling in erythroid differentiation of mouse fetal liver cells: functional analysis by a flow cytometry-based novel culture system. Blood *102*, 3938–3946.

Zhang, Y., Wolf, G.W., Bhat, K., Jin, A., Allio, T., Burkhart, W.A., and Xiong, Y. (2003b). Ribosomal protein L11 negatively regulates oncoprotein MDM2 and mediates a p53-dependent ribosomal-stress checkpoint pathway. Mol. Cell. Biol. *23*, 8902–8912.

Zhang, Z., Jia, H., Zhang, Q., Wan, Y., Zhou, Y., Jia, Q., Zhang, W., Yuan, W., Cheng, T., Zhu, X., and Fang, X. (2013). Assessment of hematopoietic failure due to Rpl11 deficiency in a zebrafish model of Diamond-Blackfan anemia by deep sequencing. BMC Genomics *14*, 896.

Zheng, J., Lang, Y., Zhang, Q., Cui, D., Sun, H., Jiang, L., Chen, Z., Zhang, R., Gao, Y., Tian, W., et al. (2015). Structure of human MDM2 complexed with RPL11 reveals the molecular basis of p53 activation. Genes Dev. *29*, 1524–1534.

Zhu, Y., Poyurovsky, M.V., Li, Y., Biderman, L., Stahl, J., Jacq, X., and Prives, C. (2009). Ribosomal protein S7 is both a regulator and a substrate of MDM2. Mol. Cell *35*, 316–326.

Cell Reports

Supplemental Information

Partial Loss of *Rpl11* in Adult Mice Recapitulates Diamond-Blackfan Anemia and Promotes Lymphomagenesis

Lucia Morgado-Palacin, Gianluca Varetti, Susana Llanos, Gonzalo Gómez-López, Dolores Martinez, and Manuel Serrano

Morgado-Palacin et al., Figure S1 (related to Fig. 1)

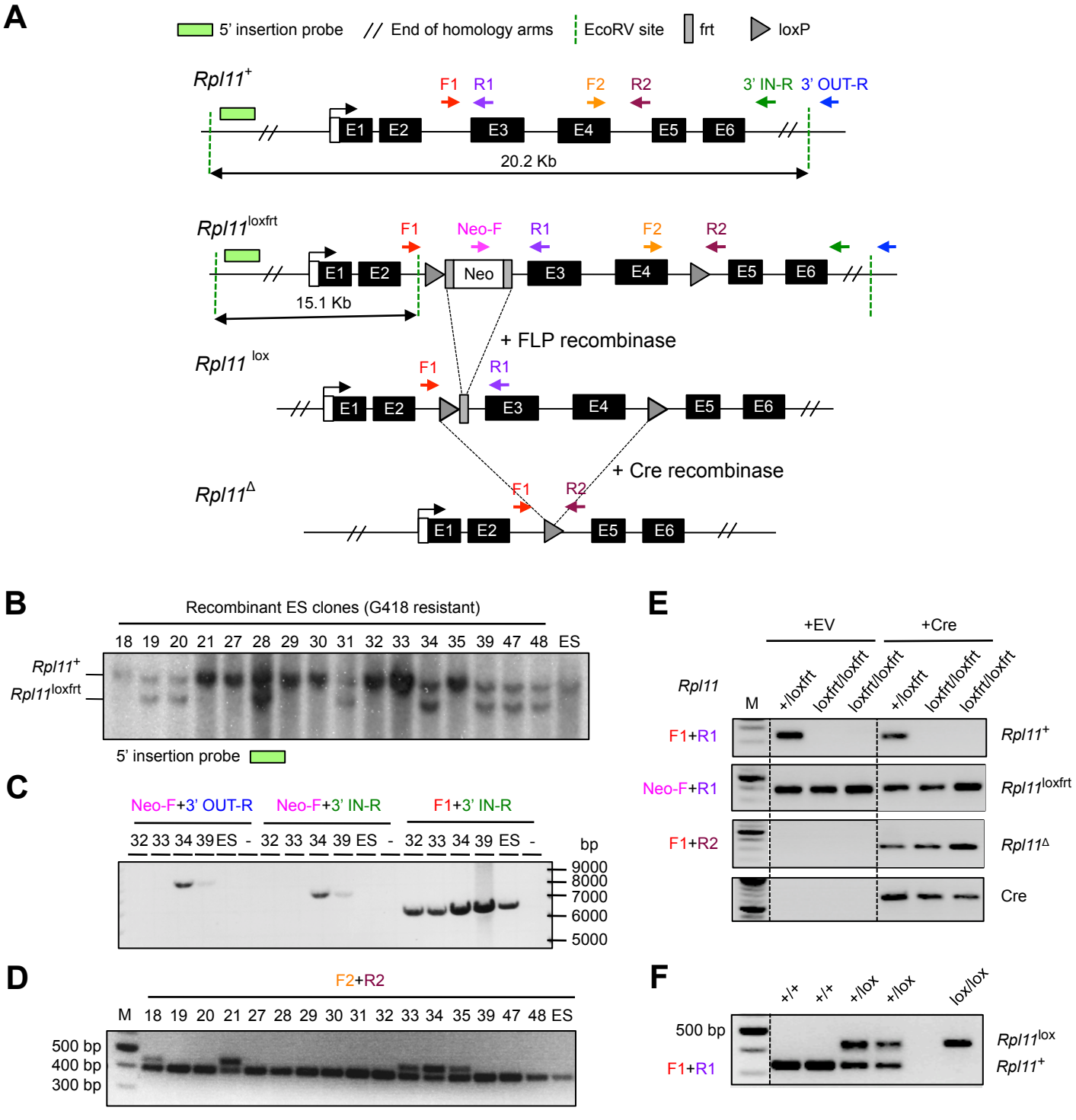

Figure S1. Generation of *Rpl11* conditional knockout mouse model, related to Figure 1.

(A) Scheme of the wt, loxfrt, lox and delta *Rpl11* alleles and location of primers used for their identification. Probe and external primers to check for 5' and 3' homology arms insertion are also shown in the picture. *Rpl11* loxfrt allele bears a neomycin cassette, flanked by frt sites, that serves for selection of recombinant ES clones. The neomycin cassette is excised upon expression of flipase recombinase (Flpe), resulting in the *Rpl11* lox allele. Exons 3 and 4 of the *Rpl11* gene, flanked by two loxP sites, are excised once Cre recombinase is expressed giving rise to the *Rpl11* Δ allele.

(B) Southern blot showing several positive recombinant ES clones for proper insertion of the 5' homology arm of the targeted *Rpl11* loxfrt allele. Digestion with EcoRV enzyme results in a DNA fragment of 20.2 Kb or 15.1 Kb in the *Rpl11* wt or loxfrt alleles, respectively. This DNA fragment contains part of the mouse chromosome 4 external to the 5' homology arm of the targeted construct.

(C) Long-range PCR displaying the amplified DNA fragments by the above-indicated primers (see location in (A)). A DNA fragment of 9.48 Kb is amplified by Neo-F and 3'OUT-R primers when correct insertion of the 3' homology arm of the targeted *Rpl11* loxfrt allele in the mouse chromosome 4 occur.

(D) PCR showing the amplification of the loxP site located in the intron 4 of the targeted *Rpl11* loxfrt allele. Those recombinant ES clones that bears loxP site in intron 4 present two bands.

(E) *Rpl11* delta (Δ) allele is correctly detected by PCR with indicated primers when Cre recombinase is present. Mouse embryonic fibroblasts (MEFs) carrying the indicated *Rpl11* alleles were infected with a plasmid expressing Cre recombinase or an empty plasmid.

(F) PCR showing the *Rpl11* lox and wt alleles with the same pair of primers. This is the regular PCR-based strategy used for genotyping and confirmation of experimental samples.

Morgado-Palacin et al., Figure S2 (related to Fig. 2)

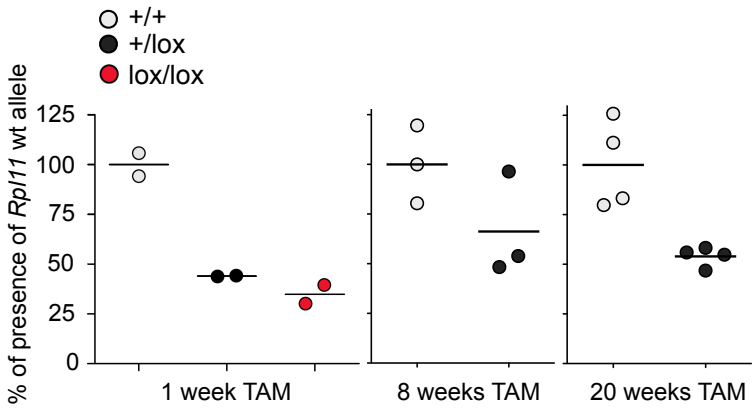

Figure S2. TAM treatment results in deletion of the *Rpl11*^{lox} allele, related to Figure 2.

Quantification by qRT-PCR of the percentage of presence of the *Rpl11* wt allele in genomic DNA from tails of mice fed with TAM for 1, 8 and 20 weeks, which is used as indication of the excision efficiency. Bars indicate the average value.

Morgado-Palacin et al., Figure S3 (related to Fig. 3)

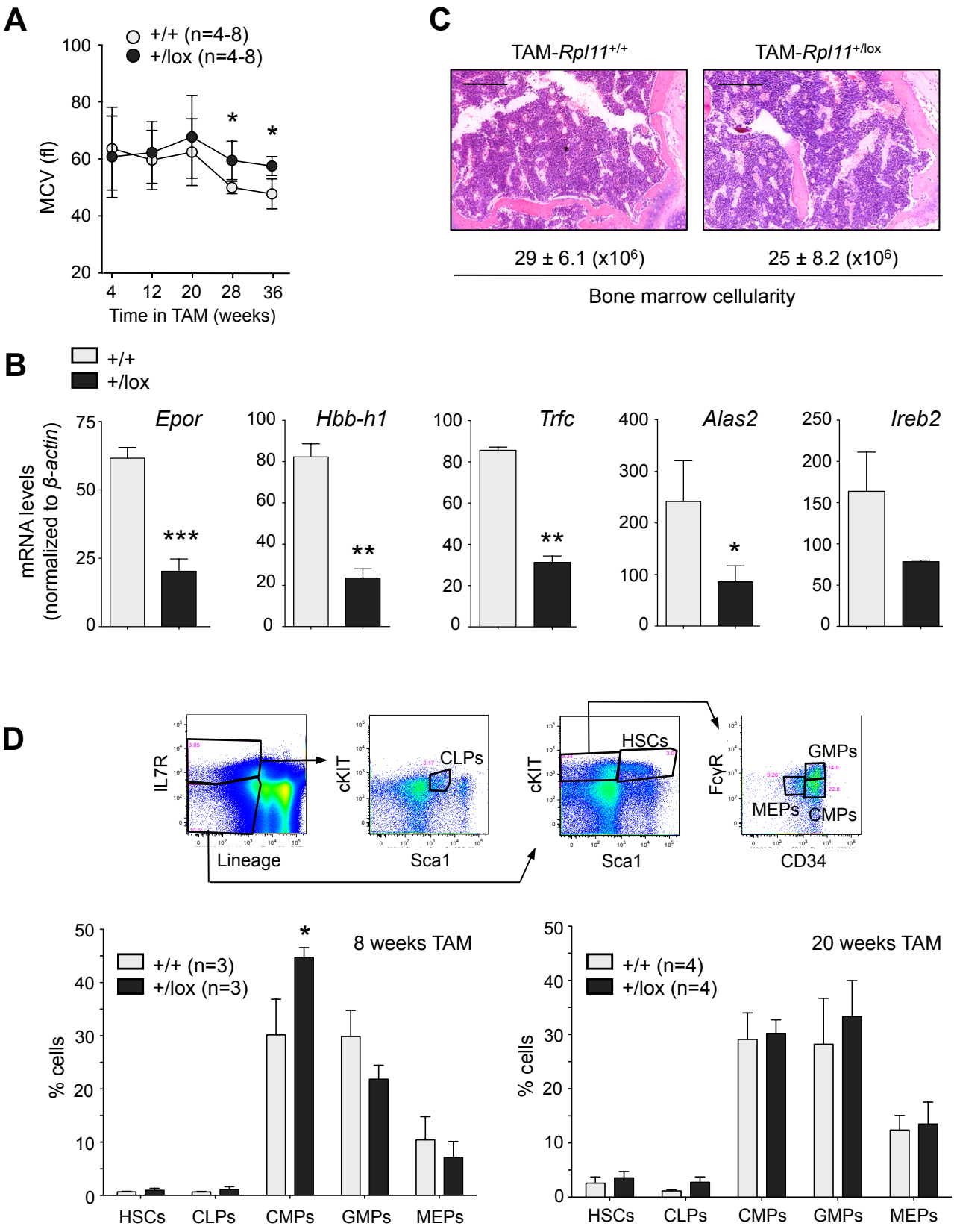

Figure S3. *Rpl11* deficiency results in impaired erythropoiesis, related to Figure 3.

(A) Mean corpuscular volume (MCV) of erythrocytes from TAM-*Rpl11*$^{+/+}$ and TAM-*Rpl11*$^{+/lox}$ mice was measured at the indicated times in TAM diet.

(B) mRNA levels of different genes involved in erythropoiesis or iron metabolism are quantified by qRT-PCR in BM cells from 8-weeks TAM-treated animals. β-actin mRNA levels are used as an endogenous control. Data correspond to 3 independent animals per genotype, except for *Ireb2* where n=2.

(C) Representative histological sections of normocellular bone marrow from TAM-*Rpl11*$^{+/+}$ or TAM-*Rpl11*$^{+/lox}$ mice. Scale bars correspond to 200 μm. Bone marrow cellularity indicates the total number of bone marrow cells extracted from the posterior limbs of each animal.

(D) Quantification by flow cytometry of the percentage of HSCs and the different subsets of hematopoietic progenitors (common lymphoid progenitors "CLPs", common myeloid progenitors "CMPs", granulocyte-monocyte progenitors "GMPs" and megakaryocyte-erythrocyte progenitors "MEPs") in BMs from 8 or 20 weeks TAM-treated animals. The gating strategy for the analyzed populations is shown above.

Values correspond to the average ± SD. Statistical t-test analysis was performed to calculate significance (* $P \leq 0.05$; ** $P \leq 0.01$; *** $P \leq 0.005$).

Morgado-Palacin et al., Figure S4 (related to Fig. 4)

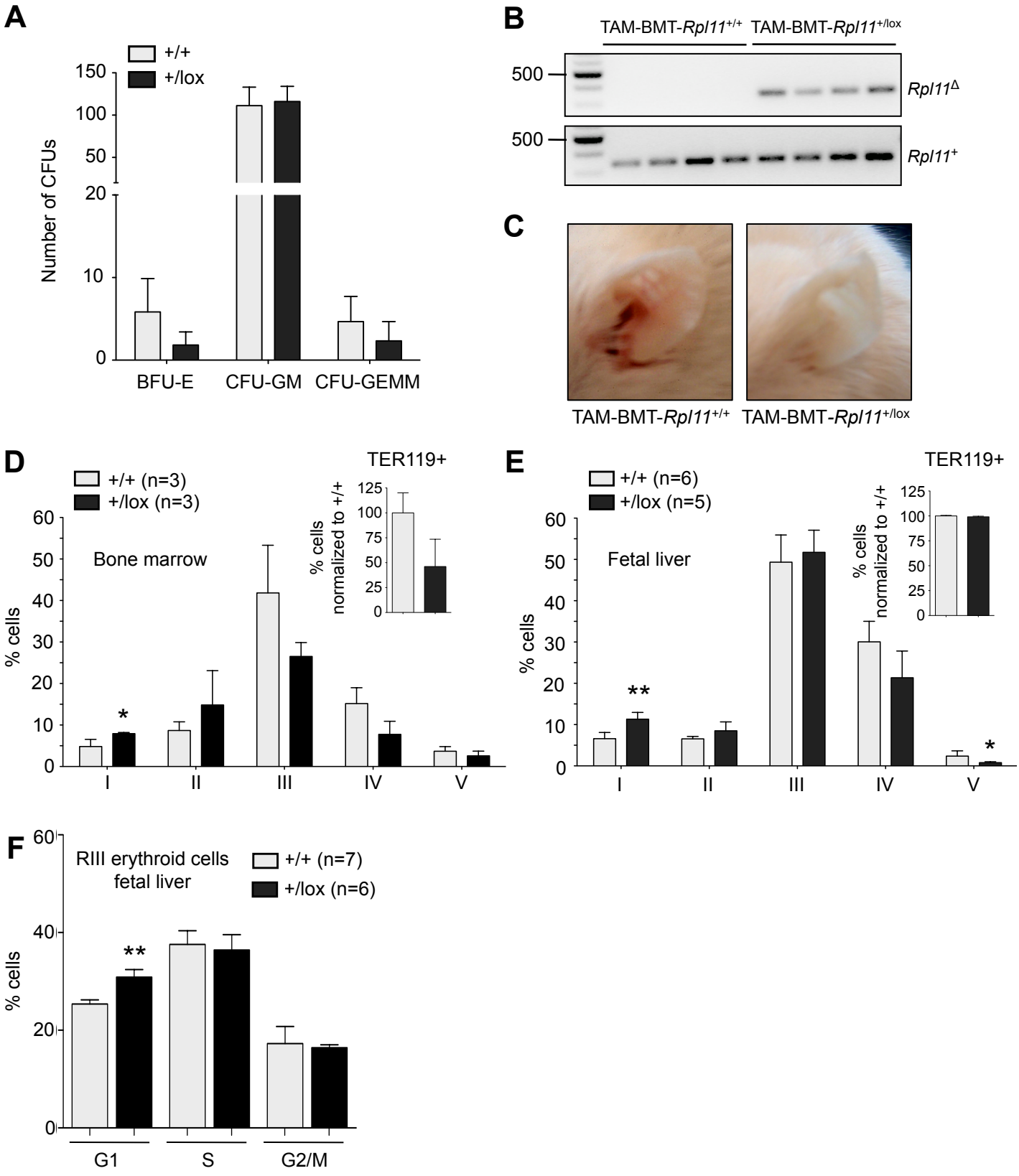

Figure S4. Erythrocyte differentiation is compromised in *Rpl11* deficient mice, related to Figure 4.

(A) Graph showing the number of colony forming units (CFUs) to evaluate the potential of the different myeloid progenitors: erythroid (BFUs, burst-forming units), "granulocyte, monocyte" (CFU-GM) or multipotential progenitor "granulocyte, erythrocyte, monocyte, megakaryocyte" (CFU-GEMM) cells. The assays were performed with bone marrow cells from a total of n=3 independent mice per genotype.

(B) PCR showing *Rpl11* alleles performed in bone marrow cells from BM-transplanted animals.

(C) Picture depicting transplanted animals with BMs from $Rpl11^{+/+}$ or $Rpl11^{+/lox}$ donors fed with tamoxifen for 12 weeks. Paleness of a TAM-BMT-$Rpl11^{+/lox}$ mouse is particularly notable in the ears.

(D) Quantification by flow cytometry of the percentage of erythroid cells from bone marrows of TAM-$Rpl11^{+/+}$ and TAM-$Rpl11^{+/lox}$ animals at different stages of erythroid maturation.

(E) Quantification by flow cytometry of the percentage of cells in the different maturational erythroid stages from $Rpl11^{+/+}$ and $Rpl11^{+/lox}$ fetal livers (E14.5) after daily injections of 4OHT in pregnant females from E11.5 to E13.5.

(F) Cell cycle analysis by flow cytometry after EdU incorporation and Hoechst staining of RIII erythroid cells from fetal livers as in (E).

Values correspond to the average ± SD. Statistical t-test analysis was performed to calculate significance (* $P \leq 0.05$; ** $P \leq 0.01$).

Morgado-Palacin et al., Figure S5 (related to Fig.5)

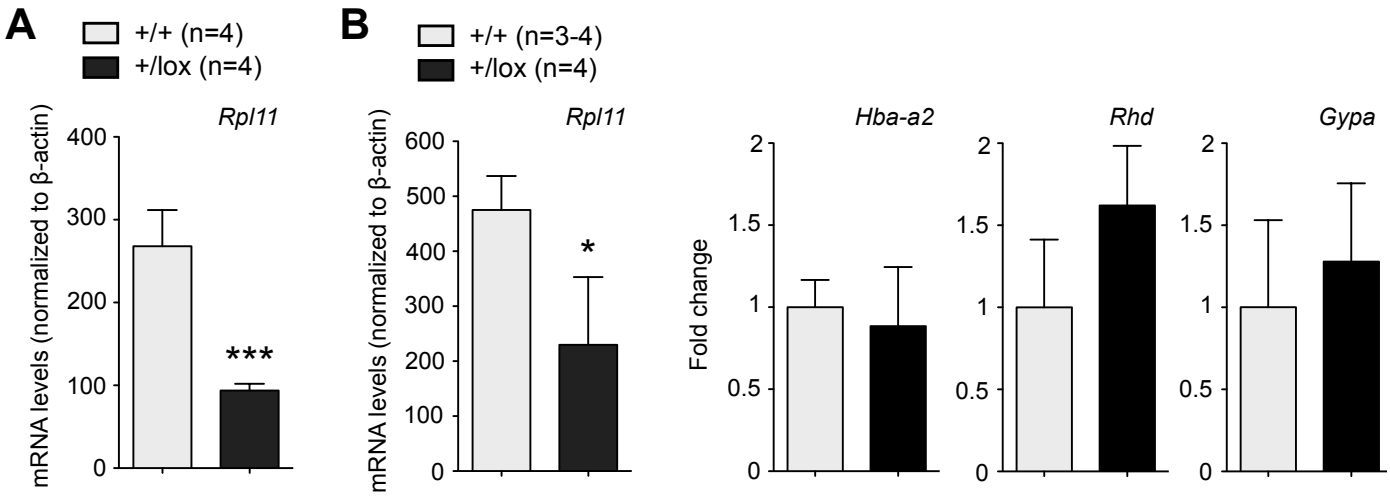

Figure S5. Expression of erythrocyte differentiation genes is not altered in adult livers from TAM-treated *Rpl11*$^{+/lox}$ mice, related to Figure 5.

(A) *Rpl11* mRNA levels of HPCs from 20 weeks TAM-treated *Rpl11*$^{+/+}$ and *Rpl11*$^{+/lox}$ mice.

(B) mRNA levels of the indicated genes of livers from 20 weeks TAM-treated *Rpl11*$^{+/+}$ and *Rpl11*$^{+/lox}$ mice. mRNA levels are normalized to β-actin housekeeping levels.

Values correspond to the average ± SD. Statistical t-test analysis was performed to calculate significance (* $P \leq 0.05$; *** $P \leq 0.005$).

Morgado-Palacin et al., Figure S6 (related to Fig. 6)

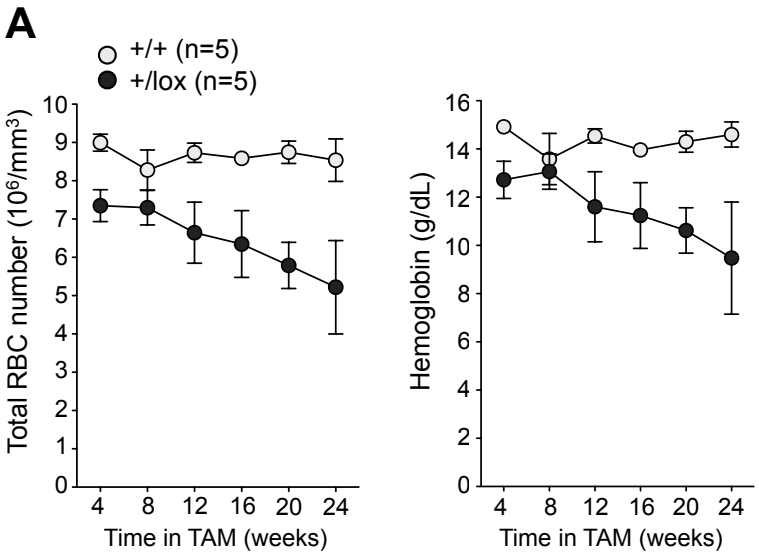

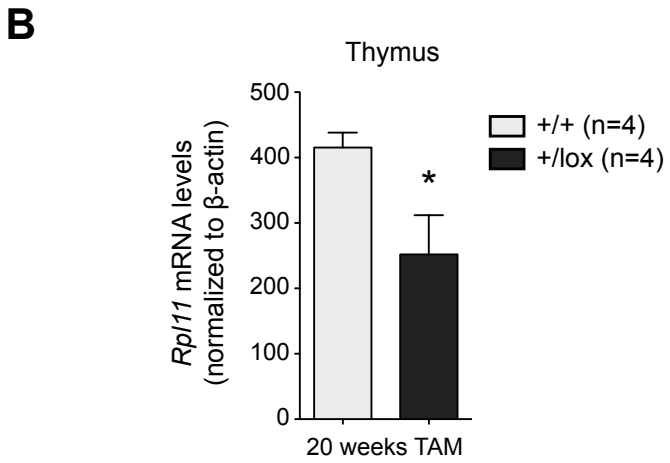

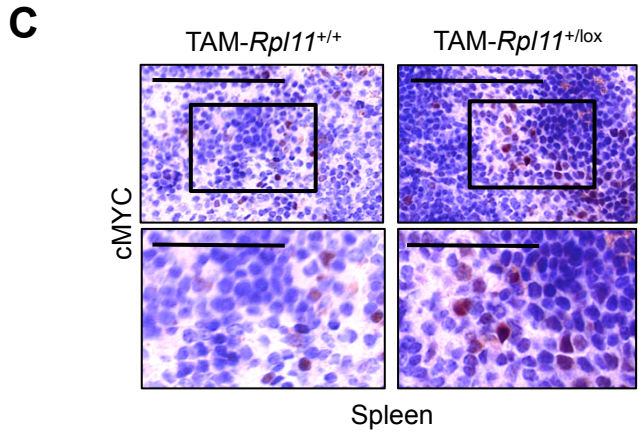

Figure S6. Anemia in γ-irradiated TAM-*Rpl11*$^{+/lox}$ mice, related to Figure 6.

(A) Red blood cells (RBC) and hemoglobin values for γ-irradiated TAM-*Rpl11*$^{+/+}$ and TAM-*Rpl11*$^{+/lox}$ mice. Differences between genotypes were significant (**$P \leq 0.01$ or *$P \leq 0.05$) for all time points with the exception of that corresponding to 8 weeks.

(B) *Rpl11* mRNA levels from thymuses of TAM-*Rpl11*$^{+/+}$ and TAM-*Rpl11*$^{+/lox}$ mice (20 weeks). β-actin mRNA levels are used as an endogenous control.

(C) Representative histological sections, stained against cMYC, from spleens of TAM-*Rpl11*$^{+/+}$ and TAM-*Rpl11*$^{+/lox}$ mice (20 weeks). Scale bars correspond to 100 μm (top images) and 50 μm (zoom in images). Pictures are representative of a total of n=4 per genotype.

Values correspond to the average ± SD. Statistical t-test analysis was performed to calculate significance (* $P \leq 0.05$; ** $P \leq 0.01$; *** $P \leq 0.005$). For panel (A), see legend.

Supplemental Tables

Table S1. Differentially regulated genes in Rpl11-deficient hematopoietic progenitors, Related to Figure 5

Annotated ranked list of those genes significantly downregulated, in blue, and significantly upregulated, in red, (FDR (q-value) < 0.15) in TAM-*Rpl11*+/lox HPCs compared to TAM-*Rpl11*+/+ controls. q-values and log_2FC are indicated. MGI, UniProt, and Ensembl databases were used for biological processes and molecular functions annotations.

Table S2. Differentially regulated gene sets in Rpl11-deficient hematopoietic progenitors, Related to Figure 5

Gene Sets with FDR (q-value) < 0.25. Eukaryotic translation (green), DNA replication/cell cycle (blue), DNA repair (yellow), iron metabolism (pink) and cancer related (orange) pathways are depicted in the indicated colors. Gene size, source and status (up or down) of the analyzed pathways are shown in the table.

Supplemental Experimental Procedures

Southern blot analysis

Approximately 15 μg of DNA from recombinant ES clones were digested o/n at 37ºC with EcoRV enzyme (ROCHE). The probe was generated by PCR amplification using the following primers: Forward 5'-GAC TCA CCG AAG GAC AGG AC-3' and Reverse 5'-TGC CTA GTT GTG TCT CCC AGT-3'.

Long-range PCR

Genomic DNA from recombinant ES clones were amplified by PCR using LA Takara enzyme and the following conditions: 1 min 94ºC, 30x (98ºC 10 sec, 58ºC 15 sec, 68ºC 10 sec), 72ºC 10 min. Primers were designed in order to amplify a DNA fragment of 9,418 bp (*Neo* F + 3' OUT R) comprised between the Neomycin cassette and the outer region of the 3' homology arm. Internal controls of amplification were also designed to amplify a DNA fragment of 7,815 bp (*Neo* F + 3' IN R) comprising the Neomycin cassette and the inner region of the 3' homology arm in those recombinant clones of ES. Primers were also ordered for amplifying a region of 6,638 bp (*Rpl11* F + 3' IN R) present in all ES samples (non recombinant and recombinant) as a control for PCR. Primers used for this strategy are listed below: *Neo* F: 5'- GCC TTC TAT CGC CTT CTT GAC GAG-3'; *Rpl11* F1: 5'-GCA TAA TCA TTG GTT GGG CCT GAT AG-3'; 3'IN R: 5'-GGC CAC TGA TGG TAA CGG TTT GC-3'; 3'OUT R: 5'-CAC GGG GAG GGG CAA CTA ACC-3'.

PCR-based genotyping for the Rpl11 alleles

To check the *Rpl11* deletion, genomic DNA isolated from mouse tissues or cells following standard procedures were subjected to PCR by using AmpliTaq DNA polymerase (N8080152 Applied Biosystems). The genotyping PCR primers are listed below:

Rpl11 F1: 5'-GCA TAA TCA TTG GTT GGG CCT GAT AG-3'

Rpl11 F2: 5'-CAC TAT GAT AAC GGC CAT TCC-3'

Rpl11 R1: 5'-CCG GAT GCC AAA GGA CCT GAC-3'

Rpl11 R2: 5'-CAC TAT GAT AAC GGC CAT TCC-3'

CRE Fw: 5'-CGG TCG ATG CAA CGA GTG ATG AGG-3'

CRE Rv: 5'-CCA GAG ACG GAA ATC CAT CGC TCG-3'

CRE recombinase transduction

Packaging 293T cells were transfected at a density of $5x10^6$ cells/p100 with XtremeGene HP transfection agent (ROCHE). 4 μg of retroviral plasmid (pBabe-empty or pBabe-CRE) was used for transfection. $0.8x10^6$ primary MEFs/p100, bearing *Rpl11*$^{+/+}$ or *Rpl11*$^{+/loxfrt}$ alleles, were transduced with the viral supernatants for 6 h and puromycin (2 μg/mL) selection was added the following day. Fibroblasts were collected for gDNA extraction at 3 days after complete selection.

Immunoblotting

Cells were harvested and lysed in NET buffer. Identical amounts of whole lysates were resolved on 4–12% SDS/PAGE gels (NuPAGE, Invitrogen) and transferred to nitrocellulose membranes. Blots were blocked in TBS, 0.2% Tween, 5% BSA and incubated with the primary antibodies anti-RPL11 (Proteintech), anti-GAPDH (71.1, Sigma), anti LAMIN A/C (N-18, Santa Cruz Biotechnology), anti-p53 (C1C12, Cell Signaling) and anti-cMYC (D84C12, Cell Signaling) and subsequently incubated with the corresponding secondary anti-IgG HRP antibodies (Dako). Signals were detected by standard ECL procedures.

Northern blot analysis of rRNA precursors

Tissues were homogenized in a Precellys homogenizer. Total RNA was isolated from cells and tissues using TRI-reagent (Sigma) following the manufacturer's instructions. 1.5 μg of total RNA were loaded onto a 1.2% MOPS/formaldehyde agarose gel and underwent electrophoresis. RNAs were transferred to a Hybond N+ nylon membrane (Amersham) through capillarity and fixed by UV crosslinking. Membranes were prehybridized in 6X SSC, 5X Denhardt's solution, 0.1% SDS, 1 μg/ml salmon sperm

DNA at 45˚C for 3 hours. The ITS2 probe (5′- ACC CAC CGC AGC GGG TGA CGC GAT TGA TCG -3′) labeled with [γ-32P]-ATP (Perkin Elmer) through PNK terminal labeling was then added to the membrane and incubated at 45˚C overnight. Membranes were washed in 2X SSC, 0.1% SDS and 1X SSC, 0.1% SDS and underwent autoradiography.

EdU incorporation assay in MEFs

Primary MEFs were seeded (3000 cells/well) onto μclear bottom 96-well plates (Greiner Bio-One) and treated with 4OHT for 3 days. Analysis of DNA synthesis by EdU incorporation was performed using Click-iT chemistry (Invitrogen) following manufacturer's instructions. Briefly, cells were incubated with EdU (10 μM) for 30 min and then, fixed with 4% paraformaldehyde, permeabilized with 0.1% Triton X-100 and incubated with Click-iT reaction cocktail (containing Alexa Fluor 647 azide). DAPI was use to counterstain cells. A total of 40 fields/well were acquired with a 20x magnification lens in the Opera HCS system (Perkin Elmer). Images were segmented using the DAPI staining to generate masks matching cell nuclei from which fluorescence intensity signals were calculated by using Acapella High Content Imaging and Analysis software (Perkin Elmer).

Colony Forming Units assay

For the colony forming units (CFU) assay, 5000 cells of adult BM from TAM fed mice (8 weeks) were plated in duplicates in methylcellulose (Methocult M3434, StemCell Technologies) in p35 non-adherent plates. Colonies were scored at 10 days according to their cellular morphology.

RNA isolation and quantitative real time PCR (qRT-PCR)

Up to 1 μg of total RNA was reverse transcribed into cDNA using iScript First Strand cDNA synthesis kit (BioRad #170-8891). Real-time PCR was performed using SYBR Green master mix (Applied Biosystems) in a 7500 Fast Real-Time PCR (Applied Biosystems). All reactions were performed in triplicates and normalized to β-*Actin* mRNA levels as an endogenous control. The sequences of the primers used are:

Alas2	Fw 5'-TGG GCT AAG AGC CAT TGT CCT-3'
	Rv 5'-GTA GGT GTG GTC CTG TTT CTT C-3'
β-actin	Fw 5'-GGC ACC ACA CCT TCT ACA ATG-3'
	Rv 5'-GTG GTG GTG AAG CTG TAG CC-3'
Bax	Fw 5'- GAC AGG GGC CTT TTT GCT A-3'
	Rv 5'- TGT CCA CGT CAG CAA TCA TC-3'
Cdkn1a	Fw 5'-GTG GGT CTG ACT CCA GCC C-3'
	Rv 5'-CCT TCT CGT GAG ACG CTT AC-3'
Cldn13	Fw 5'-GAC TTT CCC CGT TGC ATT GA-3'
	Rv 5'-CGC ATC CAG AGT CCA CTA CA-3'
Ctse	Fw 5'-GCC CCT CAG AAG ACA TCA GT-3'
	Rv 5'-CGA TGG AGA TGG TGC CAA AG-3'
Epo	Fw 5'-ACT CTC CTT GCT ACT GAT TCC T-3'
	Rv 5'-ATC GTG ACA TTT TCT GCC TCC-3'
Epor	Fw 5'-GGG CTC CGA AGA ACT TCT GTG-3'
	Rv 5'-ATG ACT TTC GTG ACT CAC CCT-3'
Gypa	Fw 5'-TGG TGG CTT CAA CTG TAG GT-3'
	Rv 5'-GAT AAT CCC TGC CAT CAC GC-3'
Hba-a2	Fw 5'-GGA TCC CGT CAA CTT CAA GC-3'

	Rv 5’-CAA GGG AGA GAA GAA GGG CA-3’
Hbb-h1	Fw 5’-GAA ACC CCC GGA TTA GAG CC-3’
	Rv 5’-GAG CAA AGG TCT CCT TGA GGT-3’
Ireb2	Fw 5’-TTC TGC CTT ACT CAA TAC GGG T-3’
	Rv 5’-AGG GCA CTT CAA CAT TGC TCT-3’
Rhd	Fw 5’-GGG TGC AGG GAA CAA TCT TG-3’
	Rv 5’-GAC CTT CTC GTC GGC AAA TC-3’
Rik	Fw 5’-TGC TGC ACA AAA GAT TCC TG-3’
	Rv 5’-TAG AAA CAC CGG CAA TGA CA-3’
Rpl11	Fw 5’-ATG GCG CAA GAT CAA GGG G-3’
	Rv 5’-GAC TGT GCA GTG AAC AGC AAT-3’
Trfc	Fw 5’-GTT TCT GCC AGC CCC TTA TTA T-3’
	Rv 5’-GCA AGG AAA GGA TAT GCA GCA-3’

DISCUSSION

The main goal of this thesis was the study of the ribosomal stress pathway in different settings, with emphasis on tumor suppression. In the first section we demonstrated that, in mouse pluripotent stem cells, imbalanced ribosome biogenesis results in the activation of the ribosomal stress pathway, which constitutes an additional checkpoint that safeguards the integrity of stem cells. Next, we exploited the ribosomal stress pathway as a potent trigger of p53-mediated responses in cancer cells; for this, we performed a chemical screen that led to the identification of compounds that alter nucleolar integrity and activate p53, in the absence of detectable DNA damage. Finally, we generated a mouse model for *Rpl11* haploinsufficiency that recapitulates the hallmarks of DBA, including cancer predisposition.

The ribosomal stress pathway in mouse pluripotent stem cells

The ribosomal stress pathway emerged more than 10 years ago as a new p53-activating pathway that monitors ribosome integrity (Zhang and Lu, 2009). Ribosome biogenesis is the most demanding energetic process in proliferating cells. Mouse embryonic pluripotent cells present extremely fast proliferation rates (8-10h duplication time), reaching cell cycles of less than 5 h in the epiblast. In order to meet the elevated energetic demands that these highly proliferating cells require, the rate of ribosome biogenesis needs to be extremely high. Consistent with this, RPs are more abundantly expressed in mESCs compared to differentiated cells (Kondrashov et al., 2011), and, interestingly, a decrease in rDNA transcription is associated to differentiation. This implies a tight coupling of replication and transcription of rRNA genes and translation of ribosomal proteins. In higher eukaryotes, replication and transcription are temporally separated to prevent collisions between the machineries involved (Bertoli et al., 2013). However, replication-transcription conflict might arise in heavily transcribed loci, such as rDNA genes. In mammalian cells, rDNA transcription is cell cycle-regulated, gradually increasing during G1 and reaching its maximum peak in S and G2, while remaining inactive in mitosis by phosphorylation of UBF, the master regulator of RNA pol I-driven transcription (Drygin et al., 2010; Klein and Grummt, 1999). Decrease in rRNA synthesis and ribosome assembly is, indeed, a prerequisite for the exit of cell cycle during mitosis (Heix et al., 1998; Kuhn et al., 1998). This mechanism differs from that of RNA pol II-transcribed genes, whose transcripts levels are maximum during G1-S transition and repressed when replication takes place (Bertoli et al., 2013), thus providing a temporal gap between transcription and replication. As an additional level of complexity, any perturbation that slows down protein synthesis, such as defective ribosomes, decreases rDNA transcription (Drygin et al., 2010) and would impact, ultimately, in the proliferation rate. Thus, ribosome biogenesis must be tightly coupled to proliferation by achieving appropriate levels of rRNA synthesis and ribosome assembly during specific windows of the cell

cycle. Failure in coupling both processes will render mouse pluripotent stem cells particularly sensitive to accumulate mutations, compromising integrity of their progeny.

The ribosomal stress pathway is in charge of monitoring ribosome biogenesis, but its functionality in pluripotent stem cells was unknown. Of note, 15 pluripotency factors, including OCT4, have been found to be associated to rDNA in mESCs and hESCs (Zentner et al., 2014). The ribosomal stress pathway relies on p53 as the ultimate effector. The role of p53 as a guardian of genome integrity in mouse pluripotent stem cells was initially dismissed because the majority of p53 protein is cytoplasmic in these cells (Aladjem et al., 1998; Sabapathy et al., 1997a; Solozobova et al., 2009). In addition, some DNA damaging agents, such as ionizing radiation (γ-irradiation), radiomimetic agents (doxorubicin) or nucleotide depletion are capable of transiently stabilizing p53 in mESCs, but trigger apoptosis independently of p53 (Aladjem et al., 1998; Corbet et al., 1999; Solozobova et al., 2009). In contrast, UV radiation and oxidative stress induce a p53-mediated apoptotic response in mESCs (Chao et al., 2000a; Corbet et al., 1999; Han et al., 2008). In this context, the functionality of the ribosomal stress pathway and the role of p53 in this response had remained unaddressed in embryonic stem cells. Only one report, published by the time our work was being peer-reviewed, demonstrated that p53-dependent apoptosis can be elicited in mESCs through RPL11-MDM2 by loss of the nucleolar protein PICT1 (Sasaki et al., 2011).

In this section of our study we have shown that p53 is active in mESCs and iPSCs in response to ribosomal stress, triggered either by treatment with ActD or by *Rpl37* depletion. As a proof-of-concept of the functionality of the ribosomal stress pathway, we have detected increased binding of RPL11 to MDM2 upon induction of ribosomal stress by low concentrations of ActD (a well-known inducer of the ribosomal stress pathway). Transcriptional upregulation of p53 target genes, including *p21*, *Mdm2*, *Puma*, *Bax* and *Noxa*, depends on RPL11 and p53, therefore confirming the activation of the ribosomal stress pathway. We have also determined that mouse pluripotent stem cells respond to perturbations in ribosome biogenesis by eliciting an apoptotic response that depends on p53. This apoptotic response is also dependent on *Puma* and *Bax*, two pro-apoptotic p53 target genes that participate in the p53-mediated apoptosis response. From our work we can conclude that mouse pluripotent stem cells possess an additional checkpoint surveillance pathway that monitors ribosome biogenesis homeostasis. The ribosomal stress pathway could be of particular relevance in developmental stages with a high cell proliferation rate, such as gastrulation (O'Farrell et al., 2004), by preventing defective cells to continue throughout specific cell lineages.

Our results also shed light to the paradoxical role of p53 in mESCs. As mentioned in the introduction section, mESCs undergo p53-dependent apoptosis upon UV or oxidative stress, but not ionizing irradiation. UV-induced photolesions are inefficiently repaired in rDNA (Balajee et al.,

1999). This could explain why UV, but not γ-IR, severely compromise nucleolar integrity (Al-Baker et al., 2004; Kurki et al., 2004; Moné et al., 2001; Rubbi and Milner, 2003; Stixova et al., 2014) resulting in mislocalization of nucleolar proteins (Kurki et al., 2004; Moore et al., 2011) and blocking of transcription (Batista et al., 2009). All these events potentially lead to ribosomal stress (Shav-tal et al., 2005; Sirri et al., 2008). Supporting UV-induced ribosomal stress, exposure of osteosarcoma cells to UV, but not to γ-IR, activates p53 through RPL11 (Bhat et al., 2004; Macias et al., 2010) and, alternatively, UV light induces degradation of RPL37 which ultimately results in ribosome unbalance and activation of the ribosomal stress pathway (Llanos and Serrano, 2010). Interestingly, oxidative stress also causes reorganization of nucleolar proteins by inhibiting RNA pol I transcription through JNK2 activity (Mayer et al., 2005), which would lead to activation of the ribosomal stress pathway.

Based on this, we speculate that UV radiation and oxidative stress trigger a p53-mediated apoptosis response in pluripotent stem cells by disturbance of the nucleolus and activation of the ribosomal stress pathway (**Figure 6**).

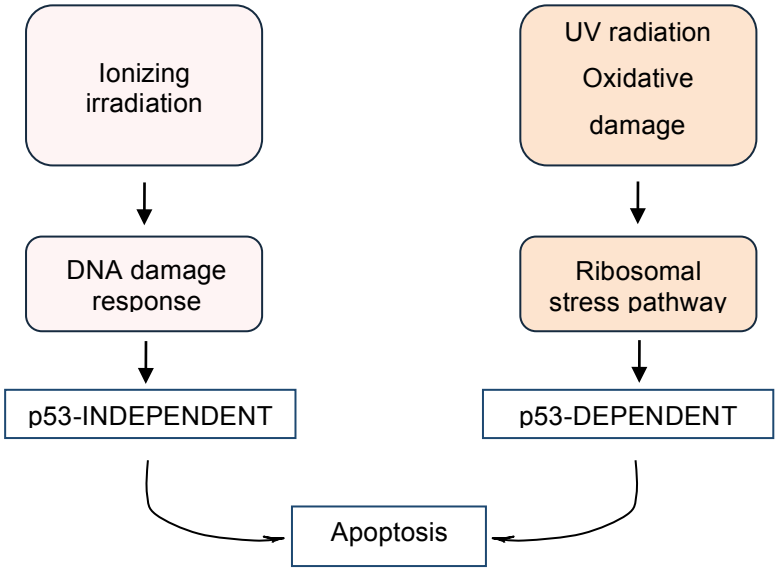

Figure 6. Scheme showing the leading stresses triggering apoptosis in mESCs.

Small molecule compound screen to identify non-genotoxic activators of p53 through the ribosomal stress pathway

Cancer cells resemble mouse pluripotent stem cells in their high proliferation rates, mainly due to their ability to bypass cellular checkpoints. In order to sustain the elevated protein synthesis levels, cancer cells increase the size and number of nucleoli, the ribosome factories (Montanaro et al., 2008). Several proto-oncogenes and tumor suppressors control RNA pol I transcription machinery in response to proliferative cues, such as nutrients and cell cycle dynamics (Drygin et al., 2010). However, cancer cells hijack RNA pol I activity by modulating tumor suppressors and oncogenes, which in turn make them addicted to high rates of rRNA synthesis in order to sustain rapid proliferation (Drygin et al., 2014; Nguyen et al., 2015). Thus, the nucleolus becomes a very attractive target in order to halt uncontrolled proliferation of cancer cells. Many chemotherapeutic drugs inhibit RNA pol I function at different levels and result in nucleolar disruption, such as actinomycin D, doxorubicin or cisplatin; however, their mechanism of action is non-selective and they can result in the acquisition of oncogenic mutations associated to genotoxic stress that ultimately result in tumour relapse (Quin et al., 2014). Few selective inhibitors of RNA pol I-mediated transcription, such as CX-5461 or BMH-21, have shown antitumorigenic activities in the absence of DNA damage, while leaving healthy cells undamaged (Bywater et al., 2012; Drygin et al., 2011; Peltonen et al., 2010, 2014). Interestingly, cancer cells with higher rates of rRNA synthesis that retain a wild-type p53 status are extremely susceptible to these inhibitors (Scala et al., 2015). Around 85-90% of blood cancers have wild-type p53 upon initial diagnosis, which make these patients appropriate for therapy with nucleolar stress agents. In this manner, the selective RNA pol I inhibitor CX-5461 is being successfully tested (phase I; clinical trial ID ACTRN12613001061729) in patients with advanced hematologic malignancies, including high-grade lymphoma, myeloma and acute leukemia. The discovery of novel genotoxic-free nucleolar disruptors is of special interest to circumvent the drawbacks of DNA damage-inducing drugs. To test large drug collections we have designed a nucleolar morphology-based screen to identify compounds that disturb nucleolar integrity. For that we have used a U2OS cell line stably expressing the GFP-tagged protein RPL37, previously generated in our lab (Llanos and Serrano, 2010). GFP signal allowed us to determine nucleolar morphology and assign an automatic nucleolar disruption score to rank potential candidates from two small chemical compounds libraries. This technical approach is robust, fast and cheap, since relies on GFP fluorescence and does not depend on immunofluorescence staining, which is usually expensive, time consuming and associated to side problems, such as inconsistent staining patterns.

Firstly, we tested an in-house made library of 640 compounds representative of the full collection (≈ 55,000 compounds) of the Experimental Therapeutics Program at the CNIO. Secondly,

we tested the Johns Hopkins University chemical library comprising 1524 compounds approved for medical use. We successfully identified and validated three related acridine derivatives that cause nucleolar disruption: CID-765471, ethacridine and aminacrine, being the last two compounds already approved for medical use as antiseptics. All these three compounds show antitumorigenic activity by activating p53 in the absence of detectable DNA damage. This makes these non-genotoxic compounds highly attractive for cancer treatment since most chemotherapeutic drugs induce DNA damage to kill cancer cells, with the risk of increase the mutational load of surviving cells. Habria que aclarar que estos agentes no son genotoxicos! Ya lo pongo en la frase subrayada en amarillo, aniado coletilla de "non-genotoxic compunds" después para hacer más énfasis.

Acridine derivatives comprise a large group of DNA intercalating agents that display different ranges of cellular toxicity according to their reactive groups. For example, platinum-based acridines are highly genotoxic (Galdino-Pitta et al., 2013; Suryadi and Bierbach, 2012), while acridine itself and its derivative CID-765471 activate p53 in a non-genotoxic manner (Dudgeon et al., 2010; Peltonen et al., 2010; Wang et al., 2005). However, the exact mechanism of p53-activation was not understood. We have addressed this question and we have demonstrated that CID-765471 causes nucleolar disruption by blocking rDNA transcription in a mechanism that involves, but does not require, selective degradation of the RNA pol I subunit RPA194. Nucleolar disruption, in turn, activates p53 through RPL11. The selective degradation of RPA194 is a shared feature with the recently characterized acridine-derivative BMH-21 (Peltonen et al., 2014). This suggests that acridine derivatives might all induce degradation of RPA194 and, therefore, disorganization of the RNA pol I holoenzyme, beyond intercalating into DNA, as an alternative mechanism to stall rDNA transcription. The activation of the ribosomal stress pathway by CID-765471 is common to CX-5461; however, CX-5461 is structurally non-related to acridines. This observation leads us to reason that any perturbation affecting RNA pol I activity would ultimately activate p53 through the ribosomal stress pathway. More importantly, our findings contribute to set the basis for additional studies on the chemotherapeutic value of non-genotoxic acridine derivatives.

As a footnote, the simplicity of our platform provides a very powerful tool for testing additional libraries. Genetic libraries designed to target nucleolar proteins, such as DNA/RNA helicases, kinases or GTP-based proteins, are good candidates to widen the spectrum of genotoxic-free compounds with capacity to disrupt the nucleolus and activate p53.

Rpl11 haploinsufficiency leads to abnormal erythroid maturation, defective ribosomal stress pathway and increased susceptibility to γ-IR induced lymphomagenesis

As we and others have previously shown, RPL11 constitutes one of the central hubs that modulates the ribosomal stress pathway in response to perturbations in ribosome biogenesis, thus resulting in activation of p53 in somatic, tumor and pluripotent stem cells (Bywater et al., 2012; Macias et al., 2010; Morgado-Palacin et al., 2012, 2014). However, *Rpl11* abrogation studies are restricted so far to the analysis of somatic/tumor cell lines, and a few *in vivo* studies in *Zebrafish* (Chakraborty et al., 2009; Danilova et al., 2011). Such *in vivo* studies have shown that morpholino-mediated downregulation of *Rpl11* in *Zebrafish* is linked to defects in brain development, hematopoiesis and metabolism (Chakraborty et al., 2009; Danilova et al., 2011). Strikingly, no mammalian organisms with full or conditional RPL11 abrogation have been generated thus far, hampering the modeling of the specific contribution of this protein to human diseases such as DBA.

To understand the *in vivo* role of RPL11 in a mammalian organism, we have generated the first mouse model of *Rpl11* haploinsufficiency. *Rpl11* heterozygosity during embryogenesis or homozygous conditional deletion of *Rpl11* in adult mice is lethal. Partial loss of *Rpl11* in adult mice recapitulates DBA, including impaired rRNA processing and defective erythroid maturation. Importantly, *Rpl11* abrogation promotes γ-IR-induced lymphomagenesis, at least in part by a defective ribosomal stress pathway and high basal levels of c-MYC oncoprotein. In summary, we have demonstrated that this mouse model is a powerful tool for modeling human congenital defects such as DBA and for studying cancer predisposition and, in particular, the role of a defective ribosomal stress pathway in oncogenic events.

Embryonic lethality of *Rpl11* heterozygous mice

As we have shown, heterozygous ablation of *Rpl11* results in embryonic lethality, suggesting an essential role for RPL11 during embryonic development. This striking phenotype is extremely unusual for mouse models bearing partial deficiencies in ribosomal proteins (Caldarola et al., 2009). We are only aware of one other ribosomal gene, *Rps6*, whose partial loss results in embryonic lethality at early developmental stages (Panić et al., 2006). *Rps6* heterozygous embryos die at E8.5, presenting defects since the beginning of gastrulation (E5.5) when ribosome biogenesis is intensely upregulated to meet the demands of a dramatic increase in the rate of proliferation and differentiation (Snow, 1977). Interestingly, embryonic lethality is only partially rescued until E12.5 in a p53 null

background, which indicates the existence of both p53-dependent and p53-independent mechanisms that monitor ribosome biogenesis during development.

Of note, ribosomal proteins are ubiquitously expressed in the organism; however, their expression levels vary notably among different RPs and such differences are cell- and tissue-specific (Kondrashov et al., 2011; Xue and Barna, 2012). One of the most paradigmatic examples is RPL38. *Rpl38* transcripts are highly expressed in the developing somites and neural tube of mouse embryos, and haploinsufficiency of *Rpl38* causes axial skeleton remodeling defects by perturbing the translation of a subset of Homeobox mRNAs (Kondrashov et al., 2011). Similar to *Rpl38* haploinsufficiency, partial loss of *Rps7* (Watkins-Chow et al., 2013) or *Rpl24* (Oliver et al., 2004) affects the skeletal tissue patterning and produces some additional malformations. In *Zebrafish*, loss of RPs or rRNA modifications leads to developmental defects (Higa-Nakamine et al., 2012; Uechi et al., 2006). Development defects in *Rpl38* and *Rps7* haploinsufficient mice are not rescued in the absence of p53, in support of extra-ribosomal functions of RPs independently of p53-mediated cell cycle arrest. In this regard, the characterization of the extra-ribosome function of *Rpl11* during embryonic development might be also useful to understand why *Rpl11*, but not *Rpl5* or *Rps19*, mutations are preferentially associated to thumb malformations in DBA (Cmejla et al., 2009; Gazda et al., 2008; Quarello et al., 2010). Our mouse model will unveil whether *Rpl11* is involved, for example, in Shh or Fgf signaling pathways that determine the digit patterning and the number of phalanges during limb development (Sanz-Ezquerro and Tickle, 2003; Suzuki, 2013).

Complete abrogation of *Rpl11* abrogation in adults is lethal

To overcome the extreme developmental phenotype of *Rpl11* heterozygous mice that hamper the characterization of its role in adult tissues, we decided to perform conditional ablation of *Rpl11* in adults. For that, we generated mice with three different genotypes ($Rpl11^{+/+}$, $Rpl11^{+/lox}$ and $Rpl11^{lox/lox}$) bearing a transgene of a ubiquitous tamoxifen-inducible Cre recombinase (Tg.UbC.*CreERT2* (Ruzankina et al., 2007)). For clarity purposes, and unless specifically mentioned, we will refer hereafter to tamoxifen-treated mice or MEFs as $Rpl11^{+/+}$ (or wild-type), $Rpl11^{+/lox}$ (or heterozygous), and $Rpl11^{lox/lox}$ (or null). Bone marrow transplanted animals followed by tamoxifen treatment will be referred as BMT-$Rpl11^{+/+}$ or BMT-$Rpl11^{+/lox}$. Animals subjected to whole body γ-irradiation, followed by tamoxifen treatment, will be referred as γ-IR $Rpl11^{+/+}$ or γ-IR $Rpl11^{+/lox}$.

Adult *Rpl11* null mice die within 8 weeks after starting the tamoxifen treatment; they present intestinal atrophy and bone marrow aplasia, which suggests that highly proliferative tissues are the first to be affected by drastic reduction of RPL11. We have also described that adult *Rpl11* null mice

present a severely reduced number of erythroid precursors (Ter119^{+} nucleated cells). Concomitant with erythroid defects, accumulation of hemosiderin is visualized in spleen and liver, suggesting a compromised iron recycling, presumably from an anemic condition. Lethality of adult mice with complete loss of *Rpl11* is not surprising given the essential function of RPL11 in the ribosome.

Partial loss of *Rpl11* recapitulates DBA features

Human DBA patients carry heterozygous mutations in ribosomal genes, which is sufficient to provoke evident symptoms that compromise their health (Boria et al., 2010; Cmejla et al., 2009; Gazda et al., 2008; Quarello et al., 2010). For this reason and due to the embryonic lethality of constitutive *Rpl11* heterozygous mice, we decided to focus our research on the effects of inducible heterozygous deletion of *Rpl11* in adult mice. Several mouse models of DBA and ribosomopathies have been reported (McGowan and Mason, 2011; Narla and Ebert, 2010), but only a subset of them recapitulate the erythropoietic defect characteristic of human DBA patients, namely, mice with partial deficiency of *Rps19* (Devlin et al., 2010; Jaako et al., 2011), *Rps6* (Keel et al., 2012; McGowan et al., 2011) and *Rps14* (Barlow et al., 2010). Interestingly, our mouse model for *Rpl11* haploinsufficiency recapitulates the main DBA features, including impaired rRNA processing, anemia as the cause of decreased erythroid progenitors, and cancer predisposition.

1. Impaired rRNA processing

RPL11, similar to many other ribosomal proteins of the large subunit, participates in the maturation of intermediate 32S rRNA, which gives rise, after further processing, to the 28S and 5.8S rRNAs (Robledo et al., 2008b; Zhang et al., 2007). Analysis of the rRNA processing of DBA patients-derived lymphoblastoid cells with mutations in *Rpl11*, as well as knockdown of *Rpl11* in HeLa cells, revealed defective processing of 32S rRNA, being this species together with 12S rRNA and 5.8S precursors accumulated (Gazda et al., 2008; Robledo et al., 2008b). Study of 32S pre-rRNA maturation in inducible *Rpl11* haploinsufficient and null MEFs (E13.5), as well as in adult spleens from these animals, confirmed the defective rRNA maturation observed in DBA, thus recapitulating another feature of this disease.

2. Defective erythroid maturation

Rpl11$^{+/lox}$ adult mice manifest macrocytic anaemia at levels that are compatible with life and elevated levels of *Epo* mRNA (coding for erythropoietin) in kidneys, consistent with the physiological response to restore normal levels of erythropoiesis. They also present a reduced number of BFU-Es

(erythroid progenitors), a severe reduction in the number of erythroblasts (nucleated Ter119+ cells) and a blockage at the early stages of erythroid maturation. Furthermore, normal mice transplanted with inducible heterozygous *Rpl11* bone marrow also developed anaemia and loss of erythroblasts upon *Rpl11* deletion. In agreement with this, many of the genes significantly downregulated in *Rpl11*$^{+/lox}$ HPCs are related to erythrocyte development and function. These erythroid-related genes remain unaffected in other tissues, such as liver. Commitment towards the erythroid lineage was partly compromised since we detected a negative trend in the number of BFU-E, the first erythroid committed cells. Although mRNA levels of the core erythroid transcription factors *Gata1*, *Tal-1* and *Klf1* (Doré and Crispino, 2011; Keller et al., 2006; Weiss et al., 1997; Wontakal et al., 2012) were not affected in *Rpl11*$^{+/lox}$ HPCs, translation of these transcripts could be hampered, similarly to what has been reported for *Gata1* upon knockdown of several RPs, including RPL11 (Ludwig et al., 2014). It would be of interest to check whether GATA1 protein levels are affected and whether mRNA expression of target genes of the erythroid core transcription network is also downregulated.

Cell cycle profiles of *Rpl11* deficient fetal liver cells revealed that erythroblasts are arrested in G1 phase. Also, we observed mRNA upregualtion of the cell cycle inhibitor *Cdkn1a* (p21) and the pro-apoptotic factor *Bax* during all stages of erythropoiesis, implying cell cycle arrest and induction of the apoptotic response as determinants of impaired maturation. Levels of p21 mRNA were also significantly increased in *Rpl11*$^{+/lox}$ HPCs, in agreement with observations in hematopoietic progenitors from DBA patients (Dutt et al., 2011). All these features recapitulate the anaemia phenotype observed in primary hematopoietic cells from DBA patients carrying mutations in *Rpl11* (Moniz et al., 2012).

Why are erythroblasts exquisitely sensitive to ribosome dysfunction?

It is still puzzling why the erythroid lineage is preferentially affected, over other cell types, in a condition of ribosomal protein haploinsufficiency. In support of this, we have demonstrated that only erythropoiesis is severely affected in *Rpl11*$^{+/lox}$ adult mice, while hematopoietic stem cells, progenitors and lymphopoiesis (B and T cell differentiation) remain largely unaffected.

Ribosomal proteins are ubiquitously expressed in all cell lineages; however, severe defects are only manifested in erythroblasts. Several hypotheses have been postulated in order to explain the vulnerability of the erythroid lineage to perturbed ribosome homeostasis: 1) inefficient translation of globin that leads to free heme groups that result in oxidative stress and finally, haemolysis of erythrocytes (Narla and Ebert, 2010), 2) defective ribosome biosynthesis at early stages of erythropoiesis to sustain high production of proteins prior to chromatin condensation and enucleation

(Sieff et al., 2010), 3) reduced translation of mRNAs required for erythrocyte function (Horos et al., 2012; Ludwig et al., 2014; Pereboom et al., 2014), and 4) selective p53 activation in the erythroid lineage that triggers cell cycle arrest and apoptosis in proerythroblasts (Dutt et al., 2013; Jaako et al., 2015).

Nonetheless, there are certain caveats in some of the proposed hypothesis. Regarding the first theory, haemoglobin levels are normal in DBA patients (Narla et al., 2011) and haemolytic anaemia has not been reported in DBA since failure relies in erythroid progenitors rather than in mature red blood cells.

Concerning the second and third theories, defective erythropoiesis should be the outcome of any ribosomal protein deficiency impinging on translation. Compromised translation of essential transcripts for erythrocyte commitment and development has been reported in several anemic RP-deficient mouse models and human cells as the main cause for erythropoiesis failure (Horos et al., 2012; Ludwig et al., 2014; Pereboom et al., 2014). For instance, although *Gata1* transcripts levels remains unaffected in *Rps19*-, *Rpl11*-, *Rpl5*-, or *Rps24*-depleted human primary erythrocyte cells, *Gata1* mRNA translation is severely hampered upon ribosome protein deficiency (Ludwig et al., 2014). Inefficient *Gata1* translation reduces expression of *Gata1* targets required for erythropoiesis, such as c-KIT (Munugalavadla and Kapur, 2005). In agreement, erythroid progenitors with reduced levels of *Rps19* express lower amounts of c-KIT (Sieff et al., 2010), which could contribute to reduced proliferation of erythroblasts. In addition, impaired polysome recruitment of a set of transcripts involved in erythrocyte development and function, including *Bag1* and *Csde1*, occurs in *Rps19*- and *Rpl11*-deficient erythroid cells (Horos et al., 2012). Furthermore, translation of *Bcat1* transcripts, required for the synthesis of branched-chain aminoacids, is also decreased in lymphoblastoid cells from DBA patients that bear mutations in RPS9 or RPL11 (Pereboom et al., 2014). Remarkably, dietary supplementation of L-leucine alleviates anaemia in DBA *Rps19*-deficient animals by activating mTOR and thus, boosts translation of proteins in a p53-independent manner (Jaako et al., 2012; Narla et al., 2014; Payne et al., 2012). Gene set enrichment analysis showed that transcriptional profiling of eukaryotic translation is impaired in $Rpl11^{+/lox}$ HPCs, but we did not follow an approach to evaluate translation activity in *Rpl11* deficient cells so whether translation of certain transcripts is preferentially affected upon loss of *Rpl11* in our model needs confirmation by, for instance, ribosome profiling.

However, not all ribosomal protein insufficiencies result in anaemia. *Rpl29*, *Rpl22*, *Rps20* and *Rps7* haploinsufficient mice do not show erythroid defects (Keel et al., 2012; Nieminen et al., 2014; Watkins-Chow et al., 2013) although they display other abnormalities, such as skeletal growth defects, impaired αβ T-cell development, dark skin hyperpigmentation and eye malformations, respectively (Anderson et al., 2007; Kirn-Safran et al., 2007; Watkins-Chow et al., 2013). This further supports the

notion that ribosomal protein deficiency results in tissue-specific phenotypes and point towards shortage of specific RPs as one of the lead cause for failure in erythropoiesis.

Intriguingly, acinar cells of the exocrine pancreas, but not erythroblasts, posses the highest protein synthesis rate in mammals (Logsdon CD, 2013), so, concomintnatly with a defective ribosome byosinthesis (possibility 2 above), it would be expected that pancreas resulted also affected. Deficiency of certain ribosomal proteins and factors involved in rRNA processing impair p53-independent pancreas development in *Zebrafish* (Provost et al., 2012, 2013; Qin et al., 2014). In agreement with this, mutations in SBDS, a nucleolar protein involved in ribosome assembly, cause exocrine pancreas insufficiency in patients with Shwachman-Diamond syndrome (SDS) (Stormon et al., 2010; Tulpule et al., 2013), a disease included in the group of ribosomopathies. Nevertheless, defects in the exocrine pancreas have not been described in DBA patients. Therefore, translation deficit by ribosome shortage does not explain the vulnerability of erythroid cells over the rest of lineages. It would be of interest to test whether SBDS deficiency causes impaired translation of certain transcripts, and if so, whether these transcripts are required for a correct pancreas function.

Cell cycle arrest and apoptosis triggered by selective activation of p53 in erythroid cells has been highlighted to be key for DBA pathogenesis. Dutt et al. (Dutt et al., 2011) showed that ribosomal protein-deficient erythroid, but not myeloid or megakaryocyte, cells accumulate p53 and its target p21. By treating healthy CD34+ hematopoietic cells with nutlin-3, a well-known p53 activator, they recapitulate accumulation of p53 selectively in erythroid cells and defective erythropoiesis in the absence of ribosome biogenesis dysfunction, similarly to defects observed upon knockdown of *Rps14* or *Rps19*. Interestingly, treating *Rps14*- or *Rps19*-deficient cells with pifithrin-α, which blocks the transcriptional transactivation activity of p53, rescues erythroid maturation. These findings point towards p53 accumulation as one of the underlying causes of DBA pathogenesis. Failure of erythroid maturation, as well as developmental defects, are restored in a p53-null background in several models of ribosomal protein haploinsufficiency, among them *Rps19* (Danilova et al., 2008; Jaako et al., 2011), *Rps14* (Barlow et al., 2010), *Rps6* (McGowan et al., 2011) and *Rpl11* in *Zebrafish* (Chakraborty et al., 2009; Danilova et al., 2011). Remarkably, anatomical defects, impaired T-cell development and dark skin hyperpigmentation in ribosomal protein-deficient models with no anaemia are also restored in a p53-deficient background (Kirn-Safran et al., 2007; McGowan et al., 2008; Nieminen et al., 2014; Watkins-Chow et al., 2013). On the contrary, *Rpl5* mutant mES cells, *Rpl5*- and *Rpl11*-depleted human lung fibroblasts and *Rpl11*-deficient fibroblasts did not display basal accumulation of p53 (Fumagalli et al., 2009, 2012; Morgado-Palacin et al., 2015; Singh et al., 2014; Teng et al., 2013b) and p53 deletion does not rescue the G2/M cell cycle arrest observed in *Rpl5* mutant mESCs (Singh et al., 2014). These observations could be reconciled by taking into consideration that activation of p53 relies on both RPL5 and RPL11 for monitoring ribosome biogenesis function through the ribosomal

stress pathway. Thus, in the case of deficiency of the ribosomal stress transducer complex (RPL11/RPL5/5S rRNA) p53 is not selectively activated. Analysis of erythroid differentiation and study of proliferative and apoptosis responses during the different erythroid stages in *Rpl11* haploinsufficient mice null for p53 would further clarify this question.

Erythroid blood malignancies (acute erythroid leukemia and its subcategory pure erythroid leukemia) in which the predominant neoplastic blasts are erythroid, are very rare, counting for less than 5% of all cases of adult acute myeloid leukemia, group in which they are classified (Hasserjian et al., 2010). Hence, selective sensitivity to p53 activation in the erythroid lineage could protect erythroid cells over the rest of hematopoietic lineages from becoming tumoral.

So far, the scenario of possibilities explaining DBA pathogenesis is increasingly complex, and additional hypotheses can be also considered. In myelodysplastic syndromes, it has been proposed that defective ligand-receptor signaling (c-KIT and Epo), rather than reduced levels of c-KIT or Epo receptors, could be one of the causes of impaired erythropoiesis (Fontenay-Roupie et al., 1999). This same theory could apply to DBA and it would be of interest to characterize downstream signaling pathways to c-KIT and Epo receptors. c-KIT and Epo signalling pathways are particularly important at the earlier stages when erythroblast depend on them for expansion and maturation. Expression of downstream proteins of Epo signalling, such as JAK2 or STAT5, is not affected in a DBA mouse model for *Rps19* deficiency (Ludwig et al., 2014) although their activity have not been checked. We observed reduced levels of Epor in *Rpl11* deficient HPCs so failure in fundamental signalling pathways could also contribute to the DBA pathogenesis.

Finally, it is worth mentioning that many chemotherapeutic drugs approved for treatment of human cancers, such as cisplatin, result in severe anaemia (Groopman and Itri, 1999). Cisplatin induces ribosomal stress by means of inhibition of RNA pol I-mediated transcription and nucleolar disruption (Burger et al., 2010; Llanos and Serrano, 2010). Vulnerability of erythroblasts to perturbations in ribosome biogenesis could explain at least in part the chemotherapy-induced anaemia in cancer patients.

3. Cancer predisposition

More than 20% of DBA patients develop cancer by around 46 years of age, including blood malignancies and solid tumours (Vlachos et al., 2012). To date, cancer incidence in mouse models for DBA (*Rps19*-deficient or mutant) or for deficiency of other RPs presenting anaemia has not been evaluated. Interestingly, haploinsufficiency of *Rps6* in the fruit fly and certain RP genes in *Zebrafish* results in increased tumour incidence (Amsterdam et al., 2004b; Stewart and Denell, 1993; Watson et

al., 1992). One of the main goals of this thesis was to address whether partial loss of *Rpl11* predispose to cancer and thus recapitulate the features of the human DBA condition. For that, we subjected mice to whole body γ-irradiation (γ-IR) followed by induction of *Rpl11* deletion one week later and monitored tumour appearance.

Fractionated or a single acute dose of whole body γ-irradiation (γ-IR) elicits thymic lymphoma due to oncogenic mutations resulting from single and double-strand breaks. Although the thymus is the target organ for tumorigenesis upon exposure to γ-IR, cells with oncogenic potential are primitive hematopoietic stem/progenitor cells, since shielding bone marrow or transplanting non-irradiated bone marrow cells prevents γ-IR-induced thymic lymphomagenesis (Kominami and Niwa, 2006). We have shown that partial loss of *Rpl11* accelerates the appearance of thymic lymphoma upon one acute dose of whole body γ-irradiation (5Gy; **Figure 7A and 7B, manuscript III**), concomitant with splenomegaly and, in certain cases, hepatomegaly. Of note, *Rpl11* gene dose was normal at the moment of γ-IR, meaning that haploinsufficiency of *Rpl11* favours tumour progression rather than initiation. However, we do not know whether partial loss of *Rpl11* could be a driving force *per se* during cancer onset. Although inconclusive, it is worth mentioning in this regard that two out of 11 *Rpl11* haploinsufficient mice in a non-irradiated cohort died between 58-70 weeks presenting tumours in spleen or splenomegaly, hepatomegaly and increased thymus size, while all their control counterparts remained alive at least 75 weeks later (data not shown). This could suggest that Rpl11 deficiency by itself migth promote lymphomagenesis in the absence of irradiation. Accelerated onset of lymphomageneis in *Rpl11* deficient mice is apparently paradoxical since impaired ribosome production should slow down cell growth and proliferation. This could reflect emerging extra-ribosomal functions of RPL11 in tumour suppression, and several non-exclusive mechanisms can be proposed.

3.1. Defective p53 surveillance pathway in response to ribosomal stress

Previous works in *Zebrafish* have shown that *Rpl11* ablation, contrary to cell lines-based studies, results in p53 activation; concurrently, the reported defects in brain development, hematopoiesis and metabolism are rescued in a p53-null background deficiency (Chakraborty et al., 2009; Danilova et al., 2011). However, we observed normal basal levels of p53 in *Rpl11* deficient fibroblasts and defective p53 activation upon ribosomal stress in primary MEFs treated with ActD, doxorubicin or CX-5461 (**Figure 7C, manuscript III**). This is not surprising considering that RPL11 is central in the ribosomal stress pathway and thus reduced levels of RPL11 would compromise this response.

Immunohistochemical analysis of bone marrow biopsies from DBA patients has shown upregulation of p53 (Dutt et al., 2011). In our model, only half of the *Rpl11*$^{+/lox}$ mice (two out of four analyzed) presented a clear accumulation of p53 in BM (data not shown). A more detailed analysis should be conducted to determine whether p53 accumulates in BM from *Rpl11*$^{+/lox}$ mice and, if so, if accumulation results from remaining *Rpl11* levels (one functional gene dose) or from alternative mechanisms, such as enhanced p53 translation by RPL26 (Takagi et al., 2005). Notably, histological analysis detecting p53 activation has been only carried out in BM biopsies from human DBA patients with mutations in *Rps19* (Dutt et al., 2011). It would be therefore of great interest to analyze peripheral blood cells or BM biopsies from *Rpl11* mutant DBA patients to understand whether it correlates with p53 activation status.

3.2. Elevated expression of c-MYC and dysregulation of potential oncogenic pathways

Finally, geneset analysis revealed several potential oncogenic pathways upregulated upon partial loss of *Rpl11* in adult HPCs; among them, MYC and MYB transcription networks and TGF-β signalling pathway. Remarkably, a very recent report showed the upregulation of the TGF-β signalling pathway in iPSCs derived from DBA patients with mutations in *Rps19* or *Rpl5* (Ge et al., 2015). We also observed elevated levels of cMYC protein in *Rpl11*-depleted fibroblasts and hematopoietic organs, more strikingly in thymus, from *Rpl11* heterozygous mice treated for 20 weeks.

Overexpression of c-MYC alone is a driver mutation in haematological malignancies, including thymic lymphomas (Morton and Sansom, 2013). Interestingly, translocations resulting in c-MYC overexpression can occur upon fragmented ionizing radiation in human breast cells (Wade et al., 2014), thus selecting c-MYC-driven cells as triggers of breast cancer. RPL11 regulates cMYC activity by several means, including activation of p53, impaired recruitment of c-MYC co-activators and control of c-MYC mRNA stability. Thus, *Rpl11* deletion could favour an oncogenic environment for the accelerated lymphomagenesis through deregulated levels of cMYC in normal tissues. Interestingly, *Rps19* deficiency cooperates with PIM kinase to increase c-MYC protein levels (Fröjmark et al., 2010). This leads to the question of whether upregulation of c-MYC levels and activity, resulting in ribosomal stress, is a common feature in DBA pathogenesis. Additionally, increased levels of c-MYC could contribute to the anaemia phenotype since overexpression of this oncogene prevents normal erythroid differentiation in erythroleukemia cells (Acosta et al., 2008; Coppola and Cole, 1986; Geiler et al., 2014).

Concluding remarks on the cancer predisposition in *Rpl11* haploinsufficient mice

It seems contradictory that reduced ribosome biosynthesis could cause uncontrolled cell growth. However, delayed cell cycle progression might increase the selective pressure for mutations that overcome reduction in ribosome biogenesis and the negative feedback on the cell cycle. This, together with upregulation of c-MYC and potential oncogenic pathways, as well as impaired p53 surveillance may finally contribute to cancer development. It would be of interest to test whether increased gene dose of *Rpl11* could potentiate p53 surveillance and delay the appearance of tumours in c-MYC-driven tumours.

Importantly, the ribosomal stress pathway has been shown to safeguard cells *in vivo*, together with ARF/MDM2 signalling, in an oncogenic c-MYC-driven lymphomagenesis model (Macias et al., 2010; Schmitt et al., 1999) and in a chemical-induced skin cancer model (squamous cell carcinoma) (Sasaki et al., 2011). Interestingly, the type of cancer registered in RPL11 mutant DBA patients (DBAR) is squamous cell carcinoma (Vlachos et al., 2012). Intriguingly, other oncogenic events, such as inactivation of pRb or Ras overexpression, do not induce the ribosomal stress pathway. Interestingly, ARF/MDM2, but not RPL11/MDM2, signalling is required for restraining tumour aggressiveness in a mouse model of prostate cancer triggered by pRb inactivation (Pan et al., 2011). It remains to be determined whether inactivation of RB family members induces ribosomal stress. These findings suggest a direct and exclusive role of c-MYC in hijacking ribosome biogenesis as a tactic to drive tumorigenesis.

In summary, we have generated a mouse model of *Rpl11* haploinsufficiency that recapitulates the anaemia and cancer susceptibility reported in human DBA patients. Findings are summarized in **Figure 7**. Based on our results, high tumour predisposition could be due two non-exclusive mechanisms: defective p53 surveillance and increased levels of basal c-MYC in heterozygous *Rpl11* fibroblast and hematopoietic organs. Nonetheless, we are still distant from unravelling the common molecular mechanism, if any, underlying any type of ribosomal protein deficiency in this disease. The feedback loop of RPL11 and c-MYC and the defective p53 surveillance can explain, at least in part, tumour predisposition in DBA patients with *Rpl11* mutations but it might be irrelevant when other ribosomal proteins are mutated. Haploinsufficiency of other RPs could impinge on tumour susceptibility by modulating other cellular processes. Cancer predisposition in DBA is still unexplored and further studies in this field would shed light on DBA pathogenesis. Additionally, our *Rpl11* haploinsufficient mouse model can be used to test the effectiveness of certain treatments and to personalize therapies for those patients with *Rpl11* mutations.

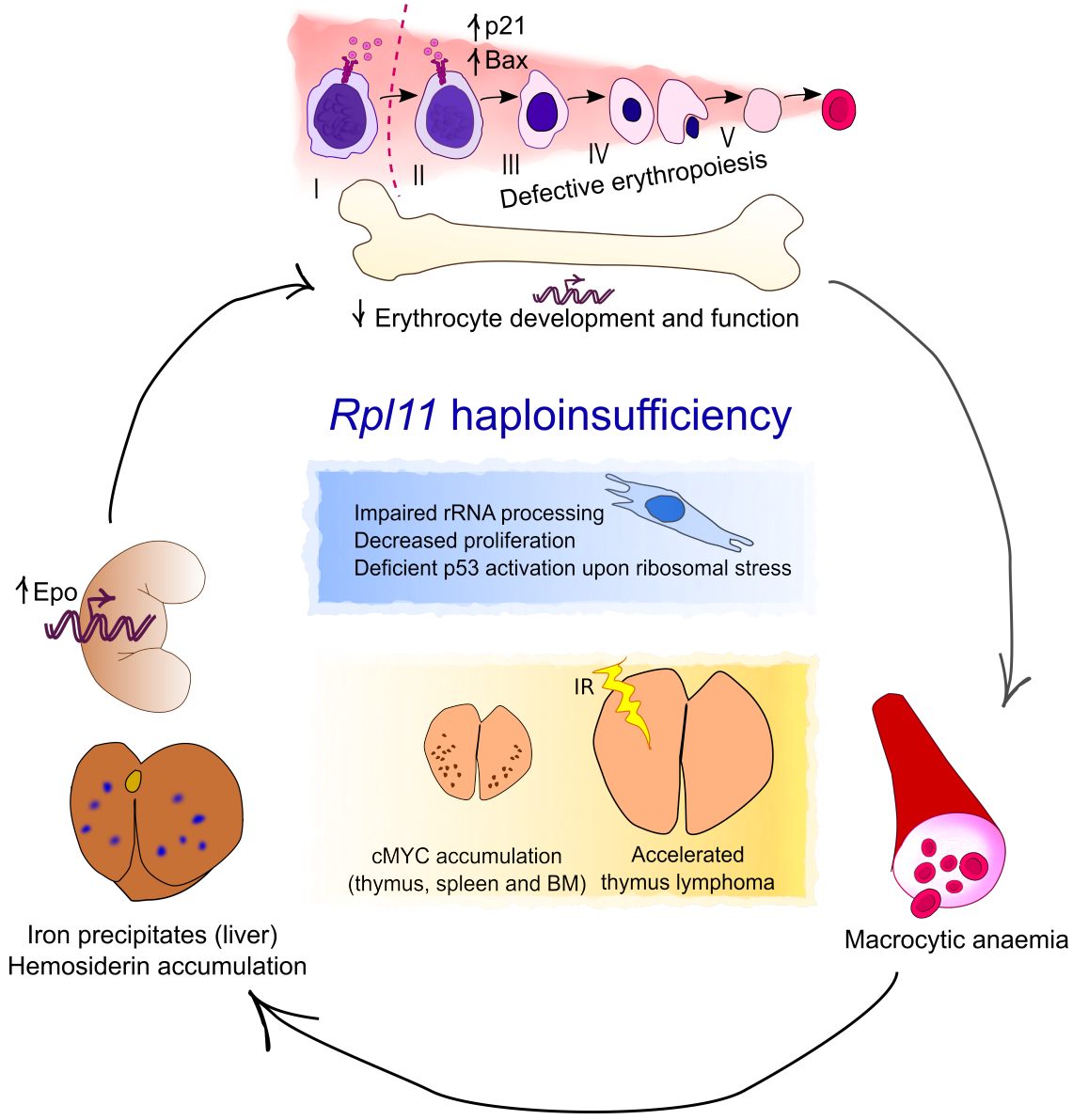

Figure 7. Partial loss of *Rpl11* recapitulates DBA and promotes lymphomagenesis.
The scheme shows the molecular features and pathologies of *Rpl11* haploinsufficient mice.

CONCLUSIONES

Con la elaboración de este trabajo de Tesis hemos alcanzado las siguientes conclusiones:

1. La vía de estrés ribosomal es funcional en células madre embrionarias de ratón y en células madre pluripotente inducidas.

2. Las células pluripotentes de ratón sometidas a estrés ribosomal activan una respuesta de apoptosis mediada por p53.

3. La morfología del nucléolo puede ser explotada para la identificación de compuestos que tengan como diana la biogénesis del ribosoma.

4. Ciertos compuestos derivados de acridina inhiben la transcripción del ADN ribosomal, inducen la degradación de la subunidad de la RNA pol II RPA194, y causan desintegración del nucléolo .

5. Ciertos derivados de acridina activan p53 en células de cáncer a través de la vía de estrés ribosomal en ausencia de daño.

6. La deleción constitutiva de un alelo de *Rpl11* es letal en ratones, así como la deleción inducible de ambos alelos en adultos.

7. La ablación de un alelo de *Rpl11* en ratones adultos recapitula las principales patologías de la anemia de Diamond-Blackfan, incluyendo un procesamiento defectivo del RNA ribosomal, anemia macrocítica debido a defectos en la maduración eritroide, y una mayor predisposición a cáncer.

8. La acelerada linfomagénesis inducida por radiación en ratones haploinsuficientes para *Rpl11* puede deberse a una función defectuosa de p53 y a mayores niveles basales de la proto-oncoproteína c-MYC.

CONCLUSSIONS

From the work carried out during this Thesis, we have reached the following conclussions:

1. The ribosomal stress pathway is operative in mouse embryonic stem cells and induced pluripotent stem cells.

2. Mouse pluripotent stem cells elicit a p53-mediated apoptotic response following ribosomal stress.

3. Nucleolar morphology can be exploited for the identification of small molecule compounds that target ribosome biogenesis.

4. Acridine derivatives cause nucleolar disruption by inhibiting rDNA transcription and promoting degradation of RPA194

5. Acridine derivatives actívate p53 through the ribosomal stress pathway in the absence of damage in cancer cells

6. Constitutive loss of one allele of *Rpl11* is lethal in mice, as well as inducible deletion of both alleles in adults.

7. Partial loss of *Rpl11* in adult mice recapitulates the main features of DBA, including impaired rRNA processing, macrocytic anemia due to a defective erythroid maturation, and cancer predisposition.

8. Accelerated whole body irradiation-induced lymphomagesis in *Rpl11* haploinsufficient mice could be due to defective p53 surveillance and higher basal levels of the proto-oncoprotein c-MYC.

REFERENCES

Acosta, J.C., Ferrándiz, N., Bretones, G., Torrano, V., Blanco, R., Richard, C., O'Connell, B., Sedivy, J., Delgado, M.D., and León, J. (2008). Myc inhibits p27-induced erythroid differentiation of leukemia cells by repressing erythroid master genes without reversing p27-mediated cell cycle arrest. Mol. Cell. Biol. *28*, 7286–7295.

Ahmad, Y., Boisvert, F.-M., Gregor, P., Cobley, A., and Lamond, A.I. (2009). NOPdb: Nucleolar Proteome Database--2008 update. Nucleic Acids Res. *37*, D181–D184.

Al-Baker, E. a, Oshin, M., Hutchison, C.J., and Kill, I.R. (2005). Analysis of UV-induced damage and repair in young and senescent human dermal fibroblasts using the comet assay. Mech. Ageing Dev. *126*, 664–672.

Al-Baker, E.A., Boyle, J., Harry, R., and Kill, I.R. (2004). A p53-independent pathway regulates nucleolar segregation and antigen translocation in response to DNA damage induced by UV irradiation. Exp. Cell Res. *292*, 179–186.

Aladjem, M.I., Spike, B.T., Rodewald, L.W., Hope, T.J., Klemm, M., Jaenisch, R., and Wahl, G.M. (1998). ES cells do not activate p53-dependent stress responses and undergo p53-independent apoptosis in response to DNA damage. Curr. Biol. *8*, 145–155.

Alt, J.R., Greiner, T.C., Cleveland, J.L., and Eischen, C.M. (2003). Mdm2 haplo-insufficiency profoundly inhibits Myc-induced lymphomagenesis. EMBO J. *22*, 1442–1450.

Amsterdam, A., Nissen, R.M., Sun, Z., Swindell, E.C., Farrington, S., and Hopkins, N. (2004a). Identification of 315 genes essential for early zebrafish development. Proc. Natl. Acad. Sci. U. S. A. *101*, 12792–12797.

Amsterdam, A., Sadler, K.C., Lai, K., Farrington, S., Bronson, R.T., Lees, J.A., and Hopkins, N. (2004b). Many ribosomal protein genes are cancer genes in zebrafish. PLoS Biol *2*, E139.

Anderson, S.J., Lauritsen, J.P.H., Hartman, M.G., Foushee, A.M.D., Lefebvre, J.M., Shinton, S. a., Gerhardt, B., Hardy, R.R., Oravecz, T., and Wiest, D.L. (2007). Ablation of Ribosomal Protein L22 Selectively Impairs T Cell Development by Activation of a p53-Dependent Checkpoint. Immunity *26*, 759–772.

Andrews, W.J., Panova, T., Normand, C., Gadal, O., Tikhonova, I.G., and Panov, K.I. (2013). Old Drug, New Target: ELLIPTICINES SELECTIVELY INHIBIT RNA POLYMERASE I TRANSCRIPTION. J. Biol. Chem. *288*, 4567–4582.

Arabi, A., Wu, S., Ridderstråle, K., Bierhoff, H., Shiue, C., Fatyol, K., Fahlén, S., Hydbring, P., Söderberg, O., Grummt, I., et al. (2005). c-Myc associates with ribosomal DNA and activates RNA polymerase I transcription. Nat. Cell Biol. *7*, 303–310.

Ayrault, O., Andrique, L., Fauvin, D., Eymin, B., Gazzeri, S., and Séité, P. (2006). Human tumor suppressor p14ARF negatively regulates rRNA transcription and inhibits UBF1 transcription factor phosphorylation. Oncogene *25*, 7577–7586.

Baker, S.J., Fearon, E.R., Nigro, J.M., Hamilton, S.R., Preisinger, a C., Jessup, J.M., vanTuinen, P., Ledbetter, D.H., Barker, D.F., Nakamura, Y., et al. (1989). Chromosome 17 deletions and p53 gene mutations in colorectal carcinomas. Science *244*, 217–221.

Balajee, A.S., May, A., and Bohr, V. a. (1999). DNA repair of pyrimidine dimers and 6-4 photoproducts in the ribosomal DNA. Nucleic Acids Res. *27*, 2511–2520.

Barak, Y., Juven, T., Haffner, R., and Oren, M. (1993). Mdm2 Expression Is Induced By Wild Type P53 Activity. EMBO J. *12*, 461–468.

Barkić, M., Crnomarković, S., Grabusić, K., Bogetić, I., Panić, L., Tamarut, S., Cokarić, M., Jerić, I., Vidak, S., and Volarević, S. (2009). The p53 tumor suppressor causes congenital malformations in Rpl24-deficient mice and promotes their survival. Mol. Cell. Biol. *29*, 2489–2504.

Barlow, J.L., Drynan, L.F., Hewett, D.R., Holmes, L.R., Lorenzo-Abalde, S., Lane, A.L., Jolin, H.E., Pannell, R., Middleton, A.J., Wong, S.H., et al. (2010). A p53-dependent mechanism underlies macrocytic anemia in a mouse model of human 5q- syndrome. Nat. Med. *16*, 59–66.

Barna, M., Pusic, A., Zollo, O., Costa, M., Kondrashov, N., Rego, E., Rao, P.H., and Ruggero, D. (2008). Suppression of Myc oncogenic activity by ribosomal protein haploinsufficiency. Nature *456*, 971–975.

Bates, S., Phillips, a C., Clark, P. a, Stott, F., Peters, G., Ludwig, R.L., and Vousden, K.H. (1998). p14ARF links the tumour suppressors RB and p53. Nature *395*, 124–125.

Batista, L.F.Z., Kaina, B., Meneghini, R., and Menck, C.F.M. (2009). How DNA lesions are turned into powerful killing structures: Insights from UV-induced apoptosis. Mutat. Res. - Rev. Mutat. Res. *681*, 197–208.

Beckerman, R., and Prives, C. (2010). Transcriptional regulation by p53. Cold Spring Harb. Perspect. Biol. *2*.

Belin, S., Beghin, A., Solano-Gonzàlez, E., Bezin, L., Brunet-Manquat, S., Textoris, J., Prats, A.-C., Mertani, H.C., Dumontet, C., and Diaz, J.-J. (2009). Dysregulation of Ribosome Biogenesis and Translational Capacity Is Associated with Tumor Progression of Human Breast Cancer Cells. PLoS One *4*, e7147.

Bertoli, C., Skotheim, J.M., and de Bruin, R. a M. (2013). Control of cell cycle transcription during G1 and S phases. Nat. Rev. Mol. Cell Biol. *14*, 518–528.

Bhat, K.P., Itahana, K., Jin, A., and Zhang, Y. (2004). Essential role of ribosomal protein L11 in mediating growth inhibition-induced p53 activation. EMBO J. *23*, 2402–2412.

Bieging, K.T., Mello, S.S., and Attardi, L.D. (2014). Unravelling mechanisms of p53-mediated tumour suppression. Nat. Rev. Cancer *14*, 359–370.

Boria, I., Garelli, E., Gazda, H.T., Aspesi, A., Quarello, P., Pavesi, E., Ferrante, D., Meerpohl, J.J., Kartal, M., Da Costa, L., et al. (2010). The ribosomal basis of Diamond-Blackfan Anemia: mutation and database update. Hum. Mutat. *31*, 1269–1279.

Boulon, S., Westman, B.J., Hutten, S., Boisvert, F.-M., and Lamond, A.I. (2010). The nucleolus under stress. Mol. Cell *40*, 216–227.

Brangwynne, C.P., Mitchison, T.J., and Hyman, a. a. (2011). Active liquid-like behavior of nucleoli determines their size and shape in Xenopus laevis oocytes. Proc. Natl. Acad. Sci. *108*, 4334–4339.

Brenner, C., Deplus, R., Didelot, C., Loriot, A., Viré, E., De Smet, C., Gutierrez, A., Danovi, D., Bernard, D., Boon, T., et al. (2005). Myc represses transcription through recruitment of DNA methyltransferase corepressor. EMBO J. *24*, 336–346.

Brooks, C.L., and Gu, W. (2011). The impact of acetylation and deacetylation on the p53 pathway. Protein Cell *2*, 456–462.

Brown, C.J., Lain, S., Verma, C.S., Fersht, A.R., and Lane, D.P. (2009). Awakening guardian angels: drugging the p53 pathway. Nat. Rev. Cancer *9*, 862–873.

Burger, K., Mühl, B., Harasim, T., Rohrmoser, M., Malamoussi, A., Orban, M., Kellner, M., Gruber-Eber, A., Kremmer, E., Hölzel, M., et al. (2010). Chemotherapeutic drugs inhibit ribosome biogenesis at various levels. J. Biol. Chem. *285*, 12416–12425.

Bursac, S., Brdovcak, M.C., Donati, G., and Volarevic, S. (2014). Activation of the tumor suppressor p53 upon impairment of ribosome biogenesis. Biochim. Biophys. Acta *1842*, 817–830.

Bursać, S., Brdovčak, M.C., Pfannkuchen, M., Orsolić, I., Golomb, L., Zhu, Y., Katz, C., Daftuar, L., Grabušić, K., Vukelić, I., et al. (2012a). Mutual protection of ribosomal proteins L5 and L11 from degradation is essential for p53 activation upon ribosomal biogenesis stress. Proc. Natl. Acad. Sci. U. S. A. *109*, 20467–20472.

Bursać, S., Brdovčak, M.C., Pfannkuchen, M., Orsolić, I., Golomb, L., Zhu, Y., Katz, C., Daftuar, L., Grabušić, K., Vukelić, I., et al. (2012b). Mutual protection of ribosomal proteins L5 and L11 from degradation is essential for p53 activation upon ribosomal biogenesis stress. Proc. Natl. Acad. Sci. U. S. A. *109*, 20467–20472.

Bywater, M.J., Poortinga, G., Sanij, E., Hein, N., Peck, A., Cullinane, C., Wall, M., Cluse, L., Drygin, D., Anderes, K., et al. (2012). Inhibition of RNA polymerase I as a therapeutic strategy to promote cancer-specific activation of p53. Cancer Cell *22*, 51–65.

Cairncross, J.G., Ueki, K., Zlatescu, M.C., Lisle, D.K., Finkelstein, D.M., Hammond, R.R., Silver, J.S., Stark, P.C., Macdonald, D.R., Ino, Y., et al. (1998). Specific genetic predictors of chemotherapeutic response and survival in patients with anaplastic oligodendrogliomas. J. Natl. Cancer Inst. *90*, 1473–1479.

Caldarola, S., De Stefano, M.C., Amaldi, F., and Loreni, F. (2009). Synthesis and function of ribosomal proteins--fading models and new perspectives. FEBS J. *276*, 3199–3210.

Cervantes, R.B., Stringer, J.R., Shao, C., Tischfield, J. a, and Stambrook, P.J. (2002). Embryonic stem cells and somatic cells differ in mutation frequency and type. Proc. Natl. Acad. Sci. U. S. A. *99*, 3586–3590.

Chae, H., Park, J., Lee, S., Kim, M., Kim, Y., Lee, J.-W., Chung, N.-G., Cho, B., Jeong, D.C., Kim, J., et al. (2014). Ribosomal protein mutations in Korean patients with Diamond-Blackfan anemia. Exp. Mol. Med. *46*, e88.

Chakraborty, A., Uechi, T., Higa, S., Torihara, H., and Kenmochi, N. (2009). Loss of ribosomal protein L11 affects zebrafish embryonic development through a p53-dependent apoptotic response. PLoS One *4*, e4152.

Challagundla, K.B., Sun, X.-X., Zhang, X., DeVine, T., Zhang, Q., Sears, R.C., and Dai, M.-S. (2011). Ribosomal protein L11 recruits miR-24/miRISC to repress c-Myc expression in response to ribosomal stress. Mol. Cell. Biol. *31*, 4007–4021.

Chan, J.C., Hannan, K.M., Riddell, K., Ng, P.Y., Peck, A., Lee, R.S., Hung, S., Astle, M. V, Bywater, M., Wall, M., et al. (2011). AKT promotes rRNA synthesis and cooperates with c-MYC to stimulate ribosome biogenesis in cancer. Sci. Signal. *4*, ra56.

Chao, C., Saito, S., Anderson, C.W., Appella, E., and Xu, Y. (2000a). Phosphorylation of murine p53 at ser-18 regulates the p53 responses to DNA damage. Proc. Natl. Acad. Sci. U. S. A. *97*, 11936–11941.

Chao, C., Saito, S., Kang, J., Anderson, C.W., Appella, E., and Xu, Y. (2000b). p53 transcriptional activity is essential for p53-dependent apoptosis following DNA damage. EMBO J. *19*, 4967–4975.

Chen, J., and Kastan, M.B. (2010). mRNA translation and provide a target for modulating p53 induction after DNA damage. 2146–2156.

Chen, D., Zhang, Z., Li, M., Wang, W., Li, Y., Rayburn, E.R., Hill, D.L., Wang, H., and Zhang, R. (2007). Ribosomal protein S7 as a novel modulator of p53-MDM2 interaction: binding to MDM2, stabilization of p53 protein, and activation of p53 function. Oncogene *26*, 5029–5037.

Cheng, Q., Chen, L., Li, Z., Lane, W.S., and Chen, J. (2009). ATM activates p53 by regulating MDM2 oligomerization and E3 processivity. EMBO J. *28*, 3857–3867.

Choesmel, V., Fribourg, S., Aguissa-Touré, A.-H.H., Pinaud, N., Legrand, P., Gazda, H.T., and Gleizes, P.-E.E. (2008). Mutation of ribosomal protein RPS24 in Diamond-Blackfan anemia results in a ribosome biogenesis disorder. Hum. Mol. Genet. *17*, 1253–1263.

Choong, M.L., Yang, H., Lee, M.A., and Lane, D.P. (2009). Specific activation of the p53 pathway by low dose actinomycin D: A new route to p53 based cyclotherapy. Cell Cycle *8*, 2810–2818.

Christophorou, M. a, Ringshausen, I., Finch, a J., Swigart, L.B., and Evan, G.I. (2006). The pathological response to DNA damage does not contribute to p53-mediated tumour suppression. Nature *443*, 214–217.

Chuykin, I. a., Lianguzova, M.S., Pospelova, T. V., and Pospelov, V. a. (2008). Activation of DNA damage response signaling in mouse embryonic stem cells. Cell Cycle *7*, 2922–2928.

Cmejla, R., Cmejlova, J., Handrkova, H., Petrak, J., Petrtylova, K., Mihal, V., Stary, J., Cerna, Z., Jabali, Y., and Pospisilova, D. (2009). Identification of mutations in the ribosomal protein L5 (RPL5) and ribosomal protein L11 (RPL11) genes in Czech patients with Diamond-Blackfan anemia. Hum. Mutat. *30*, 321–327.

Cole, M.D., and Nikiforov, M. a. (2006). Transcriptional activation by the Myc oncoprotein. Curr. Top. Microbiol. Immunol. *302*, 33–50.

Coppola, J., and Cole, M. (1986). constitutive c-myc oncogen overexpression blocks mouse erythroleukaemia cell differentiation but not commitment.

Corbet, S.W., Clarke, A.R., Gledhill, S., and Wyllie, A.H. (1999). P53-dependent and -independent links between DNA-damage, apoptosis and mutation frequency in ES cells. Oncogene *18*, 1537–1544.

Couté, Y., Burgess, J. a., Diaz, J.J., Chichester, C., Lisacek, F., Greco, A., and Sanchez, J.C. (2006). Deciphering the human nucleolar proteome. Mass Spectrom. Rev. *25*, 215–234.

Daftuar, L., Zhu, Y., Jacq, X., and Prives, C. (2013). Ribosomal Proteins RPL37, RPS15 and RPS20 Regulate the Mdm2-p53-MdmX Network. PLoS One *8*.

Dai, M.-S., and Lu, H. (2004a). Inhibition of MDM2-mediated p53 ubiquitination and degradation by ribosomal protein L5. J. Biol. Chem. *279*, 44475–44482.

Dai, M.S., and Lu, H. (2004b). Inhibition of MDM2-mediated p53 ubiquitination and degradation by ribosomal protein L5. J. Biol. Chem. *279*, 44475–44482.

Dai, M., Zeng, S., and Jin, Y. (2004). Ribosomal protein L23 activates p53 by inhibiting MDM2 function in response to ribosomal perturbation but not to translation inhibition. Mol. Cell. … *24*, 7654–7668.

Dai, M.-S., Arnold, H., Sun, X.-X., Sears, R., and Lu, H. (2007a). Inhibition of c-Myc activity by ribosomal protein L11. EMBO J. *26*, 3332–3345.

Dai, M.-S., Sears, R., and Lu, H. (2007b). Feedback regulation of c-Myc by ribosomal protein L11. Cell Cycle *6*, 2735–2741.

Dai, M.S., Shi, D., Jin, Y., Sun, X.X., Zhang, Y., Grossman, S.R., and Lu, H. (2006). Regulation of the MDM2-p53 pathway by ribosomal protein L11 involves a post-ubiquitination mechanism. J. Biol. Chem. *281*, 24304–24313.

Dang, C. V. (2012). MYC on the path to cancer. Cell *149*, 22–35.

Danilova, N., Sakamoto, K.M., and Lin, S. (2008). Ribosomal protein S19 deficiency in zebrafish leads to developmental abnormalities and defective erythropoiesis through activation of p53 protein family. Blood *112*, 5228–5237.

Danilova, N., Sakamoto, K.M., and Lin, S. (2011). Ribosomal protein L11 mutation in zebrafish leads to haematopoietic and metabolic defects. Br. J. Haematol. *152*, 217–228.

David-Pfeuty, T., Nouvian-Dooghe, Y., Sirri, V., Roussel, P., and Hernandez-Verdun, D. (2001). Common and reversible regulation of wild-type p53 function and of ribosomal biogenesis by protein kinases in human cells. Oncogene *20*, 5951–5963.

DeLeo, a B., Jay, G., Appella, E., Dubois, G.C., Law, L.W., and Old, L.J. (1979). Detection of a transformation-related antigen in chemically induced sarcomas and other transformed cells of the mouse. Proc. Natl. Acad. Sci. U. S. A. *76*, 2420–2424.

Derenzini, M., Trerè, D., Pession, a, Montanaro, L., Sirri, V., and Ochs, R.L. (1998). Nucleolar function and

size in cancer cells. Am. J. Pathol. *152*, 1291–1297.

Derenzini, M., Montanaro, L., Chillà, A., Tosti, E., Vici, M., Barbieri, S., Govoni, M., Mazzini, G., and Treré, D. (2005). Key role of the achievement of an appropriate ribosomal RNA complement for G1-S phase transition in H4-II-E-C3 rat hepatoma cells. J. Cell. Physiol. *202*, 483–491.

Derenzini, M., Montanaro, L., and Treré, D. (2009). What the nucleolus says to a tumour pathologist. Histopathology *54*, 753–762.

Devlin, E.E., Dacosta, L., Mohandas, N., Elliott, G., and Bodine, D.M. (2010). A transgenic mouse model demonstrates a dominant negative effect of a point mutation in the RPS19 gene associated with Diamond-Blackfan anemia. Blood *116*, 2826–2835.

Devlin, J.R., Hannan, K.M., Ng, P.Y., Bywater, M.J., Shortt, J., Cullinane, C., McArthur, G. a, Johnstone, R.W., Hannan, R.D., and Pearson, R.B. (2013). AKT signalling is required for ribosomal RNA synthesis and progression of Eμ-Myc B-cell lymphoma in vivo. FEBS J. *280*, 5307–5316.

Doherty, L., Sheen, M.R., Vlachos, A., Choesmel, V., O'Donohue, M.-F., Clinton, C., Schneider, H.E., Sieff, C.A., Newburger, P.E., Ball, S.E., et al. (2010). Ribosomal protein genes RPS10 and RPS26 are commonly mutated in Diamond-Blackfan anemia. Am. J. Hum. Genet. *86*, 222–228.

Donati, G., Bertoni, S., Brighenti, E., Vici, M., Treré, D., Volarevic, S., Montanaro, L., and Derenzini, M. (2011). The balance between rRNA and ribosomal protein synthesis up- and downregulates the tumour suppressor p53 in mammalian cells. Oncogene *30*, 3274–3288.

Donati, G., Peddigari, S., Mercer, C.A. a, and Thomas, G. (2013). 5S Ribosomal RNA Is an Essential Component of a Nascent Ribosomal Precursor Complex that Regulates the Hdm2-p53 Checkpoint. Cell Rep. *4*, 87–98.

Donehower, L. a, Harvey, M., Slagle, B.L., McArthur, M.J., Montgomery, C. a, Butel, J.S., and Bradley, a (1992). Mice deficient for p53 are developmentally normal but susceptible to spontaneous tumours. Nature *356*, 215–221.

Doré, L.C., and Crispino, J.D. (2011). Transcription factor networks in erythroid cell and megakaryocyte development. Blood *118*, 231–239.

Dousset, T., Wang, C., Verheggen, C., Chen, D., Hernandez-Verdun, D., and Huang, S. (2000). Initiation of nucleolar assembly is independent of RNA polymerase I transcription. Mol. Biol. Cell *11*, 2705–2717.

Drygin, D., Siddiqui-Jain, a., O'Brien, S., Schwaebe, M., Lin, a., Bliesath, J., Ho, C.B., Proffitt, C., Trent, K., Whitten, J.P., et al. (2009). Anticancer Activity of CX-3543: A Direct Inhibitor of rRNA Biogenesis. Cancer Res. *69*, 7653–7661.

Drygin, D., Rice, W.G., and Grummt, I. (2010). The RNA polymerase I transcription machinery: an emerging target for the treatment of cancer. Annu. Rev. Pharmacol. Toxicol. *50*, 131–156.

Drygin, D., Lin, A., Bliesath, J., Ho, C.B., O'Brien, S.E., Proffitt, C., Omori, M., Haddach, M., Schwaebe, M.K., Siddiqui-Jain, A., et al. (2011). Targeting RNA polymerase I with an oral small molecule CX-5461 inhibits ribosomal RNA synthesis and solid tumor growth. Cancer Res. *71*, 1418–1430.

Drygin, D., O'Brien, S.E., Hannan, R.D., McArthur, G. a., and Von Hoff, D.D. (2014). Targeting the nucleolus for cancer-specific activation of p53. Drug Discov. Today *19*, 259–265.

Dudgeon, D.D., Shinde, S., Hua, Y., Shun, T.Y., Lazo, J.S., Strock, C.J., Giuliano, K. a, Taylor, D.L., Johnston, P. a, and Johnston, P. a (2010). Implementation of a 220,000-compound HCS campaign to identify disruptors of the interaction between p53 and hDM2 and characterization of the confirmed hits. J. Biomol. Screen. *15*, 766–782.

Dutt, S., Narla, A., Lin, K., Mullally, A., Abayasekara, N., Megerdichian, C., Wilson, F.H., Currie, T., Khanna-Gupta, A., Berliner, N., et al. (2011). Haploinsufficiency for ribosomal protein genes causes selective activation of p53 in human erythroid progenitor cells. Blood *117*, 2567–2576.

Dutt, S., Narla, A., Lin, K., Mullally, A., Abayasekara, N., Wilson, F.H., Currie, T., Khanna-gupta, A., Berliner, N., Jeffery, L., et al. (2013). activation of p53 in human erythroid progenitor cells Plenary paper Haploinsufficiency for ribosomal protein genes causes selective activation of p53 in human erythroid progenitor cells. Blood *117*, 2567–2576.

Ebert, B.L., Lee, M.M., Pretz, J.L., Subramanian, A., Mak, R., Golub, T.R., and Sieff, C. a (2005). An RNA interference model of RPS19 deficiency in Diamond-Blackfan anemia recapitulates defective hematopoiesis and rescue by dexamethasone: identification of dexamethasone-responsive genes by microarray. Blood *105*, 4620–4626.

Efeyan, A., Garcia-Cao, I., Herranz, D., Velasco-Miguel, S., and Serrano, M. (2006). Tumour biology: Policing of oncogene activity by p53. Nature *443*, 159.

Elghetany, M.T., and Alter, B.P. (2002). p53 protein overexpression in bone marrow biopsies of patients with Shwachman-Diamond syndrome has a prevalence similar to that of patients with refractory anemia. Arch. Pathol. Lab. Med. *126*, 452–455.

Eliyahu, D., Raz, A., Gruss, P., Givol, D., and Oren, M. (1984). Participation of p53 cellular tumour antigen in transformation of normal embryonic cells. Nature *312*, 646–649.

Enchev, R.I., Schulman, B. a, and Peter, M. (2015). Protein neddylation: beyond cullin-RING ligases. Nat Rev Mol Cell Biol *16*, 30–44.

Farrar, J.E., Quarello, P., Fisher, R., O'Brien, K. a, Aspesi, A., Parrella, S., Henson, A.L., Seidel, N.E., Atsidaftos, E., Prakash, S., et al. (2014). Exploiting pre-rRNA processing in Diamond Blackfan anemia gene discovery and diagnosis. Am. J. Hematol. *89*, 985–991.

Fatica, A., and Tollervey, D. (2002). Making ribosomes. Curr. Opin. Cell Biol. *14*, 313–318.

Feng, L., Lin, T., Uranishi, H., Gu, W., and Xu, Y. (2005). Functional Analysis of the Roles of Posttranslational Modifications at the p53 C Terminus in Regulating p53 Stability and Activity Functional Analysis of the Roles of Posttranslational Modifications at the p53 C Terminus in Regulating p53 Stability and Ac. Society *25*, 5389–5395.

Fetherston, J., Werner, E., and Patterson, R. (1984). Processing of the external transcribed spacer of murine rRNA and site of action of actinomydn D. Nucleic Acids Res. *12*, 7187–7198.

Finlay, C.A., Hinds, P.W., and Levine, A.J. (1989). The p53 proto-oncogene can act as a suppressor of transformation. Cell *57*, 1083–1093.

Flygare, J., Kiefer, T., Miyake, K., Utsugisawa, T., Hamaguchi, I., Da Costa, L., Richter, J., Davey, E.J., Matsson, H., Dahl, N., et al. (2005). Deficiency of ribosomal protein S19 in CD34+ cells generated by siRNA blocks erythroid development and mimics defects seen in Diamond-Blackfan anemia. Blood *105*, 4627–4634.

Flygare, J., Aspesi, A., Bailey, J.C., Miyake, K., Caffrey, J.M., Karlsson, S., and Ellis, S.R. (2007). Human RPS19, the gene mutated in Diamond-Blackfan anemia, encodes a ribosomal protein required for the maturation of 40S ribosomal subunits. Blood *109*, 980–986.

Fontenay-Roupie, M., Bouscary, D., Guesnu, M., Picard, F., Melle, J., Lacombe, C., Gisselbrecht, S., Mayeux, P., and Dreyfus, F. (1999). Ineffective erythropoiesis in myelodysplastic syndromes: Correlation with fas expression but not with lack of erythropoietin receptor signal transduction. Br. J. Haematol. *106*, 464–473.

Fröjmark, A.-S., Badhai, J., Klar, J., Thuveson, M., Schuster, J., and Dahl, N. (2010). Cooperative effect of ribosomal protein s19 and Pim-1 kinase on murine c-Myc expression and myeloid/erythroid cellularity. J. Mol.

Med. Berlin Ger. *88*, 39–46.

Fumagalli, S., Cara, A. Di, Neb-gulati, A., Natt, F., Schwemberger, S., Hall, J., Babcock, G.F., Bernardi, R., Pandolfi, P.P., and Thomas, G. (2009). Absence of nucleolar disruption after impairment of 40S ribosome biogenesis reveals an rpL11-translation- dependent mechanism of p53 induction. *11*.

Fumagalli, S., Ivanenkov, V. V, Teng, T., and Thomas, G. (2012). Suprainduction of p53 by disruption of 40S and 60S ribosome biogenesis leads to the activation of a novel G2/M checkpoint. Genes Dev. *26*, 1028–1040.

Galdino-Pitta, M.R., Pitta, M.G.R., Lima, M.C.A., Galdino, L.S., and Pitta, R.I. (2013). Niche for acridine derivatives in anticancer therapy. Mini Rev. Med. Chem. *13*, 1256–1271.

Garcia-Cao, I. (2002). [ldquo]Super p53[rdquo] mice exhibit enhanced DNA damage response, are tumor resistant and age normally. Embo J. *21*, 6225–6235.

Garçon, L., Ge, J., Manjunath, S.H., Mills, J. a, Apicella, M., Parikh, S., Sullivan, L.M., Podsakoff, G.M., Gadue, P., French, D.L., et al. (2013). Ribosomal and hematopoietic defects in induced pluripotent stem cells derived from Diamond Blackfan anemia patients. Blood *122*, 912–921.

Garg, L.C., DiAngelo, S., and Jacob, S.T. (1987). Role of DNA topoisomerase I in the transcription of supercoiled rDNA gene. Proc. Natl. Acad. Sci. U.S.A. *84*, 3185–3188.

Gazda, H.T., Sheen, M.R., Vlachos, A., Choesmel, V., O'Donohue, M.F., Schneider, H., Darras, N., Hasman, C., Sieff, C.A., Newburger, P.E., et al. (2008). Ribosomal Protein L5 and L11 Mutations Are Associated with Cleft Palate and Abnormal Thumbs in Diamond-Blackfan Anemia Patients. Am. J. Hum. Genet. *83*, 769–780.

Gazda, H.T., Preti, M., Sheen, M.R., O'Donohue, M.-F., Vlachos, A., Davies, S.M., Kattamis, A., Doherty, L., Landowski, M., Buros, C., et al. (2012). Frameshift mutation in p53 regulator *RPL26* is associated with multiple physical abnormalities and a specific pre-ribosomal RNA processing defect in diamond-blackfan anemia. Hum. Mutat. *33*, 1037–1044.

Ge, J., Apicella, M., Mills, J. a., Garçon, L., French, D.L., Weiss, M.J., Bessler, M., and Mason, P.J. (2015). Dysregulation of the Transforming Growth Factor β Pathway in Induced Pluripotent Stem Cells Generated from Patients with Diamond Blackfan Anemia. PLoS One *10*, e0134878.

Geiler, C., Andrade, I., and Greenwald, D. (2014). Exogenous c-Myc Blocks Differentiation and Improves Expansion of Human Erythroblasts In vitro. *7*, 153–157.

Ghoshal, K., and Jacob, S.T. (1997). An alternative molecular mechanism of action of 5-fluorouracil, a potent anticancer drug. Biochem. Pharmacol. *53*, 1569–1575.

Giachino, C., Orlando, L., and Turinetto, V. (2013). Maintenance of genomic stability in mouse embryonic stem cells: Relevance in aging and disease. Int. J. Mol. Sci. *14*, 2617–2636.

Gilkes, D.M., Chen, L., and Chen, J. (2006). MDMX regulation of p53 response to ribosomal stress. EMBO J. *25*, 5614–5625.

Golomb, L., Bublik, D.R., Wilder, S., Nevo, R., Kiss, V., Grabusic, K., Volarevic, S., and Oren, M. (2012). Importin 7 and exportin 1 link c-Myc and p53 to regulation of ribosomal biogenesis. Mol. Cell *45*, 222–232.

Gomez-Roman, N., Grandori, C., Eisenman, R.N., and White, R.J. (2003). Direct activation of RNA polymerase III transcription by c-Myc. Nature *421*, 290–294.

Goodpasture, C., and Bloom, S.E. (1975). Visualization of nucleolar organizer regions im mammalian chromosomes using silver staining. Chromosoma *53*, 37–50.

Grandori, C., Gomez-Roman, N., Felton-Edkins, Z. a, Ngouenet, C., Galloway, D. a, Eisenman, R.N., and White, R.J. (2005). c-Myc binds to human ribosomal DNA and stimulates transcription of rRNA genes by RNA polymerase I. Nat. Cell Biol. *7*, 311–318.

Groopman, J.E., and Itri, L.M. (1999). Chemotherapy-induced anemia in adults: incidence and treatment. J. Natl. Cancer Inst. *91*, 1616–1634.

Grummt, I. (2003). Life on a planet of its own: regulation of RNA polymerase I transcription in the nucleolus. Genes Dev. *17*, 1691–1702.

Guccione, E., Martinato, F., Finocchiaro, G., Luzi, L., Tizzoni, L., Dall' Olio, V., Zardo, G., Nervi, C., Bernard, L., and Amati, B. (2006). Myc-binding-site recognition in the human genome is determined by chromatin context. Nat. Cell Biol. *8*, 764–770.

Han, M.K., Song, E.K., Guo, Y., Ou, X., Mantel, C., and Broxmeyer, H.E. (2008). SIRT1 Regulates Apoptosis and Nanog Expression in Mouse Embryonic Stem Cells by Controlling p53 Subcellular Localization. Cell Stem Cell *2*, 241–251.

Hannan, K., Hannan, R., and Smith, S. (2000). Rb and p130 regulate RNA polymerase I transcription: Rb disrupts the interaction between UBF and SL-1. Oncogene *1*, 4988–4999.

Hannan, K.M., Brandenburger, Y., Jenkins, A., Sharkey, K., Cavanaugh, A., Rothblum, L., Moss, T., Poortinga, G., McArthur, G. a, Pearson, R.B., et al. (2003). mTOR-dependent regulation of ribosomal gene transcription requires S6K1 and is mediated by phosphorylation of the carboxy-terminal activation domain of the nucleolar transcription factor UBF. Mol. Cell. Biol. *23*, 8862–8877.

Hasserjian, R.P., Zuo, Z., Garcia, C., Tang, G., Kasyan, A., Luthra, R., Abruzzo, L. V., Kantarjian, H.M., Medeiros, L.J., and Wang, S. a. (2010). Acute erythroid leukemia: A reassessment using criteria refined in the 2008 WHO classification. Blood *115*, 1985–1992.

Haupt, Y., Maya, R., Kazaz, A., and Oren, M. (1997). Mdm2 promotes the rapid degradation of p53. Nature *387*, 296–299.

Hein, N., Hannan, K.M., George, A.J., Sanij, E., and Hannan, R.D. (2013). The nucleolus: an emerging target for cancer therapy. Trends Mol. Med. *19*, 643–654.

Heix, J., Vente, A., Voit, R., Budde, A., Michaelidis, T.M., and Grummt, I. (1998). Mitotic silencing of human rRNA synthesis: Inactivation of the promoter selectivity factor SL1 by cdc2/cyclin B-mediated phosphorylation. EMBO J. *17*, 7373–7381.

Hernandez-Verdun, D., Roussel, P., Thiry, M., Sirri, V., and Lafontaine, D.L.J. (2010). The nucleolus: structure/function relationship in RNA metabolism. Wiley Interdiscip. Rev. RNA *1*, 415–431.

Heyer, B.S., MacAuley, a, Behrendtsen, O., and Werb, Z. (2000). Hypersensitivity to DNA damage leads to increased apoptosis during early mouse development. Genes Dev. *14*, 2072–2084.

Higa-Nakamine, S., Suzuki, T., Uechi, T., Chakraborty, A., Nakajima, Y., Nakamura, M., Hirano, N., Suzuki, T., and Kenmochi, N. (2012). Loss of ribosomal RNA modification causes developmental defects in zebrafish. Nucleic Acids Res. *40*, 391–398.

Hinds, P., Finlay, C., and Levine, a J. (1989). Mutation is required to activate the p53 gene for cooperation with the ras oncogene and transformation. J. Virol. *63*, 739–746.

Hinkal, G., Parikh, N., and Donehower, L. a (2009). Timed somatic deletion of p53 in mice reveals age-associated differences in tumor progression. PLoS One *4*, e6654.

Ho, J.S.L., Ma, W., Mao, D.Y.L., and Benchimol, S. (2005). p53-Dependent Transcriptional Repression of c-myc Is Required for G 1 Cell Cycle Arrest. Mol. Cell. Biol. *25*, 7423–7431.

Honda, R., Tanaka, H., and Yasuda, H. (1997). Oncoprotein MDM2 is a ubiquitin ligase E3 for tumor suppressor p53. FEBS Lett. *420*, 25–27.

Hong, Y., and Stambrook, P.J. (2004). Restoration of an absent G1 arrest and protection from apoptosis in

embryonic stem cells after ionizing radiation. Proc. Natl. Acad. Sci. U. S. A. *101*, 14443–14448.

Hong, H., Takahashi, K., Ichisaka, T., Aoi, T., Kanagawa, O., Nakagawa, M., Okita, K., and Yamanaka, S. (2009). Suppression of indued pluripotent stem cell generation by the p53-p21 pathway. Nature *460*, 1132–1135.

Horn, H.F., and Vousden, K.H. (2007). Coping with stress: multiple ways to activate p53. Oncogene *26*, 1306–1316.

Horn, H.F., and Vousden, K.H. (2008). Cooperation between the ribosomal proteins L5 and L11 in the p53 pathway. Oncogene *27*, 5774–5784.

Horos, R., Ijspeert, H., Pospisilova, D., Sendtner, R., Andrieu-Soler, C., Taskesen, E., Nieradka, A., Cmejla, R., Sendtner, M., Touw, I.P., et al. (2012). Ribosomal deficiencies in Diamond-Blackfan anemia impair translation of transcripts essential for differentiation of murine and human erythroblasts.

Huang, R., Wu, T., Xu, L., Liu, A., Ji, Y., and Hu, G. (2002). Upstream binding factor up-regulated in hepatocellular carcinoma is related to the survival and cisplatin-sensitivity of cancer cells. FASEB J. *16*, 293–301.

Itahana, K., Mao, H., Jin, A., Itahana, Y., Clegg, H. V., Lindström, M.S., Bhat, K.P., Godfrey, V.L., Evan, G.I., and Zhang, Y. (2007). Targeted Inactivation of Mdm2 RING Finger E3 Ubiquitin Ligase Activity in the Mouse Reveals Mechanistic Insights into p53 Regulation. Cancer Cell *12*, 355–366.

Jaako, P., Flygare, J., Olsson, K., Quere, R., Ehinger, M., Henson, A., Ellis, S., Schambach, A., Baum, C., Richter, J., et al. (2011). Mice with ribosomal protein S19 deficiency develop bone marrow failure and symptoms like patients with Diamond-Blackfan anemia. Blood *118*, 6087–6096.

Jaako, P., Debnath, S., Olsson, K., Bryder, D., Flygare, J., and Karlsson, S. (2012). Dietary L-leucine improves the anemia in a mouse model for Diamond-Blackfan anemia. Blood *120*, 2225–2228.

Jaako, P., Debnath, S., Olsson, K., Zhang, Y., Flygare, J., Lindström, M.S., Bryder, D., and Karlsson, S. (2015). Disruption of the 5S RNP-Mdm2 interaction significantly improves the erythroid defect in a mouse model for Diamond-Blackfan anemia. Leukemia 2221–2229.

Jacks, T., Remington, L., Williams, B., Schmitt, E.M., Halachmit, S., Bronson, R.T., and Weinberg, R.A. (1994). Tumor spectrum analysis in p53-mutant mice. *4*, 1–7.

Jäkel, S., and Gürlich, D. (1998). Importin β, transportin, RanBP5 and RanBP7 mediate nuclear import of ribosomal proteins in mammalian cells. EMBO J. *17*, 4491–4502.

James, M.J., and Zomerdijk, J.C.B.M. (2004). Phosphatidylinositol 3-Kinase and mTOR Signaling Pathways Regulate RNA Polymerase I Transcription in Response to IGF-1 and Nutrients. J. Biol. Chem. *279*, 8911–8918.

Jenkins, J.R., Rudge, K., and Currie, G.A. (1984). Cellular immortalization by a cDNA clone encoding the transformation-associated phosphoprotein p53. Nature *312*, 651–654.

Jin, A., Itahana, K., Keefe, K.O., and Zhang, Y. (2004). Inhibition of HDM2 and Activation of p53 by Ribosomal Protein L23. *24*, 7669–7680.

Joerger, a C., and Fersht, a R. (2007). Structure–function–rescue: the diverse nature of common p53 cancer mutants. Oncogene *26*, 2226–2242.

Jones, S.N., Roe, a E., Donehower, L. a, and Bradley, a (1995). Rescue of embryonic lethality in Mdm2-deficient mice by absence of p53. Nature *378*, 206–208.

Jones, S.N., Hancock, a R., Vogel, H., Donehower, L. a, and Bradley, a (1998). Overexpression of Mdm2 in mice reveals a p53-independent role for Mdm2 in tumorigenesis. Proc. Natl. Acad. Sci. U. S. A. *95*, 15608–15612.

Kamijo, T., Zindy, F., Roussel, M.F., Quelle, D.E., Downing, J.R., Ashmun, R.A., Grosveld, G., and Sherr, C.J. (1997). Tumor suppression at the mouse INK4a locus mediated by the alternative reading frame product p19ARF. Cell *91*, 649–659.

Kamijo, T., Van De Kamp, E., Chong, M.J., Zindy, F., Diehl, J.A., Sherr, C.J., and McKinnon, P.J. (1999). Loss of the ARF tumor suppressor reverses premature replicative arrest but not radiation hypersensitivity arising from disabled Atm function. Cancer Res. *59*, 2464–2469.

Kawai, H., Wiederschain, D., and Yuan, Z. (2003). Critical Contribution of the MDM2 Acidic Domain to p53 Ubiquitination. Society *23*, 4939–4947.

Kawamura, T., Suzuki, J., Wang, Y. V, Menendez, S., Morera, B., Raya, A., Wahl, G.M., Carlos, J., and Belmonte, I. (2010). Linking the p53 tumor suppressor pathway to somatic cell reprogramming. Nature *460*, 1140–1144.

Kazyken, D., Kaz, Y., Kiyan, V., and Zhylkibayev, A. (2014). The nuclear import of ribosomal proteins is regulated by mTOR. Oncotarget *5*, 9577–9593.

Keel, S.B., Phelps, S., Sabo, K.M., O'Leary, M.N., Kirn-Safran, C.B., and Abkowitz, J.L. (2012). Establishing Rps6 hemizygous mice as a model for studying how ribosomal protein haploinsufficiency impairs erythropoiesis. Exp. Hematol. *40*, 290–294.

De Keersmaecker, K., Atak, Z.K., Li, N., Vicente, C., Patchett, S., Girardi, T., Gianfelici, V., Geerdens, E., Clappier, E., Porcu, M., et al. (2013). Exome sequencing identifies mutation in CNOT3 and ribosomal genes RPL5 and RPL10 in T-cell acute lymphoblastic leukemia. Nat. Genet. *45*, 186–190.

Keller, M. a, Addya, S., Vadigepalli, R., Banini, B., Delgrosso, K., Huang, H., and Surrey, S. (2006). Transcriptional regulatory network analysis of developing human erythroid progenitors reveals patterns of coregulation and potential transcriptional regulators. Physiol. Genomics *28*, 114–128.

Kirn-Safran, C.B., Oristian, D.S., Focht, R.J., Parker, S.G., Vivian, J.L., and Carson, D.D. (2007). Global growth deficiencies in mice lacking the ribosomal protein HIP/RPL29. Dev. Dyn. *236*, 447–460.

Klein, J., and Grummt, I. (1999). Cell cycle-dependent regulation of RNA polymerase I transcription: the nucleolar transcription factor UBF is inactive in mitosis and early G1. Proc. Natl. Acad. Sci. U. S. A. *96*, 6096–6101.

Kominami, R., and Niwa, O. (2006). Radiation carcinogenesis in mouse thymic lymphomas. Cancer Sci. *97*, 575–581.

Kondrashov, N., Pusic, A., Stumpf, C.R., Shimizu, K., Hsieh, A.C., Xue, S., Ishijima, J., Shiroishi, T., and Barna, M. (2011). Ribosome-mediated specificity in Hox mRNA translation and vertebrate tissue patterning. Cell *145*, 383–397.

Kress, M., May, E., Cassingena, R., and May, P. (1979). Simian virus 40-transformed cells express new species of proteins precipitable by anti-simian virus 40 tumor serum. J. Virol. *31*, 472–483.

Kressler, D., Hurt, E., and Bassler, J. (2010). Driving ribosome assembly. Biochim. Biophys. Acta *1803*, 673–683.

Kubbutat, M.H., Jones, S.N., and Vousden, K.H. (1997). Regulation of p53 stability by Mdm2. Nature *387*, 299–303.

Kuhn, a, Vente, a, Dorée, M., and Grummt, I. (1998). Mitotic phosphorylation of the TBP-containing factor SL1 represses ribosomal gene transcription. J. Mol. Biol. *284*, 1–5.

Kuramitsu, M., Sato-Otsubo, A., Morio, T., Takagi, M., Toki, T., Terui, K., Wang, R., Kanno, H., Ohga, S., Ohara, A., et al. (2012). Extensive gene deletions in Japanese patients with Diamond-Blackfan anemia. Blood

119, 2376–2384.

Kurki, S., Peltonen, K., Latonen, L., Kiviharju, T.M., Ojala, P.M., Meek, D., and Laiho, M. (2004). Nucleolar protein NPM interacts with HDM2 and protects tumor suppressor protein p53 from HDM2-mediated degradation. Cancer Cell *5*, 465–475.

Kuroda, T., Murayama, A., Katagiri, N., Ohta, Y., Fujita, E., Masumoto, H., Ema, M., Takahashi, S., Kimura, K., and Yanagisawa, J. (2011). RNA content in the nucleolus alters p53 acetylation via MYBBP1A. EMBO J. *30*, 1054–1066.

Kussie, P.H., Gorina, S., Marechal, V., Elenbaas, B., Moreau, J., Levine, a J., and Pavletich, N.P. (1996). Structure of the MDM2 oncoprotein bound to the p53 tumor suppressor transactivation domain. Science *274*, 948–953.

Labib, K., and Hodgson, B. (2007). Replication fork barriers: pausing for a break or stalling for time? EMBO Rep. *8*, 346–353.

Landau, D. a., Tausch, E., Taylor-Weiner, A.N., Stewart, C., Reiter, J.G., Bahlo, J., Kluth, S., Bozic, I., Lawrence, M., Böttcher, S., et al. (2015). Mutations driving CLL and their evolution in progression and relapse. Nature.

Landowski, M., O'Donohue, M.-F., Buros, C., Ghazvinian, R., Montel-Lehry, N., Vlachos, A., Sieff, C. a, Newburger, P.E., Niewiadomska, E., Matysiak, M., et al. (2013). Novel deletion of RPL15 identified by array-comparative genomic hybridization in Diamond-Blackfan anemia. Hum. Genet. *132*, 1265–1274.

Lane, D.P., and Crawford, L. V (1979). T antigen is bound to a host protein in SV40-transformed cells. Nature *278*, 261–263.

Laptenko, O., and Prives, C. (2006). Transcriptional regulation by p53: one protein, many possibilities. Cell Death Differ. *13*, 951–961.

Larson, D.E., Xie, W., Glibetic, M., O'Mahony, D., Sells, B.H., and Rothblum, L.I. (1993). Coordinated decreases in rRNA gene transcription factors and rRNA synthesis during muscle cell differentiation. Proc. Natl. Acad. Sci. U. S. A. *90*, 7933–7936.

Lee, J.T., and Gu, W. (2010). The multiple levels of regulation by p53 ubiquitination. Cell Death Differ. *17*, 86–92.

Lessard, F., Morin, F., Ivanchuk, S., Langlois, F., Stefanovsky, V., Rutka, J., and Moss, T. (2010). The ARF tumor suppressor controls ribosome biogenesis by regulating the RNA polymerase I transcription factor TTF-I. Mol. Cell *38*, 539–550.

Li, H., Collado, M., Villasante, A., Strati, K., Ortega, S., Can, M., Blasco, M.A., and Serrano, M. (2009). The Ink4 / Arf locus is a barrier for iPS cell reprogramming. *460*, 2–7.

Li, M., Chen, D., Shiloh, A., Luo, J., Nikolaev, A.Y., Qin, J., and Gu, W. (2002). Deubiquitination of p53 by HAUSP is an important pathway for p53 stabilization. Nature *416*, 648–653.

Li, M., Brooks, C.L., Wu-Baer, F., Chen, D., Baer, R., and Gu, W. (2003). Mono- versus polyubiquitination: differential control of p53 fate by Mdm2. Science *302*, 1972–1975.

Li, M., He, Y., Dubois, W., Wu, X., Shi, J., and Huang, J. (2012a). Distinct regulatory mechanisms and functions for p53-activated and p53-repressed DNA damage response genes in embryonic stem cells. Mol. Cell *46*, 30–42.

Li, T., Kon, N., Jiang, L., Tan, M., Ludwig, T., Zhao, Y., Baer, R., and Gu, W. (2012b). Tumor suppression in the absence of p53-mediated cell-cycle arrest, apoptosis, and senescence. Cell *149*, 1269–1283.

Lin, T., Chao, C., Saito, S., Mazur, S.J., Murphy, M.E., Appella, E., and Xu, Y. (2005). p53 induces

differentiation of mouse embryonic stem cells by suppressing Nanog expression. Nat. Cell Biol. *7*, 165–171.

Lindström, M.S., Jin, A., Deisenroth, C., White Wolf, G., and Zhang, Y. (2007). Cancer-associated mutations in the MDM2 zinc finger domain disrupt ribosomal protein interaction and attenuate MDM2-induced p53 degradation. Mol. Cell. Biol. *27*, 1056–1068.

Linzer, D., and Levine, A. (1979). Characterization of a 54K Dalton Cellular SV40 Tumor Antigen and Uninfected Present in SV40-Transformed Cells and Uninfected Embryonal Carcinoma Cells. Cell *17*, 43–52.

Llanos, S., and Serrano, M. (2010). Depletion of ribosomal protein L37 occurs in response to DNA damage and activates p53 through the L11/MDM2 pathway. Cell Cycle *9*, 4005–4012.

Logsdon CD, J.B. (2013). The role of protein synthesis and digestive enzymes in acinar cell injury. Nat Rev Gastroenterol Hepatol *10*, 362–370.

Lohrum, M. a, Woods, D.B., Ludwig, R.L., Bálint, E., and Vousden, K.H. (2001). C-terminal ubiquitination of p53 contributes to nuclear export. Mol. Cell. Biol. *21*, 8521–8532.

Lohrum, M. a E., Ludwig, R.L., Kubbutat, M.H.G., Hanlon, M., and Vousden, K.H. (2003). Regulation of HDM2 activity by the ribosomal protein L11. Cancer Cell *3*, 577–587.

Loughery, J., and Meek, D. (2013). Switching on p53: an essential role for protein phosphorylation? Biodiscovery 1–20.

Louvet, E., Junéra, H.R., Berthury, I., and Hernandez-Verdun, D. (2006). Compartmentation of the Nucleolar Processing Proteins in the Granular Component Is a CK2-driven Process. Mol. Biol. Cell *17*, 2537–2546.

Ludwig, L.S., Gazda, H.T., Eng, J.C., Eichhorn, S.W., Thiru, P., Ghazvinian, R., George, T.I., Gotlib, J.R., Beggs, A.H., Sieff, C. a, et al. (2014). Altered translation of GATA1 in Diamond-Blackfan anemia. Nat. Med. *20*, 748–753.

Lundgren, K., Montes d Oca Luna, R., Boddie, Y., Elena, M., Spencer, B., Rahn, C., Guillermina, B., Michael, L., and Finley, C. a. (1997). Targeted expression of MDM2 uncouples S phase from mitosis and inhibits mammary gland development independent of p53. Genes Dev. *11*, 714–725.

Macias, E., Jin, A., Deisenroth, C., Bhat, K., Mao, H., Lindström, M.S., and Zhang, Y. (2010). An ARF-Independent c-MYC-activated tumor suppression pathway mediated by ribosomal protein-Mdm2 interaction. Cancer Cell *18*, 231–243.

Mahata, B., Sundqvist, a, and Xirodimas, D.P. (2012). Recruitment of RPL11 at promoter sites of p53-regulated genes upon nucleolar stress through NEDD8 and in an Mdm2-dependent manner. Oncogene *31*, 3060–3071.

Mariani, L., Deiana, G., Vassella, E., Fathi, A.-R., Murtin, C., Arnold, M., Vajtai, I., Weis, J., Siegenthaler, P., Schobesberger, M., et al. (2006). Loss of heterozygosity 1p36 and 19q13 is a prognostic factor for overall survival in patients with diffuse WHO grade 2 gliomas treated without chemotherapy. J. Clin. Oncol. *24*, 4758–4763.

Marion, R.M., Strati, K., Li, H., Murga, M., Blanco, R., Ortega, S., Mario, R.M., Fernandez-Capetillo, O., Serrano, M., and Blasco, M.A. (2009). A p53-mediated DNA damage response limits reprogramming to ensure iPS cell genomic integrity. *460*.

Martins, C.P., Brown-Swigart, L., and Evan, G.I. (2006). Modeling the therapeutic efficacy of p53 restoration in tumors. Cell *127*, 1323–1334.

Matsson, H., Davey, E.J., Fröjmark, a S., Miyake, K., Utsugisawa, T., Flygare, J., Zahou, E., Byman, I., Landin, B., Ronquist, G., et al. (2006). Erythropoiesis in the Rps19 disrupted mouse: Analysis of erythropoietin response and biochemical markers for Diamond-Blackfan anemia. Blood Cells. Mol. Dis. *36*, 259–264.

Mayer, C., and Grummt, I. (2006). Ribosome biogenesis and cell growth: mTOR coordinates transcription by all

three classes of nuclear RNA polymerases. Oncogene *25*, 6384–6391.

Mayer, C., Zhao, J., Yuan, X., and Grummt, I. (2004). mTOR-dependent activation of the transcription factor TIF-IA links rRNA synthesis to nutrient availability. Genes Dev. *18*, 423–434.

Mayer, C., Bierhoff, H., and Grummt, I. (2005). The nucleolus as a stress sensor: JNK2 inactivates the transcription factor TIF-IA and down-regulates rRNA synthesis. Genes Dev. *19*, 933–941.

McBride, K. a, Ballinger, M.L., Killick, E., Kirk, J., Tattersall, M.H.N., Eeles, R. a, Thomas, D.M., and Mitchell, G. (2014). Li-Fraumeni syndrome: cancer risk assessment and clinical management. Nat. Rev. Clin. Oncol. *11*, 260–271.

McGowan, K. a., and Mason, P.J. (2011). Animal models of diamond Blackfan anemia. Semin. Hematol. *48*, 106–116.

McGowan, K. a, Li, J.Z., Park, C.Y., Beaudry, V., Tabor, H.K., Sabnis, A.J., Zhang, W., Fuchs, H., de Angelis, M.H., Myers, R.M., et al. (2008). Ribosomal mutations cause p53-mediated dark skin and pleiotropic effects. Nat. Genet. *40*, 963–970.

McGowan, K. a, Pang, W.W., Bhardwaj, R., Perez, M.G., Pluvinage, J. V, Glader, B.E., Malek, R., Mendrysa, S.M., Weissman, I.L., Park, C.Y., et al. (2011). Reduced ribosomal protein gene dosage and p53 activation in low-risk myelodysplastic syndrome. Blood *118*, 3622–3633.

McStay, B., and Grummt, I. (2008). The epigenetics of rRNA genes: from molecular to chromosome biology. Annu. Rev. Cell Dev. Biol. *24*, 131–157.

Mélèse, T., and Xue, Z. (1995). The nucleolus: an organelle formed by the act of building a ribosome. Curr. Opin. Cell Biol. *7*, 319–324.

Mendrysa, S.M., O'Leary, K. a., McElwee, M.K., Michalowski, J., Eisenman, R.N., Powell, D. a., and Perry, M.E. (2006). Tumor suppression and normal aging in mice with constitutively high p53 activity. Genes Dev. *20*, 16–21.

Meulmeester, E., Frenk, R., Stad, R., de Graaf, P., Marine, J.-C., Vousden, K.H., and Jochemsen, A.G. (2003). Critical role for a central part of Mdm2 in the ubiquitylation of p53. Mol. Cell. Biol. *23*, 4929–4938.

Mirabello, L., Macari, E.R., Jessop, L., Ellis, S.R., Myers, T., Giri, N., Taylor, A.M., McGrath, K.E., Humphries, J.M., Ballew, B.J., et al. (2014). Whole-exome sequencing and functional studies identify RPS29 as a novel gene mutated in multicase Diamond-Blackfan anemia families. Blood *124*, 24–32.

Mitsui, K., Tokuzawa, Y., Itoh, H., Segawa, K., Murakami, M., Takahashi, K., Maruyama, M., Maeda, M., and Yamanaka, S. (2003). The Homeoprotein Nanog Is Required for Maintenance of Pluripotency in Mouse Epiblast and ES Cells. Cell *113*, 631–642.

Miyake, K., Utsugisawa, T., Flygare, J., Kiefer, T., Hamaguchi, I., Richter, J., and Karlsson, S. (2008). Ribosomal protein S19 deficiency leads to reduced proliferation and increased apoptosis but does not affect terminal erythroid differentiation in a cell line model of Diamond-Blackfan anemia. Stem Cells *26*, 323–329.

Momand, J., Zambetti, G., Olson, D., George, D., and Levine, A. (1992). The mdm-2 oncogene product forms a complex with the p53 protein and inhi- bits p53-mediated transactivation.pdf.crdownload. Cell *69*, 1237–1245.

Moné, M.J., Volker, M., Nikaido, O., Mullenders, L.H.F., Zeeland, A.A. Van, Verschure, P.J., Manders, E.M.M., and Driel, R. Van (2001). Local UV-induced DNA damage in cell nuclei results in local transcription inhibition. *2*, 1013–1017.

Moniz, H., Gastou, M., Leblanc, T., Hurtaud, C., Crétien, a, Lécluse, Y., Raslova, H., Larghero, J., Croisille, L., Faubladier, M., et al. (2012). Primary hematopoietic cells from DBA patients with mutations in RPL11 and RPS19 genes exhibit distinct erythroid phenotype in vitro. Cell Death Dis. *3*, e356.

Montanaro, L., Treré, D., and Derenzini, M. (2008). Nucleolus, ribosomes, and cancer. Am. J. Pathol. *173*, 301–310.

Montes de Oca Luna, R., Wagner, D.S., and Lozano, G. (1995). Rescue of early embryonic lethality in mdm2-deficient mice by deletion of p53. Nature *378*, 203–206.

Moore, H.M., Bai, B., Boisvert, F.-M., Latonen, L., Rantanen, V., Simpson, J.C., Pepperkok, R., Lamond, A.I., and Laiho, M. (2011). Quantitative proteomics and dynamic imaging of the nucleolus reveal distinct responses to UV and ionizing radiation. Mol. Cell. Proteomics *10*, M111.009241.

Morgado-Palacin, L., Llanos, S., and Serrano, M. (2012). Ribosomal stress induces L11- and p53-dependent apoptosis in mouse pluripotent stem cells. Cell Cycle *11*, 503–510.

Morgado-Palacin, L., Llanos, S., Urbano-Cuadrado, M., Blanco-Aparicio, C., Megias, D., Pastor, J., and Serrano, M. (2014). Non-genotoxic activation of p53 through the RPL11-dependent ribosomal stress pathway. Carcinogenesis *35*, 2822–2830.

Morgado-Palacin, L., Varetti, G., Llanos, S., Gomez-Lopez, G., Martinez, D., and Serrano, M. (2015). Partial Loss of Rpl11 in Adult Mice Recapitulates Diamond-Blackfan Anemia and Promotes Lymphomagenesis. Cell Rep. *13*, 1–11.

Morton, J.P., and Sansom, O.J. (2013). MYC-y mice: from tumour initiation to therapeutic targeting of endogenous MYC. Mol. Oncol. *7*, 248–258.

Munugalavadla, V., and Kapur, R. (2005). Role of c-Kit and erythropoietin receptor in erythropoiesis. Crit. Rev. Oncol. Hematol. *54*, 63–75.

Narla, A., and Ebert, B.L. (2010). Ribosomopathies: human disorders of ribosome dysfunction. Blood *115*, 3196–3205.

Narla, A., Vlachos, A., and Nathan, D.G. (2011). Diamond Blackfan Anemia Treatment: Past, Present, and Future. Semin. Hematol. *48*, 117–123.

Narla, A., Payne, E.M., Abayasekara, N., Hurst, S.N., Raiser, D.M., Look, a. T., Berliner, N., Ebert, B.L., and Khanna-Gupta, A. (2014). L-Leucine improves the anaemia in models of Diamond Blackfan anaemia and the 5q- syndrome in a TP53-independent way. Br. J. Haematol. *167*, 524–528.

Nguyen, L.X.T., Raval, A., Garcia, J.S., and Mitchell, B.S. (2015). Regulation of Ribosomal Gene Expression in Cancer. J. Cell. Physiol. *230*, 1181–1188.

Nichols, J., Zevnik, B., Anastassiadis, K., Niwa, H., Klewe-Nebenius, D., Chambers, I., Schöler, H., and Smith, A. (1998). Formation of pluripotent stem cells in the mammalian embryo depends on the POU transcription factor Oct4. Cell *95*, 379–391.

Nieminen, T.T., O'Donohue, M.-F., Wu, Y., Lohi, H., Scherer, S.W., Paterson, A.D., Ellonen, P., Abdel-Rahman, W.M., Valo, S., Mecklin, J.-P., et al. (2014). Germline Mutation of RPS20, Encoding a Ribosomal Protein, Causes Predisposition to Hereditary Nonpolyposis Colorectal Carcinoma Without DNA Mismatch Repair Deficiency. Gastroenterology *147*, 595–598.e5.

O'Farrell, P.H., Stumpff, J., and Su, T.T. (2004). Embryonic Cleavage Cycles: How Is a Mouse Like a Fly? Curr. Biol. *14*, 35–45.

Oliner, J.D., Kinzler, K.W., Meltzer, P.S., George, D.L., and Vogelstein, B. (1992). Amplification of a gene encoding a p53-associated protein in human sarcomas. Nature *358*, 80–83.

Oliver, E.R., Saunders, T.L., Tarlé, S.A., and Glaser, T. (2004). Ribosomal protein L24 defect in belly spot and tail (Bst), a mouse Minute. Development *131*, 3907–3920.

Olivier, M., Hollstein, M., and Hainaut, P. (2010). TP53 mutations in human cancers: origins, consequences, and

clinical use. Cold Spring Harb. Perspect. Biol. *2*, 1–17.

Oren, M., Maltzman, W., and Levine, a J. (1981). Post-translational regulation of the 54K cellular tumor antigen in normal and transformed cells. Mol. Cell. Biol. *1*, 101–110.

Orford, K.W., and Scadden, D.T. (2008). Deconstructing stem cell self-renewal : genetic insights into cell-cycle regulation. *9*.

Palmero, I., Pantoja, C., and Serrano, M. (1998). p19ARF links the tumour suppressor p53 to Ras. Nature *395*, 125–126.

Pan, W., Issaq, S., and Zhang, Y. (2011). The in vivo role of the RP-Mdm2-p53 pathway in signaling oncogenic stress induced by pRb inactivation and Ras overexpression. PLoS One *6*.

Panić, L., Tamarut, S., Sticker-Jantscheff, M., Barkić, M., Solter, D., Uzelac, M., Grabusić, K., and Volarević, S. (2006). Ribosomal protein S6 gene haploinsufficiency is associated with activation of a p53-dependent checkpoint during gastrulation. Mol. Cell. Biol. *26*, 8880–8891.

Parada, L.F., Land, H., Weinberg, R. a, Wolf, D., and Rotter, V. (1984). Cooperation between gene encoding p53 tumour antigen and ras in cellular transformation. Nature *312*, 649–651.

Patel, J.H., Loboda, A.P., Showe, M.K., Showe, L.C., and McMahon, S.B. (2004). Analysis of genomic targets reveals complex functions of MYC. Nat. Rev. Cancer *4*, 562–568.

Payne, E.M., Virgilio, M., Narla, A., Sun, H., Levine, M., Paw, B.H., Berliner, N., Look, A.T., Ebert, B.L., and Khanna-Gupta, A. (2012). L-leucine improves the anemia and developmental defects associated with Diamond-Blackfan anemia and del(5q)MDSby activating themTORpathway. Blood *120*, 2214–2224.

Pellagati, A., Marafioti, T., Paterson, J.C., Barlow, J.L., Drynan, L.F., Giagounidis, A., Pileri, S.A., Cazzola, M., McKenzie, A.N.J., Wainscoat, J.S., et al. (2015). Induction of p53 and up-regulation of the p53 pathway in the human 5q- syndrome. Blood *99*, 2721–2723.

Peltonen, K., Colis, L., Liu, H., Jäämaa, S., Moore, H.M., Enbäck, J., Laakkonen, P., Vaahtokari, A., Jones, R.J., af Hällström, T.M., et al. (2010). Identification of novel p53 pathway activating small-molecule compounds reveals unexpected similarities with known therapeutic agents. PLoS One *5*, e12996.

Peltonen, K., Colis, L., Liu, H., Trivedi, R., Moubarek, M.S., Moore, H.M., Bai, B., Rudek, M. a, Bieberich, C.J., and Laiho, M. (2014). A targeting modality for destruction of RNA polymerase I that possesses anticancer activity. Cancer Cell *25*, 77–90.

Pereboom, T.C., Bondt, A., Pallaki, P., Klasson, T.D., Goos, Y.J., Essers, P.B., Groot Koerkamp, M.J. a, Gazda, H.T., Holstege, F.C.P., Costa, L. Da, et al. (2014). Translation of branched-chain aminotransferase-1 transcripts is impaired in cells haploinsufficient for ribosomal protein genes. Exp. Hematol. *42*, 394–403.e4.

Perry, R.P., and Kelley, D.E. (1970). Inhibition of RNA synthesis by actinomycin D: characteristic dose-response of different RNA species. J. Cell. Physiol. *76*, 127–139.

Perry, M.E., Piette, J., Zawadzki, J. a, Harvey, D., and Levine, a J. (1993). The mdm-2 gene is induced in response to UV light in a p53-dependent manner. Proc. Natl. Acad. Sci. U. S. A. *90*, 11623–11627.

Pestov, D.G., Strezoska, Z., and Lau, L.F. (2001). Evidence of p53-Dependent Cross-Talk between Ribosome Biogenesis and the Cell Cycle : Effects of Nucleolar Protein Bop1 on G 1 / S Transition Evidence of p53-Dependent Cross-Talk between Ribosome Biogenesis and the Cell Cycle : Effects of Nucleolar Protei. Mol. Cell. Biol. *21*, 4246–4255.

Pichiorri, F., Suh, S.-S., Rocci, A., De Luca, L., Taccioli, C., Santhanam, R., Zhou, W., Benson, D.M., Hofmainster, C., Alder, H., et al. (2010). Downregulation of p53-inducible microRNAs 192, 194, and 215 Impairs the p53/MDM2 Autoregulatory Loop in Multiple Myeloma Development. Cancer Cell *18*, 367–381.

Pomerantz, J., Schreiber-Agus, N., Liégeois, N.J., Silverman, a, Alland, L., Chin, L., Potes, J., Chen, K., Orlow, I., Lee, H.W., et al. (1998). The Ink4a tumor suppressor gene product, p19Arf, interacts with MDM2 and neutralizes MDM2's inhibition of p53. Cell *92*, 713–723.

Pospisilova, D., Cmejlova, J., Hak, J., Adam, T., and Cmejla, R. (2007). Successful treatment of a Diamond-Blackfan anemia patient with amino acid leucine. Haematologica *92*, e66–e67.

Provost, E., Wehner, K. a., Zhong, X., Ashar, F., Nguyen, E., Green, R., Parsons, M.J., and Leach, S.D. (2012). Ribosomal biogenesis genes play an essential and p53-independent role in zebrafish pancreas development. Development *139*, 3232–3241.

Provost, E., Weier, C. a, and Leach, S.D. (2013). Multiple ribosomal proteins are expressed at high levels in developing zebrafish endoderm and are required for normal exocrine pancreas development. Zebrafish *10*, 161–169.

Qin, W., Chen, Z., Zhang, Y., Yan, R., Yan, G., Li, S., Zhong, H., and Lin, S. (2014). Nom1 mediates pancreas development by regulating ribosome biogenesis in zebrafish. PLoS One *9*, 1–10.

Quarello, P., Garelli, E., Carando, A., Brusco, A., Calabrese, R., Dufour, C., Longoni, D., Misuraca, A., Vinti, L., Aspesi, A., et al. (2010). Diamond-Blackfan anemia: genotype-phenotype correlations in Italian patients with RPL5 and RPL11 mutations. Haematologica *95*, 206–213.

Quin, J.E., Devlin, J.R., Cameron, D., Hannan, K.M., Pearson, R.B., and Hannan, R.D. (2014). Targeting the nucleolus for cancer intervention. Biochim. Biophys. Acta *1842*, 802–816.

Ray-Coquard, I., Blay, J.-Y., Italiano, A., Le Cesne, A., Penel, N., Zhi, J., Heil, F., Rueger, R., Graves, B., Ding, M., et al. (2012). Effect of the MDM2 antagonist RG7112 on the P53 pathway in patients with MDM2-amplified, well-differentiated or dedifferentiated liposarcoma: an exploratory proof-of-mechanism study. Lancet Oncol. *13*, 1133–1140.

Reynolds, R.C., Montgomery, P.O., and Hughes, B. (1964). Nucleolar "Caps" Produced By Actinomycin D. Cancer Res. *24*, 1269–1277.

van Riggelen, J., Yetil, A., and Felsher, D.W. (2010). MYC as a regulator of ribosome biogenesis and protein synthesis. Nat. Rev. Cancer *10*, 301–309.

Robledo, S., Idol, R.A., Crimmins, D.A.N.L., Ladenson, J.H., Mason, P.J., and Bessler, M. (2008a). The role of human ribosomal proteins in the maturation of rRNA and ribosome production. 1918–1929.

Robledo, S., Idol, R. a, Crimmins, D.L., Ladenson, J.H., Mason, P.J., and Bessler, M. (2008b). The role of human ribosomal proteins in the maturation of rRNA and ribosome production. RNA *14*, 1918–1929.

Rodriguez, M.S., Desterro, J.M., Lain, S., Lane, D.P., and Hay, R.T. (2000). Multiple C-terminal lysine residues target p53 for ubiquitin-proteasome-mediated degradation. Mol. Cell. Biol. *20*, 8458–8467.

de Rozieres, S., Maya, R., Oren, M., and Lozano, G. (2000). The loss of mdm2 induces p53-mediated apoptosis. Oncogene *19*, 1691–1697.

Rubbi, C.P., and Milner, J. (2003). Disruption of the nucleolus mediates stabilization of p53 in response to DNA damage and other stresses. EMBO J. *22*, 6068–6077.

Ruggero, D., and Shimamura, A. (2015). Marrow failure : a window into ribosome biology. *124*, 2784–2793.

Russell, J., and Zomerdijk, J.C.B.M. (2005). RNA-polymerase-I-directed rDNA transcription, life and works. Trends Biochem. Sci. *30*, 87–96.

Ruzankina, Y., Pinzon-Guzman, C., and Asare, A. (2007). Deletion of the Developmentally Essential Gene ATR in Adult Mice Leads to Age-Related Phenotypes and Stem Cell Loss. Cell Stem Cell *1*, 113–126.

Sabapathy, K., Klemm, M., Jaenisch, R., and F.wagner, E. (1997a). Regulation of ES cell differentiation by functional and conformational modulation of p53. EMBO J. *16*, 6217–6229.

Sabapathy, K., Klemm, M., Jaenisch, R., and F.wagner, E. (1997b). Regulation of ES cell differentiation by functional and conformational modulation of p53. EMBO J. *16*, 6217–6229.

Sachdeva, M., Zhu, S., Wu, F., Wu, H., Walia, V., Kumar, S., Elble, R., Watabe, K., and Mo, Y.-Y. (2009). p53 represses c-Myc through induction of the tumor suppressor miR-145. Proc. Natl. Acad. Sci. U. S. A. *106*, 3207–3212.

Sage, J. (2012). The retinoblastoma tumor suppressor and stem cell biology. Genes Dev. *26*, 1409–1420.

Sankaran, V.G., Ghazvinian, R., Do, R., Thiru, P., Vergilio, J.-A., Beggs, H., Sieff, C. a, Orkin, S.H., Nathan, D.G., Lander, E.S., et al. (2012). Exome Sequencing Identifies GATA1 Mutations Resulting in Diamond-Blackfan Anemia. J. Clin. Invest. *122*, 1–5.

Sanz-Ezquerro, J.J., and Tickle, C. (2003). Fgf Signaling Controls the Number of Phalanges and Tip Formation in Developing Digits. Curr. Biol. *13*, 1830–1836.

Sarnow, P., Ho, Y.S., Williams, J., and Levine, a J. (1982). Adenovirus E1b-58kd tumor antigen and SV40 large tumor antigen are physically associated with the same 54 kd cellular protein in transformed cells. Cell *28*, 387–394.

Sasaki, M., Kawahara, K., Nishio, M., Mimori, K., Kogo, R., Hamada, K., Itoh, B., Wang, J., Komatsu, Y., Yang, Y.R., et al. (2011). Regulation of the MDM2-P53 pathway and tumor growth by PICT1 via nucleolar RPL11. Nat. Med. *17*, 944–951.

Scala, F., Brighenti, E., Govoni, M., Imbrogno, E., Fornari, F., Treré, D., Montanaro, L., and Derenzini, M. (2015). Direct relationship between the level of p53 stabilization induced by rRNA synthesis-inhibiting drugs and the cell ribosome biogenesis rate. Oncogene 1–13.

Scheffner, M., Werness, B. a., Huibregtse, J.M., Levine, a. J., and Howley, P.M. (1990). The E6 oncoprotein encoded by human papillomavirus types 16 and 18 promotes the degradation of p53. Cell *63*, 1129–1136.

Schlosser, I., Hölzel, M., Mürnseer, M., Burtscher, H., Weidle, U.H., and Eick, D. (2003). A role for c-Myc in the regulation of ribosomal RNA processing. Nucleic Acids Res. *31*, 6148–6156.

Schmidt, E. V (1999). The role of c-myc in cellular growth control. Oncogene *18*, 2988–2996.

Schmitt, C. a, McCurrach, M.E., de Stanchina, E., Wallace-Brodeur, R.R., and Lowe, S.W. (1999). INK4a/ARF mutations accelerate lymphomagenesis and promote chemoresistance by disabling p53. Genes Dev. *13*, 2670–2677.

Shav-tal, Y., Blechman, J., Darzacq, X., Montagna, C., Dye, B.T., Patton, J.G., Singer, R.H., and Zipori, D. (2005). Dynamic Sorting of Nuclear Components into Distinct Nucleolar Caps during Transcriptional Inhibition. *16*, 2395–2413.

Sherr, C.J. (1998). Tumor surveillance via the ARF – p53 pathway. Genes Dev. *12*, 2984–2991.

Shiue, C.-N., Berkson, R.G., and Wright, a P.H. (2009). c-Myc induces changes in higher order rDNA structure on stimulation of quiescent cells. Oncogene *28*, 1833–1842.

Sieff, C. a., Yang, J., Merida-Long, L.B., and Lodish, H.F. (2010). Pathogenesis of the erythroid failure in Diamond Blackfan anaemia. Br. J. Haematol. *148*, 611–622.

Singh, S. a, Goldberg, T. a, Henson, A.L., Husain-Krautter, S., Nihrane, A., Blanc, L., Ellis, S.R., Lipton, J.M., and Liu, J.M. (2014). p53-Independent cell cycle and erythroid differentiation defects in murine embryonic stem cells haploinsufficient for Diamond Blackfan anemia-proteins: RPS19 versus RPL5. PLoS One *9*, e89098.

Sirri, V., Urcuqui-Inchima, S., Roussel, P., and Hernandez-Verdun, D. (2008). Nucleolus: the fascinating nuclear body. Histochem. Cell Biol. *129*, 13–31.

Sjögren, S.E., Siva, K., Soneji, S., George, A.J., Winkler, M., Jaako, P., Wlodarski, M., Karlsson, S., Hannan, R.D., and Flygare, J. (2015). Glucocorticoids improve erythroid progenitor maintenance and dampen *Trp53* response in a mouse model of Diamond-Blackfan anaemia. Br. J. Haematol. n/a – n/a.

Smith, J.S., Alderete, B., Minn, Y., Borell, T.J., Perry, a, Mohapatra, G., Hosek, S.M., Kimmel, D., O'Fallon, J., Yates, a, et al. (1999). Localization of common deletion regions on 1p and 19q in human gliomas and their association with histological subtype. Oncogene *18*, 4144–4152.

Snow, M.H.L. (1977). Gastrulation in the mouse: growth and regionalization of the epiblast. J. Embryol. Exp. Morphol. *Vol. 42*, 293–303.

Solozobova, V., Rolletschek, A., and Blattner, C. (2009). Nuclear accumulation and activation of p53 in embryonic stem cells after DNA damage. BMC Cell Biol. *10*, 46.

De Stanchina, E., McCurrach, M.E., Zindy, F., Shieh, S.Y., Ferbeyre, G., Samuelson, A. V., Prives, C., Roussel, M.F., Sherr, C.J., and Lowe, S.W. (1998). E1A signaling to p53 involves the p19(ARF) tumor suppressor. Genes Dev. *12*, 2434–2442.

Stewart, M.J., and Denell, R. (1993). Mutations in the Drosophila gene encoding ribosomal protein S6 cause tissue overgrowth. Mol. Cell. Biol. *13*, 2524–2535.

Stixova, L., Hruskova, T., Sehnalova, P., Legartova, S., Svidenska, S., Kozubek, S., and Bartova, E. (2014). Microscopy Techniques Used for Comparison of UVA- and γ-Irradiation-Induced DNA Damage in the Cell Nucleus and Nucleolus. Folia Biol. *60*, 76–84.

Stormon, M.O., Ip, W.F., Ellis, L., Schibli, S., Rommens, J.M., and Durie, P.R. (2010). Evidence of a generalized defect of acinar cell function in Shwachman-Diamond syndrome. J. Pediatr. Gastroenterol. Nutr. *51*, 8–13.

Sun, X.-X., Dai, M.-S., and Lu, H. (2008). Mycophenolic Acid Activation of p53 Requires Ribosomal Proteins L5 and L11. J. Biol. Chem. *283*, 12387–12392.

Sun, X.-X., Wang, Y.-G., Xirodimas, D.P., and Dai, M.-S. (2010). Perturbation of 60 S ribosomal biogenesis results in ribosomal protein L5- and L11-dependent p53 activation. J. Biol. Chem. *285*, 25812–25821.

Sun, X.X., Dai, M.S., and Lu, H. (2007). 5-fluorouracil activation of p53 involves an MDM2-ribosomal protein interaction. J. Biol. Chem. *282*, 8052–8059.

Sundqvist, A., Liu, G., Mirsaliotis, A., and Xirodimas, D.P. (2009). Regulation of nucleolar signalling to p53 through NEDDylation of L11. EMBO Rep. *10*, 1132–1139.

Suryadi, J., and Bierbach, U. (2012). DNA metalating-intercalating hybrid agents for the treatment of chemoresistant cancers. Chem. - A Eur. J. *18*, 12926–12934.

Suzuki, T. (2013). How is digit identity determined during limb development? Dev. Growth Differ. *55*, 130–138.

Takagi, M., Absalon, M.J., McLure, K.G., and Kastan, M.B. (2005). Regulation of p53 translation and induction after DNA damage by ribosomal protein L26 and nucleolin. Cell *123*, 49–63.

Tang, Y., Zhao, W., Chen, Y., Zhao, Y., and Gu, W. (2008). Acetylation Is Indispensable for p53 Activation. Cell *133*, 612–626.

Tanimura, S., Ohtsuka, S., Mitsui, K., Shirouzu, K., Yoshimura, A., and Ohtsubo, M. (1999). MDM2 interacts with MDMX through their RING finger domains. FEBS Lett. *447*, 5–9.

Taylor, A.M., Humphries, J.M., White, R.M., Murphey, R.D., Burns, C.E., and Zon, L.I. (2012). Hematopoietic

defects in rps29 mutant zebrafish depend upon p53 activation. Exp. Hematol. *40*, 228–237.e5.

Teng, T., Thomas, G., and Mercer, C. a (2013a). Growth control and ribosomopathies. Curr. Opin. Genet. Dev. *23*, 63–71.

Teng, T., Mercer, C. a, Hexley, P., Thomas, G., and Fumagalli, S. (2013b). Loss of tumor suppressor RPL5/RPL11 does not induce cell cycle arrest but impedes proliferation due to reduced ribosome content and translation capacity. Mol. Cell. Biol. *33*, 4660–4671.

Tolbert, D., Lu, X., Yin, C., Tantama, M., and Van Dyke, T. (2002). p19(ARF) is dispensable for oncogenic stress-induced p53-mediated apoptosis and tumor suppression in vivo. Mol. Cell. Biol. *22*, 370–377.

Toledo, F., and Wahl, G.M. (2006). Regulating the p53 pathway: in vitro hypotheses, in vivo veritas. Nat. Rev. Cancer *6*, 909–923.

Torihara, H., Uechi, T., Chakraborty, A., Shinya, M., Sakai, N., and Kenmochi, N. (2011). Erythropoiesis failure due to RPS19 deficiency is independent of an activated Tp53 response in a zebrafish model of Diamond-Blackfan anaemia. Br. J. Haematol. *152*, 648–654.

Treiber, D.K., Zhai, X., Jantzen, H.M., and Essigmann, J.M. (1994). Cisplatin-DNA adducts are molecular decoys for the ribosomal RNA transcription factor hUBF (human upstream binding factor). Proc. Natl. Acad. Sci. *91*, 5672–5676.

Trerè, D. (2000). AgNOR staining and quantification. Micron *31*, 127–131.

Tulpule, A., Kelley, J.M., Lensch, M.W., McPherson, J., Park, I.H., Hartung, O., Nakamura, T., Schlaeger, T.M., Shimamura, A., and Daley, G.Q. (2013). Pluripotent stem cell models of shwachman-diamond syndrome reveal a common mechanism for pancreatic and hematopoietic dysfunction. Cell Stem Cell *12*, 727–736.

Uechi, T., Nakajima, Y., Nakao, A., Torihara, H., Chakraborty, A., Inoue, K., and Kenmochi, N. (2006). Ribosomal protein gene knockdown causes developmental defects in zebrafish. PLoS One *1*.

Utikal, J., Polo, J.M., Stadtfeld, M., Maherali, N., Kulalert, W., Walsh, R.M., Khalil, A., Rheinwald, J.G., and Hochedlinger, K. (2009). Immortalization eliminates a roadblock during cellular reprogramming into iPS cells. Nature *460*, 1145–1148.

Valente, L.J., Gray, D.H.D., Michalak, E.M., Pinon-Hofbauer, J., Egle, A., Scott, C.L., Janic, A., and Strasser, A. (2013). P53 Efficiently Suppresses Tumor Development in the Complete Absence of Its Cell-Cycle Inhibitory and Proapoptotic Effectors p21, Puma, and Noxa. Cell Rep. *3*, 1339–1345.

Ventura, A., Kirsch, D.G., McLaughlin, M.E., Tuveson, D. a., Grimm, J., Lintault, L., Newman, J., Reczek, E.E., Weissleder, R., and Jacks, T. (2007). Restoration of p53 function leads to tumour regression in vivo. Nature *445*, 661–665.

Vlachos, A., and Muir, E. (2010). How I treat Diamond-Blackfan anemia. Bl *116*, 3715–3723.

Vlachos, A., Rosenberg, P.S., Atsidaftos, E., Alter, B.P., and Lipton, J.M. (2012). Incidence of neoplasia in Diamond Blackfan anemia: a report from the Diamond Blackfan Anemia Registry. Blood *119*, 3815–3819.

Vlachos, A., Dahl, N., Dianzani, I., and Lipton, J.M. (2013). Clinical utility gene card for: Diamond – Blackfan Anemia – update 2013. Eur. J. Hum. Genet. *21*, 2–5.

Vogelstein, B., Lane, D., and Levine, A.J. (2000). Surfing the p53 network. Nature *408*, 307–310.

Voit, R., Schäfer, K., and Grummt, I. (1997). Mechanism of repression of RNA polymerase I transcription by the retinoblastoma protein. Mol Cell Biol *17*, 4230–4237.

Volarevic, S., Stewart, M.J., Ledermann, B., Zilberman, F., Terracciano, L., Montini, E., Grompe, M., Kozma, S.C., and Thomas, G. (2000). Proliferation, but not growth, blocked by conditional deletion of 40S ribosomal

protein S6. Science *288*, 2045–2047.

Wade, M., Li, Y.-C., and Wahl, G.M. (2013). MDM2, MDMX and p53 in oncogenesis and cancer therapy. Nat. Rev. Cancer *13*, 83–96.

Wade, M. a, Sunter, N.J., Fordham, S.E., Long, a, Masic, D., Russell, L.J., Harrison, C.J., Rand, V., Elstob, C., Bown, N., et al. (2014). c-MYC is a radiosensitive locus in human breast cells. Oncogene *34*, 1–10.

Wang, W., Ho, W.C., Dicker, D.T., MacKinnon, C., Winkler, J.D., Marmorstein, R., and El-Deiry, W.S. (2005). Acridine derivatives activate p53 and induce tumor cell death through Bax. Cancer Biol. Ther. *4*, 893–898.

Warner, J.R. (1999). The economics of ribosome biosynthesis in yeast. Trends Biochem. Sci. *24*, 437–440.

Watkins-Chow, D.E., Cooke, J., Pidsley, R., Edwards, A., Slotkin, R., Leeds, K.E., Mullen, R., Baxter, L.L., Campbell, T.G., Salzer, M.C., et al. (2013). Mutation of the diamond-blackfan anemia gene Rps7 in mouse results in morphological and neuroanatomical phenotypes. PLoS Genet. *9*, e1003094.

Watson, K.L., Konrad, K.D., Woods, D.F., and Bryant, P.J. (1992). Drosophila homolog of the human S6 ribosomal protein is required for tumor suppression in the hematopoietic system. Proc. Natl. Acad. Sci. U. S. A. *89*, 11302–11306.

Wei, S., Chen, X., McGraw, K., Zhang, L., Komrokji, R., Clark, J., Caceres, G., Billingsley, D., Sokol, L., Lancet, J., et al. (2012). Lenalidomide promotes p53 degradation by inhibiting MDM2 auto-ubiquitination in myelodysplastic syndrome with chromosome 5q deletion. Oncogene *32*, 1110–1120.

Weiss, M.J., Yu, C., and Orkin, S.H. (1997). Erythroid-cell-specific properties of transcription factor GATA-1 revealed by phenotypic rescue of a gene-targeted cell line. Mol. Cell. Biol. *17*, 1642–1651.

White, J., and Dalton, S. (2005). Cell cycle control of embryonic stem cells. Stem Cell Rev. *1*, 131–138.

Wontakal, S.N., Guo, X., Smith, C., MacCarthy, T., Bresnick, E.H., Bergman, a., Snyder, M.P., Weissman, S.M., Zheng, D., and Skoultchi, a. I. (2012). A core erythroid transcriptional network is repressed by a master regulator of myelo-lymphoid differentiation. Proc. Natl. Acad. Sci. *109*, 3832–3837.

Xiong, X., Zhao, Y., He, H., and Sun, Y. (2011). Ribosomal protein S27-like and S27 interplay with p53-MDM2 axis as a target, a substrate and a regulator. Oncogene *30*, 1798–1811.

Xirodimas, D.P., Saville, M.K., Bourdon, J.C., Hay, R.T., and Lane, D.P. (2004). Mdm2-mediated NEDD8 conjugation of p53 inhibits its transcriptional activity. Cell *118*, 83–97.

Xue, S., and Barna, M. (2012). Specialized ribosomes: a new frontier in gene regulation and organismal biology. Nat. Rev. Mol. Cell Biol. *13*, 355–369.

Xue, W., Zender, L., Miething, C., Dickins, R. a., Hernando, E., Krizhanovsky, V., Cordon-Cardo, C., and Lowe, S.W. (2007). Senescence and tumour clearance is triggered by p53 restoration in murine liver carcinomas. Nature *445*, 656–660.

Yadavilli, S., Mayo, L.D., Higgins, M., Lain, S., Hegde, V., and Deutsch, W. a. (2009). Ribosomal protein S3: A multi-functional protein that interacts with both p53 and MDM2 through its KH domain. DNA Repair (Amst). *8*, 1215–1224.

Yip, B.H., Vuppusetty, C., Attwood, M., Giagounidis, a, Germing, U., Lamikanra, a a, Roberts, D.J., Maciejewski, J.P., Vandenberghe, P., Mecucci, C., et al. (2013). Activation of the mTOR signaling pathway by L-leucine in 5q- syndrome and other RPS14-deficient erythroblasts. Leukemia *27*, 1760–1763.

Young, R. a. (2011). Control of the embryonic stem cell state. Cell *144*, 940–954.

Yuan, J., Luo, K., Zhang, L., Cheville, J.C., and Lou, Z. (2010). USP10 Regulates p53 Localization and Stability by Deubiquitinating p53. Cell *140*, 384–396.

Yuan, X., Zhou, Y., Casanova, E., Chai, M., Kiss, E., Gröne, H.-J., Schütz, G., and Grummt, I. (2005). Genetic inactivation of the transcription factor TIF-IA leads to nucleolar disruption, cell cycle arrest, and p53-mediated apoptosis. Mol. Cell *19*, 77–87.

Zemp, I., and Kutay, U. (2007). Nuclear export and cytoplasmic maturation of ribosomal subunits. FEBS Lett. *581*, 2783–2793.

Zentner, G.E., Balow, S. a, and Scacheri, P.C. (2014). Genomic characterization of the mouse ribosomal DNA locus. Genes|Genomes|Genetics *4*, 243–254.

Zhai, W., and Comai, L. (2000). Repression of RNA Polymerase I Transcription by the Tumor Suppressor p53 Repression of RNA Polymerase I Transcription by the Tumor Suppressor p53. *20*, 5930–5938.

Zhang, Y., and Lu, H. (2009). Signaling to p53: ribosomal proteins find their way. Cancer Cell *16*, 369–377.

Zhang, C., Comai, L., and Johnson, D.L. (2011a). PTEN Represses RNA Polymerase I Transcription by Disrupting the SL1 Complex †. *25*, 6899–6911.

Zhang, J., Harnpicharnchai, P., Jakovljevic, J., Tang, L., Guo, Y., Oeffinger, M., Rout, M.P., Hiley, S.L., Hughes, T., and Woolford, J.L. (2007). Assembly factors Rpf2 and Rrs1 recruit 5S rRNA and ribosomal proteins rpL5 and rpL11 into nascent ribosomes. Genes Dev. *21*, 2580–2592.

Zhang, L., Prak, L., Rayon-Estrada, V., Thiru, P., Flygare, J., Lim, B., and Lodish, H.F. (2013a). ZFP36L2 is required for self-renewal of early burst-forming unit erythroid progenitors. Nature *499*, 92–96.

Zhang, Q., Xiao, H., Chai, S.C., Hoang, Q.Q., and Lu, H. (2011b). Hydrophilic residues are crucial for ribosomal protein L11 (RPL11) interaction with zinc finger domain of MDM2 and p53 protein activation. J. Biol. Chem. *286*, 38264–38274.

Zhang, Y., Xiong, Y., and Yarbrough, W.G. (1998). ARF promotes MDM2 degradation and stabilizes p53: ARF-INK4a locus deletion impairs both the Rb and p53 tumor suppression pathways. Cell *92*, 725–734.

Zhang, Y., Wolf, G.W., Bhat, K., Jin, A., Allio, T., Burkhart, W.A., and Xiong, Y. (2003). Ribosomal Protein L11 Negatively Regulates Oncoprotein MDM2 and Mediates a p53-Dependent Ribosomal-Stress Checkpoint Pathway. *23*, 8902–8912.

Zhang, Z., Jia, H., Zhang, Q., Wan, Y., Zhou, Y., Jia, Q., Zhang, W., Yuan, W., Cheng, T., Zhu, X., et al. (2013b). Assessment of hematopoietic failure due to Rpl11 deficiency in a zebrafish model of Diamond-Blackfan anemia by deep sequencing. BMC Genomics *14*, 896.

Zhao, Y., Bernard, D., and Wang, S. (2013). Small Molecule Inhibitors of MDM2-p53 and MDMX-p53 Interactions as New Cancer Therapeutics. Biodiscovery 4.

Zheng, J., Lang, Y., Zhang, Q., Cui, D., Sun, H., Jiang, L., Chen, Z., Zhang, R., Gao, Y., Tian, W., et al. (2015). Structure of human MDM2 complexed with RPL11 reveals the molecular basis of p53 activation. Genes Dev. 1524–1534.

Zhong, S., Zhang, C., and Johnson, D.L. (2004). Epidermal Growth Factor Enhances Cellular TATA Binding Protein Levels and Induces RNA Polymerase I- and III-Dependent Gene Activity Epidermal Growth Factor Enhances Cellular TATA Binding Protein Levels and Induces RNA Polymerase I- and III-Dependent Gene . *24*, 5119–5129.

Zhou, X., Hao, Q., Liao, J., Zhang, Q., and Lu, H. (2013). Ribosomal protein S14 unties the MDM2-p53 loop upon ribosomal stress. Oncogene *32*, 388–396.

Zindy, F., Eischen, C.M., Randle, D.H., Kamijo, T., Cleveland, J.L., Sherr, C.J., and Roussel, M.F. (1998). Myc signaling via the ARF tumor suppressor regulates p53-dependent apoptosis and immortalization. Genes Dev. *12*, 2424–2433.